




LUCA @ CAHA 3.5m

LUCA Feasibility Study

Rev. No.	Document authors / contributors	Approval	Date
1	F. Prada, E. Pérez, J.M. Ibáñez, J. Sánchez, R. Content, J. Lawrence, G. Murray, <i>Winlight System</i>	 Francisco Prada (PI)	12 July 2019

Principal Investigator: Francisco Prada
f.prada@csic.es



Outline

1. Introduction
2. LUCA Team and Collaborators
3. LUCA Science
4. LUCA Survey Strategy
5. IFU-6000 Instrument Proposal
6. Project Layout: work packages
7. Project cost and timeline
8. LUCA in the world-wide context
9. Conclusions and remarks
10. Acknowledgements
11. Appendix A: IFU-6000 Fiber System Feasibility Study by Durham University
12. Appendix B: IFU-6000 Feasibility Study Report (pre-optics and spectrograph) by AAO-Macquarie
13. Appendix C: IFU-6000 spectrograph technical and proposal reports by Winlight System
14. Appendix D: IFU-6000 Instrument Control System Feasibility Study by IAA-CSIC



Audentes fortuna iuvat.
Publio Virgilio, Eneida, 10, 284.

Ex nihilo nihil fit.



1. Introduction

LUCA (Local Universe from Calar Alto) is proposed as a new generation science program for the Calar Alto Observatory (CAHA) 3.5-m telescope. The LUCA Project faces the construction of large Integral Field Unit (IFU) spectrograph with six thousands optical fibers (named IFU-6000), that will allow astronomers to map our universe neighborhood in 3D with an unprecedented spatial resolution. LUCA will be able to observe large pieces of the sky generating a massive quantity of spectral data cubes in the visible range, which aims to unravel physical processes at small enough scale to study how the star formation and evolution affects the formation and evolution of galaxies in our local universe.

The project, conceived and led by the Instituto de Astrofísica de Andalucía (IAA-CSIC), was selected by the CAHA's advisory committee to finance its feasibility study. The feasibility study phase extended over the period from on Oct. 1st, 2018 and July 12th, 2019, and a total of 243,300 euro was required for its accomplishment. Out of the awarded 100,000 euro by the Junta de Andalucía, and managed by the University of Almería, we spent 76,300 euro to pay the consultancy work done by AAO-Macquarie (35,000 euro), Durham University (31,700 euro) and Winlight System (9600 euro). The human resources devoted by the IAA-CSIC to the feasibility study sum a total of 161,000 euro which corresponds to a total of 2.35FTE: 0.25 FTE Hardware/Software Control Engineer; 0.30 FTE Instrument Engineer; 0.80 FTE Project Scientist; and 1.00 FTE Principal Investigator, Project Manager, Instrument Scientist. In addition 6,000 euro was spent by the IAA-CSIC in travel and meetings.

This document presents a detailed Feasibility Study of the LUCA Project. The work included in this report has been performed by a team of engineers and scientists at the IAA-CSIC in collaboration with the institutions and consultants listed below (see Sec. 2). We provide science specifications and requirements, science overview and survey strategy, a technical description of the instrument proposal, performances and designs, work packages, an expected schedule and costs. Conclusions and remarks are given in Sec 9.



2. LUCA Team and Collaborators

The work presented in this feasibility study document has been performed and led by the LUCA Team at the IAA-CSIC in collaboration with AAO-Macquarie University, Durham University and Winlight System.

LUCA Team at IAA-CSIC:

- Francisco Prada, *Principal Investigator, Project Manager, Instrument Scientist*
- Enrique Pérez, *Project Scientist*
- Justo Sánchez, *Instrument Engineer*
- José Miguel Ibáñez, *Software & Control Engineer*

Consultant Collaborators:

- Graham Murray (Durham University), *Fiber System and Slit Assembly*
- Robert Content and Jon Lawrence (AAO-Macquarie), *Pre-optics and Spectrograph System*
- *Winlight System, Spectrograph Design*

See Sec. 10 for Acknowledgements.

3. LUCA Science

The large-scale structure of the Universe is a complex web of clusters, filaments, and voids. Hierarchical clustering cosmology has been successful to explain the large-scale structures. However, at small and intermediate scales, there is a significant number of problems to explain how galaxies form and how they evolve depending on their environment. Recently, high spatial resolution cosmological simulations of galaxy formation and evolution have started to be developed. These models require the implementation of accurate phenomenological prescriptions for the sub-grid physics governing galaxy evolution, in particular those that link the star formation processes with the galactic feedback, which occur at ~few tens parsec scales.

Galaxies are a complex mix of baryonic (stars, gas, and dust) and dark matter and radiation, spatially distributed in galaxy components (bulge, thin and thick disks, halo, etc) at kpc scales. However, the physical processes that lead to star formation and the modes by which this activity couples to the broader environment where galaxies flow occur on smaller scales, of a few tens of



parsecs. Here, we propose to study the local universe from these small parsec scales to the scales of the nearest galaxy cluster. This will improve by more than an order of magnitude the spatial resolution of current IFS galaxy surveys (e.g. CALIFA, MaNGA).

As defined by the IAU, based on current resolution of individual stars, the Local Universe comprises a sphere of radius 15 Mpc centered in the Local Group, and it includes the Local Volume and the Virgo cluster.

Galaxies in the Local Universe offer us the unique opportunity to map the kinematics, physical and chemical properties of the stellar populations, the interstellar medium, and dark matter at spatial scales from a few pc, as in M31 or M33, to less than 100 pc in the Virgo cluster. This is the range of spatial scales needed to constrain the sub-grid physics in models of galaxy formation and evolution.

Furthermore, because over this local volume all the galaxies are considered to be at roughly the same cosmic epoch, but the local density field varies by a factor of ~ 100 , the large-scale evolutionary effects are due more to the underlying density than to any variation in epoch. Thus, LUCA will enable us to map the bulge, disk, and halo properties with unprecedented high spatial resolution, and to study the effects of the environment on these galaxy components at different levels of field density, isolated galaxies, galaxy groups, and the nearest galaxy cluster.

In addition to this main global science case, many other science cases can be carried out with the proposed instrumentation, including extended stellar and nebular targets in the Milky Way or the mapping of the local cosmic flow.

Science Requirement	Parameter
Telescope	CAHA 3.5 m
IFU FoV	9 arcmin ²
Spatial sampling	2.5''
# spaxels	6000
Fiber core on CCD	< 4 pixels
On sky FoV effective coverage	> 90%
Fiber cable length	< 40 m
Spectral resolution @ 500nm	2000
Wavelength range	360-700 nm
Fiber cross-talk	< 5%

Table. Summary of main science technical requirements.

3.1 LUCA Sample

Following the IAU definition of the Local Universe, LUCA is a survey of nearby galaxies selected to be in the Local Volume and in the Virgo cluster. Thus, the survey contains two samples.

First sample: Local Volume

A selection of galaxies from the complete sample of galaxies in the Local Volume, up to 11 Mpc, compiled by Klypin et al. 2015, that are visible from CAHA and are more luminous than $M_B = -16$. This selection includes all spirals and early type galaxies of the Local Volume with stellar mass above $10^9 M_{\text{sun}}$. Excluding M31, M33, and M101, that are members of this sample⁽¹⁾, the galaxies have a size (a_{26} , the isophotal diameter at a surface brightness $SB_B=26 \text{ mag/arcsec}^2$) that ranges from 1 to 30 arcmin, with mean 7.4 arcmin and median 5.6 arcmin.

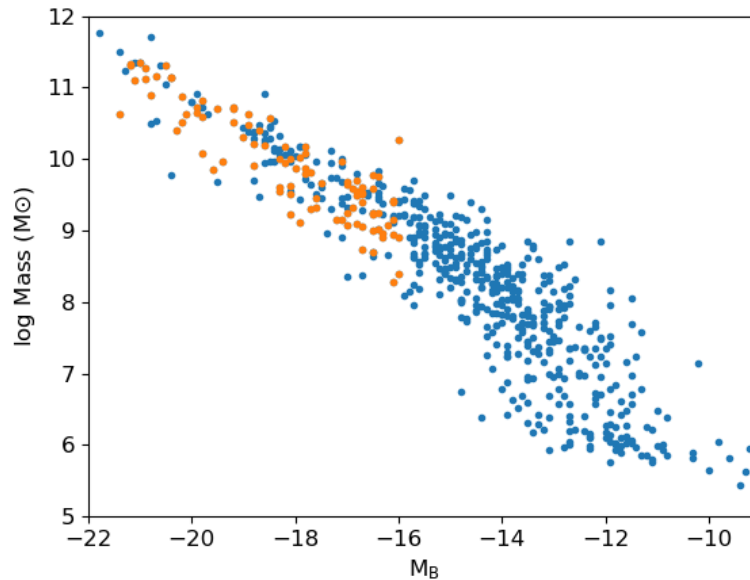


Figure. Blue points represent all the 603 LV galaxies (Klypin et al. 2015) with a measured M_B and estimated dynamical mass. In orange the 102 galaxies of the LUCA LV sample, with $M_B < -16$ and visible from CAHA.

¹ From now on, these three galaxies are excluded from the LV sample in this document, as they are the specific target of an independent study at the CAHA Schmidt telescope, with documentation already submitted to the CAHA director for the consideration of the CAHA executive committee.

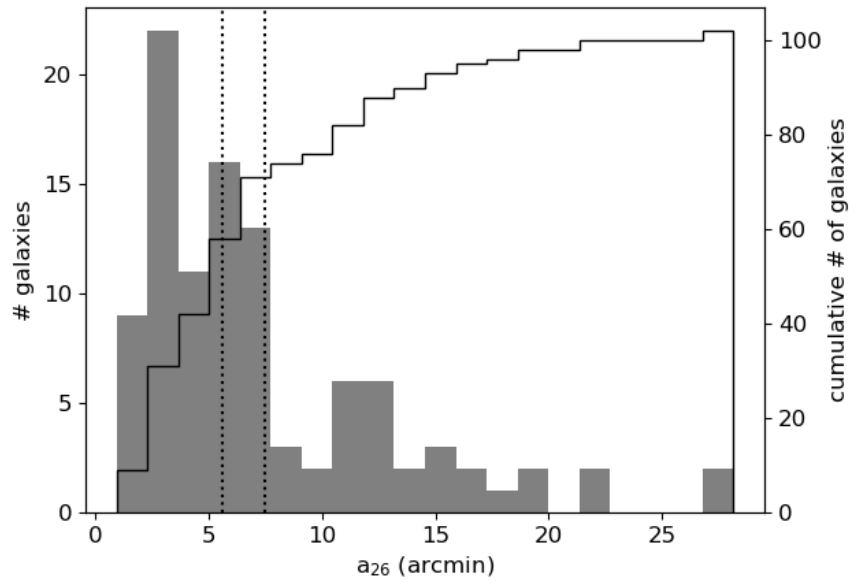


Figure. Distribution of galaxy sizes (a_{26} , the isophotal diameter at a surface brightness $SB_B=26 \text{ mag/arcsec}^2$) for the Local Volume sample. The grayscale filled histogram corresponds to the left Y-axis, while the black hollow line shows the cumulative distribution (right hand Y-axis), to a total of 102 galaxies. Vertical dotted lines indicate mean ($7.4'$) and median ($5.6'$) values.

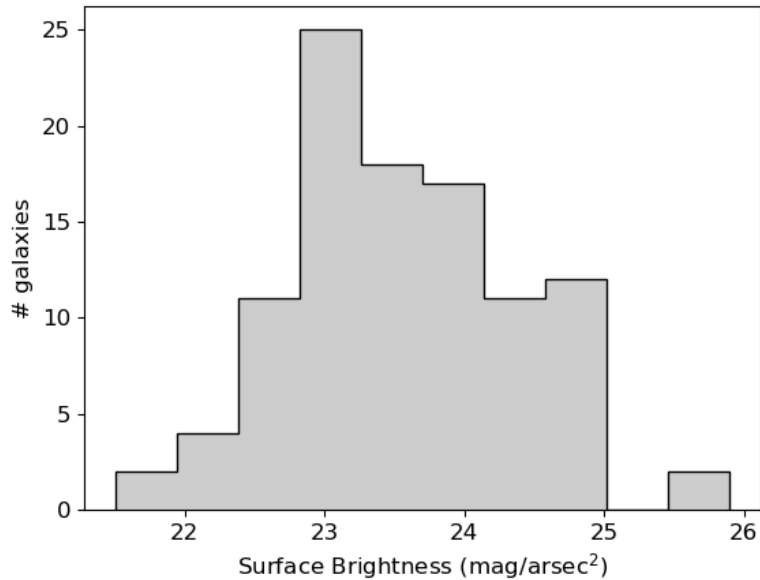


Figure. Distribution of surface brightness for the LV sample.

Thus, the LV sample is formed by 102 galaxies at a mean distance 6.7 Mpc, providing a spatial scale of 32 pc/arcsec, and having a mean diameter size of 7.4 arcmin.

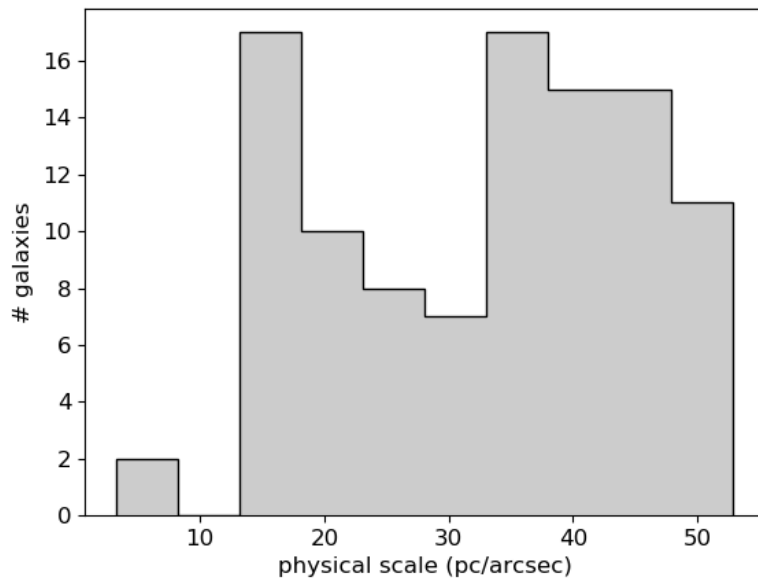


Figure. Distribution of linear physical scales in parsec/arcsec for the LV sample.

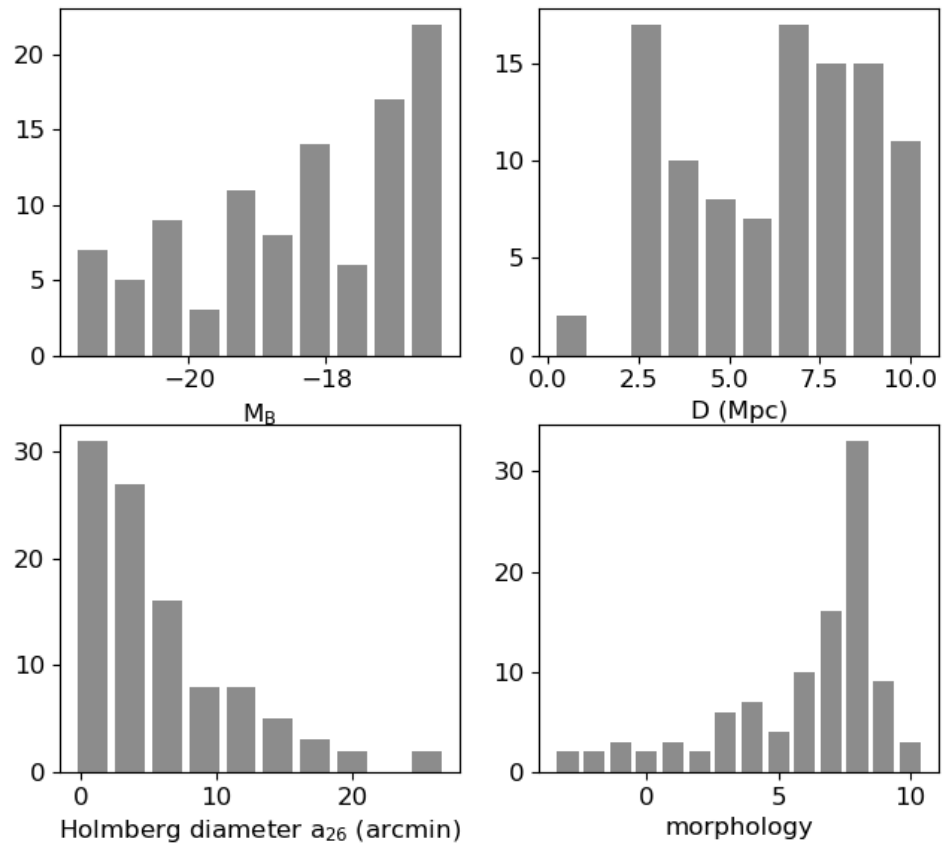


Figure. Distribution of magnitude, distance, size, and morphology for the LV sample.

Second sample: Virgo cluster

A selection of 218 galaxies from the Virgo Cluster Catalog (VCC, Binggeli, Sandage & Tammann 1985) more luminous than $M_g < -17$ and visible from CAHA. This sub-sample includes galaxies of all morphological types and are spatially well distributed within the cluster covering its main filamentary structures. The sample is complete for galaxies with stellar mass $> 10^9 M_\odot$, it provides a spatial scale of 80 pc/arcsec and a mean size of 2.4 arcmin.

We will seek ways to provide synergy with current and upcoming surveys of the local universe at different wavelengths, such as those provided by Spitzer FIR (LVL survey), SKA and ngVLA (SWG2) HI, and other optical surveys (HST/LEGUS, J-PLUS/J-PAS).

To our knowledge, no other project is planned to map with IFS such an extent of the local volume. The closest competitor beyond 2020 will be SDSS-V, which includes as one of its three main surveys the local volume mapper concentrating on the MW and LMC. For M31, M33 and other galaxies out to 5 Mpc they will have a sparse IFS sampling: "Statistical samples of H II regions (green) observed at 20 pc resolution across M31, and at ~ 50 pc resolution across other nearby galaxies" (cf. arXiv1711.03234). In the North they will have only ~ 2000 fibers, compared to the ~ 6000 for LUCA. We will likely reach the sky at about the same time.

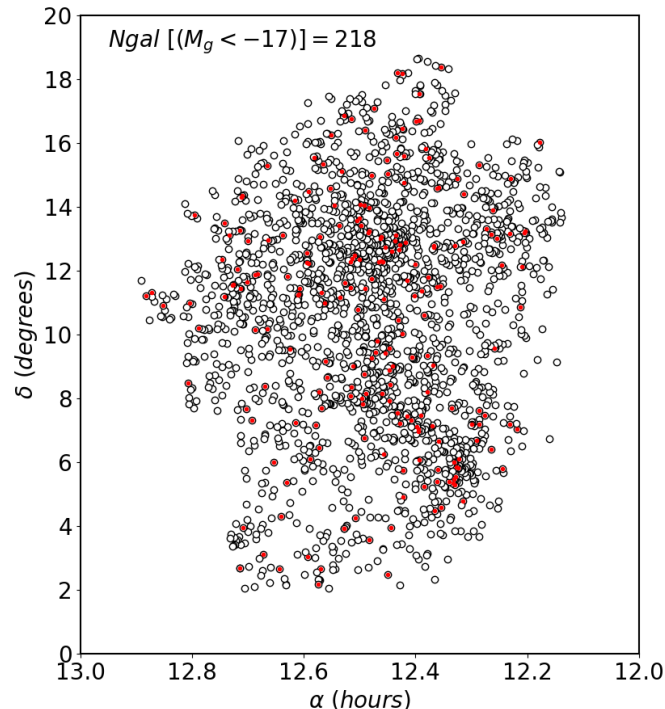


Figure. Spatial distribution of galaxies in the Virgo Cluster Catalog. In red the galaxies selected in the LUCA VCC sample, with $M_g < -17$ and visible from CAHA.

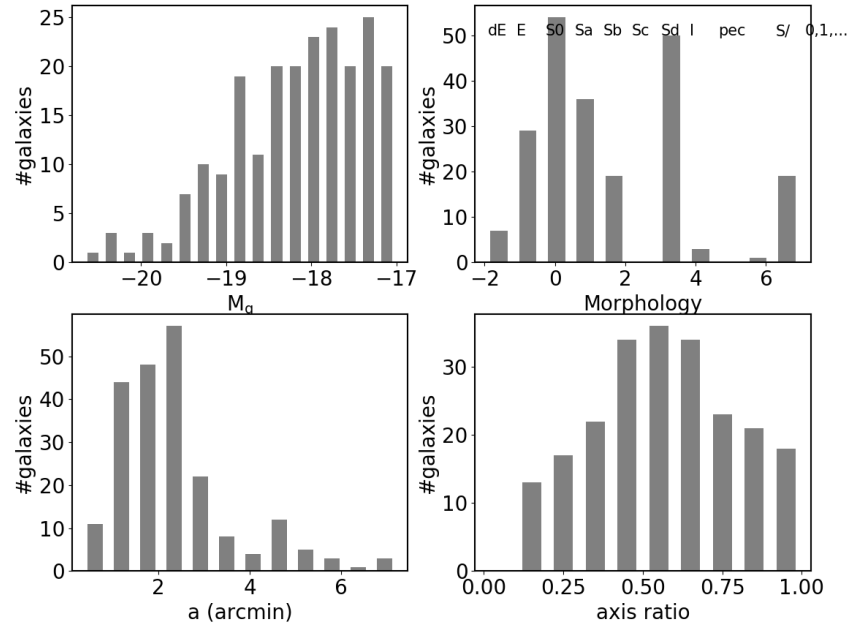


Figure. Distribution of properties of the galaxies in the LUCA VCC sample. M_g is the absolute magnitude in the SDSS g band, the morphological type, the semimajor axis size (in arcmin) and the galaxies axis ratio (0.1 for edge on, 1 for face on).

4. LUCA Survey Strategy

The LV sample is drawn from the work of Karachentsev et al (2013, AJ, 145, 101) ⁽²⁾

Selection criteria:

- Range of declination so that the target is visible at least one hour, equivalent to a target maximum altitude of at least 50° . This results in $(\text{dec} > -2.77) \ \& \ (\text{dec} < 77.23)$
- The Local Volume is defined as the universe within a radius of $D \leq 11$ Mpc from the Milky Way. Data compiled by Klypin et al. (2015, MNRAS, 454, 1789).
- Limiting absolute blue magnitude $M_B \leq -16$
- Measured galaxy major axis smaller than $30'$ to exclude the very large galaxies (M31, M33, and M101) that will be done with LUCA@Schmidt. Thus: $(a_{26} > 0) \ \& \ (a_{26} < 30)$.

² <http://www.sao.ru/lv/lvgdb/>

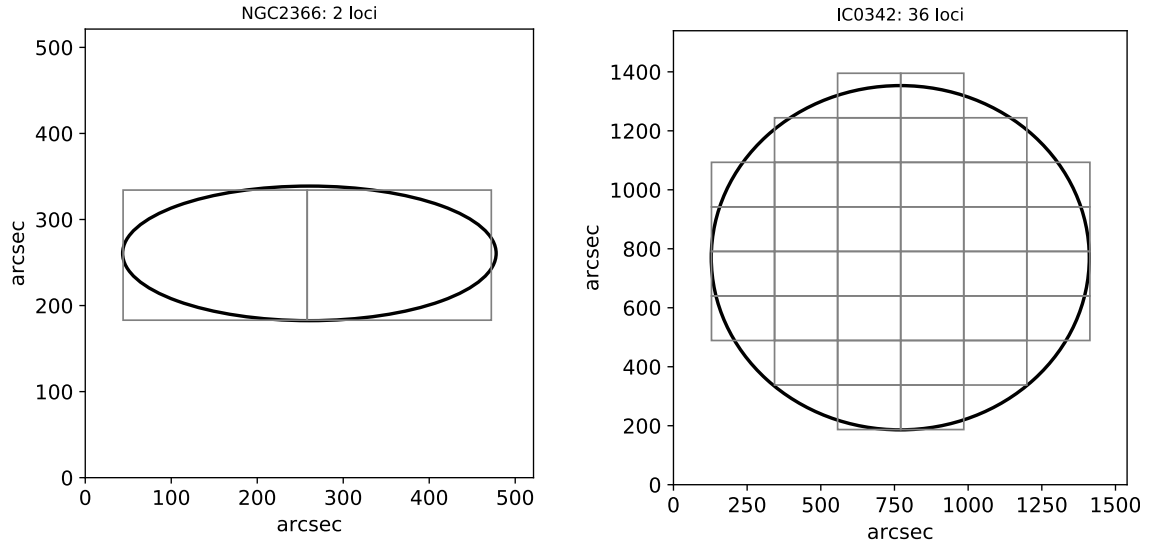


Figure. Examples of low and high number of pointings needed to completely map a galaxy with the 8 spectrographs system. Each box represents the IFU FoV of 9.1 arcmin^2 . The ellipse represents the galaxy by its semimajor axis and axis ratio.

The figure below shows the number of loci⁽³⁾ required to cover each galaxy, with the full 8 spectrographs system of FoV 9.1 arcmin^2 . The spread along the vertical axis for a given a_{26} is produced by the inclination of the galaxy; for the same major axis, edge-on galaxies require less pointings than face-on galaxies. This is illustrated with the dotted lines, that represent the limiting cases.

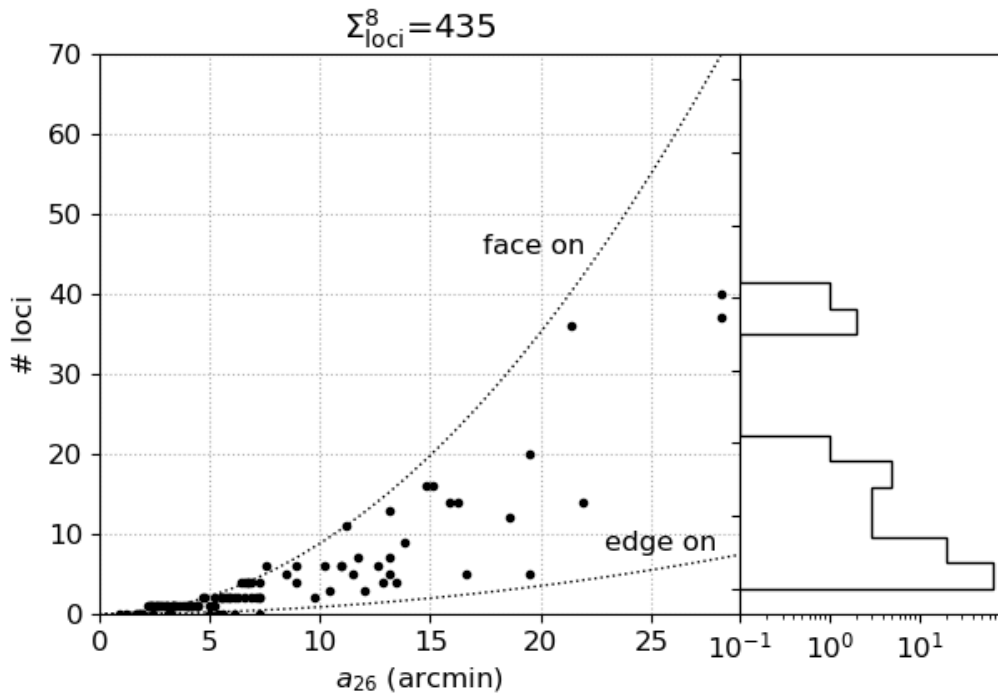


Figure. Number of loci per galaxy in the LV sample, for a total of 435 for the 102 galaxies.

³ We use the term locus/loci as meaning pointing/pointings.

The VCC sample is drawn from many works, originally by Binggeli et al (1985, AJ,90, 1681), and more recently the Next Generation Virgo Cluster Survey (NGVS) (Ferrarese et al 2012 ApJS, 200, 4, and series of papers). We have obtained the data tables from Simbad.

Selection criteria:

- Range of declination so that the target is visible at least one hour, equivalent to a target maximum altitude of at least 50° . This results in $(\text{dec} > -2.77) \ \& \ (\text{dec} < 77.23)$
- Limiting absolute blue magnitude $M_g \leq -17$.

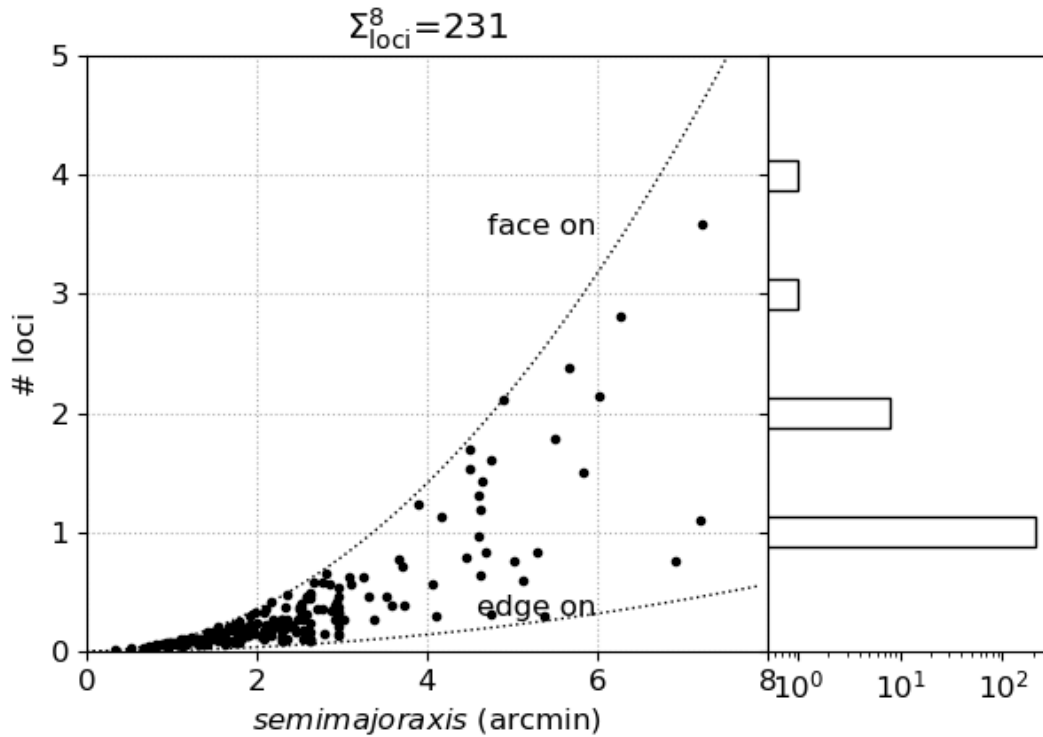


Figure. Number of pointings per galaxy in the VCC sample, for a total of 231 loci required for the 218 galaxies. Notice that the points with fractional values of loci are in fact upgraded to their ceiling value, as shown in the histogram on the right.



We have found a linear relation between the total area of loci needed to cover a galaxy and the area of the galaxy, such that

$$\#loci * arealFU = 0.255 * area_gx$$

From this relation, the number of loci is given by

$$\#loci = 0.255 * area_gx / arealFU$$

This relationship is independent of the number of spectrographs used, as illustrated in the figure for the whole IFU of 8 spectrographs and for the same system when only the first spectrograph has been commissioned and is used.

Notice that although this relationship can give a fractional number of loci, meaning that the galaxy is smaller than the IFU FoV, in practice values less than 1 are upgraded to 1, and in general fractional loci are upgraded to their ceiling value.

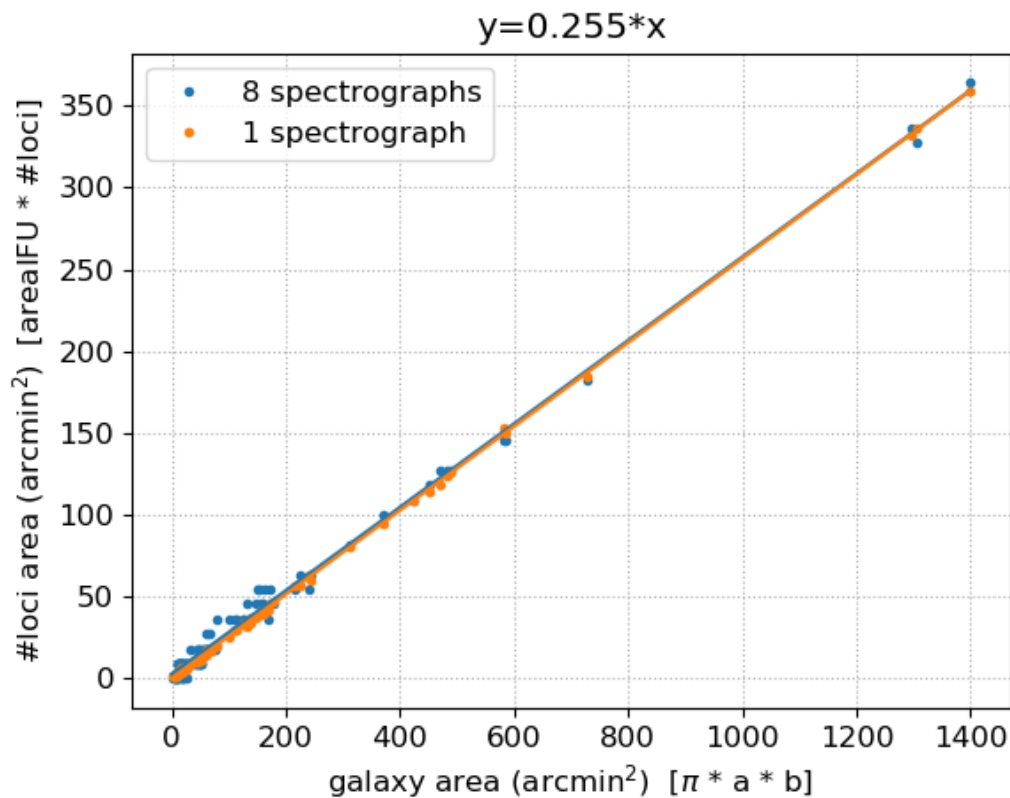


Figure. Linear relationship between the area of the galaxy and the area of loci needed to cover the galaxy.

The table shows, for the two samples, the number of galaxies, the total number of loci needed to observe them with the complete 8 spectrograph system (FoV 9.1 arcmin²), and (the right two columns) the number of galaxies that can be observed with just one pointing (one loci, FoV 1.1



arcmin²) either with the full 8 spectrograph system or with only the first spectrograph. Thus, we can see that if the first spectrograph is commissioned first, about half of the Virgo sample can be efficiently observed with just one pointing per galaxy, while only three galaxies of the LV sample could be observed with just one pointing and one spectrograph.

sample	constraint	# gxs	# loci	8 specs, 9.1 [□]	1 spec, 1.1 [□]
Local Volume	$MB \leq -16$	102	435	53	3
Virgo Cluster	$Mg \leq -17$	218	231	208	114

Table summary of the total number of galaxies and pointings for the two samples, and the number of galaxies that can be observed with just one pointing, with 8 and with 1 spectrographs.

The total number of observing hours is computed as

$$\text{hours} = \sum(\text{loci}) \times \text{hours_per_loci} \times \text{overhead}$$

Assuming 2 hours total integration per pointing, and 20% overhead, we arrive at

LV : 1044 hours

VCC : 555 hours

If we assume that, year round average, a night has 5 useful hours integrating on target, this translates into:

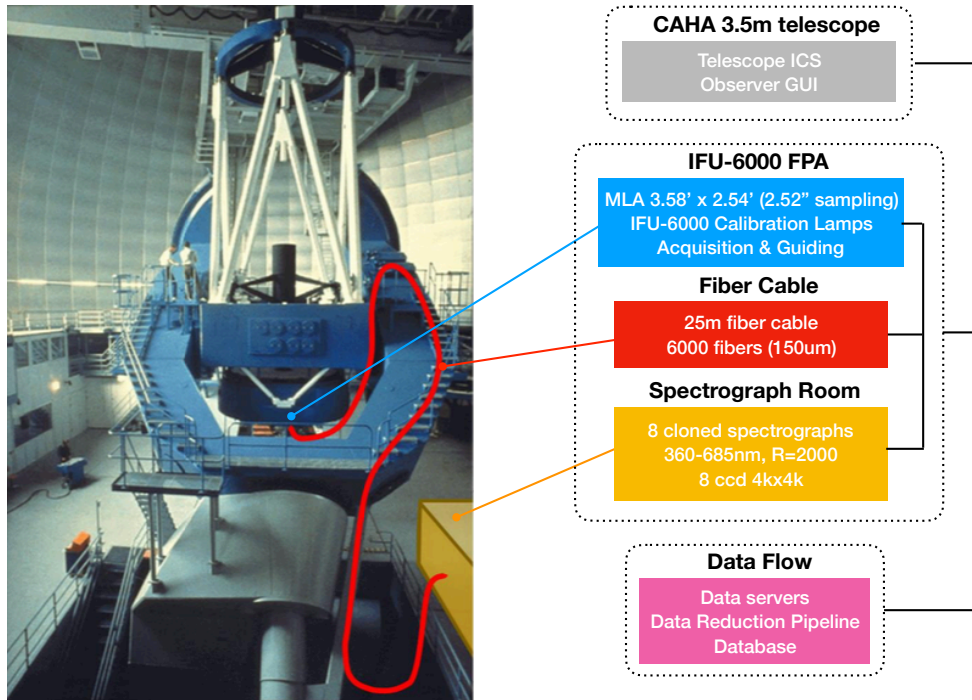
LV : 209 nights

VCC : 111 nights

Where the useful nights for LUCA include gray and dark, spectroscopic conditions and seeing below 1.5 arcsec

5. IFU-6000 Instrument Proposal

The chart below shows a schematic view of the IFU-6000 instrument at the CAHA 3.5m telescope.



System view of the IFU-6000 instrument at the CAHA 3.5m telescope

The main IFU-6000 instrument parameters are listed in this table:

IFU-6000 Parameter	As-designed
Telescope f/ratio	f/10
IFU injection	Microlens Array (MLA) – Hexagonal
On-sky FoV diameter per aperture (arcsec)	2.52
Output f/ratio MLA	f/3.51
Total number of fibers for the IFU	6000
FoV for the IFU in arcmin ² ($\sqrt{2}$ aspect size)	9.1 (3.58' x 2.54')
IFU fill factor	>95%
Fiber cable length (meters)	30
Number of fibers per spectrograph	750
Number of spectrographs	8
Wavelength coverage in single arm (nm)	360-685
Resolution at 500nm	2000
Resolution range (over band-pass)	1440-2740
Projected slit width (μ m)	150
Slit length (mm)	162.6
Detector format (number of pixels)	4k x 4k
Detector pixel size (μ m)	15
Number of detectors	8
Fiber core average on CCD (pixels)	3.73
Spectrograph f/ratio collimator	f/3.43
Spectrograph f/ratio camera	f/1.28
As-designed PSF (maximum <i>r.m.s.</i>)	12.6



We describe each of the instrument systems, including the CAHA 3.5m telescope, as follows.

A. CAHA 3.5m telescope

The CAHA 3.5-meter equatorial telescope is located at 2168 m above the sea level in Sierra de los Filabres, Almería, Spain. It is the largest telescope on the continental Europe. The Observatory has excellent facilities, being operated by the Centro Astronómico Hispano Alemán A.I.E., a partnership between the Spanish National Research Council (CSIC) and the Junta de Andalucía regional government (JA).

Calar Alto is a good astronomical site. Its main properties are similar in many aspects to those of other major observatories. The median seeing is ~0.90" and zenith-corrected values of the moonless night-sky surface brightness are 22.39, 22.86, 22.01, 21.36, and 19.25 mag arcsec⁻² in U, B, V, R and I, which indicates that Calar Alto is a particularly dark site for optical observations up to the I band. The fraction of astronomical useful nights at the observatory is ~70%, with ~30% of photometric nights. See Sánchez et al. for all site characterization details (PASP, 119, 1186, 2007).

The table below displays the main optical parameters of the CAHA 3.5m telescope. Our large IFU will be placed at the focal plane of the RC-system focus.

corrector		prime-system		RC-system	IR-system
		2 lens	3 lens		
aperture	mm	3 500			
focal length	mm	12 195	13 761	35 000	157 500
central obscuration	mm ø	820		1367	281.66
eff. coll. area	m ²	9.093		8.153	8.969*
f/ratio		1/3.48	1/3.93	1/10.0	1/45
FOV	mm	100	243	300	109
	arcmin	28.19	60.71	29.47	2.38
scale	"/mm	16.9	15.0	5.89	1.31
radius of field curvature	mm	infinite		-3786	
hourangle range	h	-7 to +7			

Table. Main optical parameters of the CAHA 3.5m telescope.

Our Team has been in close contact with the CAHA staff to follow up their upgrades and feedback regarding the telescope control system (ICS) and had several visits and meetings to evaluate the assessment of the LUCA needs and specifications for the Focal Plane Assembly, specifications and logistics for the focal cable and spectrograph room. We also got access to the *Zemax* optical model of the CAHA 3.5m telescope, which was necessary to perform the optical design of the spectrograph.

B. IFU-6000 Focal Plane Assembly

The nominal Focal Plane of the RC focus of the 3.5 m telescope has a practicable circular FoV of 29.47' (300 mm) diameter. The large science IFU with a FoV of 3.58' x 2.54' will be placed on the optical axis at the center of the focal plane, and four Acquisition & Guiding (A&G) cameras, each with a FoV of 3'x3', will be located around at the East, North, West and South locations. See below a schematic view of the Focal Plane Assembly (FPA) as seeing from above.

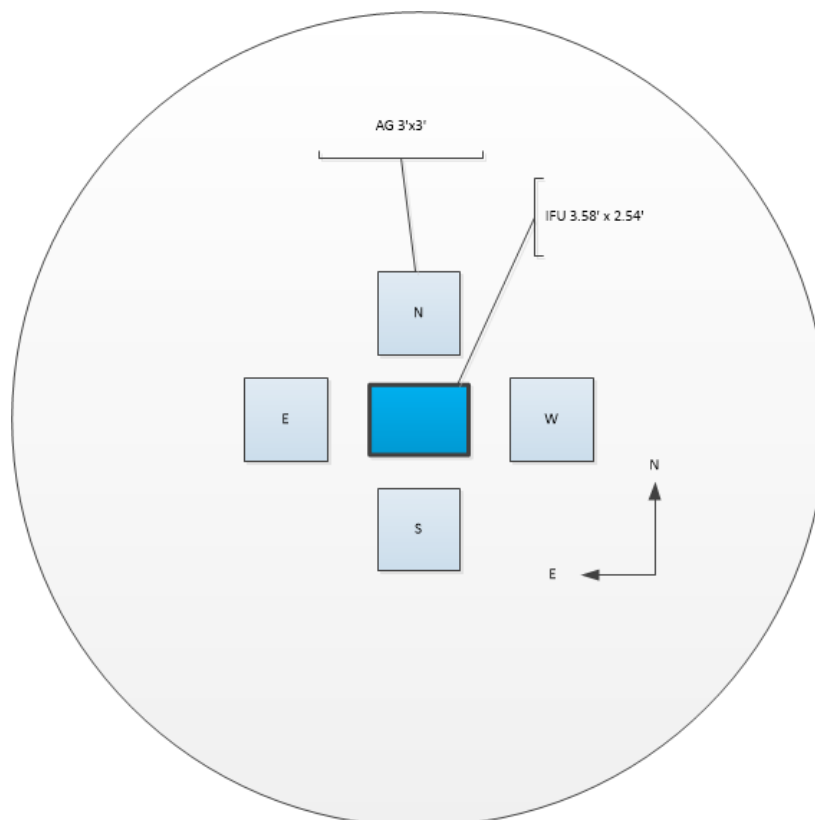


Figure. Frontal view of the IFU-6000 Focal Plane Assembly at the RC focus. The large science IFU is surrounded by 4 A&G cameras. The outer circle has a diameter of 300 mm, i.e. the entire FoV of the RC focus.

The IFU-6000 FPA will be attached to the 3.5 m A&G box. Inside the A&G box we will place the Calibration Unit, using the same space that currently uses the PMAS Calibration Unit. We will also allow switching from IFU-6000 to CARMENES by moving a mirror into the telescope beam. The PMAS Guiding System can be removed completely, which will allow having more space inside the A&G box. A technical assessment of the 3.5 m A&G box in this new context must be performed in the next phase of the project. So far we do not find any critical or risky aspects.

Acquisition & Guiding:

The hardware details of the A&G camera system can be found in Appendix E. We use the Gaia database through the *astroquery* interface to generate sky fields with stars. The FoV to search for available guiding stars at any of the 4 locations on the sky is 3'x3' (see figure above).

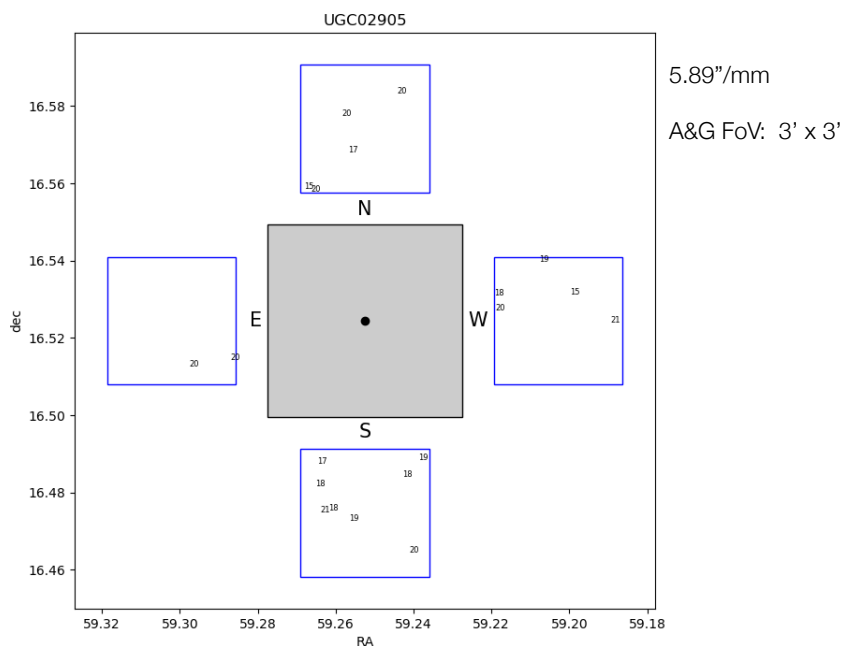


Figure. Schematic view of the 20 Gaia guide stars available for the example galaxy UGC02905. The central gray box represents the IFU and the four outer blue boxes the four autoguide cameras.

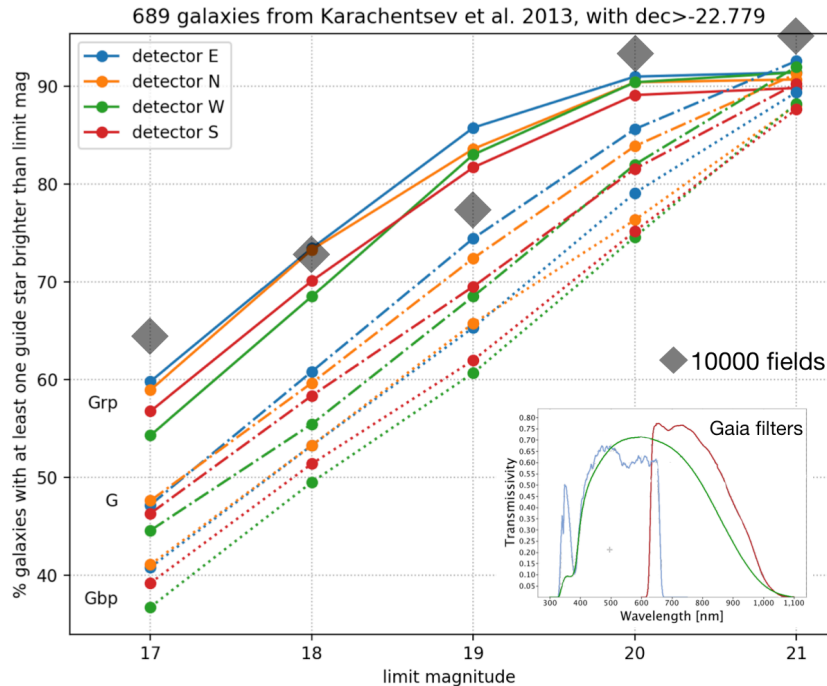


Figure. To study the availability of stars for guiding, we generate random locations on a sphere and select 10000 fields with declination above -22.78° (so that maximum airmass < 2). We then count the stars brighter than a given magnitude (Gaia 'phot_g_mean_mag'). The gray large squares in the figure show the percent number of these fields with at least one guide star brighter than a given magnitude. The lines show the actual number of stars for the 689 galaxies in the Karachentsev et al 2013 LV catalog. The four colors are for the four guide cameras, while the three different line types indicate the values in the three Gaia filters shown in the inset.

C. IFU-6000 Fiber System

The document in Appendix A addresses the practical aspects of constructing the fibre system for the proposed IFU-6000 instrument to be deployed on the 3.5 metre Calar Alto Equatorial Telescope following the LUCA baseline science requirements. IFU-6000 will furnish the telescope with a powerful short wavelength (360 nm – 680 nm) integral field spectroscopic facility, wherein an optical fibre integral field unit at the Cassegrain focus of the telescope will feed a suite of duplicate spectrographs within a dedicated environmentally controlled enclosure sited on the observatory dome floor, to the east of the equatorial plinth. The IFU will cover 9 square arcminutes of sky with 6000-spaxel, 2.5 arcsecond sampling. This study examines all relevant aspects of the fibre system, outlining baseline requirements and identifying the most technologically appropriate, low-risk solutions in each case. Recommendations are guided by many years of expertise and experience accumulated at Durham University CfAI working with fibre-based instrument projects (GMOS & IMACS IFUs, FMOS, PFS, and DESI, amongst others). The document also includes timeline and cost estimates.

The document in Appendix A includes the study of the following aspects:

- Fiber selection: transmission, fiber numerical aperture, focal ratio degradation, fiber core size, fiber clad size, fiber buffer material and size, batch variation
- Fiber cable design: functional requirements, planetary stranding
- Cable production: furcation tube, installing the fibers into the furcation tube, the tensile element, the stranding production line, conduits, strain relief boxes
- Constraints and specific considerations for the cable scheme
- Cable terminations: IFU input (chosen field format and IFU input hardware and optics) and IFU output – slit assemblies
- Test strategy
- Timeline and Cost estimates

As a reference we show below a plot Plot of percentage transmission calculated for 30 meter sections of FBPI versus FIP Polymicro fibre from Molex. The desired bandwidth of 360 nm to 680 nm is bounded by the green lines. With the exception of a small absorption feature centred around 592 nm, the FIP fibre shows a consistently higher transmission than the FBPI product, with the greatest gains evident towards the UV end of the plots (more details in Appendix A).

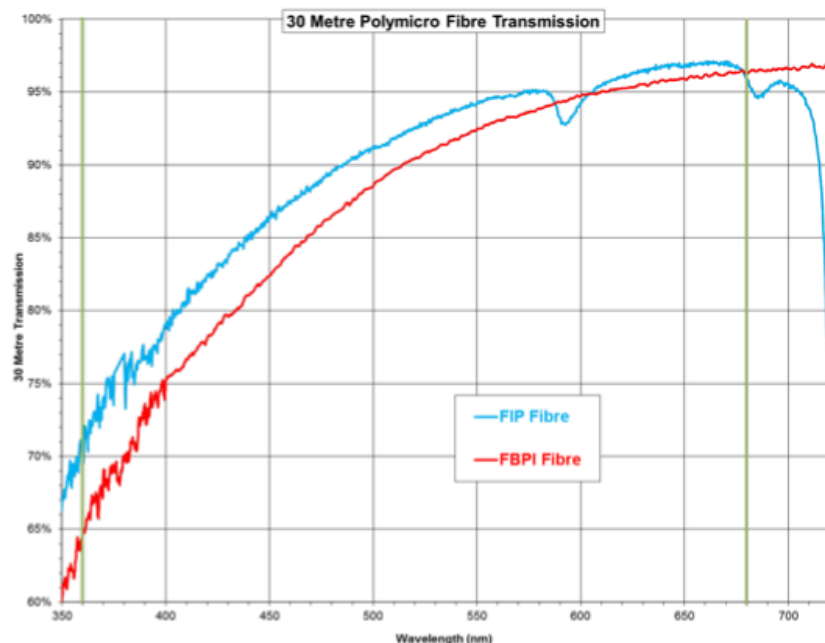


Figure. Percent transmission for 30 meter sections of FBPI versus FIP Polymicro fibre from Molex. The desired bandwidth of 360 nm to 680 nm is bounded by the green lines.

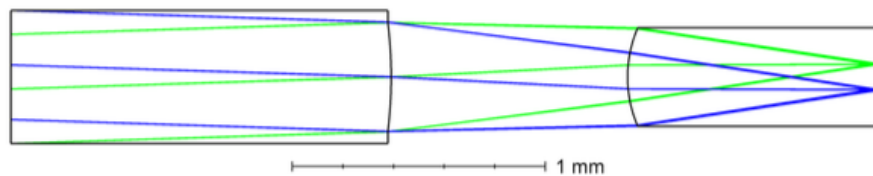
IFU with microlenses vs. bare fibres:

An IFU can be built using only the bare fibers or having a microlens system in front of the fibers. If microlenses are used, they can typically have one or 2 lenses along the optical axis, and they can reimaging the pupil or the field on the fiber core at the input and on the slit. If the pupil is imaged on the slit, then the field is imaged on the stop of the spectrograph and reversely. While the image on

the slit directly affects the image on the detector, the image on the spectrograph stop affects the PSF on the detector. Each solution has its specific advantages and disadvantages that must be studied to determine the best option. So far we have adopted as our nominal spectrograph design that with an IFU microlens array (MLA), i.e. the AAO-Macquarie “MLA-design” (see Appendix C for details, and Section C.5 below).

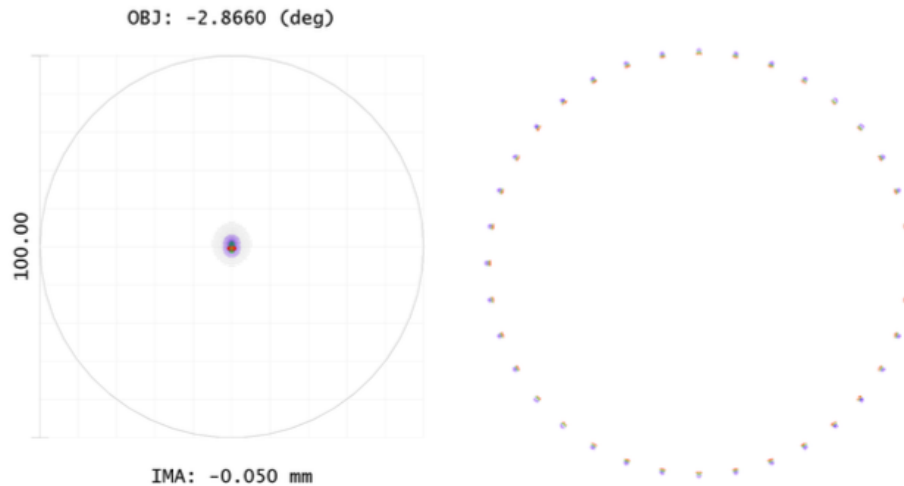
Microlenses at the input help to have a very high Fill Factor: 91% with touching circular microlenses and theoretically almost 100% with hexagonal microlenses. With the relatively slow F/10 speed of the CAHA 3.5m secondary that will be used, it is also possible to avoid fore-optics. Manufacturing is simpler than bare fibres for an IFU with 6000 fibres. It may however cause incomplete scrambling problems that bare fibres do not have depending on the exact design.

Figure below shows a design of input microlenses. It uses 2 microlens arrays. The focal plane of the telescope is on the first microlens array, which is on the second surface. Compared to single array systems, it avoids a type of FRD called geometric FRD. Without fore-optics, it also permits to correct the small non-telecentricity of the telescope. There are however additional tolerances from the additional array. The system images the pupil of the telescope, so an image of the primary, on the fibre core. It is also possible to image instead the focal plane of the telescope, so the first microlens, on the fibre core.



Input microlens system

The image quality at the edge of the fibre core is shown in the figure below (left panel). This is the only place where the image quality matters. A bad image quality in the center for example would have no consequences since all the light would go through while the PSF at the edge creates losses of light by vignetting. Oversizing the fibres to avoid losses of light seems an evident solution at first sight but it increases the Etendue product so the spectrographs must be bigger and more expensive.



Left: PSF on the fibre core edge of the input microlens system; the circle has the diameter of the fibre core.

Right: Aberration FRD of the output beam of the input microlens system.

The right panel of the figure above shows the degradation of the beam entering the fibre. That degradation is an average FRD. Both the image qualities on the fibre core and of the beam edge are excellent.

The most critical problem of the IFU-6000 is that the seeing is much smaller than the IFU sampling. A typical seeing at Calar Alto is 0.9" (median) while the sampling of our IFU is 2.52". In principle, the width of the PSF on the IFU should be at least twice the width of the spatial sampling to respect the Nyquist sampling criterion, so 6.5" for IFU-6000. This would however significantly reduce the resolution and is not that easy to achieve. For example, a defocus of the telescope does not give a Gaussian PSF. It reduces the problem but does not solve it. While the Nyquist sampling criterion is for the ability to precisely reconstruct the intermediate intensities between fibres or microlenses assuming perfect measurements by the spectrograph, it is also valid for the different kinds of measurement errors introduced by the fibre system with or without microlenses. Understanding the consequences on the measurements of all the options is important to determine the best option and calculate its specifications. This study will be performed during the next phase of the project.

Fiber cross-talk along the slit:

A single IFU pointing generates a spectral-spatial 2D image in the detector, with fibers arranged along the spatial direction. A slice of this image along the spatial direction is shown on the top plot of the enclosed image, with a zoomed in shown in the insert, where the single fiber PSF can be seen. A PSF model (e.g., a Gaussian) is fitted to each fiber PSF as shown in the bottom-left figure (in orange in the figure below), and the cross-talk is defined as the fraction of the PSF that falls below neighboring fibers (darker orange wings).

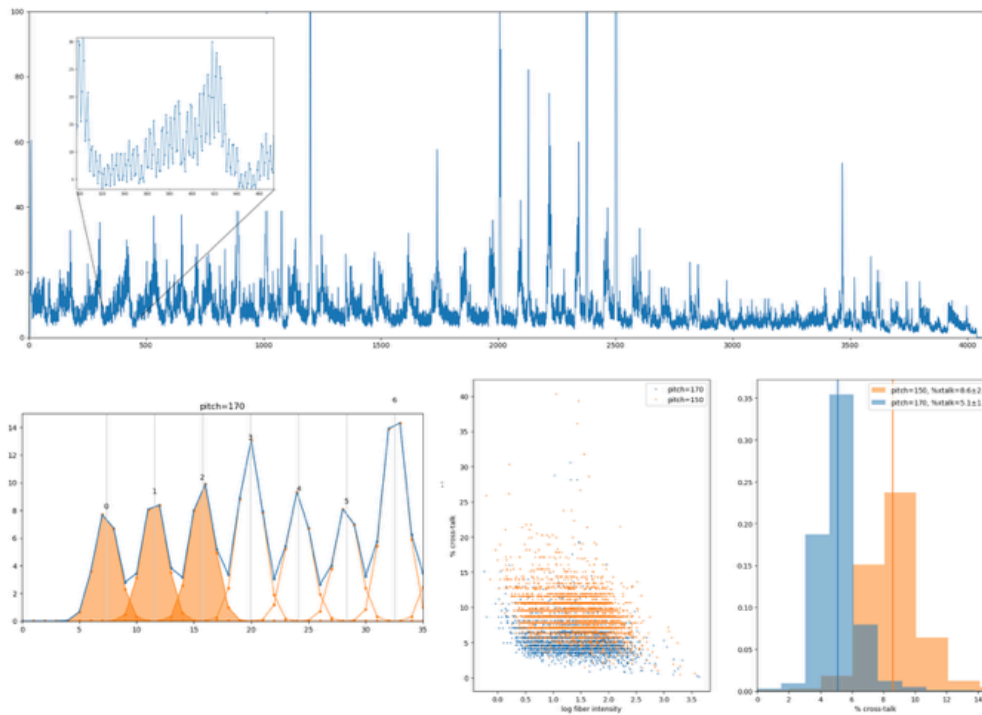
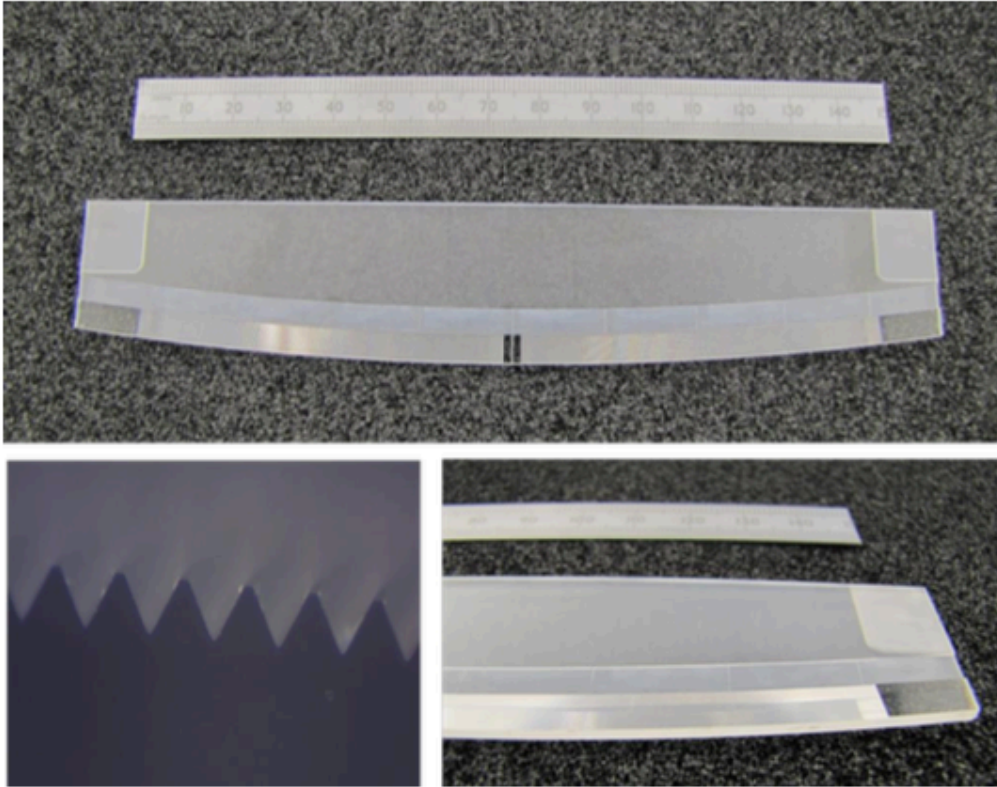


Figure. Section along the spatial dimension in the CCD and inset with zoom in where each individual fiber profile can be seen. Bottom left shows the profile fits to extract the flux in each fiber, and the corresponding cross-talk computed and plotted in the bottom right.

The two bottom-right figures give the values of cross-talk extracted for two different values of the fiber pitch along the slit (the peak-to-peak separation of fibers along the slit) with values of 150 and 170 micron. We set-up a requirement of a 2% contamination as it was adopted in the AAO spectrograph design, see Appendix B.

D. Spectrograph Slit Assembly

Slit Units have been made in Durham for many instruments – fibre arrays with large fibre counts, from simple parallel schemes to complex, curved / non-telecentric / off-axis geometries. Details are shown Appendix A.



The monolithic v-groove array prototyped to the PFS design is shown. Cut from a single piece of borosilicate glass, this v-groove array exhibits extremely high tolerances, high thermal stability, low profile (< 3 mm height).

The slit unit often is built from individual blocks of 50-100 fibers. We propose for the IFU-6000 spectrographs a monolithic V-groove slit design – a prototype concept done at Durham University based on Subaru PFS slit geometry; see Appendix A for details, and figure above with pictures of the prototype. This is a unique innovation that will improve significantly the quality and stability of the PSF, and hence this solution will improve the spectrograph performance as compared to the classical pseudo-slits.

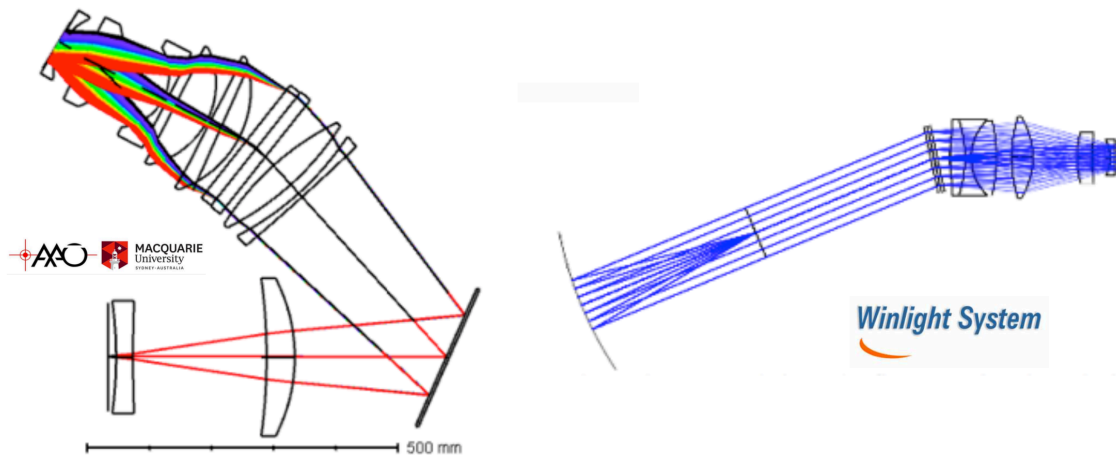
E. IFU-6000 Spectrograph System

To meet the science requirements of LUCA we require building a new IFU fiber-fed spectrograph (IFU-6000) at the CAHA 3.5m telescope that will allow observing in the optical spectral range 360-700nm with resolution 2000. The IFU will have a unique large FoV of 9 arcmin² with 6000 fibers and a spatial sampling of 2.5" on the sky.

Our collaborators at AAO-Macquarie and Winlight System have performed a design study for the IFU-6000 spectrograph (see Appendixes B and C). Note that only the AAO-Macquarie

spectrograph design has also included the necessary pre-optics system. Our LUCA Team has been in close contact and had the necessary interaction and feedback with both groups during the development of the feasibility study. We also had a face-to-face meeting at Winlight Systems in Marseille at the start of the work, and had the visit of Jon Lawrence, Head of Technology of AAO-Macquarie, at the IAA on Feb. 18-19, 2019.

AAO-Macquarie have developed designs for a baseline version that uses bare fiber injection and a version that uses microlens arrays (MLA). They also have done a compact design (smaller optics that accommodates 25% smaller number of fibers per spectrograph) with lower spectrograph unit cost, but that increases considerably the number of spectrographs, i.e. 13 units vs. 8 units for the baseline version. See Appendix B for all details, including performance. Here, we have considered the ‘MLA design’, see figure below, as our preferred option as compared to that with bare fibers since guarantees a nearly perfect homogeneity in S/N over the entire FoV (hard to get with bare fiber IFU which only have a 54% filling factor as compare to >95% obtained with an hexagonal MLA). In addition the ‘MLA design’ doesn’t need any additional pre-optics. This saves cost and complexity. The design with a bare-fibre IFU needs a pre-optics, which is a doublet and 2 singlet lenses as an optical relay converting the f/10 beam from the telescope focus to give f/3.5 at the intermediate focus where the fibre IFU is located. Three of the surfaces are aspheric (see Appendix B for details, and also the discussion above of MLA vs. bare fibers).



Designs of the IFU-6000 spectrograph. Left: optical layout for the AAO-Macquarie “MLA design”. This design shows a mirror in the collimator but this would be removed to follow a straight-through layout or be replaced by a dichroic in case a red-arm camera wants to be developed as future upgrade. The slit is flat. Right: Winlight System optical layout of their “DESI 1-arm” design proposal. In this case the collimator is a spherical mirror and the slit is curved. Both designs use VPH as disperser element.

The Winlight System proposed design for the IFU-6000 spectrograph is an update of the DESI blue optical configuration (fiber n.a.=0.14, curved slit and spherical collimator mirror), the main difference being the addition of a lens (see figure above). The asphere is also moved from the field



lens to this new lens. The collimator is also slightly updated. See Appendix C for all details, including performance.

The opto-mechanical design for both AAO-Macquarie and Winlight System spectrographs are described in detail in Appendix B and C. Note that the AAO-Macquarie design does not require any moving parts. In the case of Winlight System their design requires two moving elements: the collimator Hartman doors and the shutter, which is placed at the collimated beam. In the case of the AAO-Macquarie the shutter is behind the spectrograph camera and attached to the CCD camera.

Below we collect a number of reasons that justify the preference of the AAO-Macquarie proposal over that from Winlight System, after taking in consideration science and technical requirements:

- 1) To get a spectral resolution of $R=2000$ @ 500 nm and a FoV of 9 arcmin^2 on the sky, the Winlight fibers would need to be 1.59" wide instead of 2.52". Then 15,050 fibers would be needed, and hence 19 Winlight spectrographs compared to 8 AAO-Macquarie spectrographs with a total of 6000 fibers (see Table below).
- 2) The slit of the Winlight spectrograph has its pupil behind it. This creates collision between the fibers at the back of the slit so more space may be needed. The AAO-Macquarie design has the pupil in front of the slit so there is more space behind the slit and no losses.
- 3) The Winlight slit is on-axis right in the path of the light reflected by the mirror. This has similar effect than a spider in a Schmidt camera. Apart from vignetting some light, probably 1 to a few percent, it generates diffraction spikes, which may also affect the PSF.
- 4) The light density in $\text{arcsec}^2/\text{pixel}$ is smaller on the Winlight spectrographs than on the AAO-Macquarie 's by a factor of 1.84. This means much more detector noise (read-out + dark current) on the Winlight spectra. The SNR degradation will be at its maximum at the blue end.
- 5) AAO-Macquarie slit is flat as compared to the curved Winlight slit. The latter won't allow having microlenses on it in case we do need them to optimize the spectrograph performance.
- 6) There is not much difference between the two designs in terms of average transmission of the optics.
- 7) The spectral bandwidth of AAO-Macquarie (360-685nm) vs. Winlight (365-730nm) offers an advantage thanks to its bluer minimum wavelength. The AAO-Macquarie 685nm red limit also guarantees to observe all main relevant spectral features. There is no a significant gain in terms of science performance going up to 730nm.
- 8) Despite the cost of a Winlight spectrograph is about 40% cheaper than one AAO-Macquarie unit, a total of 19 Winlight units are needed as compare to the 8 AAO-



Macquarie's, which will largely increase the total cost of the project by a factor of 2 only due to the spectrographs, ignoring the increase of cost by the needed of additional 11 CCDs!

	AAO	WinLight
Slit length (mm)	162.9	121.0
Usable slit length (mm)	162.9	115.0
Collimator NA	0.1456	0.1400
Input fibre NA	0.1423	0.1368
Spectral demagnification	0.371	0.496
Spatial demagnification	0.361	0.496
Camera F-ratio (spectral)	1.273	1.77
Camera F-ratio (spatial)	1.241	1.77
Minimum wavelength (nm)	360	365
Maximum wavelength (nm)	685	730
Bandwidth (nm)	325	365
Spectral length (mm)	60.69	59.88
Dcore image on detector (μm)	55.62	48.86
Fibre diameter (μm)	150	98.52
Fibre diameter (arcsec)	2.52	1.59
Number of fibres	6000	15049
Nfibres per spectrograph	750	806
Number of spectrographs	8	19

AAO-Macquarie vs. Winlight spectrograph parameters

See below a chart with the main features of the IFU-6000 spectrograph adopting the AAO-Macquarie "MLA desing" as our proffered option.

AAO-Macquarie 'MLA design'

360-685 nm R=2000 @ 500nm

Spatial sampling = 2.52" on sky
 fiber core projects on 3.73 CCD pixels

fibers < 750

Slit length = 162.6 mm

4k x 4k CCD with 15 μ/pixel

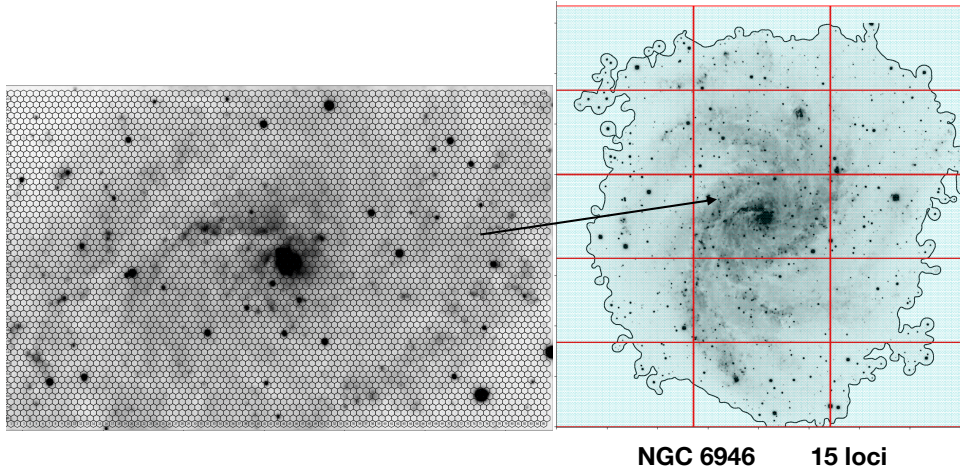
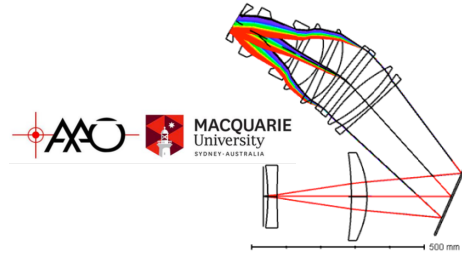


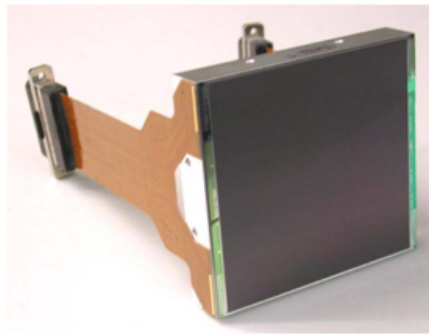
Figure. Global summary of the AAO-Macquarie spectrograph design, parameters, and view of an example galaxy.

The AAO-Macquarie design will be optimized and developed further in the next phase of the project to complete its Final Design Review.

E) Detector & Cryostat System

E.1) CCD detectors

We are considering the scientific e2v CCD Sensor 4096 x 4096 Pixels (CCD231-84 Back Illuminated). This CCD meets our science requirements; see below a table with a summary of its characteristics. The CCD for the first spectrograph will be provided by CAHA. We will need to purchase another 7 e2v CCDs for the remaining 7 spectrographs.



SUMMARY PERFORMANCE (Typical)

Number of pixels	4096(H) x 4112(V)
Pixel size	15 μm square
Image area	61.4 mm x 61.4 mm
Outputs	4
Package size	63.0 x 69.0 mm
Package format	silicon carbide with two flexi connectors
Focal plane height, above base	15.0 mm
Height tolerance	$\pm 10 \mu\text{m}$
Connectors	two 37-way micro-D
Fiatness	<20 μm (peak to valley)
Amplifier sensitivity	7 $\mu\text{V}/\text{e}^-$
Readout noise	5 e^- at 1 MHz 2 e^- at 50 kHz
Maximum pixel data rate	3 MHz
Charge storage (pixel full well)	350,000 e^-
Dark signal	3 $\text{e}^-/\text{pixel}/\text{hour}$ (at $-100 \text{ }^\circ\text{C}$)

F. Cryostats

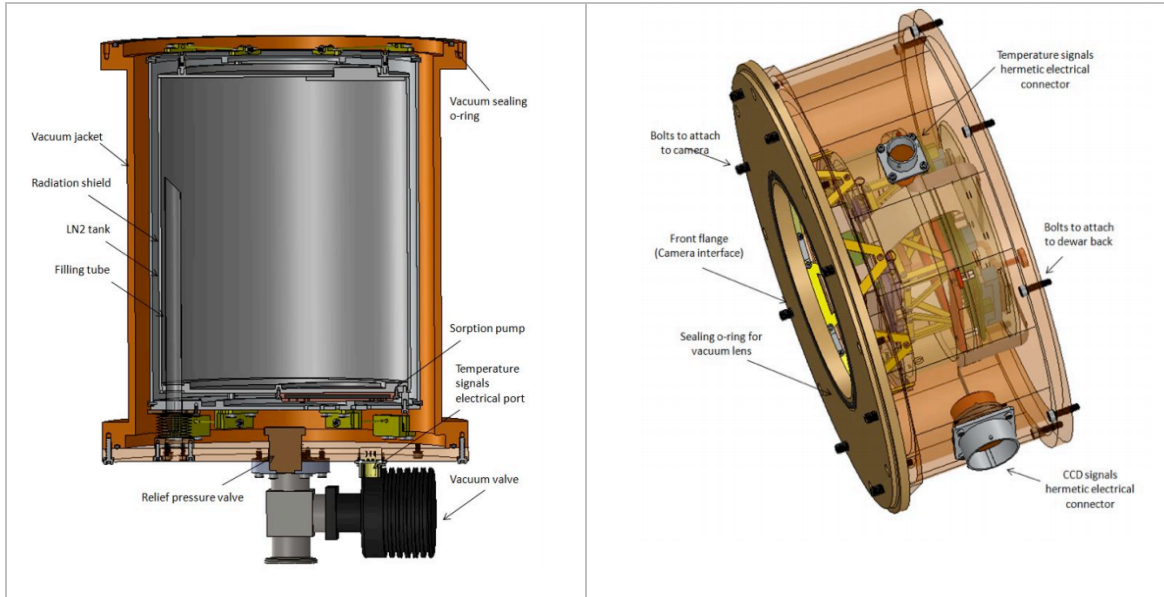
Regarding the cryogenic device to harbor the CCD cameras, so far, we have considered two options. One based on Liquid Nitrogen (LN₂) open-cycle cryostat and provided by INAOE in Mexico (TBC) in a similar design of the MEGARA instrument, and other that would be based on cryostats developed by CEA-Saclay in France, which uses a closed-cycle pulse tube cooler, as implemented in the DESI instrument. Additionally, for the option based on LN₂, the AAO spectrograph study also includes a cryostat solution similar to the proposed by the INAOE (see Appendix B).

LN₂ cryostat (MEGARA):

The LN₂ open-cycle cryostat would be a custom-made product, designed by the INAOE astronomical instrumentation group and based on design for the MEGARA cryostat. This cryostat would offer modular stages for the easy assembly and testing whilst also allowing future modifications to accommodate the required CCD, electronics and optics. This system offers to be the cheapest option for the LUCA Project if it will be provided by INAOE as an in-kind contribution.

The complete cryostat assembly would consist of two main parts: the dewar back and the CCD Head. The dewar back (or main body) serves as vacuum jacket and contains the liquid nitrogen tank; it also has on the rear part the liquid nitrogen fill tube, an electrical port for temperature

monitor and two vacuum ports. The CCD head is assembled on top of the main body and will contain the CCD detector and its associated electronics.

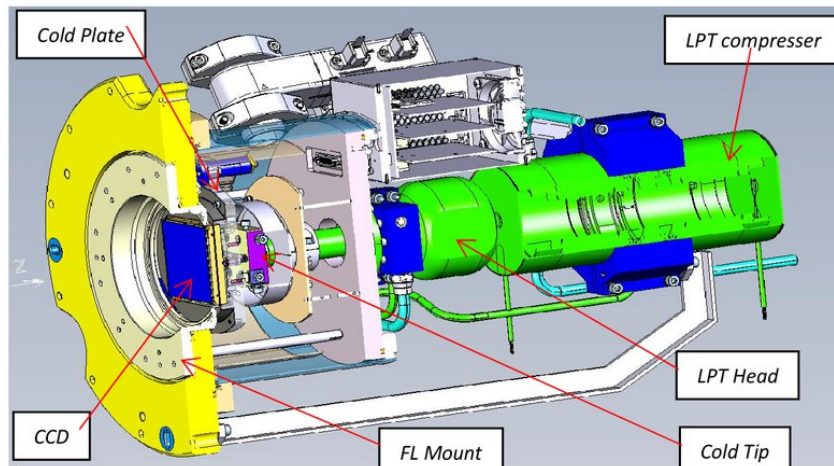


MEGARA Cryostat: dewar back view and CCD-head.

For more details see “MEGARA cryostat advanced design” by D. Ferrusca, Proc. SPIE 9147, (July 2014).

Cryocooler cryostat (DESI):

The DESI based cryocooler cryostat would be developed by the CEA Saclay (France), and would provide the mechanical connection to the spectrograph camera, support the thermal and vacuum conditions, and interface with the control system and the CCD electronics. The figure below shows a rendered cross section of this cryostat.



Model of the DESI cryostat and camera interface.

The cooling system would use a closed pulse tube cooler (Thales LPT9310 Cryocooler) cooling the CCDs to 163K with a precision of 1 K and regulate the temperature to ± 0.1 K.

For more details see “The DESI spectrograph system and production” by J. Edelstein, Proc. SPIE 10702 (July 2018).

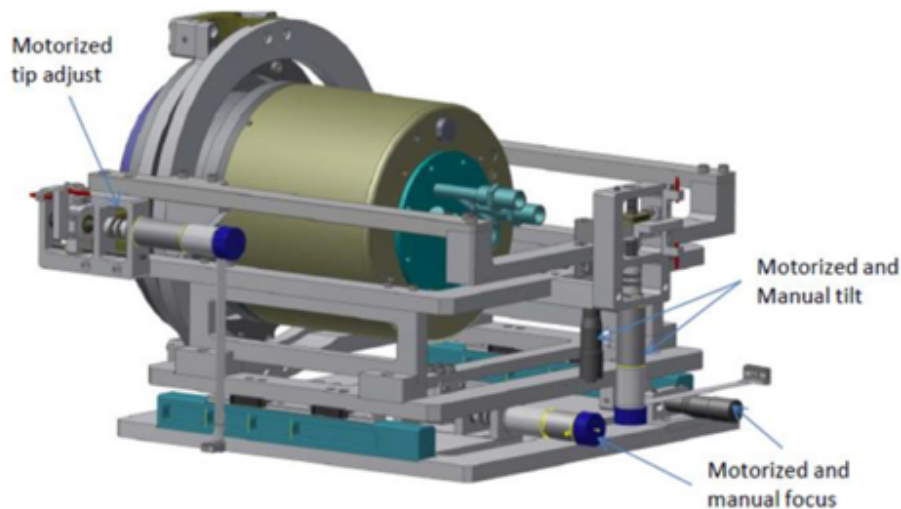


Figure. Detector mount cradle design.

The detector mount cradle design for the spectrograph with 5-axis adjustment will be based on the design for Hector at AAO, see above.

G. Electronics, Software Control and Data system

The feasibility study of the control system of the IFU-6000 instrument at the CAHA 3.5m instrument was led by the IAA-CSIC and can be found in Appendix D. In this document we present the scale and feasibility of the IFU-6000 Instrument Control System (ICS), including: electronics, number of motor/actuators/sensors, cabinet control and distribution, A&G cameras, power consumption, data rates, control software, observation software tools, GUIs, data handling, etc., and also assess the compliance of the ICS with the hardware and software recommendations applicable to the CAHA Observatory. It contains the technological baseline and will be the reference for further IFU-6000 activities during the preliminary and detailed design phases.

The document gives a general description of the IFU-6000 control electronics and software based on the AAO spectrograph design summarized above and described in Appendix B, consisting in eight 1-arm spectrographs. Standard features, such as e.g. data processing, cryogenic control,



telescope control, are not addressed in detail at this phase of the project. Some specifications from CAHA that are specifically driving the design were extracted from the various applicable documents and highlighted in that document.

The scale of the IFU-6000 instrument control system is unprecedented in the Calar Alto Observatory; as is the dimension of the IFU-6000 instrument project. The most challenging parts identified are the simultaneous readout of the 8 CCD detectors, because of their complexity and the number of devices involved for the 8 spectrographs.

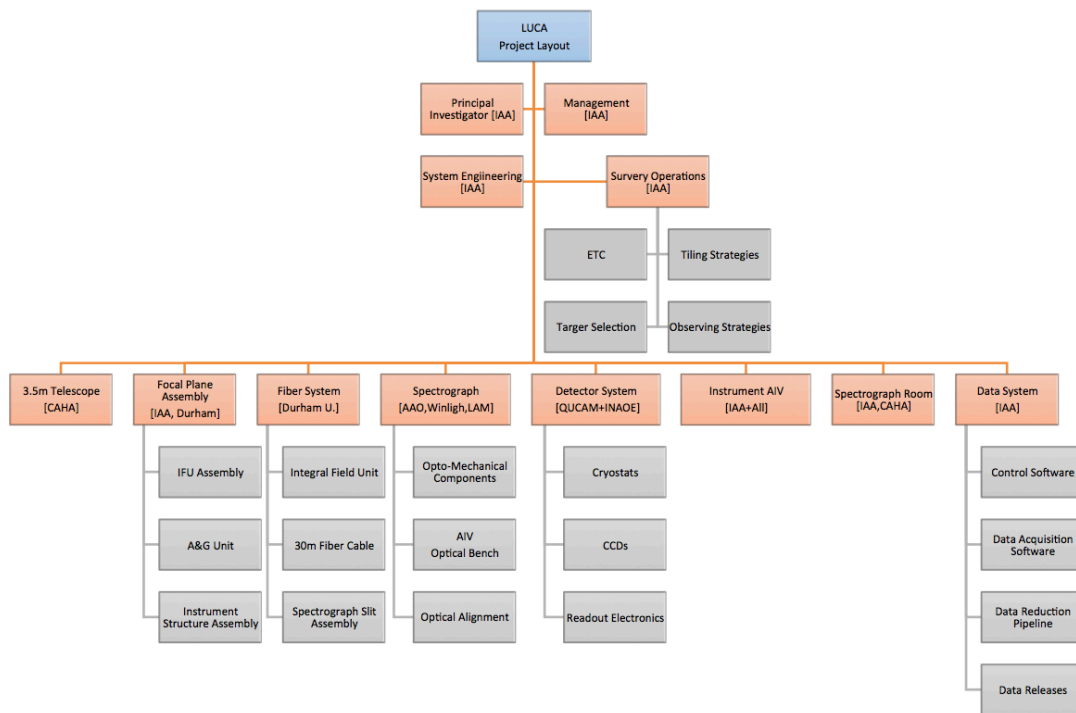
However, we can conclude at the moment of this study that no electronics or software feasibility issues were raised.

6. Project Layout: work packages

The chart flow below provides the work packages together with the institutions responsible for the instrument and science delivery towards the development, construction and science exploitation of the LUCA Project. This is pending of having a formal proposal and agreement which must be signed between the institution that will form the LUCA Consortium and CAHA.

The chart flow below provides the work-packages together with the institutions responsible for the instrument and science delivery towards the development, construction and science exploitation of the LUCA Project.

This is pending of having a formal proposal and agreement which must be signed between CAHA and the institutions that will form the LUCA Consortium.



LUCA Project layout

7. Project cost and timeline

We present here a summary of the project cost estimates. Figures are based on experience with previous projects. Actual quotations shall be requested during the Final Design Phase; therefore a 20% contingency should be factored into these baseline estimates for hardware. Details can be found in Appendices A, B, and D. See the table below.

Description	Cost (Kilo-euro)	Details
Fiber System (hardware and material)	800	Appendix A
8 Spectrographs (complete units)	5930	Appendix B
8 CCD science detectors	800	Appendix D
CCD read-out electronics (hardware)	90	Appendix D
Control electronics, A&G, sensors, connectors, Lab misc. (hardware)	95	Appendix D
8 CCD Cryostats	---	In-kind (TBC)
Computers	48	Appendix D
Spectrograph Room	25	TBC
Total	7788	



We have also estimated the human resources required over a 5-year period to complete the instrument design, construction, AIV, and commissioning, see below. A detailed estimation will be done during the Final Design Review Phase of the Project.

Description	FTE (5-year)	Details
Fiber Engineering	2.5	Durham University contract services (See Appendix A)
Detector Engineering	2.5	QUCAM contract services (See Appendix D)
Control Software Engineering	4.5	IAA-CSIC (See Appendix D)
Electronic Engineering	4.5	IAA-CSIC (See Appendix D)
Data Science Engineer	4.5	IAA-CSIC (See Appendix D)
Project Manager	5	IAA-CSIC
System Engineer	5	IAA-CSIC
Mechanical Engineer	5	IAA-CSIC
Total	33.5	

We have a tentative timeline for the construction of the different instrument systems. They can be found in Appendix A for the Fiber System, Appendix B for the spectrographs, and Appendix D for the Control and Software. However, at this stage of the project we cannot provide a detailed schedule at the Project level with a Gantt chart that describes all activities and milestones involved. This can only be done during the Final Design Review Phase of the Project that will take a complete year. We can certainly confirm that a total of 5-years will be needed for the completion of the Project. This estimate is based on the work done in this feasibility study and previous experience of our collaborators on similar instruments.

Milestone	Year 1	Year 2	Year 3	Year 4	Year 5
Final Design Review Phase					
1 st spectrograph construction					
+ 3 spectrograph units					
+ 4 spectrograph units					
'1/8 FoV' science operations					
'1/2 FoV' science operations					
'100% FoV' science operations					

LUCA timeline estimate

It is worth mentioning that the construction of the 1st spectrograph can be finalized in 17 months after the completion of the FDR. This is a realistic plan given the expertise of our team. Due to the modularity of the IFU-6000 instrument, this planning will allow us to have first light at the CAHA 3.5m telescope with 1/8 of the FoV, and thus to start the LUCA science operations in 2.5 years. As shown above, in the Survey Planning Section, there will be enough galaxies in our sample to be observed with a single spectrograph. Three additional spectrographs can be completed and delivered to Calar Alto by the end of the 4th year, which will allow observations with 50% of the FoV. The remaining 4 spectrographs will complete the entire FoV during the fifth and final year of the Project. The table above shows this tentative planning.

8. LUCA in the worldwide context

We compare LUCA with the most competitive existing and upcoming IFUs: MaNGA at the SDSS 2.5m telescope, CALIFA at the CAHA 3.5m telescope, SDSS-V Local Volume Mapper at the SDSS 2.5m telescope, WEAVE at the WHT 4.2m telescope, and MUSE at the VLT 8.2m telescope. We display in the figure below all these IFUs given their total number of pixels and total number of spectral resolution elements. The solid lines indicate IFUs with the same ratio of #spaxels and #spectral elements.

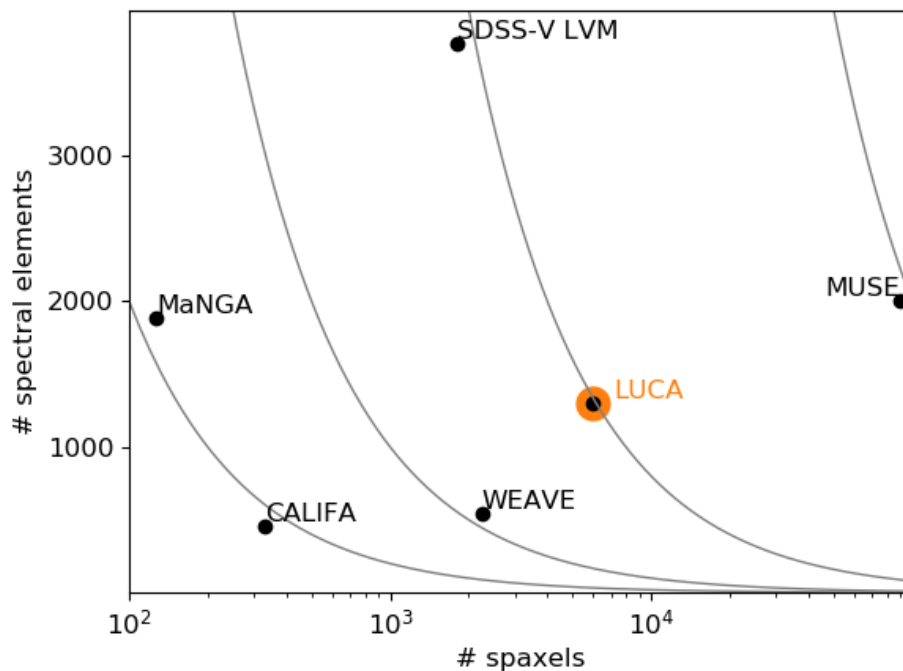


Figure. Number of spectral elements versus number of spatial elements for the worldwide current major IFU instruments/surveys. The full lines indicate different values of the constant ratio of the two parameters.

The competitiveness of an IFU to perform the proposed survey of the Local Volume galaxies relies on its capability of being efficient in mapping a given area of the sky that covers each galaxy down to some limiting surface magnitude (see Sec. 3). In this regard the IFU Etendue is the key parameter that drives the speed of the survey. In the figure below, we compare the *Etendue* and the ratio of #spaxels to #spectral elements of LUCA with the other IFUs. It can be clearly seen that LUCA has by far the largest *Etendue*, being a factor of almost one order of magnitude larger than the SDSS-V LVM. Interestingly, we have discovered that the existing and planned IFUs obey some “law” as shown by the solid curve. LUCA appears many sigmas away from the “law”, which demonstrates its outstanding unique and competitive niche for IFU surveys.

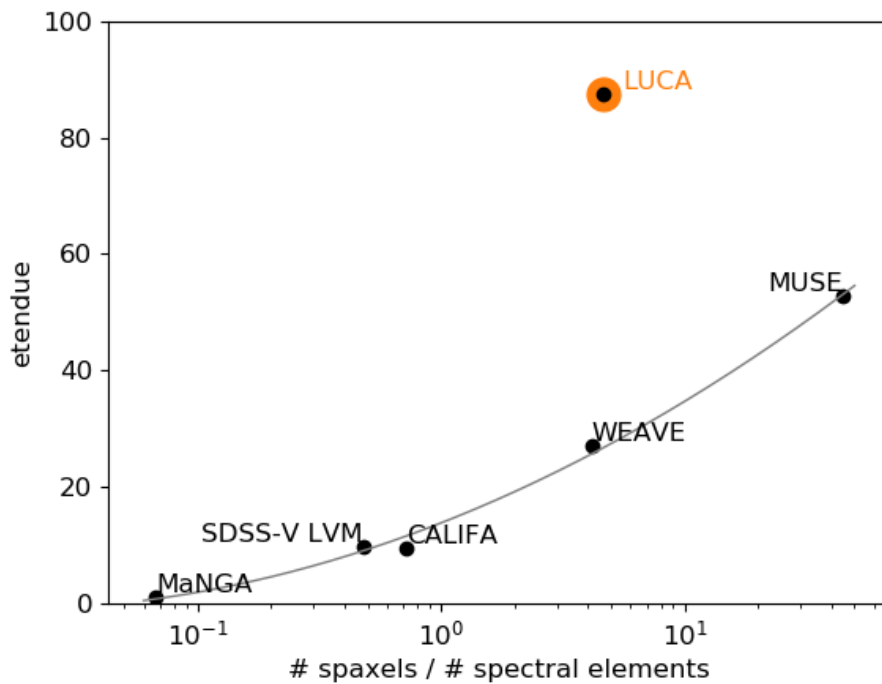
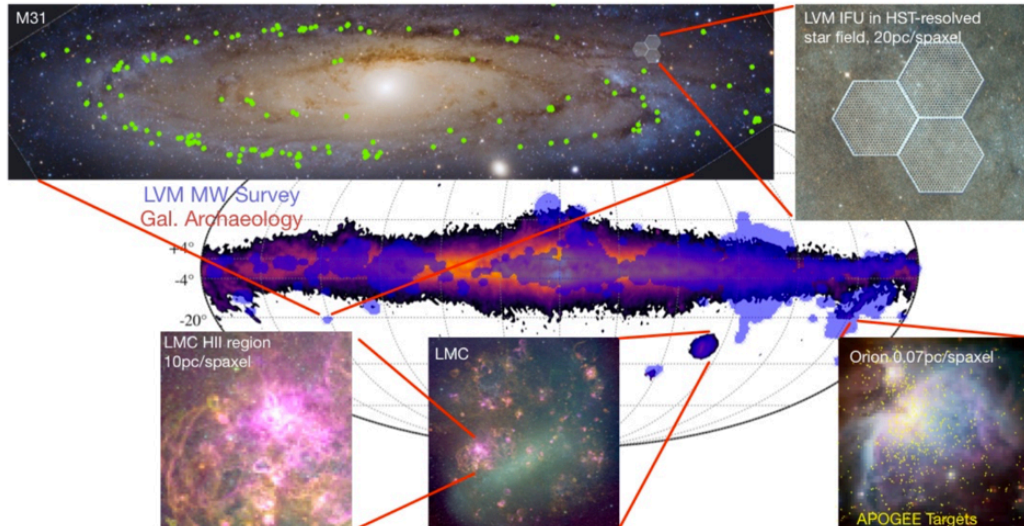


Figure. Etendue versus the ratio of spatial to spectral elements for the current major IFU instruments/surveys. LUCA stands out high above all other projects in etendue. Overall, the systems seem to lie along a curve given by a law. This is an interesting result that needs to be explored further. The full line is a second order poly fit.

The SDSS-V Local Volume Mapper is planned to start observations beyond 2020. The details can be found in arXiv:1711.03234. In the Chart below one can see a summary of the project, which intends to perform IFU mapping of the Milky Way, LMC, M31, M33, and other galaxies out to 5 Mpc. They plan to do sparse spatial sampling of these galaxies, and also statistical samples of HII regions at 20 pc resolution in M31 and ~50 pc in other galaxies. See below an overview chart of the SDSS-V LVM project.

The SDSS-V LVM footprint and sampling strategy is shown below.



SDSS-V LVM is complementary to LUCA since it does not intend to perform an entire IFU spatial mapping of all galaxies within our Local Volume. On the other hand, as seen above, the *Etendue* of LUCA is almost one order of magnitude larger than that of the SDSS-V LVM! Thus, LUCA will be a unique IFU spectroscopic facility that will offer CAHA and the IAA-CSIC, and the worldwide astronomical community an invaluable legacy, which will be fundamental in our understanding of galaxy formation and evolution, and will result key for follow-up detailed studies in the ELT era.

9. Conclusions and remarks

This document faces the Feasibility Study of a new fiber-fed IFU spectrograph (IFU-6000) at the CAHA 3.5m telescope. IFU-6000 has a huge *Etendue* and large number of spatial/spectral elements compared to other existing and upcoming worldwide IFUs. The new instrument facility will allow astronomers to complete the LUCA Local Volume and Virgo surveys, which aim to map our universe neighborhood in 3D with an unprecedented spatial resolution (better than 100 pc) to unveil the sub-grid physics of galaxy formation.

The work included in this report provides an overview of the LUCA science program, science specifications and requirements of the instrument, science survey strategy, a technical description of the instrument technical proposal (designs and performances, instrument system work packages), discuss the project competitiveness worldwide and also expected costs and timeline.

We have shown technical solutions and feasibility for all instrument systems. There are no high-risk items identified because this project will follow closely other very similar projects built by the LUCA Team using the same vendors for which there is a good track record. This is especially important



for the serial production of the cloned spectrographs. For the remaining project phases, the risk matrix will be further developed and updated with the participation of all team members and in consultation with the key stakeholders during the Final Design Review phase.

We will provide to CAHA by September 15th a new document with the additional information requested by the CAHA Director.

10. Acknowledgements

We thank the CAHA staff Gilles Bergond, Jens Helming, Luis Hernández, and Santiago Reinhart for their feedback on the CAHA 3.5m telescope specifications, interfaces and observatory infrastructures. We acknowledge María Balaguer, Head of UDIT at IAA-CSIC, for her comments and recommendations on Project Management, System Engineering and AIV. We also thank Rubén García Benito, Luca Izzo, and Enrique Pérez Montero at the IAA-CSIC for useful science discussions, and Johan Comparat at MPE in Garching for help with the exposure time estimations. We want to thank Rosa González Delgado for her involvement and work in the LUCA Proposal that was submitted to CAHA in the call for new instrumentation. We are grateful to Eric Prieto at LAM in Marseille for his feedback on the *Winlight* spectrograph design, and Simon Tulloch (QUCAM) for his advice and suggestions on the Detector System.



APPENDIX A



IFU-6000 Fiber System Feasibility Study

LUCA - Calar Alto 3.5 metre Telescope - IFU-6000 Fibre System Feasibility Study

Graham J. Murray

LUCA

Calar Alto 3.5 metre Telescope

IFU – 6000

Fibre System Feasibility Study

Durham University
Physics Department Centre for Advanced Instrumentation
South Road
Durham
DH1 3LE UK

Email: g.j.murray@durham.ac.uk
Tel: +44 191 334 3541

Revision Number	Document Authors	Signature	Date
1	Graham J. Murray		Sunday 12 th May 2019
2	Graham J. Murray		Thursday 26 th June 2019
3	Graham J. Murray		Friday 27 th June 2019

LUCA - Calar Alto 3.5 metre Telescope - IFU-6000 Fibre System Feasibility Study

Contents

1.	Introduction	3
2.	Baseline requirements	3
3.	Fibre selection	4
3.1.	Transmission	4
3.2.	Fibre numerical aperture	5
3.3.	Focal ratio degradation.....	5
3.4.	Fibre core size	7
3.5.	Fibre clad size.....	7
3.6.	Fibre buffer material, size.....	7
3.7.	Batch variation	7
4.	Fibre cable design	7
4.1.	Functional requirements.....	7
4.2.	Planetary Stranding.....	8
5.	Cable production.....	10
5.1.	Furcation tube.....	10
5.2.	Installing the fibres into the furcation tube.....	11
5.3.	The tensile element	12
5.4.	The stranding production line.....	12
5.5.	Conduits	13
5.6.	Strain relief boxes	13
6.	Constraints & specific considerations for the cable scheme	14
7.	Cable terminations.....	15
7.1.	IFU Input.....	16
7.1.1.	Chosen field format.....	16
7.1.2.	IFU input hardware and optics.....	17
7.2.	IFU output – slit assemblies	18
8.	Test strategy.....	20
9.	Timeline estimates	21
10.	Cost estimates.....	21
11.	References	22

LUCA - Calar Alto 3.5 metre Telescope - IFU-6000 Fibre System Feasibility Study

1. Introduction

This document addresses the practical aspects of constructing the fibre system for the proposed IFU-6000 instrument to be deployed on the 3.5 metre Calar Alto Equatorial Telescope. IFU-6000 will furnish the telescope with a powerful short wavelength (360 nm – 680 nm) integral field spectroscopic facility, wherein an optical fibre integral field unit at the Cassegrain focus of the telescope will feed a suite of duplicate spectrographs within a dedicated environmentally controlled enclosure sited on the observatory dome floor, to the east of the equatorial plinth. The IFU will cover 9 square arcminutes of sky with 6000-spaxel, 2.5 arcsecond sampling. This study will examine all relevant aspects of the fibre system, outlining baseline requirements and identifying the most technologically appropriate, low-risk solutions in each case. Recommendations are guided by many years of expertise and experience accumulated at Durham University CfAI working with fibre-based instrument projects (GMOS & IMACS IFUs, FMOS, PFS, and DESI, amongst others).

2. Baseline requirements

The fibre system samples light over a pre-defined, fixed 2-D field and delivers this light to the spectrographs. The fibre cabling scheme must thus provide an optically matched, optically efficient, optically stable, and mechanically robust interface between the telescope focal plane and the spectrograph entrance focal planes. The schematic in Figure 1 shows the system elements. On the left is the IFU input, consisting of a 2-D fibre array formed by arranging the fibres in a 2-D hole-matrix. The fibres transition through an intermediate input cable section, leading to a monolithic loop box and cable breakout; inside the loop box each fibre is configured in a single loop. This serves as a reservoir of spare fibre (in case of fibre breakage) and strain relief, decoupling residual fibre tension between the main cable and the IFU input. The main cable sections emerge from this loop box, one cable per spectrograph. Each cable is ruggedised, and designed such that bend-induced stresses and tensile stress will be minimised. The spectrograph ends of the cables transition through further (output) loop boxes and into spectrograph pseudo-slits via output cable sections.

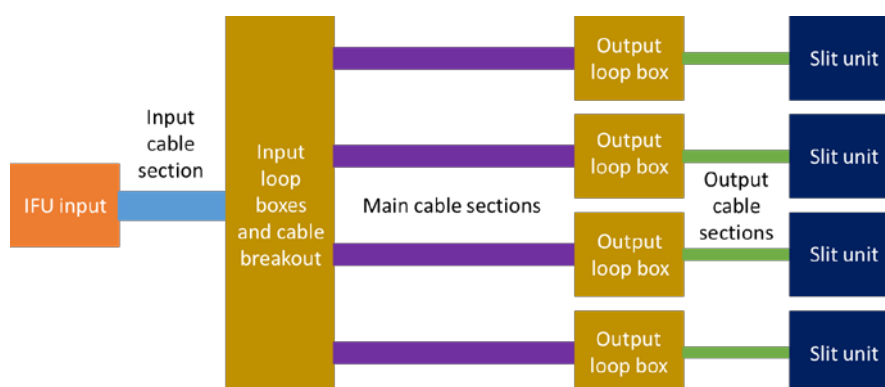


Figure 1. Schematic of cable system. To simplify, four slit channels only are shown.

Studies of the telescope structure and fibre cable routing paths have revealed that cable lengths of 25 metres will be adequate to connect the focal plane through to the anticipated location of the spectrographs. Keeping the cable lengths as short as is practical is important for minimising intrinsic absorption loss in the fibre, however some additional fibre is required for the loop boxes (≈ 1 metre each) and for routing around the telescope right ascension and declination axes. 5 metres of additional length seems reasonable, therefore a total end-to-end fibre length of 30 metres is proposed. The cable location is indicated by a red line in Figure 2.

LUCA - Calar Alto 3.5 metre Telescope - IFU-6000 Fibre System Feasibility Study

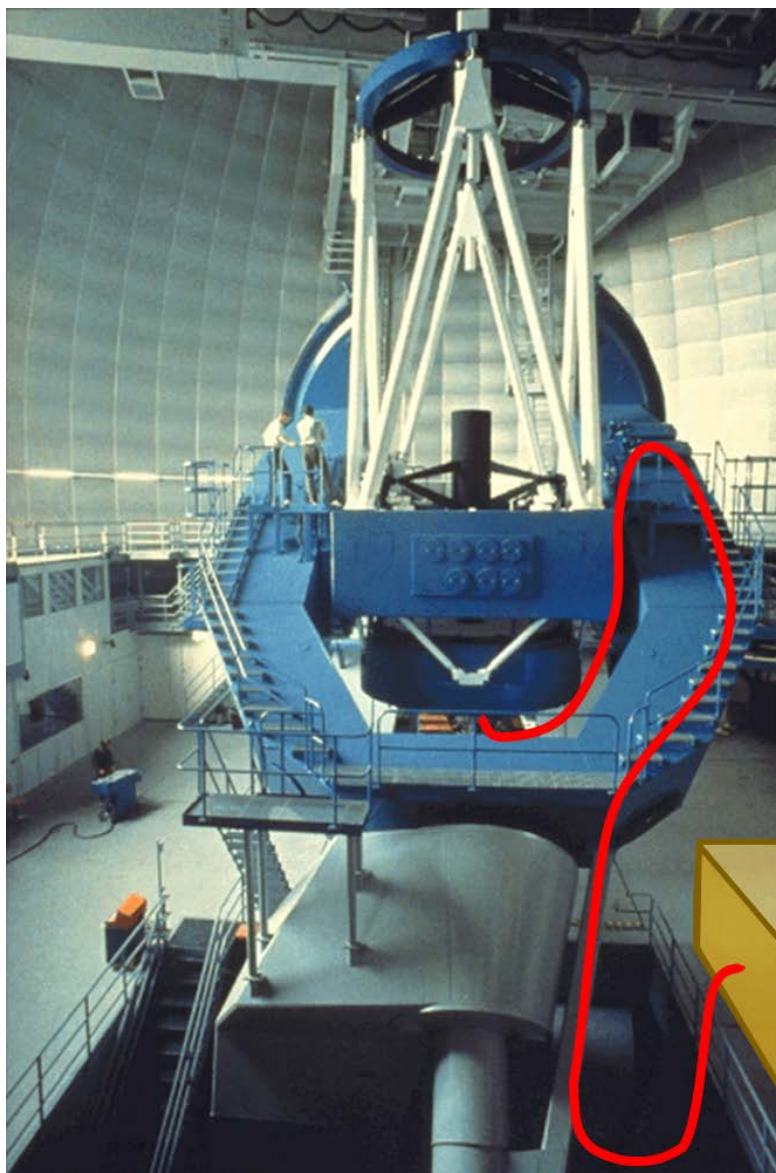


Figure 2. A photograph of the telescope, looking in a northerly direction. The approximate location of the cable route is indicated by the red line. A box sketched to the right of the right ascension axis shows where the spectrograph environmentally controlled enclosure will be sited.

3. Fibre selection

3.1. Transmission

The wavelength range required for the IFU-6000 application is comparatively narrow so does not present any significant challenges for the optical fibre selection. Regarding the choice of vendor, the least risk would be to use a known and tested product from a supplier with a good track record for providing optical fibre for astronomical applications. Polymicro - Molex Inc. fits these requirements. Over the wavelength range of 360 nm – 680 nm, the high-OH content FIP fibre wins out by a few percent over more traditional broadband fibres such as FBPI. See the comparative transmission plots for 30 m fibre sections in Figure 3.

LUCA - Calar Alto 3.5 metre Telescope - IFU-6000 Fibre System Feasibility Study

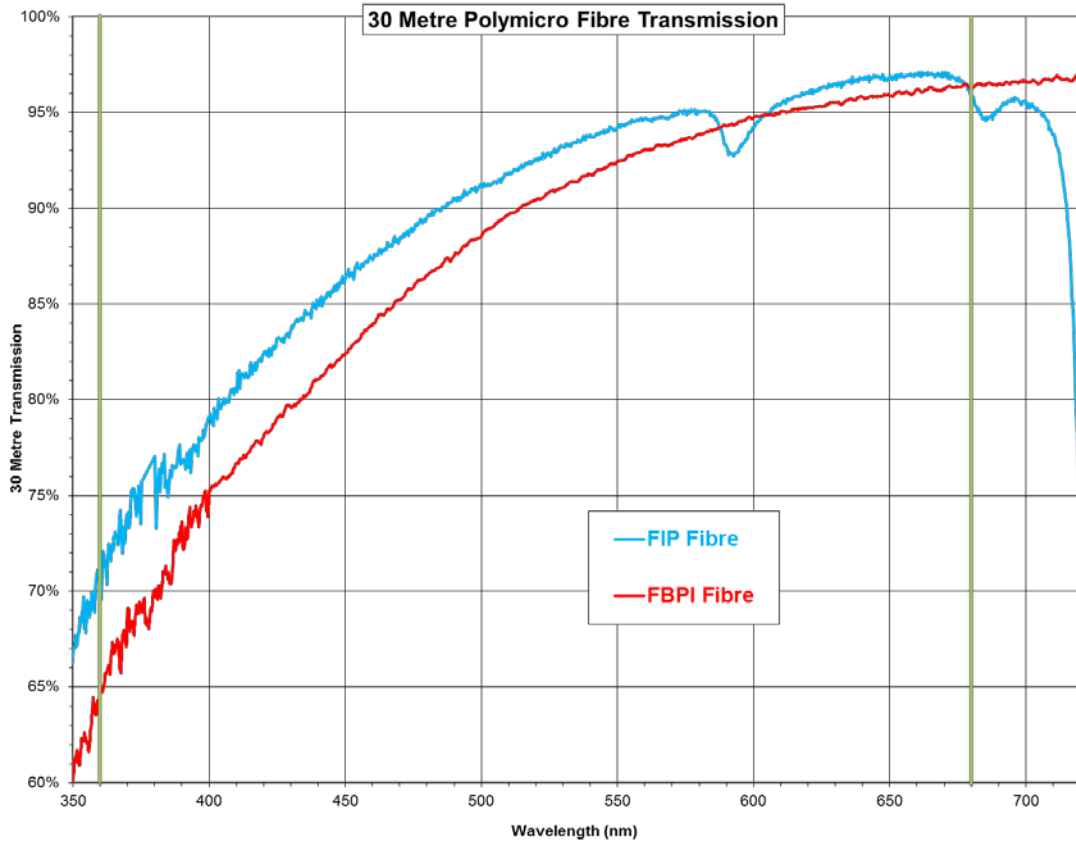


Figure 3. Plot of percentage transmission calculated for 30 metre sections of FBPI versus FIP Polymicro fibre from Molex. The desired bandwidth of 360 nm to 680 nm is bounded by the green lines. With the exception of a small absorption feature centred around 592 nm, the FIP fibre shows a consistently higher transmission than the FBPI product, with the greatest gains evident towards the UV end of the plots.

3.2. Fibre numerical aperture

The fibres will be microlens-coupled, with incident light at the fibre entrance faces having undergone a F/# conversion to $\approx F/3.5$ from the F/# delivered by the fore-optics. Unusually high numerical aperture fibres are not therefore anticipated, and standard 0.22 N.A. product will be sufficient. Exact specifications for the input microlenses are still TBD.

3.3. Focal ratio degradation

In addition to absorption within the fibre, another critical loss mechanism is Focal Ratio Degradation (FRD). FRD can be considered as a “blurring” of incident F/# that occurs as light propagates down an optical fibre, causing light exiting the fibre to distribute over a wider angular range. It is a fundamental concern for photon-starved applications such as astronomy because rays which emerge at faster F/# than the designed clear aperture of the spectrograph will be lost due to over-filling. Indeed, if the FRD is present to such an extent that the critical angle of the fibre is exceeded, further losses will occur at the core/clad boundary throughout the fibre length.

FRD can originate from intrinsic Rayleigh scattering within the glass of the fibre, stresses and microbending, as well as poor end preparation. All Polymicro fibres that have seen use in astronomical applications have been extensively tested for intrinsic FRD and they are generally consistently good. Nevertheless the selected fibre will be subject to FRD verification tests to retire any such risks with the FIP product.

LUCA - Calar Alto 3.5 metre Telescope - IFU-6000 Fibre System Feasibility Study

There are two widely used FRD tests which are applicable; the filled cone method and the collimated beam (or ring) method.

The filled cone method mimics to some extent the optical configuration of the telescope – a source of finite size (typically an illuminating source fibre) will be re-imaged onto the input face of the fibre core under test, with a $F/\#$ equivalent to the intended application. The output far field pattern is then analysed to assess the encircled energy over a range of $F/\#$ ’s. This test is thorough and provides a realistic representation of the fibre performance in the instrument. However it is time-consuming and difficult to align the fibre accurately, so the test can be prone to error. This test is therefore applicable to qualifying a small number of samples of fibre in the early stages, and for final verification testing.

The collimated beam method in contrast is the fastest, simplest, most robust and least error-prone. It relies on the fact that fibres are very efficient at optically scrambling/mixing azimuthally about the optical axis of the core, but conversely, scrambling of the radial (angular) component is minimal. Figure 4 shows the principle. A uniform-profile collimated beam is launched into the fibre core at an angle θ with respect to the optical axis of the fibre. Azimuthal scrambling within the fibre produces a cone of light, having an angle of divergence 2θ . However while the barycentre of a cross-section through the ring will indeed correspond to an angle θ from the axis, FRD will cause a spread of light either side of this peak, forming a pseudo-Gaussian intensity distribution. The FWHM thickness of the far field projected annulus corresponds directly to the level of FRD present.

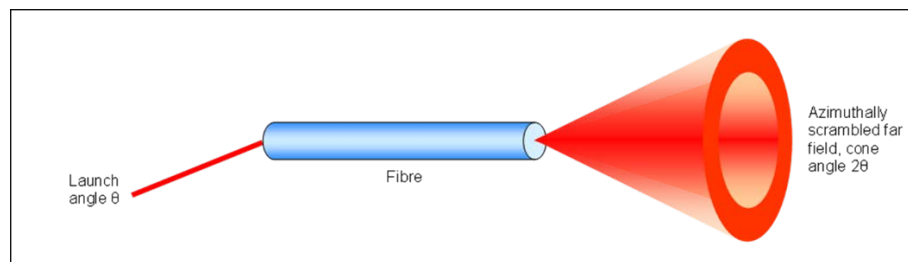


Figure 4. Sketch illustrating focal ratio degradation (FRD) in an optical fibre revealed via the collimated beam test. FRD is seen as a spread in the thickness of a far field annulus.

There is a direct correspondence between the two test methods, but the collimated beam test only provides a “snapshot” of FRD affecting rays at a single angle. A full model of the fibre FRD *can* be derived by sweeping the launch angle through a full range of θ , however the collimated beam test is usually employed for fixed angle measurements only, and it sees application at intermediate stages during fibre system production, where large numbers of fibres are assessed to statistically quantify the effects of successive production stages. It can be readily configured as a portable test, so for example it is ideal for use at the cable production factory or at the telescope. Durham CfAI has built permanent cone and collimated beam lab-based test benches, and a portable test bench that has seen extensive use for PFS cable work offsite.

Low FRD termination and end preparation strategies have been explored and developed over a number of astronomy projects at Durham University CfAI. These include careful selection of the epoxies to be used and low stress thermal cure schedules, combined with minimum epoxy use. Completed terminations are processed to achieve high optical quality using state-of-the-art fibre polishing and inspection. The cable will be designed in such a way that stress due to fibre packing, bending, and tensile forces will be minimised. This will be detailed in section 4.

LUCA - Calar Alto 3.5 metre Telescope - IFU-6000 Fibre System Feasibility Study

3.4. Fibre core size

The fibre core size is pre-defined as $150 \pm 3 \mu\text{m}$. This has been determined from the nearest available off-the-shelf core size from the Polymicro catalogue that meets the science and optical requirements; fill factor resulting from spaxel size on the sky and incident F/#, and the desired line spread function in the spectrographs.

3.5. Fibre clad size

The standard $150 \mu\text{m} \pm 3 \mu\text{m}$ core Polymicro fibre comes with a cladding diameter of $165 \pm 3 \mu\text{m}$ (tolerances are non-cumulative). A rule of thumb for minimising evanescent wave loss is that the cladding should be at least $10 \times$ the longest wavelengths captured by the instrument. Here we have:

$$680 \text{ nm} \times 10 = 6.8 \mu\text{m}, \text{ and } 15 \mu\text{m} \div 2 = 7.5 \mu\text{m};$$

$7.5 \mu\text{m} > 6.8 \mu\text{m}$, so the clad is within the acceptable range.

3.6. Fibre buffer material, size

The fibre buffer material will be a Polymicro standard baked Polyimide coat. The off-the-shelf diameter for the $150 \mu\text{m}$ core product is $195 \pm 3 \mu\text{m}$ (tolerances once again are non-cumulative). Since the fibre buffer can be produced with a high diameter tolerance (and extremely well controlled concentricity, typically sub-micron) then where fibres are bonded into input and output terminations, fibre centration errors will not be significantly affected. The buffer material does not therefore need to be stripped before gluing fibre ends into assemblies. Retaining the buffer results in reduced risk of breakage during assembly, in addition to lower fibre stress, thus lower FRD.

3.7. Batch variation

For procurements of large quantities of fibre, the fibre must originate from a number of different fibre pre-forms. This raises the possibility that a variation from pre-form to pre-form could be seen in the delivered fibre product. However, Polymicro fibre data obtained from the early stages of the DESI project has shown that the product from the company is remarkably consistent. Relying on the Polymicro in-house quality control testing prior to shipment is therefore considered perfectly acceptable.

4. Fibre cable design

4.1. Functional requirements

The fibre cable should retain the fibres in robust, flexible conduits that will impart minimal packing, bending, and tensile stresses to the fibres, to minimise FRD and FRD variation. To achieve this the cable is typically an assembly of polymer furcation tubes, each containing a sub-set of the fibres, and housed inside a PVC-clad (watertight) steel-helicoil outer sheath. Provision must be made for tensile support, and the effects of differential path-length variation through the furcation tubes should be also be minimised, so there is no tension induced in the fibres by so-called "race-tracking"¹. There will be sections where there is a transition in tube cable size, and/or number of cables (downstream of the IFU input but before the loop box, and upstream of the slits but after the loop boxes). The cable pattern that is decided upon must accommodate these features.

¹ Where the path-lengths within a tube will vary around a bend in a tube depending upon whether the fibres route on the inside or the outside of the bend.

LUCA - Calar Alto 3.5 metre Telescope - IFU-6000 Fibre System Feasibility Study

4.2. Planetary Stranding

A successful cable solution that will meet the IFU-6000 cable requirements was originally developed for the Subaru Fibre Multi Object Spectrograph (FMOS) project [1]. The production technique is referred to as “planetary stranding”. Outside of astronomy, the method is widely employed as a stress minimising strategy in industrial cable manufacture for such applications as marine telecommunications. Here, multi-fibre cables having large cross sections are typically many kilometres in length and have to endure bending and substantial external tensile load, especially during deployment. This innovation was applied on a smaller scale for making the FMOS fibre cables and it proved very effective. A typical stranded cable is shown in Figure 4 as a cutaway sketch. Since FMOS was completed the production process has been improved significantly, specifically for the Subaru Prime Focus Spectrograph (PFS) cables [2]. This work was funded by the PFS project and undertaken in collaboration with PPC Broadband Fiber Ltd. in the UK, where a dedicated production line and stranding machine were devised [3]. The same facilities and methods were subsequently adopted for the Dark Energy Spectroscopic Experiment (DESI) fibres [4]. This cable construction method is proposed for IFU-6000.

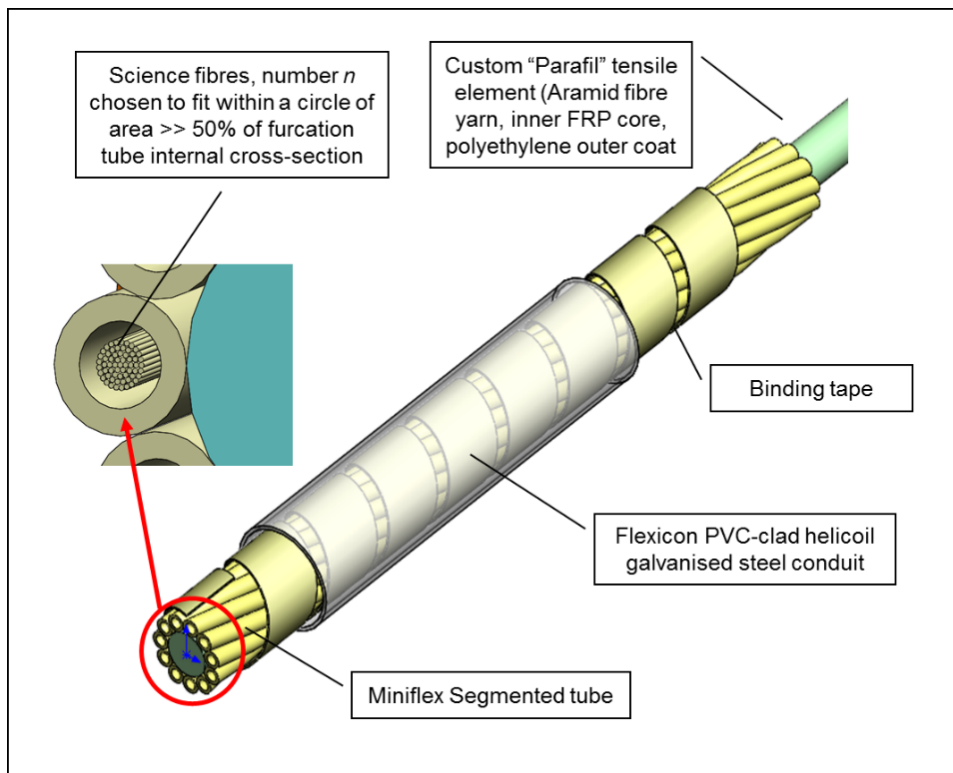


Figure 5. Cutaway view showing the composition of a stranded cable. “Miniflex” segmented furcation tubes containing science fibres are stranded around a central tensile element. Fill-factor, cable diameter, stranding pitch are all optimised for minimum fibre stress. Cables are produced in collaboration with PPC Broadband Fiber Ltd. – inventors of the Miniflex tube.

The planetary stranding process utilises a machine that winds furcation tubes spirally around a central high-strength core without imparting a twist to the tubes. In order to do this the stranding head carrying the spools of tube de-rotates each spool one full counter-rotation for a complete rotation of the stranding head itself. The fibres in a cable thus formed cannot be easily put under tension if the cable is bent or pulled, because stranding around a core of finite size results in additional fibre per unit length incorporated into the cable, thus the fibres are always in a relaxed state. Incorporation of additional fibre per unit length is most readily visualised with reference to Figure 6.

LUCA - Calar Alto 3.5 metre Telescope - IFU-6000 Fibre System Feasibility Study

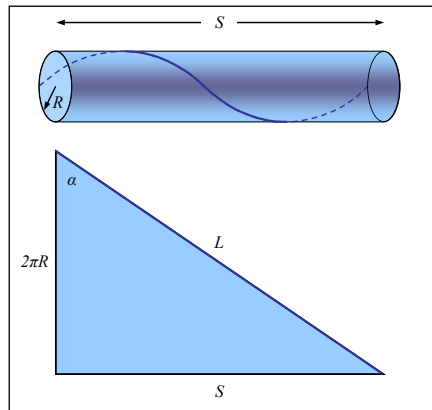


Figure 6. In a stranded cable, where the stranding element is located a distance R from the centre, it follows a path around the surface of a cylinder. If the cylinder is ‘unwrapped’ flat, the stranding element length L (the fibre) can be seen to be greater than the lay length S .

The pitch of the winding, i.e. the length over which the spiral winding has described 360° is more commonly known in cable engineering terminology as the ‘lay length’ and this is an important factor in the cable design. The percentage additional stranding element per unit-length Z is given by:

$$Z = \frac{L - S}{S} \cdot 100\% = \left\{ \sqrt{1 + \left(\frac{2\pi R}{S}\right)^2} - 1 \right\} \cdot 100\% \tag{1}$$

Where: S = the winding pitch (lay length).

L = the stranding length.

R = the stranding radius (distance from the centre to a circle on the centres of the azimuthally distributed furcation tubes).

For a given furcation tube diameter d and number of tubes n , the stranding radius R itself is given by:

$$R = \frac{d}{2 \sin\left(\frac{180}{N}\right)} \tag{2}$$

Three “rules of thumb” should be considered when deriving the optimal lay length S :

1) It has been found empirically that the cable performs effectively if the additional fibre length incorporated per unit length of cable is greater than 2.5% or so.

2) Corning Cable Systems GmbH & Co. KG [4] advise that further advise that a lay length should be (very approximately) equivalent to one quarter circumference of the cable when coiled at minimum bend radius, in order that fibres will remain free to adjust position, move differentially and equalise *localised* tension during manipulation of the cable. This is a simplified but effective empirical solution to an otherwise complex problem that encompasses factors such as stranding radius, coefficient of friction of fibres within the tube, the minimum bend that the cable is likely to experience, packing density of the fibres within the tube, and so-on. The physical minimum bend limit is actually defined by the outer ruggedised cable conduit which will be used (see Section 5.5) since this has a generous mechanical bend limit, dependent on the conduit diameter. From the manufacturer’s catalogue the minimum bend radius (MBR) for Adaptaflex SPL40 conduit is listed as 180 mm. The deployed science cables when in use will not see a bend radius close to this (the smallest bends are typically closer to 300 mm). Nevertheless if a cable is designed using the manufacturer’s minimum figure as a guide then we can be assured that the stranded cable will function correctly in all circumstances. So, as an

LUCA - Calar Alto 3.5 metre Telescope - IFU-6000 Fibre System Feasibility Study

example, following equation (1) for a 40 mm O.D. conduit, the minimum I.D. of a stranded cable core that will fit freely is 32.7 mm. (actual limits are the bores inside the conduit end fittings, which are smaller than the conduit I.D. itself). So assuming we use 12-off 6.35 mm furcation tubes, first check that the core will fit:

$$R = 12.3 \text{ mm.}$$

Adding d , one furcation tube diameter, to the stranding diameter $2R$ gives a overall cable core O.D. = 30.9 mm.

30.9 mm < 32.7 mm - so the cable core will fit SPL40.

Then:

$$S = \pi (180 \text{ mm}/2) \approx 283 \text{ mm, so } Z = 3.7\% - 3.7\% > 2.5\% \text{ minimum.}$$

3) Thirdly, the true radius of the helix should be significantly greater than the minimum long-term bend radius (MBR_{LT}) of the fibre (typically 100 times the fibre core diameter). The stranded helix is a three-dimensional curve that has an equivalent radius, which is given by:

$$Q = R \cdot \left\{ 1 + \left(\frac{S}{4\pi R} \right)^2 \right\} \quad (3)$$

Where: Q = the three dimensional radius, or *bending radius* of the helix.

Calculating the value Q for the cabling application yields a bending radius of approximately 54 mm; close to 4 times the MBR_{LT} for a fibre. However this is simplistic because it presumes a cable in a straight line. The smallest bend radius seen by the fibre in a real, worst case would be when the cable is taken to its minimum bend radius. Here, the curvatures directly combine. If the Cable MBR is combined with the true helical curvature Q at this point, the fibre sees a compound radius of around 42 mm, again well clear of the fibre MBR_{LT} .

5. Cable production

The background and detailed specifics of the principles and techniques involved in producing the PFS cables are covered in the referenced paper [3] but there are several key aspects which should be covered here:

- The choice of furcation tube and how the fibres are installed.
- How a stranded cable core is formed.
- How the cable core is packaged.

5.1. Furcation tube

PPC Broadband Fiber Ltd. produce a patented furcation tube which has seen widespread use in astronomical projects. The tube is marketed as 'Miniflex Optical Fibre Protection Tubing' (OFPT). This is a single layer polybutylene terephthalate (PBT) polymer tube having a comparatively thick wall, hence high crush resistance. While offering a high degree of fibre protection it nevertheless exhibits good flexibility due to a novel segmented design. The tube is resistant to tensile loads, and the segmentation and offers a degree of protective bend limitation. The smooth inner bore meanwhile supports the fibre with low friction and eliminates fibre micro bending. Figure 7 shows a range of sizes of Miniflex OFPT.

LUCA - Calar Alto 3.5 metre Telescope - IFU-6000 Fibre System Feasibility Study



Figure 7. Examples of various sizes of Miniflex Optical Fibre Protection Tubing (OFPT).

5.2. Installing the fibres into the furcation tube

PPC Broadband Fiber Ltd. install fibres into the furcation tubing at the factory. This enables better control of fibre tension and a uniform, high parallelism in the fibre packing (minimum crossing/interweaving of fibre) in comparison to bundles made by drawing the fibre into tubes by hand in the laboratory. The feed process involves controlled channelling of fibres into the Miniflex extruder under carefully controlled conditions. The first section of the feed scheme consists of a set of “pay-off” towers that support spools of fibre. The towers are simple steel frames that each have a capacity of 16 spools. Currently there are four pay-off towers, giving a maximum capacity of 64 spools / fibres. The fibres converge at guide plate where an array of smooth, low friction ceramic inserts (eyelets) define the positions of the fibres in a regular grid as they converge over a narrowed range of angles into the extruder. A controlled convergence here is important because it ensures the fibres are separated, receiving an even coating of powder lubricant as they pass through a powder coating bath which sits between the eyelet plate and the extruder itself. Lubricant is essential for preventing the fibres sticking to each other, to the inside walls of the Miniflex tube, and it ensures free differential movement between fibres in a bundle. The result is a highly parallel fibre bundle laid in the furcation tube with neutral tension. Figure 8 shows the configuration of the various component parts comprising the fibre feed prior to the Miniflex extrusion line. There are some additional considerations that must be taken into account with this process:

- The fibre must be purchased in specific, matched lengths. Clearly if 64 fibres are to be inserted into a furcation tubes, spools of fibres must be purchased / organised into batches of 64, and the lengths of these fibres should be similar. Polymicro are able to supply matched fibre batches for such manufacturing schemes.
- The production line is run more slowly than might be the case for a small number of fibres. This simply reduces risk and ensures all fibres can be monitored to ensure they are feeding into the production line smoothly.

LUCA - Calar Alto 3.5 metre Telescope - IFU-6000 Fibre System Feasibility Study

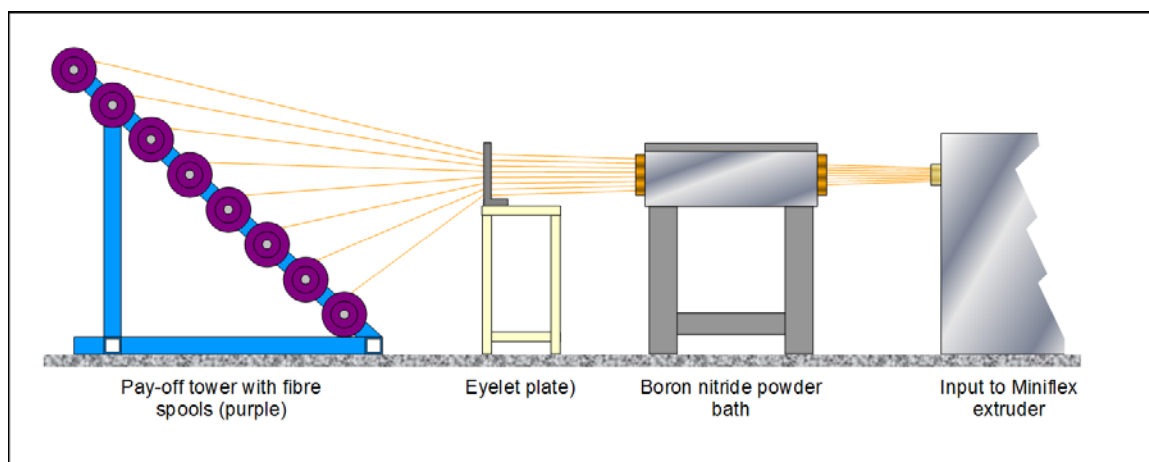


Figure 8. The fibre feed scheme for channeling fibre into the Miniflex extrusion line. Introducing the fibre during the production of the Miniflex tube results in a highly parallel lay and minimal tensile stress. Fibres are first drawn through an agitated boron nitride powder coating bath to apply a uniform and continuous coat of the dry powder lubricant.

5.3. The tensile element

For existing astronomical cables a tensile element was selected for high tensile strength and minimum extension under load. Tensile ropes formed from Aramid yarn meet these requirements. A typical rope will consist of a core of many fine Aramid fibres surrounded by a soft polyethylene sheath, the diameter of which is built up to match the packing of furcation tubes stranded around it. Aramid possesses a very low, slightly negative CTE, typically $-2 \times 10^{-6}/^{\circ}\text{C}$. However when considering applications in lower temperature environments, the Aramid soft Aramid fibres will offer no stiffness, hence no mechanical support against shrinkage. For this reason, cable tensile elements contain a central CTE-stabilising solid core, typically a small diameter rod of glass fibre reinforced polymer.

5.4. The stranding production line

The production line is sketched out in Figure 9. Core to the cable stranding process is the “planetary strander”. This machine was designed and built collaboratively by PPC Broadband Fiber Ltd. and Durham University. The functioning is relatively simple; spools of fibres in Miniflex tubes are held on spool-carriers which are synchronised to counter-rotate as the machine turns – remaining upright – so no twist is imparted. Power is delivered by a drive motor and drive belt coupled to a set of secondary drive belts & pulleys to synchronise the spool counter-rotations with the rotation of the machine overall. The tensile element is fed through the central axis of the machine and when the machine turns, tubes are laid around the tensile element in a helix.

Tensile element is pulled through the machine from the passive tensile element pay-off by the haul-off machine. Between this and the strander a tape binder wraps a consolidating Mylar film around the stranded cable core. All three driven units are synchronised and cable transfer rate through the production line is monitored with a tachometer.

LUCA - Calar Alto 3.5 metre Telescope - IFU-6000 Fibre System Feasibility Study

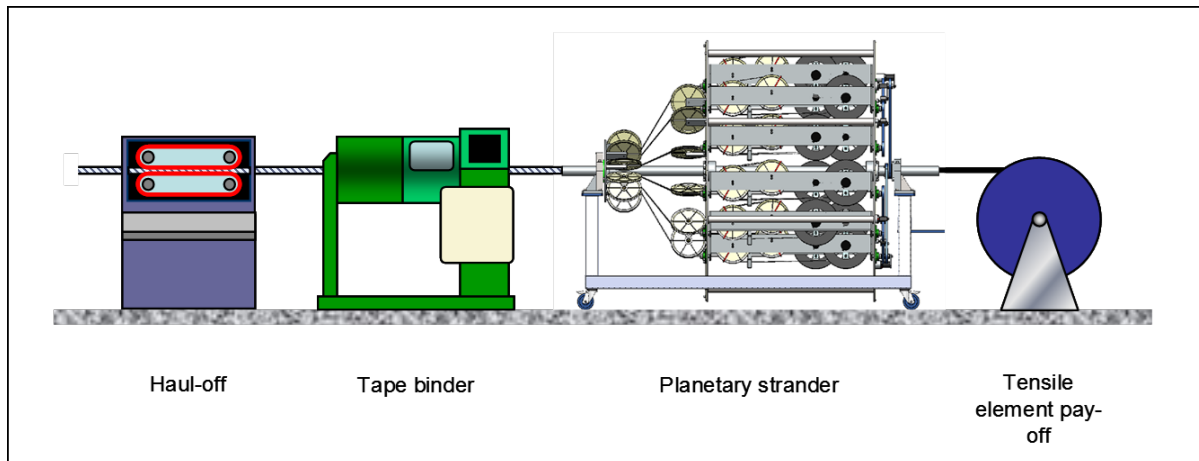


Figure 9. The cable production line, starting with the tensile element on the right. This feeds into a planetary strander which carries spools of Miniflex furcation tubes containing the fibres. The tubes are wound around the tensile element in planetary-fashion (no twist). The stranded cable is then bound with consolidating tape, resulting in a stranded and tape-bound cable core emerging on the left. The haul-off pulls cable through the production line at a constant rate.

5.5. Conduits

The completed cable cores will be managed within ruggedised, PVC-clad helicoil conduit and hardware. Examples of conduits and fittings are shown in Figure 11. The mechanical strength, crush resistance and flexibility are imparted by an interlocked steel helicoil construction. The PVC outer coat prevents the ingress of moisture. Watertight fittings will also be used. Adaptaflex, Flexicon, and similar conduits have been used extensively for astronomical fibre systems.



Figure 10. Examples of Adaptaflex PVC-clad steel helicoil ruggedised conduit systems.

5.6. Strain relief boxes

It has been stated already that the strain relief boxes allow for fibre differential movement / dissipation of tensile stress, but more importantly, they serve as fibre reservoir from which additional fibre can be extracted if fibres are broken during the preparation of end terminations. For a fibre system longer than a few metres, loop boxes would normally be located close to both ends of the cable scheme, as is proposed here. They are simple box structures that have cable conduit interfaces at the entrance and exit ports. Within the box, bundles of fibres from each furcation tube are configured in loose loops, typically separated by divider plates. If the cable needs to breakout into

LUCA - Calar Alto 3.5 metre Telescope - IFU-6000 Fibre System Feasibility Study

several cables, or transition to a conduit of different size, the strain relief boxes are the most convenient location to do this.

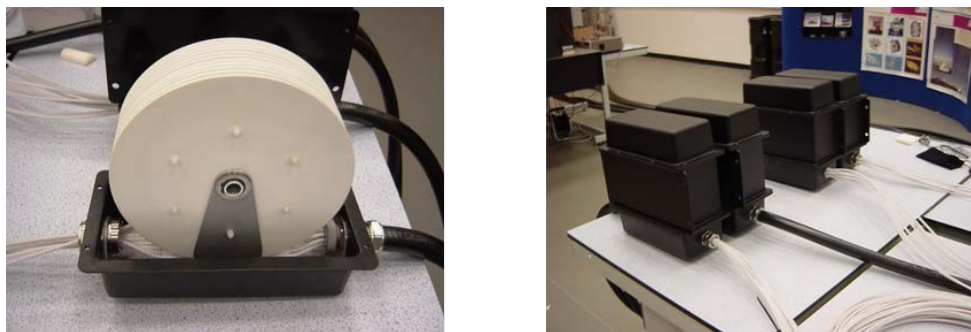


Figure 11. Examples of the strain relief boxes employed in the FMOS cable system, shown at various stages during construction. On the left a box is shown open, revealing partition discs. On the right strain relief boxes are near completion.

6. Constraints & specific considerations for the cable scheme

The spectrograph will be of an AAO design, employing 6000 fibres across 8 spectrographs, each slit, having 750 fibres. A DESI-like design was proposed by Winlight System, however to meet the science requirements for field coverage and spectral resolution the fibre core size reduced to 100 μm and the fibre count more than doubled, to 15,000 elements addressing 19 spectrographs. This scheme was therefore ruled out.

So employing the AAO instrument design, we can begin to refine the options by applying fibre management and the cable construction constraints to reveal what the cable scheme might look like. We can first state that:

- The 150 μm core fibre O.D. is 195 μm
- For simplicity, the number of cables should be either 1 or 2 per spectrograph slit. Fewer cables will result in cable cross-sections that are impractically large, with complicated fibre routing / breakouts at the spectrographs.

Furthermore, from the cable production process:

- The most fibres that the payoff can safely handle is 64 (4 \times 16-spool payoff towers)².
- The maximum handling capacity of the strander is 12 cables.

Another empirically derived³, approximate rule of thumb comes into play when considering packing the fibres into furcation tubes. Clearly a tightly packed furcation tube will lead to compressive stress on the fibres, but even comparatively loose packed tubes can see elevated FRD in the fibres when the furcation tube is manipulated and flexed. This originates in stress points where the fibres cross / overlap, and it is related also to the degree of disorder in the bundle. For regular-sized multimode

² The fibres should not arrive at the eyelet plate with large angles. Angles become excessive with more payoffs. In addition, larger numbers of fibres become difficult to manage in the semi-automated production process. For higher fibre counts we would consider hand-pulling fibre into tubes, but this can result in less tensile uniformity and parallelism in the fibre lay.

³ Derived from PFS fibre testing on low OH fibres manufactured by Fujikura.

LUCA - Calar Alto 3.5 metre Telescope - IFU-6000 Fibre System Feasibility Study

fibres ($> 50 \mu\text{m}$, $< 500 \mu\text{m}$ OD) it has been observed that the cross sectional area of the fibre bundle⁴ should not exceed significantly more than 20% of the cross-sectional area of the furcation tube I.D. in order to maintain minimum packing stress on individual fibres. This is a conservative figure, and to some extent it is dependent on the physical characteristics of the fibre itself. It is the case that some fibre types can be managed with a higher packing fraction (fibres from different manufacturers can exhibit different sensitivity to external stress - there is evidence for example that Polymicro fibres fare better than competitors, packing by an additional 10% to 20% or more without substantial degradation in performance). In addition, fibre buffer thickness will have a significant impact. Fibre packing will therefore be subject to proof-testing with candidate fibre at the detailed design stage, and results used to finalise the cable scheme. However $\approx 20\%$ packing fraction will be considered for the purposes of this study.

The number N of fibre diameters d that can pack into an enclosing circle of diameter D is governed by the specific geometry of the packing, which varies with N . Look-up tables in Machinery's handbook [6] list diameter factors K for specific numbers of D , so N can be derived. The table below lists values of N obtained for three of the common sizes of Miniflex conduit:

Miniflex (mm)	O.D.	Miniflex I.D. (mm)	D, O.D. of 20% cross sectional area (mm)	Calculated dia. factor K_c D/d	\geq Nearest dia. factor K_{ref} from ref tables	Matching N for K_{ref}
4.0		2.6	1.16	5.95	5.62	19
5.0		3.1	1.39	7.12	7.11	34
6.35		4.2	1.88	9.64	9.186	61

Table 1. $\approx 20\%$ packing fractions for a $195 \mu\text{m}$ O.D. fibre for a variety of furcation tube sizes.

The 4.0 mm Miniflex solution is rejected because a significantly larger number of furcation tubes will be required to accommodate all the fibres.

Assuming the maximum 12 tubes per cable, 5.0 mm Miniflex \rightarrow 34 fibres each, 15 cables would be required. Not ideal.

Assuming the maximum 12 tubes per cable, 6.35 mm Miniflex \rightarrow 61 fibres each; 8 cables would be required, (with an overfill of a couple of fibres per tube including spares, which is acceptable). A 12-off 6.35 mm cable solution would therefore work.

Each cable will thus have 12 furcation tubes stranded around an 18 mm O.D. tensile element. The impact of increased packing can be explored if fewer cables are desired. As has already been shown in Section 4.2, 12-off 6.35 mm Miniflex tubes yields a cable core OD of 30.9 mm which fits comfortably within the ID of a commercial 40 mm Adaptaflex or similar conduit.

7. Cable terminations

The fibre cable system terminates at the input in a 2-D parallel fibre array which will address a sub-field of 9 square arcminutes on the sky (initial schemes had a $3' \times 3'$ square field). At the output the fibres are formatted into fibre pseudo-slits located at the spectrograph focal planes; the curvature and optical pointing of these slit units are matched to the optical requirements of the spectrographs. Durham University CfAI has more than 20 years' experience developing fibre based integral field units. CfAI has undertaken extensive R&D programmes to develop advanced hardware and strategies for

⁴ Note: The cross-sectional area of the bundle here is *not* defined as the sum total of fibre cross-sectional areas, but rather the diameter of an enclosing circle that encompasses the fibre bundle at its most disordered.

LUCA - Calar Alto 3.5 metre Telescope - IFU-6000 Fibre System Feasibility Study

making 2-D and 1-D fibre arrays. These provide accurate, low FRD fibre assemblies and have been well demonstrated.

7.1. IFU Input

At the input of the fibre system the fibre ends are arranged in a regular 2-D array, which coherently maps to the spectrograph slit. Integral field units can have a variety of formats, for example hexagonal, truncated-hexagonal, square, or rectangular. For very high multiplex schemes the IFU input can also be formed from “tiles” of sub-modules to keep the fibre bundles manageable. For IFU-6000 it is practical to construct the input as a single monolithic unit, so tiling is not considered.

7.1.1. Chosen field format

Throughout the survey work to be undertaken by the IFU, 1/3 of the galaxies are to be acquired in a single pointing. If a set of galaxies are considered as simple disc-shaped forms with random orientations, the most effective topology for efficient acquisition is a rectangle, and the optimal aspect ratio is $1/\sqrt{2}$ (approximately 1:1.41). The fibre packing in the rectangular 2-D arrays should be hexagonal. Square packing incurs a significant geometric FRD penalty, as a consequence of the geometry of incident rays bounded by the microlens aperture. Simplistically, for a given pitch p and focal length f the incident F/# at the fibre core will include rays that are faster because f/p is only true for a circular aperture of diameter p . A ray bundle bounded by a square aperture of side length p will include 27% of rays outside this circle. A similar effect applies to a hexagonal aperture, but less so, delivering 10% of rays at a faster F/#.

The nearest 1:1.41 fit to 6000 hexagonally packed fibres gives a field size of: 61 x 99 fibres = 6039 fibres⁵. Figure 12 shows a sketch of the 6039-fibre field divided into spectrograph-specific field formats.

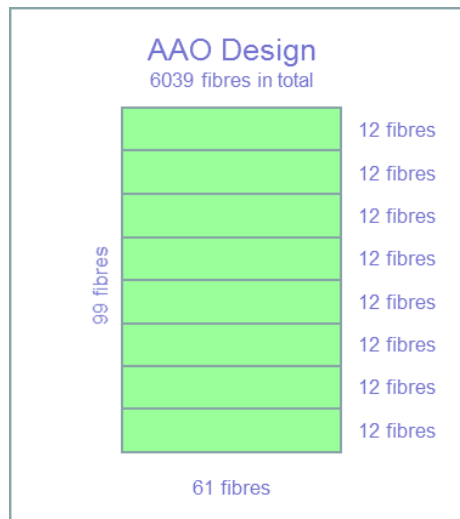


Figure 12. The field format for the AAO Spectrograph design.

The input will be microlens coupled, increasing the fill factor and transforming the slow F/# incident light from the telescope to fast F/# coupling into the fibres, with a microlens pitch of 2.5” on sky. The use of a positive microlens in combination with a fibre array results in a larger fibre pitch than would

⁵ The ratio of 61:99 is of course 1:1.62. However because the field will be hexagonally packed (assuming the packing is configured in rows of 61) the long axis is shortened by a factor $\cos 30^\circ$. $99(\cos 30^\circ):61 = 1:1.41$ approximately.

LUCA - Calar Alto 3.5 metre Telescope - IFU-6000 Fibre System Feasibility Study

be the case if the fibres were simply close-packed with no gaps. The precise physical pitch in μm that this spatial sampling translates into is still TBD but shall be derived from an optimisation including the telescope, fore-optics, fibre core size, and spectrograph clear aperture.

7.1.2. IFU input hardware and optics

The fibres must be supported in a highly toleranced, regular 2-D matrix of channels. They will be bonded into this hole-array, which will then be polished flat, in preparation for bonding a microlens array onto the surface. For an IFU comprising 6000 sampling elements the most suitable technology is a hole-array made from a stack of hole-array plates, typically 6 mm – 8 mm thick, located within a precision steel frame. The picture shown in Figure 13 illustrates the principle. The pattern of holes is cut with an excimer laser. A variety of materials can be used for the hole-array plate substrates; and silicon, Cirlex⁶, glasses and ceramics have all been demonstrated. Individual plate thickness can be in the region 0.5 mm – 1 mm (chosen following maximum cut-depth recommendations from the laser machining company). There is an argument for using a dark or transparent substrate material rather than white / reflective, if it is considered advantageous to minimise back-scattering. However a final choice will be based on an assessment of test cuts provided by the manufacturer using substrate samples. Tolerances on all laser cut features are typically $\leq 2 \mu\text{m}$ (this is non-cumulative across the hole-matrix). Since the pitch can be arbitrarily selected, the microlens array would typically be manufactured first, the pitch of the lenslets would be accurately measured and the hole-arrays produced to match. The laser-cut holes exhibit a small, very repeatable taper due to erosive ablation as material is ejected during each cut-pulse from the laser. If the tapers are aligned when the plates are assembled into a stack, it eases significantly the task of inserting fibre through the matrix.

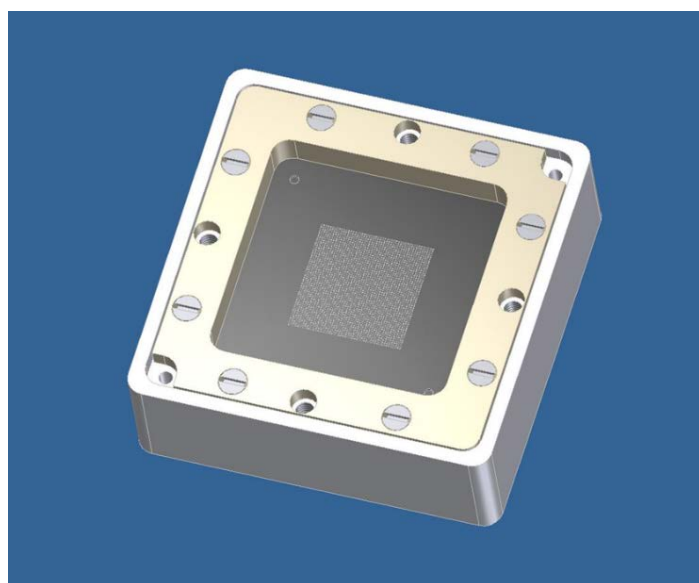


Figure 13. A rendering showing an example of a 2-D hole-array matrix for a several thousand fibre IFU.

Fibres are inserted into the hole-array matrix under a microscope. Initially it was anticipated that additional holes to support guide pins would be useful for accurately co-registering the hole-array plates. However in practice this was found to be unnecessary; putting a couple of fibre stubs temporarily at or near opposite corners of the hole matrix performs the same function. Population of

⁶ A polyimide sheet supplied in highly toleranced thicknesses. It has a near-black appearance so it absorbs the laser light efficiently during the cutting process leading to very clean features.

LUCA - Calar Alto 3.5 metre Telescope - IFU-6000 Fibre System Feasibility Study

the array occurs *after* the slit ends of the cable have been completed. The fibres in each slit are scanned with a focused laser spot to identify fibres in the input bundle, to facilitate the coherent mapping of fibres between the input and output.

When assembly of the array is complete the fibres are trimmed and bonded into place by dipping the front of the array into epoxy resin. Capillary action fills the voids in the stack. A two-part low stress epoxy with an elevated temperature cure schedule is ideal, and a number of such products are available for fibre optic assembly (Angstrombond or Epotek resins are typically used). The cured assembly would then be optically polished and the microlens array installed. A suitable antireflection coating will be applied to the microlens array when it is manufactured to improve optical efficiency. The microlens array is bonded with an optical grade UV cure epoxy (Epotek and Norland supply products that are well tailored to fused silica and other glasses). Alignment is undertaken with the microlens “floating” on a film of uncured adhesive. Back illumination at the slits projects light from the 2-D array, through the microlenses onto a pre-configured target. The location of the projected pattern translates with microlens offset. Using a precision x, y manual positioner, co-registration < 5 µm can be achieved.

An engineered shell will be designed to support the IFU input assembly in the focal plane of the telescope. This also protects the bare fibres, and serves as a mechanical interface to the downstream cable conduit.

7.2. IFU output – slit assemblies

One of the most effective methods to create linear arrays of optical fibres is to use v-groove arrays. Exceptionally high positional tolerance and pointing can be realised, and the technology is standard for a number of telecommunications applications, where e.g. for multi-fibre connectors, sets of fibres are mounted in parallel v-channel plates and polished. With appropriate design and selection of adhesive, very low FRD is achieved (close to equivalent bare fibre performance).

For a number of pseudo-slits that have been made in Durham for fibre-based spectroscopic instruments (GMOS-IFUs, FMOS, DESI) the slits have been built up from sets of individual, parallel-channel v-groove array sub-blocks. This is effective for flat slits, and curved slits can be created reasonably well with this method also. However the fibre pointing is in parallel sets, thus it is only approximate. Furthermore there must be a nominal clearance between blocks leaving in gaps in the 1-D fibre pattern and inefficient use of detector real-estate. To address these deficiencies, Durham University CfAI in collaboration with an industrial partner, SQS Vlaknova Optika A.S. has undertaken a successful development programme to mature monolithic v-groove array technology. Figure 14 and Figure 15 show such a component (a flat lid cut to cover the v-groove section is not included). The v-groove plate was cut with a dedicated laser cutting machine tailored to cut glass to very high tolerances. The substrate is Borofloat 33 wafer, a borosilicate glass that cuts with a high surface finish and has a higher toughness than e.g. fused silica, so there is less fragility in regions with fine / sharp features. This v-groove array was prototyped to have the same specifications as the fibre slit for PFS. Indeed it also happens to be quite similar in specification to the DESI slit (albeit the DESI scheme employs significantly smaller fibres). Metrology was undertaken to ascertain the pointing accuracy of the v-groove pattern. The results are given in Table 2, with PFS required specifications included for comparison. In terms of format, the monolithic v-groove pseudo-slit solution is extremely versatile, capable of supporting a wide variety of slit topologies. The versatility and other advantages can be summarised as:

LUCA - Calar Alto 3.5 metre Telescope - IFU-6000 Fibre System Feasibility Study

- No gaps, as seen with slit block schemes.
- The slit front face can have a true (not approximate) concave or convex curved profile.
- In the example shown the v-groove is planar, creating a flat linear array of fibres. However the linear array of fibres itself can be given a curvature.
- The fibres have true (not approximate) pointing. The fibre axes can be divergent, convergent, &/or off-axis – indeed they can tilt out of the plane if required.
- The pitch of the fibres can vary across the array.
- Different fibre sizes can be accommodated in the same slit.
- The assembled component can have an extremely low profile.
- Antireflection coatings can be directly applied.

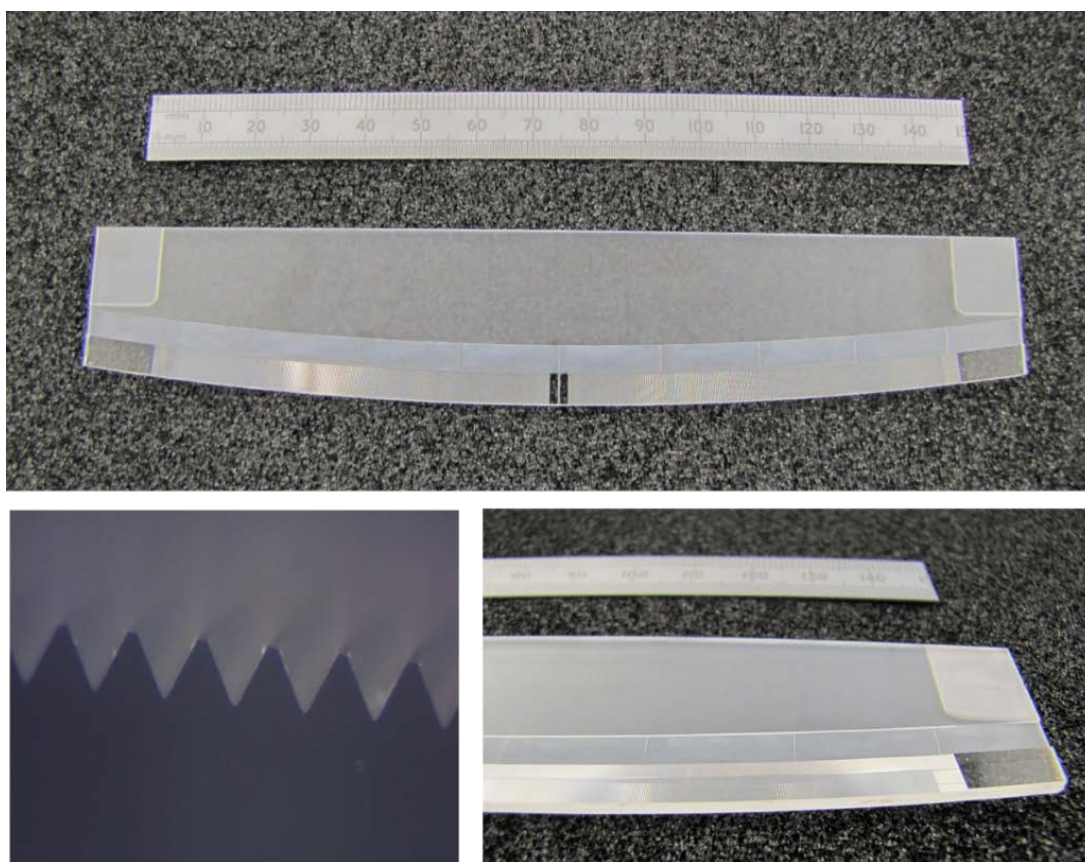


Figure 14. A monolithic fibre slit developed in collaboration with SQS Vlaknova Optika A.S.

Fibre assembly is relatively straightforward. Several fibre stub spacers are temporarily located at regular intervals in the v-channels and the lid is placed on top, secured lightly with a custom clamp. With the v-groove array and lid now possessing the correct separation, fibres can be slid in, channel by channel. UV-cure epoxy is introduced and drawn into the array from the front by capillary action. Appropriate masking when exposed to a UV curing light ensures only adhesive in the v-channels is hardened - excess uncured adhesive can be washed away subsequently with solvent. A specialist external contractor undertakes the assembly polishing, and afterwards the polished face can be AR coated directly (applying a thin AR coated glass window – a so-called “meniscus lens” - is a practical alternative). A protective housing will be designed to support each pseudo slit in the focal plane, with provision of suitable furcation tubing / conduit to route fibres out of the spectrograph enclosure.

LUCA - Calar Alto 3.5 metre Telescope - IFU-6000 Fibre System Feasibility Study

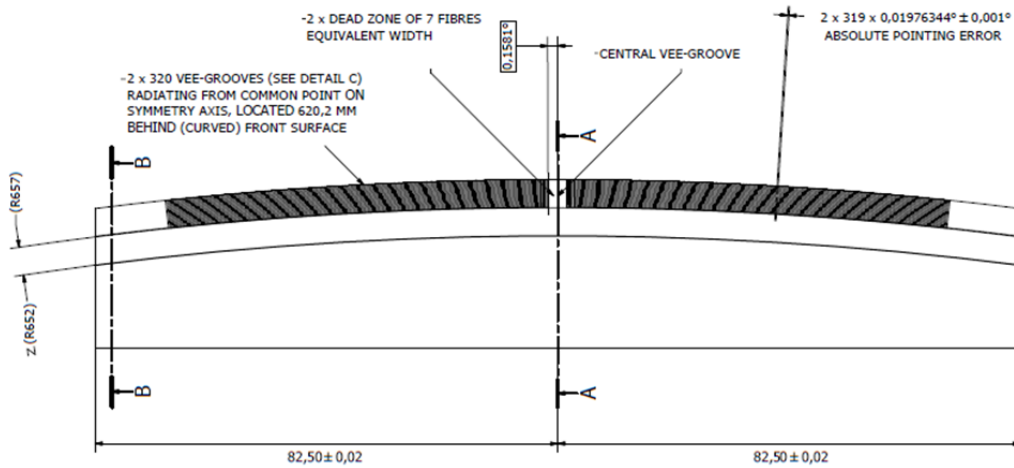


Figure 15. Layout of the v-groove array. Lid not shown

Description	Measured Value	Requirement
V-groove angular spacing	$0.019749 \pm 0.000003^\circ$	$0.01976344 \pm 0.001^\circ$
Location of convergence point	620.5 ± 0.2 mm	620.2
V-Groove twist at extremes	$\pm 45 \mu\text{rad}$	

Table 2. Actual measurement data from this prototype.

At the time of writing the specifics of the fibre slit format are still being refined, it is likely to have non-parallel pointing and a flat front face in the current scheme. The pitch is going to be somewhere in the region of 200 μm .

8. Test strategy

A staged test strategy is of importance to the construction of a large fibre system, in order to retire potential risk wherever possible. A preliminary outline of such a strategy can be summarised as follows:

- 1) **Pre-CDR** - Initial test of a sample of fibre, to verify the intrinsic FRD & spectral transmission.
- 2) **Pre-CDR (preferably)** - Undertake a fill-factor test – fibres are installed into a candidate furcation tube to ascertain the FRD performance versus packing fraction.
- 3) **At the cable factory**
 - a) FRD test of a sample of fibres after feeding fibres into furcation tube.
 - b) After stranding the cable - Continuity test of all fibres to confirm none broken, then FRD test (again a sample of fibres in system).
- 4) **In parallel**
 - a) Metrology of 2-D hole-array components.
 - b) FRD test of assembled 2-D monolithic input prototype (few fibres, to verify bonding strategy).
 - c) Optical quality test of microlens array.
 - d) Metrology (pitch) and optical quality test of microlens array.
 - e) Bonding strategy refined with a sample v-groove array.
 - f) FRD test of this sample v-groove assembly.
 - g) Metrology of actual v-groove pseudo-slit plates.
- 5) FRD testing and pointing test following slit construction.
- 6) IFU pointing verification after microlens array installation.
- 7) End to end fibre system performance tests.

LUCA - Calar Alto 3.5 metre Telescope - IFU-6000 Fibre System Feasibility Study

9. Timeline estimates

Below is a preliminary estimate of the timeline of the construction phases of the fibre system following FDR. The schedule is tentative and relates to the fibre system only. In practice this will need to be considered within the framework of the overall project plan and will be revised accordingly.

Item	Year 1						Year 2						Year 3		
	J/F	M/A	M/J	J/A	S/O	N/D	J/F	M/A	M/J	J/A	S/O	N/D	J/F	M/A	M/J
Fibre manufacture															
Cable production															
Slit design															
Slit hardware mfr															
Slit assembly															
Slit polishing															
Input hardware design															
Input hardware mfr															
µlens mfr, AR coat															
µlens test															
Input assembly															
Input polish															
Microlens install, test															

10. Cost estimates

Figures are based on experience with previous projects. Actual quotations shall be requested during the Final Design phase, therefore a 20% contingency should be factored into these baseline estimates.

Estimated costs – AAO Design (hardware and materials only)			
Item	Unit cost	Quantity	Sub-total
Fibre	€1.2 / metre	216km	€260K
Slit unit hardware	€35K / slit	8	€280K
Slit unit polishing	€5K / slit	8	€40K
IFU Input hardware and optics	€20K	1	€20K
Cable production at PPC (hardware)	€25K / cable	8	€200K
	Total:		€800K

Estimate of total staff time required – similar for both cases: 2 × FTEs over 2.5 years.

LUCA - Calar Alto 3.5 metre Telescope - IFU-6000 Fibre System Feasibility Study

11. References

- [1] Murray, G. J. et al. "Design and construction of the fibre system for FMOS" Proc. SPIE 7014, 70145L (2008)
- [2] Tamura, N. et al. "Prime Focus Spectrograph (PFS) for the Subaru Telescope: Overview, recent progress, and future perspectives" Proc. SPIE. 9908, 99081M (2016)
- [3] Schmoll, J. et al. "Design and production of the DESI fibre cables" Proc. SPIE 10702, 107027N (2018)
- [4] Murray, G. J. et al. "An optimal method for producing low-stress fibre optic cables for astronomy", Proc. SPIE 10401 (2017)
- [5] Mahlke, G. Gössing, P. [Fiber Optic Cables, Fundamentals, Cable Design, Systems Planning], 4th Edition, Publicis MCD Corporate Publishing, pp 126-128 (2001)
- [6] Oberg, E. Jones, F. Horton, H. Ryffel, H. McCauley, C. [Machinery's Handbook], 28th Edition, Industrial Press, pp. 87-91 (2008)





APPENDIX B



IFU-6000 Feasibility Study Report (pre-optics and spectrograph)



LUCA FEASIBILITY STUDY REPORT

Rev No.	Document Authors/Contributors	Approval	Date
1	J. Lawrence, R. Content, A. Lopez Sanchez, M. Mahesh, H. McGregor		27 June 2019
		J. Lawrence	
2	J. Lawrence, R. Content, A. Lopez Sanchez, M. Mahesh, H. McGregor		1 July 2019
		J. Lawrence	



1	INTRODUCTION	6
1.1	Report Scope	6
2	OPTICAL DESIGN	7
2.1	System	7
2.2	Fore-Optics, IFU, and Spectrograph Injection	8
2.2.1	Baseline Design	8
2.2.2	MLA Design	8
2.2.3	Compact Design	9
2.3	Spectrograph.....	9
2.3.1	Reference Designs	9
2.3.2	LUCA Baseline Design	10
2.3.3	MLA Design	11
2.3.4	Compact Design	13
3	PERFORMANCE	14
3.1	Image Quality	14
3.1.1	Baseline Design	14
3.1.2	MLA Design	17
3.1.3	Compact Design	20
3.2	Throughput	22
4	FIBRE SLIT	23
4.1	Considerations	23
4.2	Reference Instruments	23
5	MECHANICAL DESIGN	24
5.1	Reference Designs	24
5.2	Overall Mechanical Assembly	25
5.3	Structure	28
5.4	Collimator.....	29
5.5	Grating.....	30
5.6	Camera.....	31
5.7	Detector Cryostat.....	32
5.8	Fore-Optics Mechanical Design.....	33
6	COST AND SCHEDULE TO FINAL DESIGN	34
6.1	Scope of Work.....	34
6.2	Costing.....	34
6.3	Schedule	34
7	COST AND SCHEDULE TO SPECTROGRAPH DELIVERY	35
7.1	Scope of Work.....	35
7.2	Cost Estimate.....	35
7.3	Schedule	36



7.4	Co-Contributions	36
8	RISK ANALYSIS	37
9	AAO-MQ CAPABILITIES AND HERITAGE	38
9.1	The AAO-MQ Technology Group	38
9.2	Key Staff Expertise	40
9.3	AAO Consortium	42
9.4	Astronomy Linkages	42
10	ADDITIONAL SCIENCE PROGRAMS	43
10.1	Galactic HII Regions	43
10.2	Evolved Low-Mass Stars and Planetary Nebulae	43
10.3	Non-Local Galaxies, Galaxy Groups and Galaxy Clusters	44

GLOSSARY OF TERMS

2dF	2 degree field; a 400 fibre robotic positioner and field corrector at the AAT
4MOST	4 Metre Multi-object spectrograph Telescope; a high multiplex spectrograph for the VISTA telescope
AAO	Australian Astronomical Optics – formerly the Australian Astronomical Observatory
AAO-MQ	Australian Astronomical Optics at Macquarie University
AAO-Stromlo	Australian Astronomical Optics at the Research School of Astronomy and Astrophysics, Mount Stromlo, Australian National University
AAO-USyd	Australian Astronomical Optics at the University of Sydney
AAOmega	a multi-object spectrograph on the AAT
AAT	Anglo-Australian Telescope
AESOP	AAO-ESO Positioner; a fibre positioner for 4MOST
AIT	assembly, integration and testing (phase)
AGB	active galactic nuclei
AGN	asymptotic giant branch
AST3-NIR	a near-infrared camera for a wide field Antarctic Telescope
COTS	commercial off the shelf (product)
CYCLOPS-2	fibre feed for UCLES at the AAT
ESO	European Southern Observatory
FMOS-Echidna	Fibre Multi-Object Spectrograph for Subaru
FOV	field of view
FRD	focal ratio degradation
G-CLEF	a high resolution spectrograph for the GMT
GHOST	Gemini High resolution Optical SpecTrograph
GMACS	a multi-object spectrograph for the GMT
GMT	Giant Magellan Telescope
GNOSIS	a photonic OH suppression fibre feed for the AAT
Hector	a highly multiplexed deployable IFS for the AAT
HERMES	High Efficiency and Resolution Multi-Element Spectrograph, on the AAT
ICD	interface control document
IFU	integral field unit
IRIS2	infrared multi-object spectrograph for the AAT
KOALA	1000 element integral field unit fibre system for the AAT



LUCA	Local Universe from Calar Alto
MANIFEST	a fibre positioner for the GMT
MLA	microlens array
MOS	multi-object spectrograph
MQAAstro	Macquarie University Astronomy, Astrophysics and Astrophotonics Research Centre
OzPoz	a fibre positioner for ESO's VLT
PNe	planetary nebula
PRAXIS	an OH suppression system and spectrograph
PSF	point spread function
SAMI	a deployable IFU fibre system at the AAT
TAIPAN	multi-object spectrograph and positioner system for UKST
UCLES	a high resolution echelle at the AAT
UKST	United Kingdom Schmidt Telescope at Siding Spring Observatory
Veloce	a fibre-fed high resolution Echelle spectrograph at the AAT
VISTA	a 4m telescope at ESO's Paranal Observatory
VLT	Very Large Telescope; four 8m telescopes run by ESO
VPH	volume phase holographic (grating)

1 INTRODUCTION

This document presents the AAO-MQ contribution to the Local Universe from Calar Alto (LUCA) instrument feasibility study. LUCA is a new instrument concept for a fibre-optic integral-field-unit spectrograph for the 3.5 m Calar Alto Telescope.

1.1 Report Scope

Following the service proposal described in the contract research agreement executed on 21 Jan 2019, this report covers the following items that are presented as separate Chapters:

- the optical design for the complete instrument system, including fore-optics, fibre input and output microlens arrays, and the spectrograph;
- an analysis of the performance of the optical design, including system spot diagrams, image quality analysis, throughput estimates, and efficiency calculations;
- recommendations on fibre packaging at the spectrograph entrance slits;
- details of the opto-mechanical approach to design and assembly for the instrument spectrographs, including the detector cryostat and interface;
- a cost estimate and timeline for the final optical design and optical engineering for the complete instrument system;
- a cost estimate and timeline for the mechanical design, parts procurement, assembly, integration, testing, and delivery of the instrument spectrographs;
- a risk analysis associated with the spectrograph delivery;
- details of the capabilities and heritage of the AAO's Technology Group; and
- identification of additional science programs for the instrument.

2 OPTICAL DESIGN

2.1 System

The optical design for the overall instrument system is driven by the specifications shown in Table 1.

Table 1. Specifications for key system parameters

Parameter	Baseline design	MLA design	Compact design
Telescope injection	f/10	f/10	f/10
IFU injection	bare fibre	MLA	bare fibre
On-sky FOV diameter per aperture (arcsec)	2.52	2.52	2.18
On-sky FOV per aperture (arcsec ²)	5.0	5.0	3.7
Total number of fibres for the IFU	6000	6000	7722
On-sky FOV for IFU (arcmin ²)	8.3	8.3	8.0
Total FOV for IFU (arcmin ²)	15.3	9.1	14.8
IFU fill factor	54%	91%	54%
Number of fibres per spectrograph	750	750	594
Number of spectrographs	8	8	13
Wavelength coverage (nm)	360-685	360-685	360-685
Spectrograph arms	1	1	1
Resolution at 500 nm	2000	2000	2000
Detector format (number of pixels)	4k x 4k	4k x 4k	4k x 4k
Detector pixel size (µm)	15	15	15
Resolution range (over bandpass)	1440-2740	1440-2740	1440-2740
Fibre core/cladding/buffer (µm)	150/170/190	100/TBD/TBD	150/170/190
Projected slit width (µm)	150	150	150
Slit length (mm)	162.9	162.6	128.9
Output f/ratio fore-optics	f/3.51	f/3.51	f/4.06
Input f/ratio collimator	f/3.43	f/3.43	f/3.97
Camera f/ratio	f/1.26	f/1.28	f/1.47
Fibre core average diameter (pixel)	3.71	3.73	3.73
As-designed PSF (maximum RMS in micron at the 9 designed wavelengths)	12.6	12.6	12.6

We have developed designs for a baseline version that uses bare fibre injection, a version that uses microlens arrays (MLAs), and a compact design with lower spectrograph unit cost (and lower areal coverage per spectrograph).

2.2 Fore-Optics, IFU, and Spectrograph Injection

2.2.1 Baseline Design

The optical design layout for the fore-optics for the baseline version, with bare-fibre injection, is shown in Figure 1. This is a relatively simple design using a doublet and 2 singlet lenses as an optical relay converting the $f/10$ beam from the telescope focus to give $f/3.5$ at the intermediate focus where the fibre IFU is located. Three of the surfaces are aspheres.

The fibre IFU consists of 6000 fibres in a close-packed array. The $150\ \mu\text{m}$ core diameter fibres are packed with a pitch of $\sim 194\ \mu\text{m}$ (representing the fibre buffer plus tolerance) giving a total field-of-view of $15.3\ \text{arcmin}^2$. This IFU has a fill factor of $\sim 54\%$.

At the output of the fibre cable is a bare fibre slit that is bonded or gelled to the first spectrograph lens. The nominal pitch of fibres along the slit is $\sim 220\ \mu\text{m}$ – though this must be modified to account for any additional sky fibres, calibration fibres, or for spacing between slit blocks.

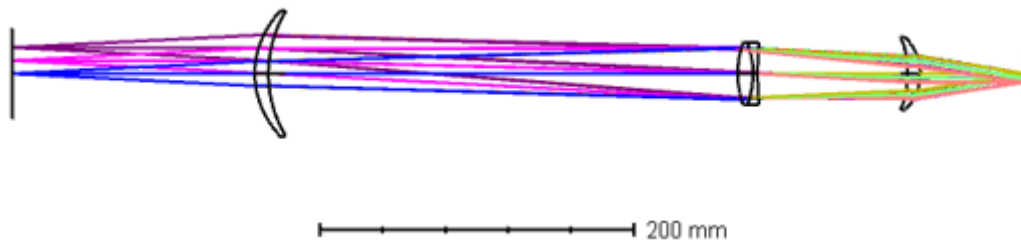


Figure 1. Fore-optics optical design.

2.2.2 MLA Design

For injection into the MLA system, we have arrived at a solution that does not require any fore-optics. An air-spaced pair of MLAs is mounted to the fibre array (see Figure 2). In this option, a $100\ \mu\text{m}$ core fibre is used (to avoid vignetting with a larger fibre), though the actual fibre core size should be optimised based on further analysis. This has an equivalent sky slit width per aperture to the bare fibre version (i.e., the output MLA gives $150\ \mu\text{m}$ wide images). The MLA fore-optics are mounted directly at the telescope $f/10$ Cassegrain focus. The use of 2 MLAs is used to minimise geometric FRD, though solutions may be also possible using a single MLA.

Circular microlens arrays are used in this version with a fill-factor of $\sim 91\%$. In further iterations of the design higher fill-factor hexagonal microlens arrays may be considered instead for the MLAs.

At the output of the fibre cable, the fibre slit (of bare fibres) is bonded to a MLA (Figure 3). The pitch of the fibres matches the pitch for the MLA and is approximately equivalent to that in the baseline version (i.e., $\sim 220\ \mu\text{m}$) with the same caveats. In this option, there is a spacing between the MLA and the first spectrograph lens.

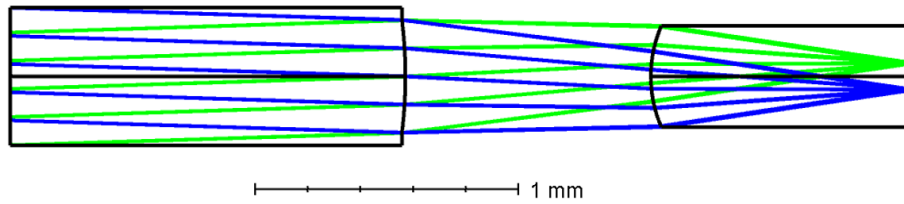


Figure 2. MLA optical design for injection into the fibre array. The telescope focal plane lies at the first surface on the left. The fibre is bonded to the rear of the right-most surface.

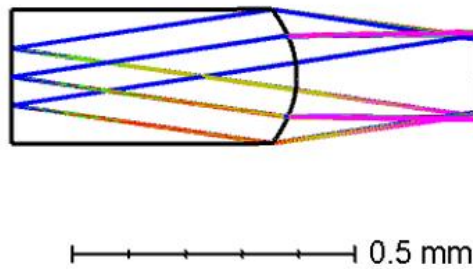


Figure 3. MLA design for injection into the spectrograph. The output fibre slit lies at the first surface on the left. The projected spectrograph slit is at the right of the fibre.

2.2.3 Compact Design

The fore-optics and IFU designs for the compact spectrograph will be similar to the optical layout as presented for the baseline design. No specific optical layout has been produced for this option. The same core diameter 150 μm fibres are used as for the baseline design, though the fore-optics magnification should be changed to give smaller sky coverage per fibre (2.18" compared to 2.52"). To achieve the same total sky area will thus require more fibres, 7722, in the IFU. Like the baseline solution the IFU is close-packed array with a fill factor of $\sim 54\%$.

At the output of the compact design is a bare-fibre slit that is bonded to the first spectrograph lens. As for the baseline design, the nominal pitch of fibres along the slit is $\sim 220 \mu\text{m}$ – though this must be modified to account for any additional sky fibres, calibration fibres, or for spacing between slit blocks.

2.3 Spectrograph

2.3.1 Reference Designs

The spectrograph optical design for LUCA is based on the Hector spectrograph currently being delivered for the Anglo-Australian Telescope. The optical layout for Hector is shown for reference in Figure 4. Hector is an all-refractive dual channel design that has been cost optimised to provide high throughput and efficiency. Substantial trade-off studies have arrived at the selection of the Hector configuration based on cost and provided scientific benefit. These trade-offs considered other design styles, such as catadioptric systems with Schmidt collimators and/or Schmidt cameras.

Hector was itself based around a scaled up version of the relatively low resolution ($R \sim 2300$) TAIPAN spectrograph (see Figure 5) that was installed at the UK Schmidt Telescope in 2017 for use with the TAIPAN fibre positioner system.

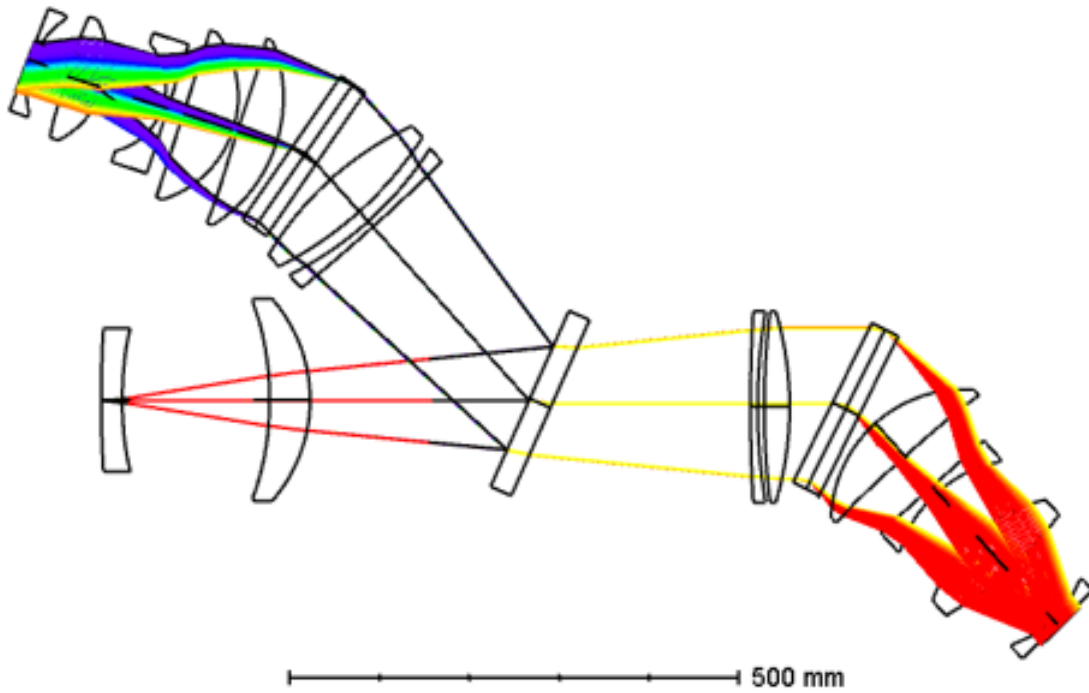


Figure 4. Optical design layout for the Hector spectrograph for the AAT.

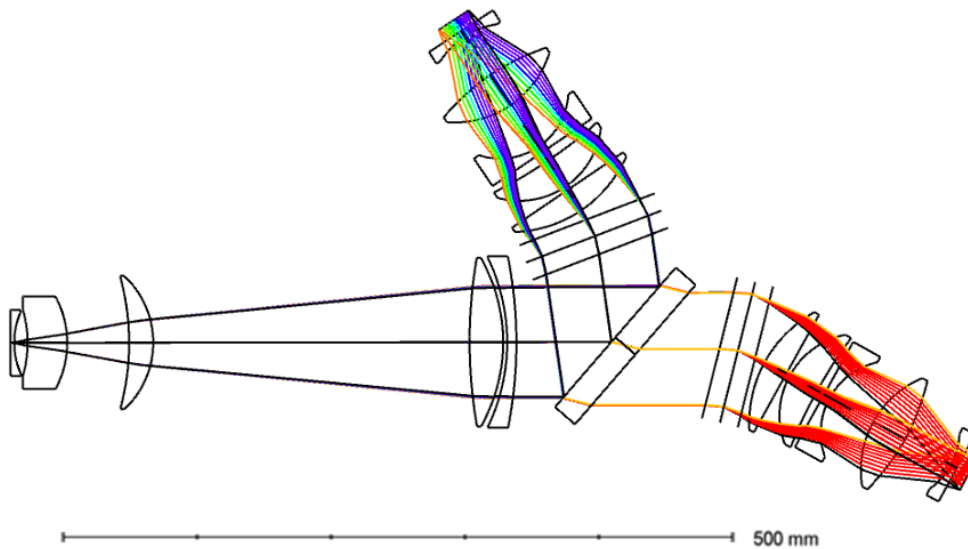


Figure 5. Optical design layout for the TAIWAN spectrograph for the UKST. Note optics relative to scale bar in comparison to the other designs.

2.3.2 LUCA Baseline Design

The optical design layout for the LUCA spectrograph is given in Figure 6. The design is a single channel using all singlet lens. For the baseline we assume no MLAs are included on the slit, rather the fibres output $\sim f/3.4$ directly to the spectrograph. The fibres are mounted against the first spectrograph lens using glue or index matching gel.

This design incorporates a four element collimator (including the slit lens) and a five element camera. All lenses have one aspheric surface, though the degree of aspheric departure is quite low ($<200\ \mu\text{m}$) for all the lenses except two. All glasses use have low absorption across the full wavelength range for the spectrograph. The average lens diameter is $\sim 200\ \text{mm}$.

There is a large spacing between the 3rd and 4th collimating lenses. This could be used to add an upgrade with a longer wavelength second arm in the future if desired.

The dispersive element in the baseline design is a volume phase holographic grating, as used in both Hector and TAIPAN spectrographs. The LUCA grating is $\sim 700\ \text{lines/mm}$ with a diameter of $\sim 240\ \text{mm}$ (cf., Hector uses a $220\ \text{mm}$ grating with a line frequency of $1200\ \text{lines/mm}$ grating, and TAIPAN uses a $108\ \text{mm}$ grating with a line frequency of $900\ \text{lines/mm}$).

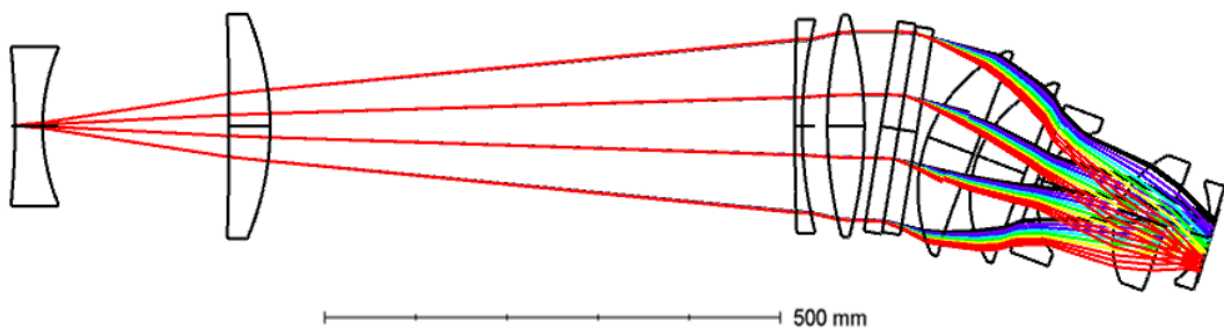


Figure 6. Optical layout for LUCA baseline design.

2.3.3 MLA Design

The design is modified to provide the possibility of using microlens arrays to adjust the focal ratio and allow tighter fibre packing. The full trade-off to understand which option is preferred should be completed during the next phase of the project. The modified design is shown in Figure 7 which provides a flat focal surface for mounting the fibre slit array to the MLA. Spacing is provided before the first spectrograph lens to allow opto-mechanical mounts.

This design uses the same layout and glass types as for the baseline design. Most lenses are very similar in thickness, diameter, and curvature. The average lens diameter increases by $\sim 1\%$ and the average aspheric departure increases by $\sim 10\%$.

As for the baseline, this version uses a VPH grating with a line frequency of $\sim 700\ \text{lines/mm}$ and a diameter of $\sim 240\ \text{mm}$.

Note that the optical design layout shows a mirror between the 3rd and 4th collimating lenses. This is an artefact of the way the file was set up in Zemax. This mirror would be removed in practise so the design is similar to shown in the baseline layout.

As for the previous design, there is a large spacing between the 3rd and 4th collimating lenses. This could be used to add an upgrade with a longer wavelength second arm in the future if desired.

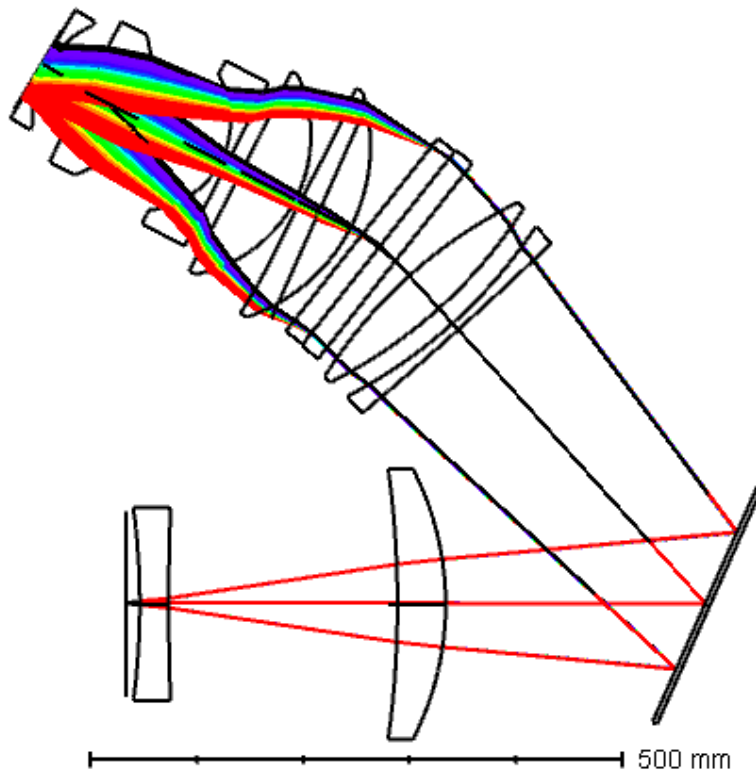


Figure 7. Optical layout for LUCA microlens array design. This design shows a mirror in the collimator but this would be removed to follow the same straight-through layout as the baseline option.

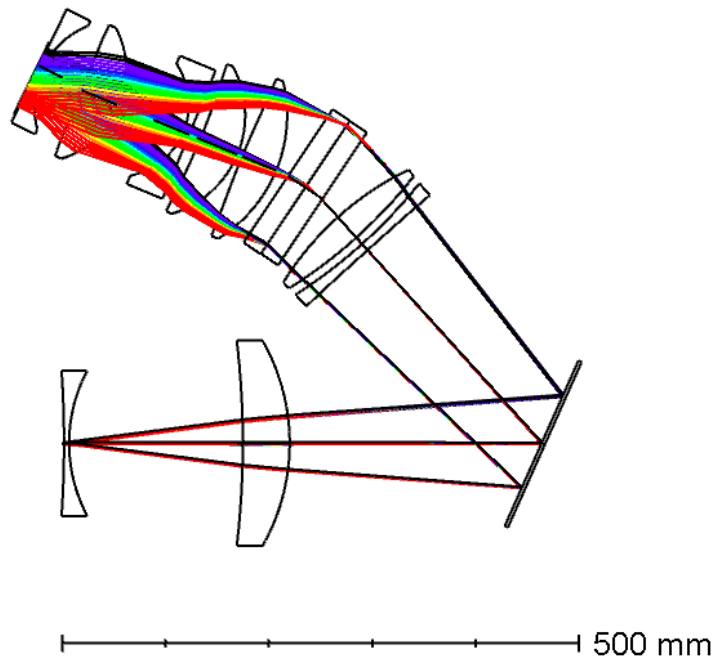


Figure 8. Optical layout for LUCA compact design. Note optics relative to scale bar in comparison to the other designs. This design shows a mirror in the collimator but this would be removed to follow the same straight-through layout as the baseline option.



2.3.4 Compact Design

To reduce unit cost, a reduced scope version is presented here. This variant has a reduced slit length and collimator focal ratio. This is thus accompanied by a reduction in the overall efficiency of the spectrograph via a decrease in the sky areal coverage (i.e., number of fibres) per spectrograph. The optical layout for this variant is shown in Figure 8. This design follows closely the lens glass type, curvatures, and element spacings as for the versions presented above but the lens diameters reduced to ~75% of the baseline design, and aspheric departures also reduced (to ~85% relative to the baseline). Note that this version is far from being cost optimized. The number of aspheres and possibly the number of lenses can likely be reduced as the specifications have been easily obtained. The compact design uses a 150 mm VPH grating of size ~150 mm.

3 PERFORMANCE

3.1 Image Quality

3.1.1 Baseline Design

The fore-optics for the bare-fibre baseline solution are designed to give excellent image quality over a 15 arcmin² field of view – see Figure 9.

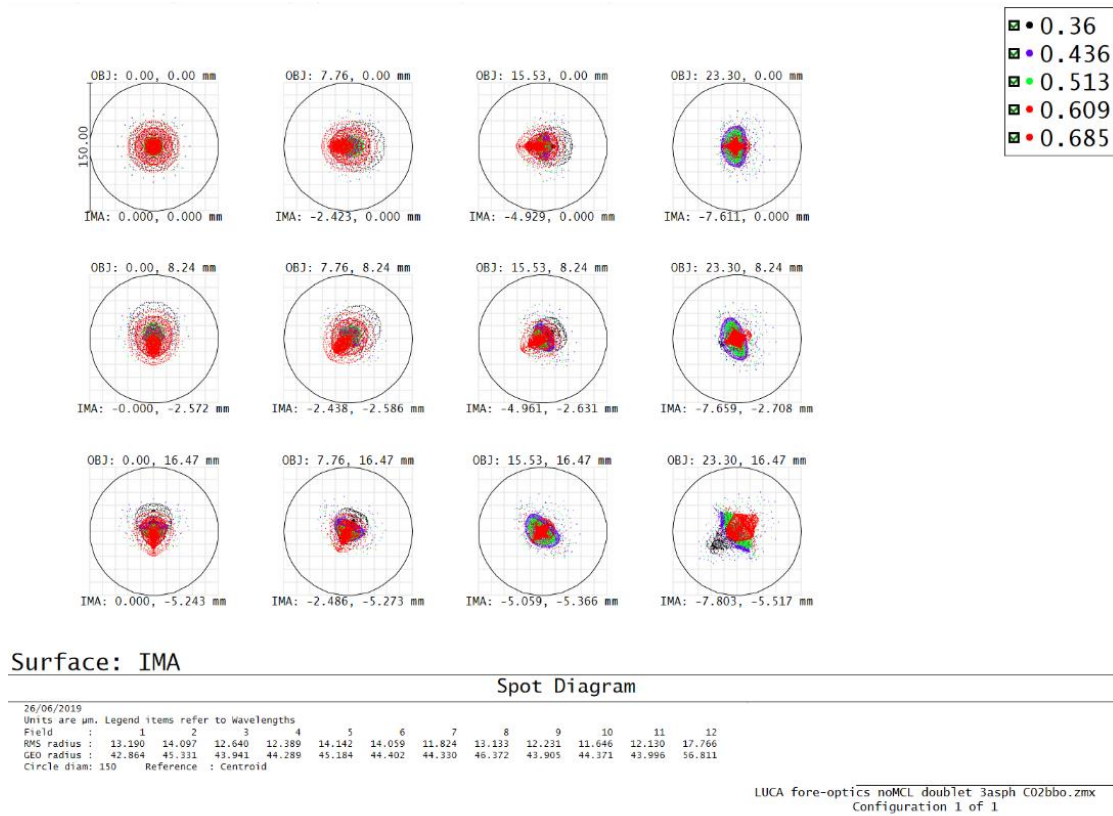


Figure 9. Fore-optics full field spot diagram at wavelengths across the full bandpass relative to the fibre core size for the baseline design.

For the spectrograph spot diagrams across the field are given in Figure 10, Figure 11, and Figure 12 for blue, center, and red edge wavelengths respectively for the baseline LUCA design. Good image quality is obtained relative to the projected fibre core size (3.7 pixels). It should be noted that the design was done to get a maximum RMS of 12.6 μm but with a limited number of wavelengths (9), fields (7) and a ray grid to fasten the calculations. This has left some regions between the used wavelengths and fields with larger RMS than 12.6 μm and even some calculated values due to the limited ray sampling. A complete optimization has been left for the next phase. The full optimisation will also include a reduction of the 45 degree PSF elongation seen in Figure 12, which could be problematic as it may lead to cross-contamination of spectra.

The Zemax reported RMS spot radius is shown versus wavelength and field position in Figure 13.

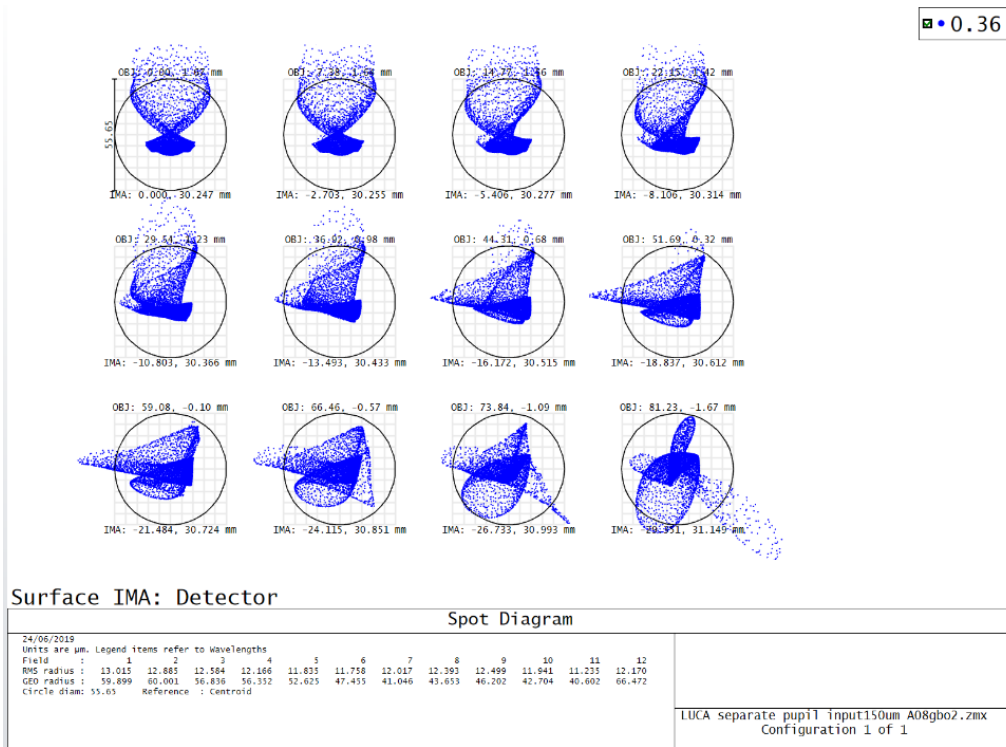


Figure 10. Full field spot diagram for the baseline design at 360 nm. The circle is the fibre core footprint.

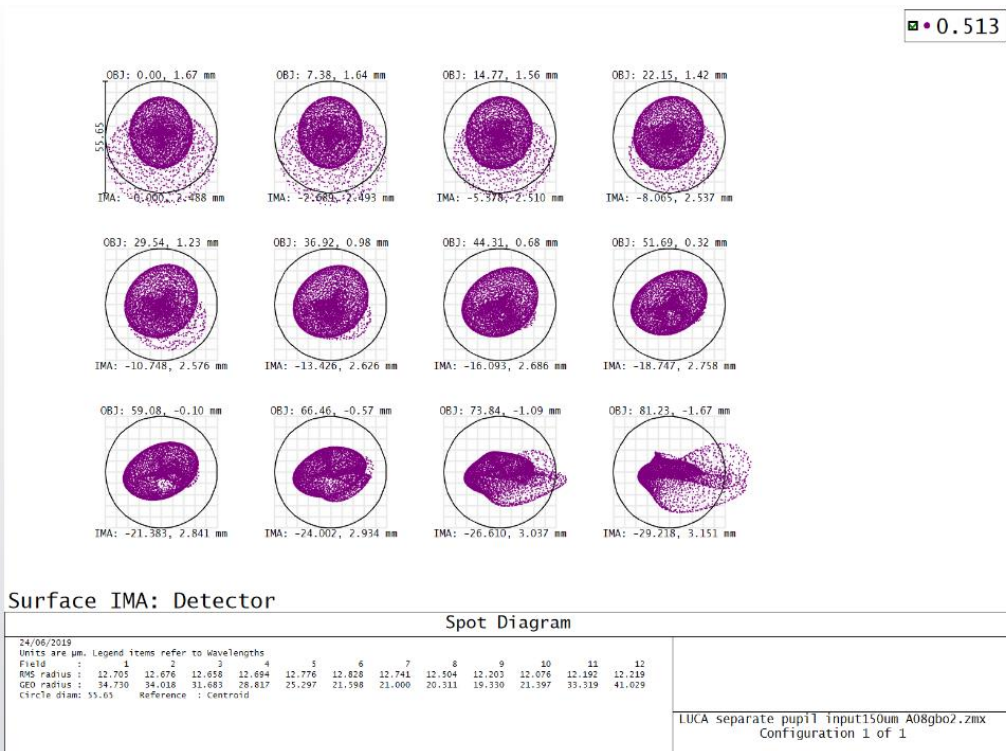


Figure 11. Full field spot diagram for the baseline design at 513 nm. The circle is the fibre core footprint.

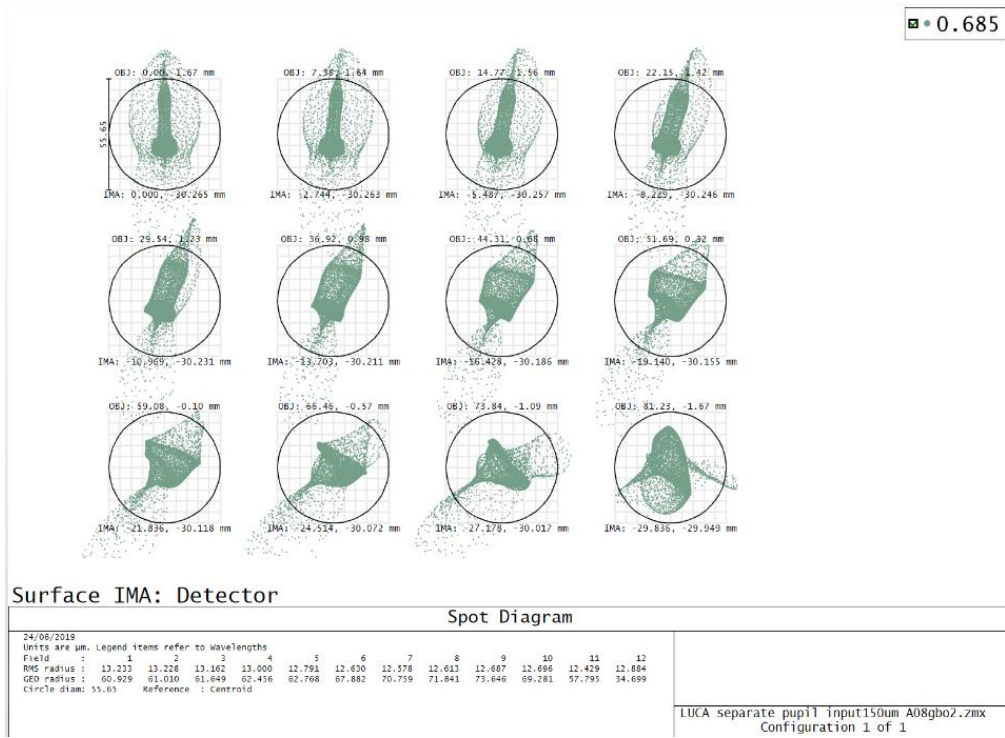


Figure 12. Full field spot diagram for the baseline design at 685 nm. The circle is the fibre core footprint.

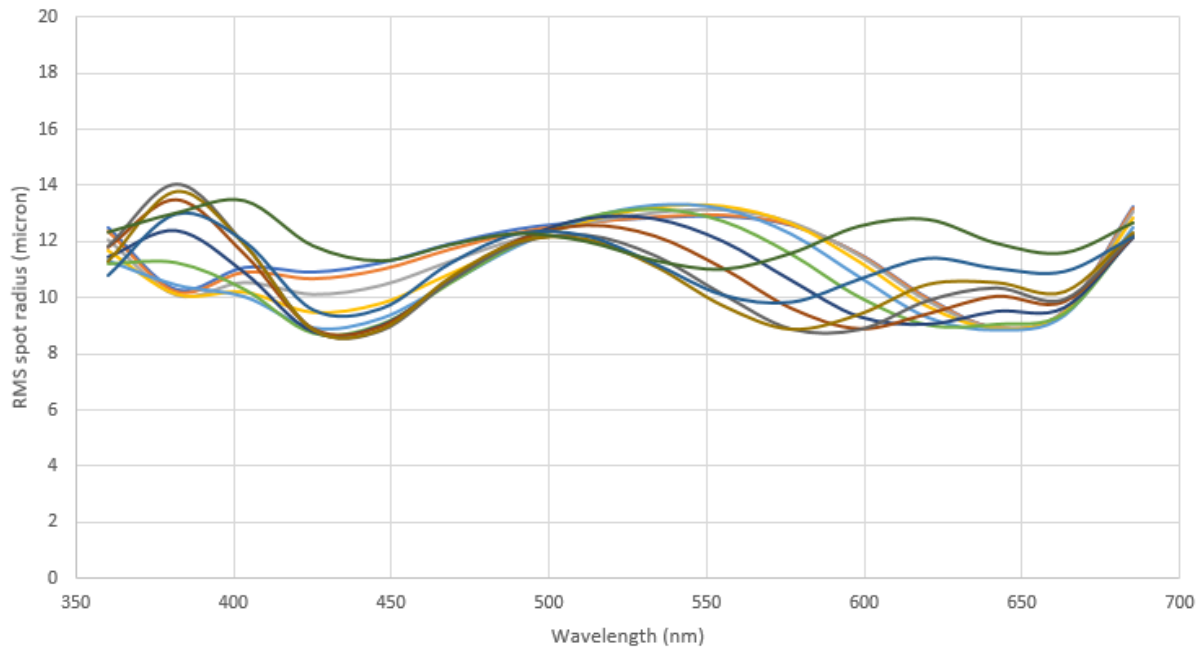


Figure 13. RMS spot radius versus wavelength for field angles along the slit for the baseline design.

3.1.2 MLA Design

Spot diagrams for the injection using the MLA pair are shown in Figure 14. Excellent image quality is obtained.

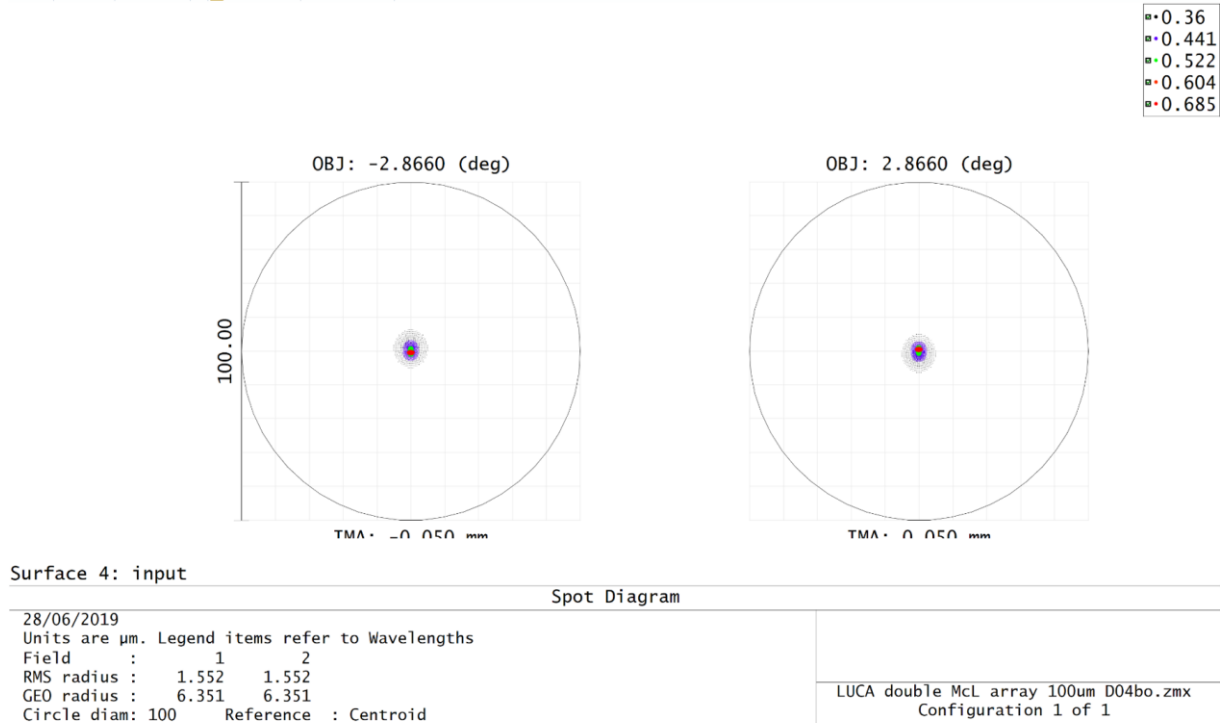


Figure 14. Spot diagram for the MLA injection system relative to the fibre core size.

For the MLA design spectrograph spot diagrams across the field are given in Figure 15, Figure 16, and Figure 17 for blue, center, and red edge wavelengths respectively for the baseline LUCA design. Good image quality is obtained relative to the projected fibre core size (3.7 pixels).

The Zemax reported RMS spot radius is shown versus wavelength and field position in Figure 18.

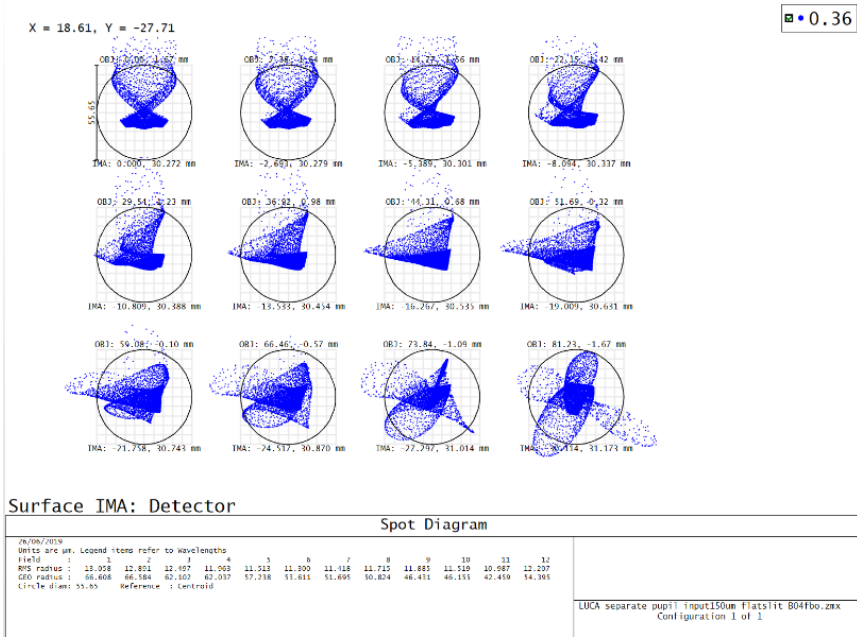


Figure 15. Full field spot diagram for the MLA design at 360 nm. The circle is the fibre core footprint.

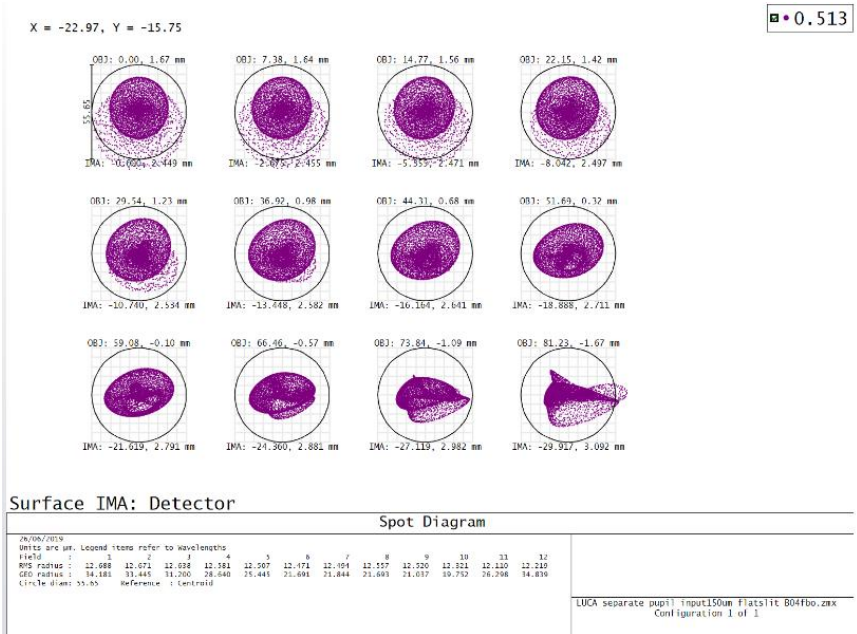


Figure 16. Full field spot diagram for the MLA design at 513 nm. The circle is the fibre core footprint.

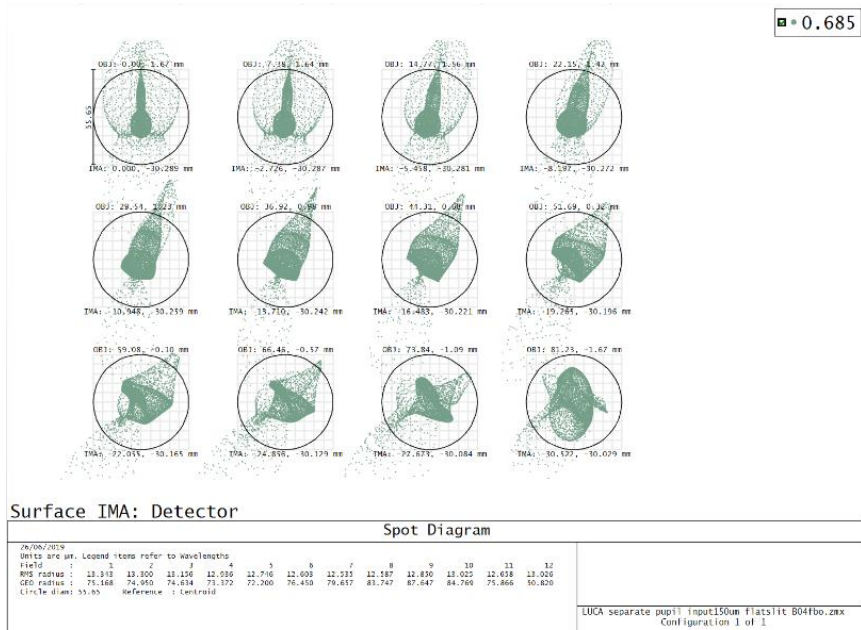


Figure 17. Full field spot diagram for the MLA design at 685 nm. The circle is the fibre core footprint.

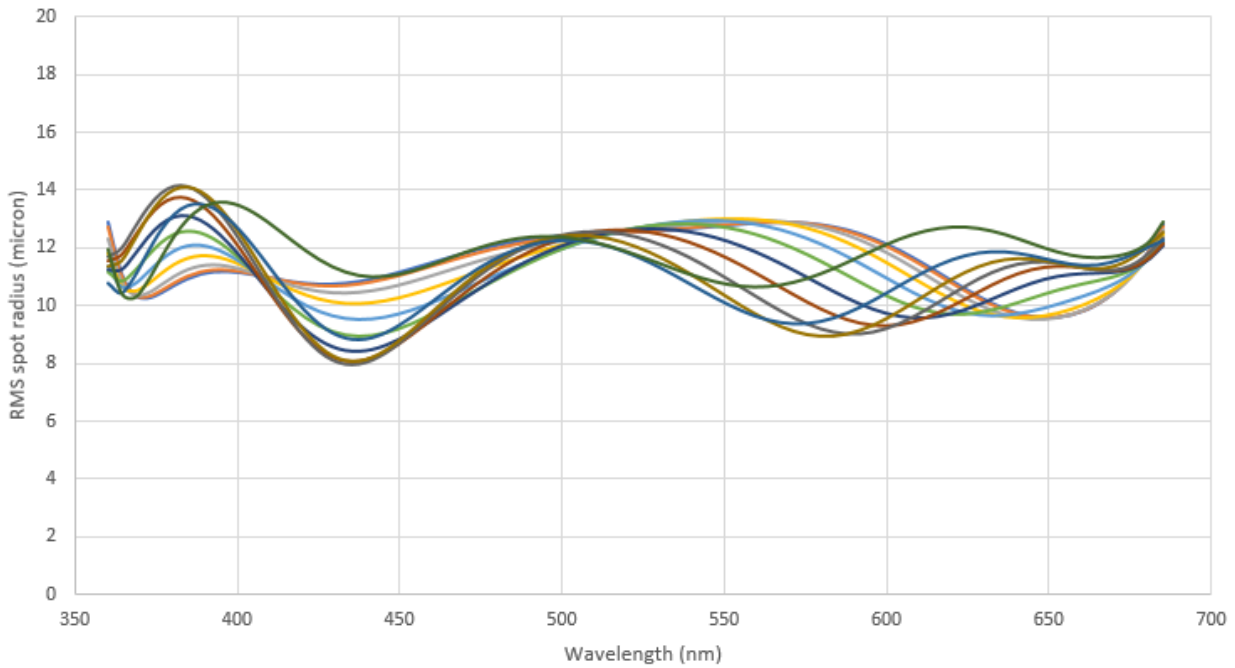


Figure 18. RMS spot radius versus wavelength for field angles along the slit for the MLA design.

3.1.3 Compact Design

For the compact design spectrograph spot diagrams across the field are given in Figure 19, Figure 20, and Figure 21 for blue, center, and red edge wavelengths respectively. Good image quality is obtained relative to the projected fibre core size (3.7 pixels). The Zemax reported RMS spot radius is shown versus wavelength and field position in Figure 22.

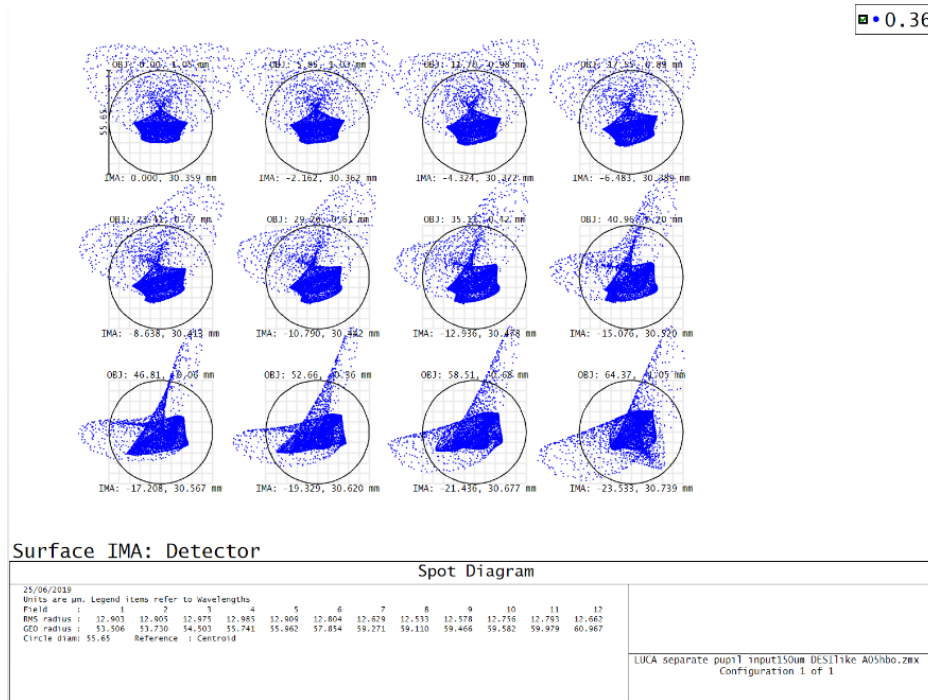


Figure 19. Full field spot diagram for the compact design at 360 nm. The circle is the fibre core footprint.

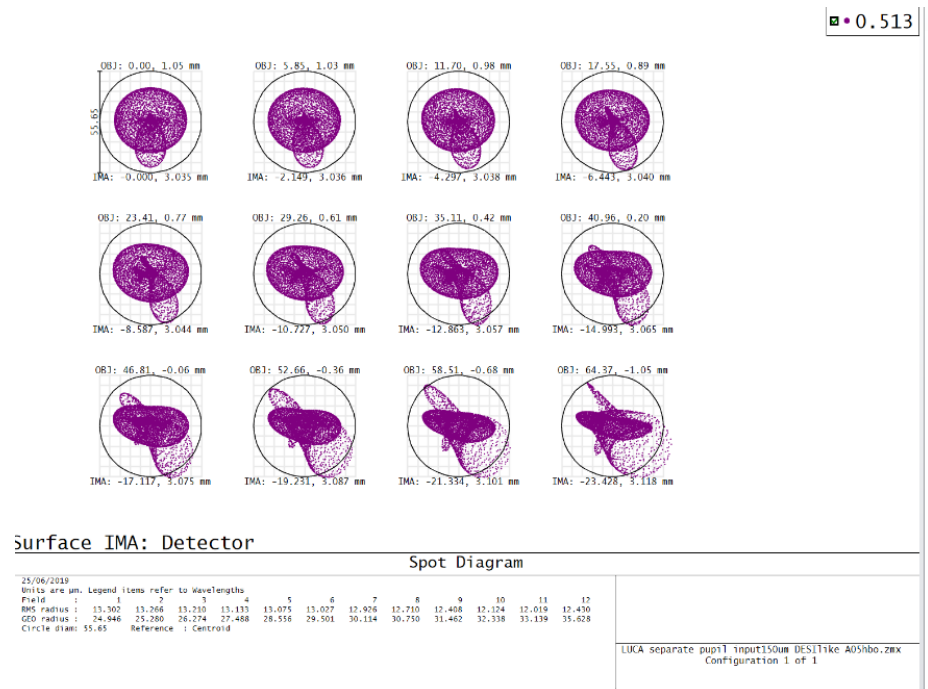


Figure 20. Full field spot diagram for the compact design at 513 nm. The circle is the fibre core footprint.

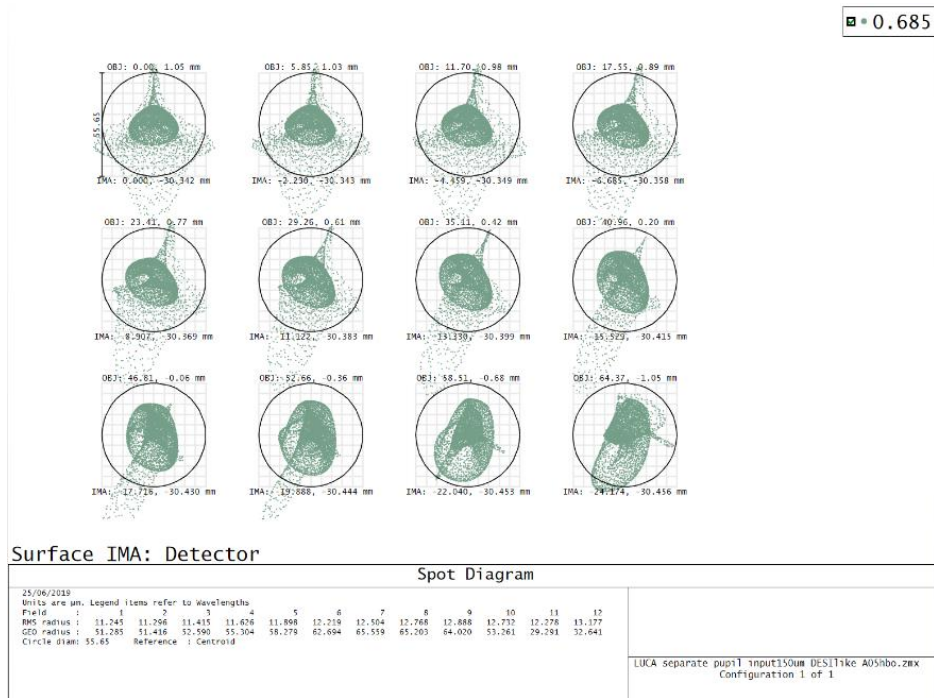


Figure 21. Full field spot diagram for the compact design at 685 nm. The circle is the fibre core footprint.

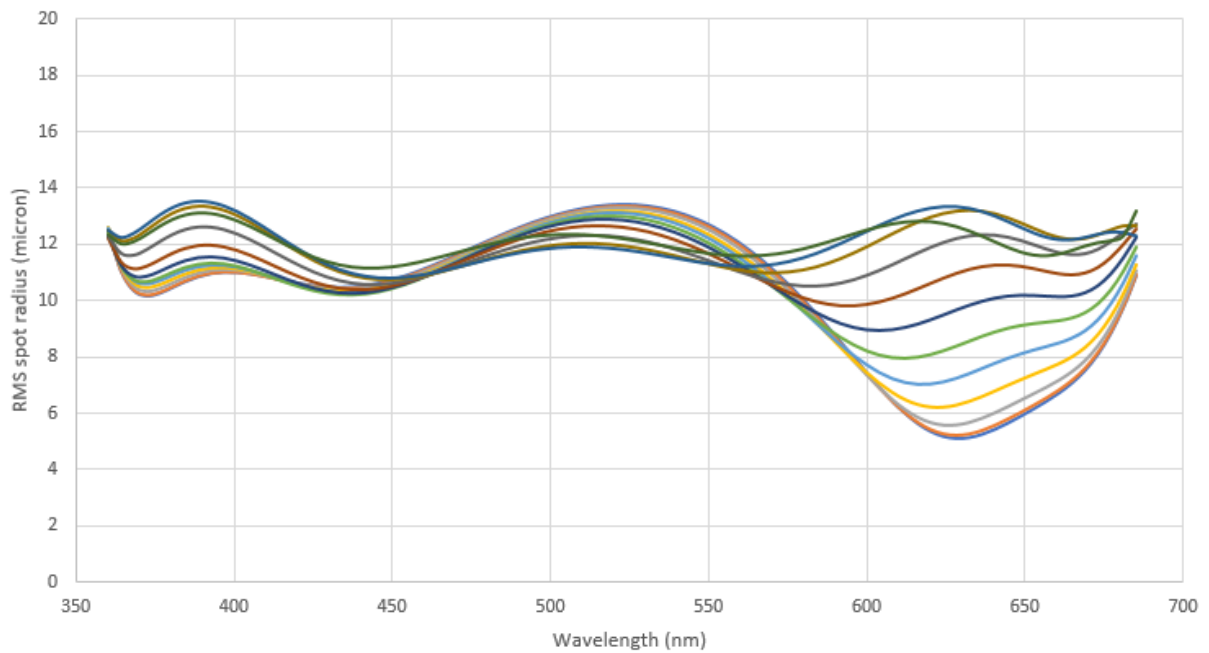


Figure 22. RMS spot radius versus wavelength for field angles along the slit for the compact design.

3.2 Throughput

Spectrograph throughput from internal absorption and lens anti-reflection coatings is shown in Figure 23. Note there is high throughput with very little dependence on wavelength for all designs. The graph is shown for the baseline design, though the other variants show only minor deviation in the blue.

No modelling of the VPH grating diffraction efficiency has been completed. The efficiency curve for this element will likely dominate the wavelength response for the instrument at the extreme edges. Some example VPH grating efficiency curves are given in Figure 24. Values should be considered for reference/illustrative purposes only. VPH grating efficiency is a function of all design parameters for the grating and thus a specific model must be developed. The bandwidth is quite large for a VPH and thus significant drop in efficiency away from the centre wavelength should be expected.

Further work should be done in the following phase to develop the full throughput model that will incorporate the grating and fibre efficiencies, and the losses due to vignetting within the spectrograph.

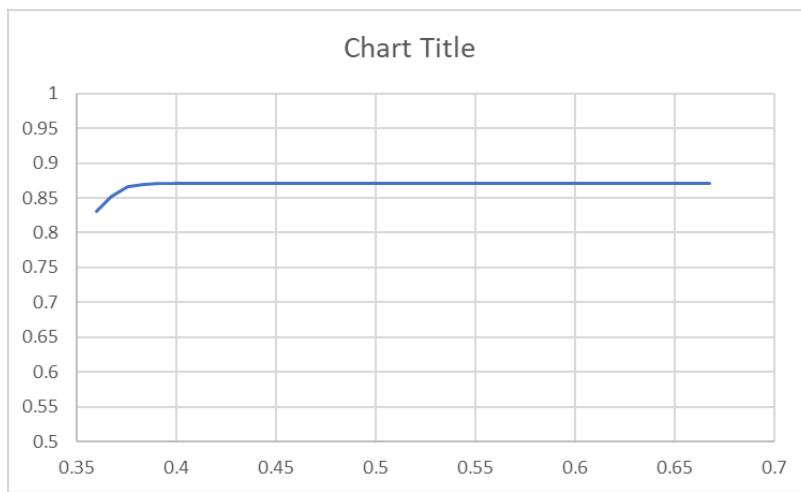


Figure 23. Spectrograph throughput from internal absorption and coatings.

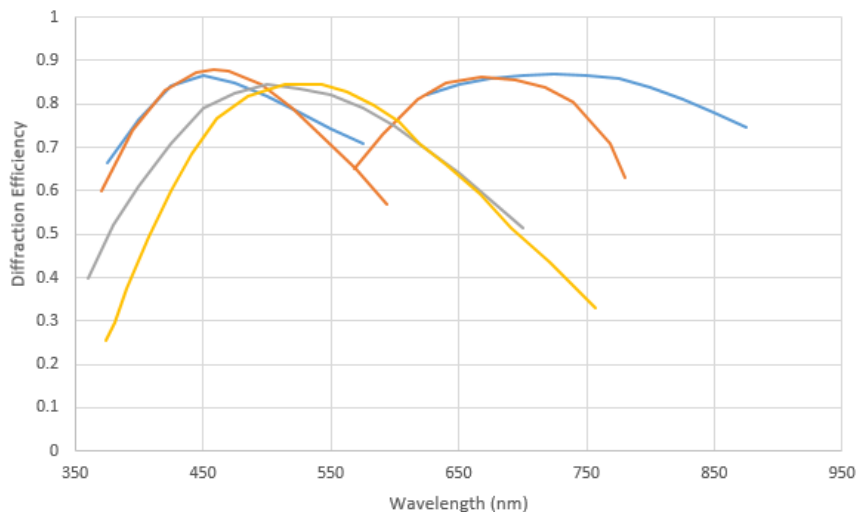


Figure 24. Illustrative VPH grating diffraction efficiencies for TAIPAN (blue), Hector (orange), and two gratings (yellow, grey) from the literature (Barden et al. 2000, Rallison et al. 2003).

4 FIBRE SLIT

4.1 Considerations

Specifications for the fibre slit, particularly concerning the packing density of fibres relative to the core size, have been developed after consideration of a number of issues:

- the overall system requirements (including the pixels per resolution element and the desired wavelength coverage);
- the size and cost of the spectrograph (i.e., as influenced by the slit length);
- the ease of spectral extraction (i.e., related to the cross talk between neighboring fibres); and
- the feasibility of construction.

For both bare-fibre baseline and microlens designs the total number of fibres is 750. For the compact version the total fibre number is 594.

4.2 Reference Instruments

For reference, the proposed fibre slit parameters can be compared to several other instruments that the AAO have experience with, as shown in Table 2. The pitch to core ratio for LUCA is consistent with large IFUs on a similar scale telescope.

Table 2. Reference instrument fibre slits

Instrument	Instrument type	Pitch of spectra (pixel)	Core diameter (pixels)	Ratio
2df at the AAT	single object MOS	10.1	3.4	3.0
HERMES at the AAT	single object MOS	10.1	5.0	2.0
Hector at the AAT	mini-IFUs	5	2.8	1.8
SAMI at the AAT	mini-IFUs	4.9	3.0	1.6
LUCA at the CAT	large monolithic IFU	5.3	3.7	1.4
KOALA at the AAT	large monolithic IFU	4.0	2.9	1.4

5 MECHANICAL DESIGN

5.1 Reference Designs

The opto-mechanical design for LUCA will follow the approach as for the TAIPAN and Hector spectrographs. The TAIPAN spectrograph, delivered and installed to the UKST is shown in Figure 25. The Hector spectrograph mechanical design is shown in Figure 26. Hector is now in fabrication phase and is due for assembly to commence in late 2019.

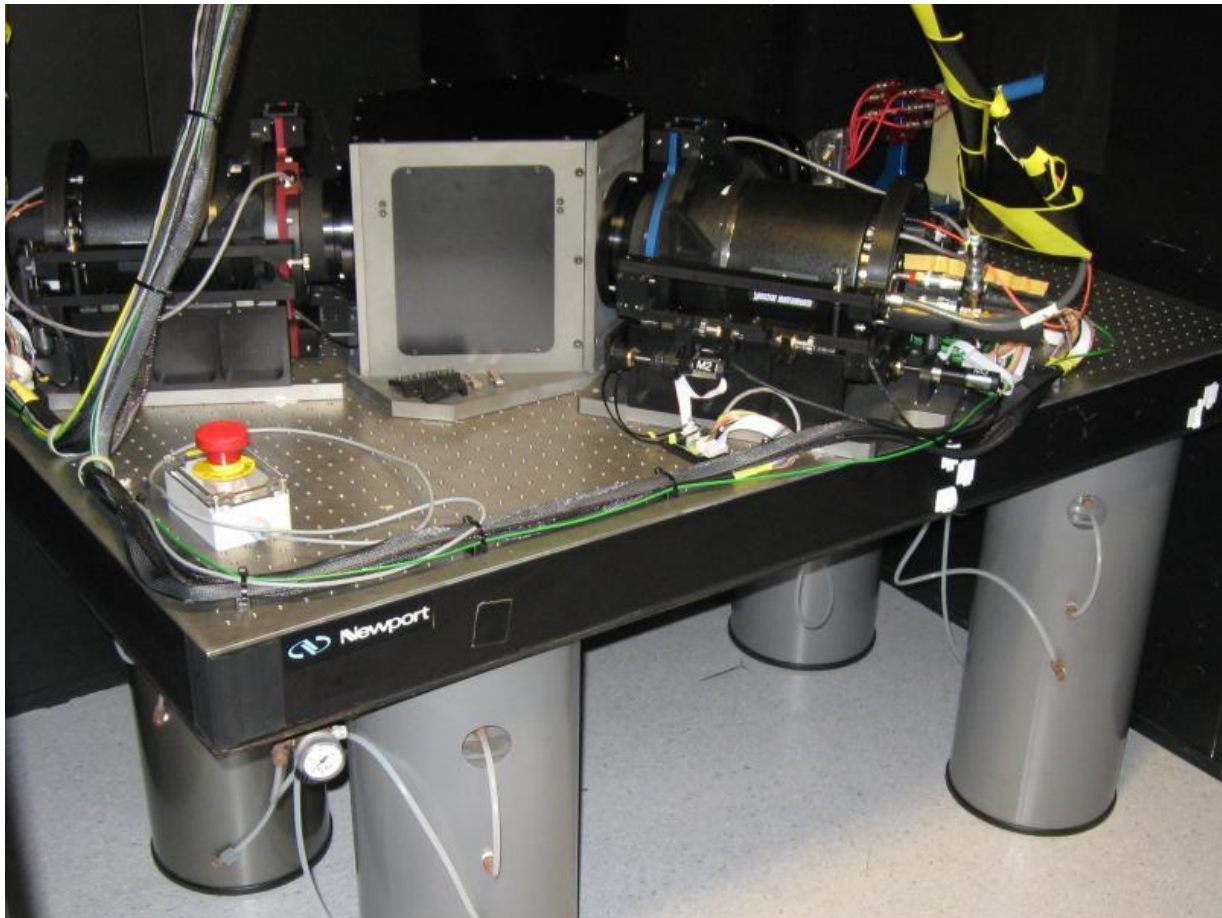


Figure 25. TAIPAN spectrograph installed at the UKST at Siding Spring Observatory.

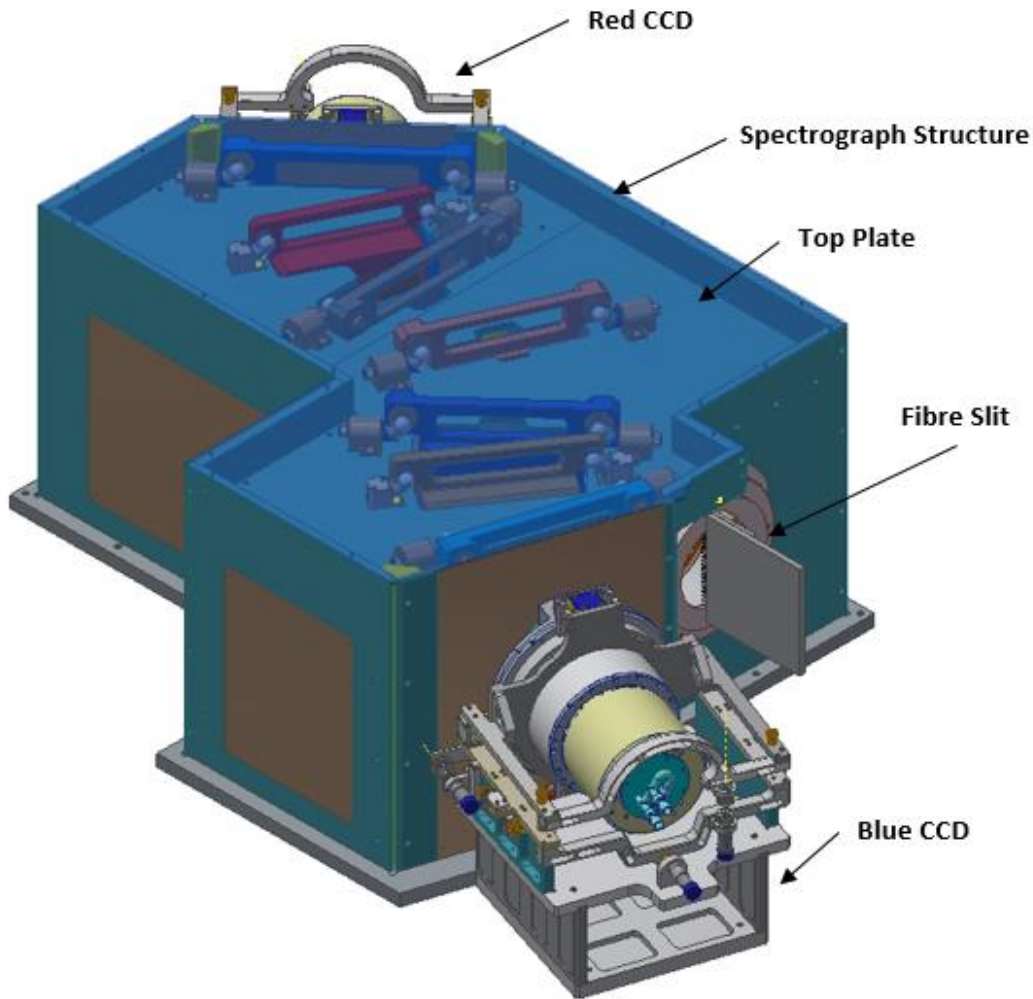


Figure 26. Hector spectrograph mechanical layout.

5.2 Overall Mechanical Assembly

The optical-mechanical layout for the LUCA spectrograph is shown in Figure 27, with labelled optical components. This layout, and the mechanical design presented in the following sections, refers to the baseline design. Only minor changes are required for the MLA design. For the compact design, the mechanical parts would be scaled down, though would follow the same principle.

The overall spectrograph mechanical assembly is to be mounted on a commercial optical table as shown in Figure 28. Cross-sections with the optical element locations are shown in Figure 29 and Figure 30. The overall assembly consists of a structural frame to which lens barrels are mounted to the frame walls. The second collimator group and the VPH grating are both installed on kinematic mounts from the top plate of the assembly frame.

A complete tolerancing analysis has not yet been conducted on the spectrograph optical design. However, detailed Monte-Carlo simulations have been completed for the Hector spectrograph. Such analysis drives requirements on the positional accuracy of optical elements to be typically 15-120 arcsec in tilt, 10-50 μm in decenter, 50-100 μm in focus. These tolerances are met with the mechanical concept design for Hector upon which this design is based.

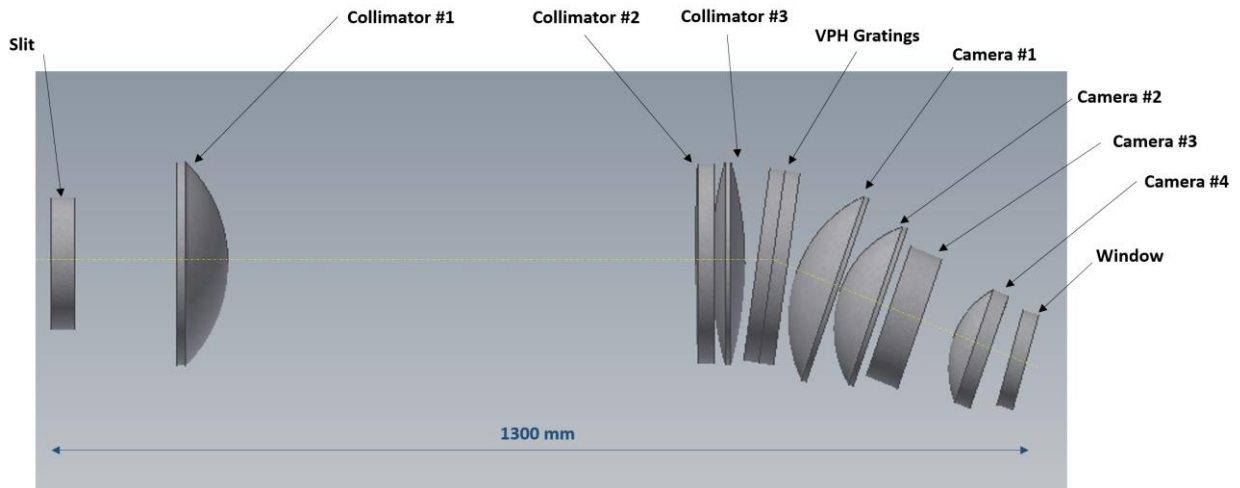


Figure 27. Opto-mechanical layout for the LUCA spectrograph.

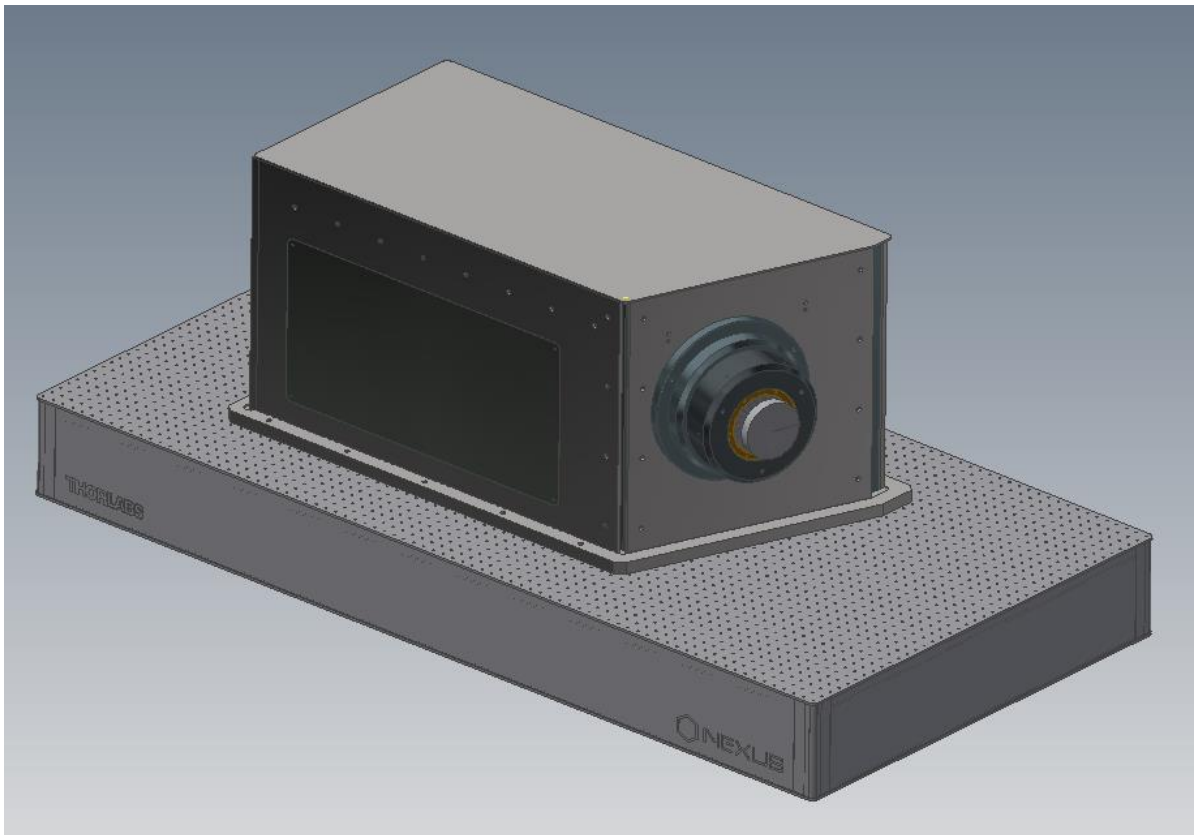


Figure 28. The LUCA spectrograph assembly mounted on COTS optical table.

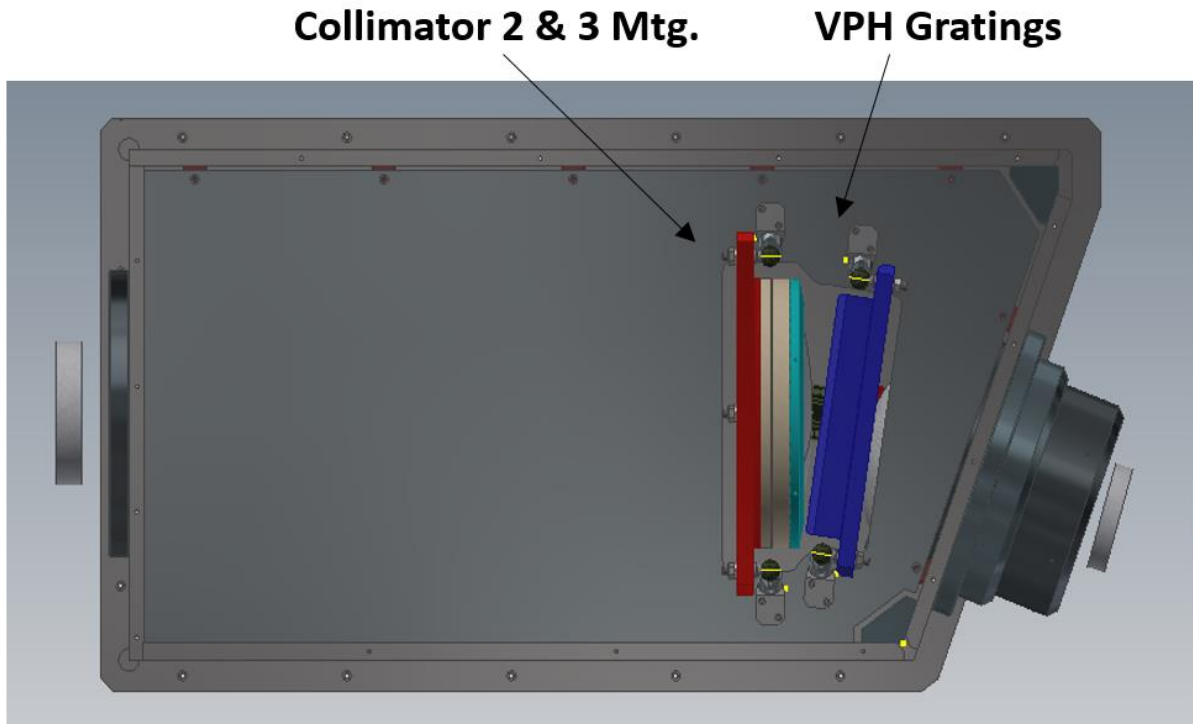


Figure 29. Cross-section from above showing the spectrograph assembly with top mounted elements.

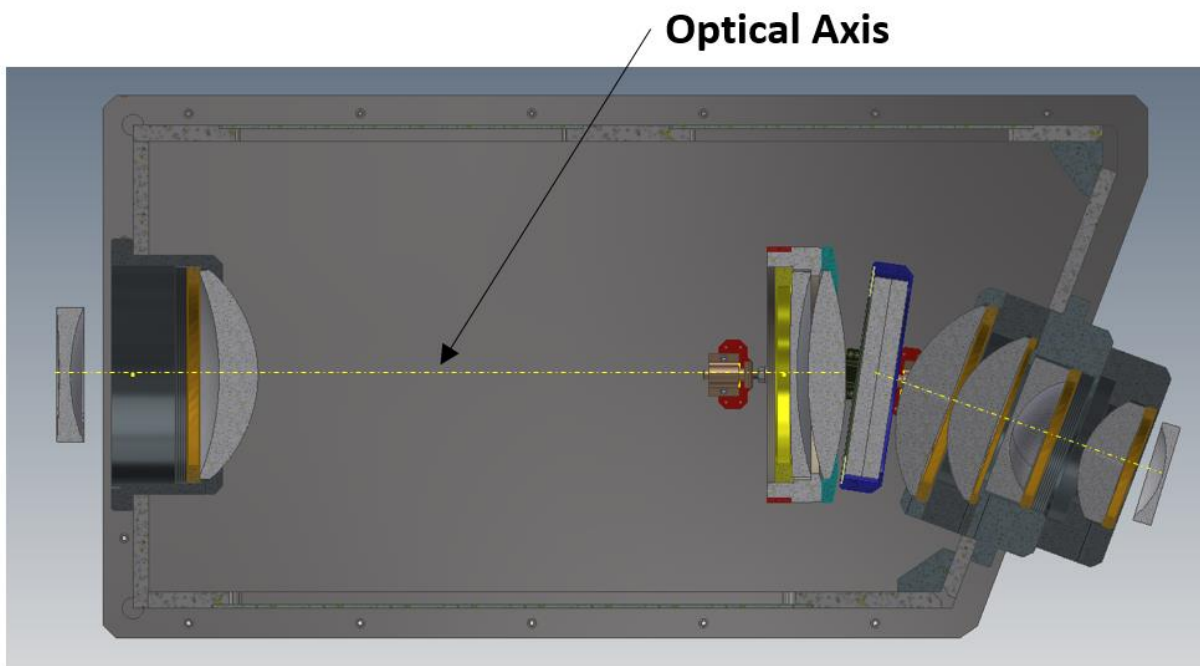


Figure 30. Cross-section from above showing the spectrograph assembly with position of all optical elements and mounting cells.

5.3 Structure

The spectrograph structural assembly is shown in Figure 31 and Figure 32. The structural material is from MIC-6 Aluminium cast jig plate. The structure sets the foundation for the built and alignment of mounted elements. The structure base plate has a profile machined to position the camera mounting plate at the required angle. The vertical plate holding the collimator has a precision bore to locate the collimator and to establish the optical axis. An intermediate plate includes pockets to hold the kinematic mounts for the volume phase holographic grating and the collimator assembly. A top plate is used to cover the whole assembly.

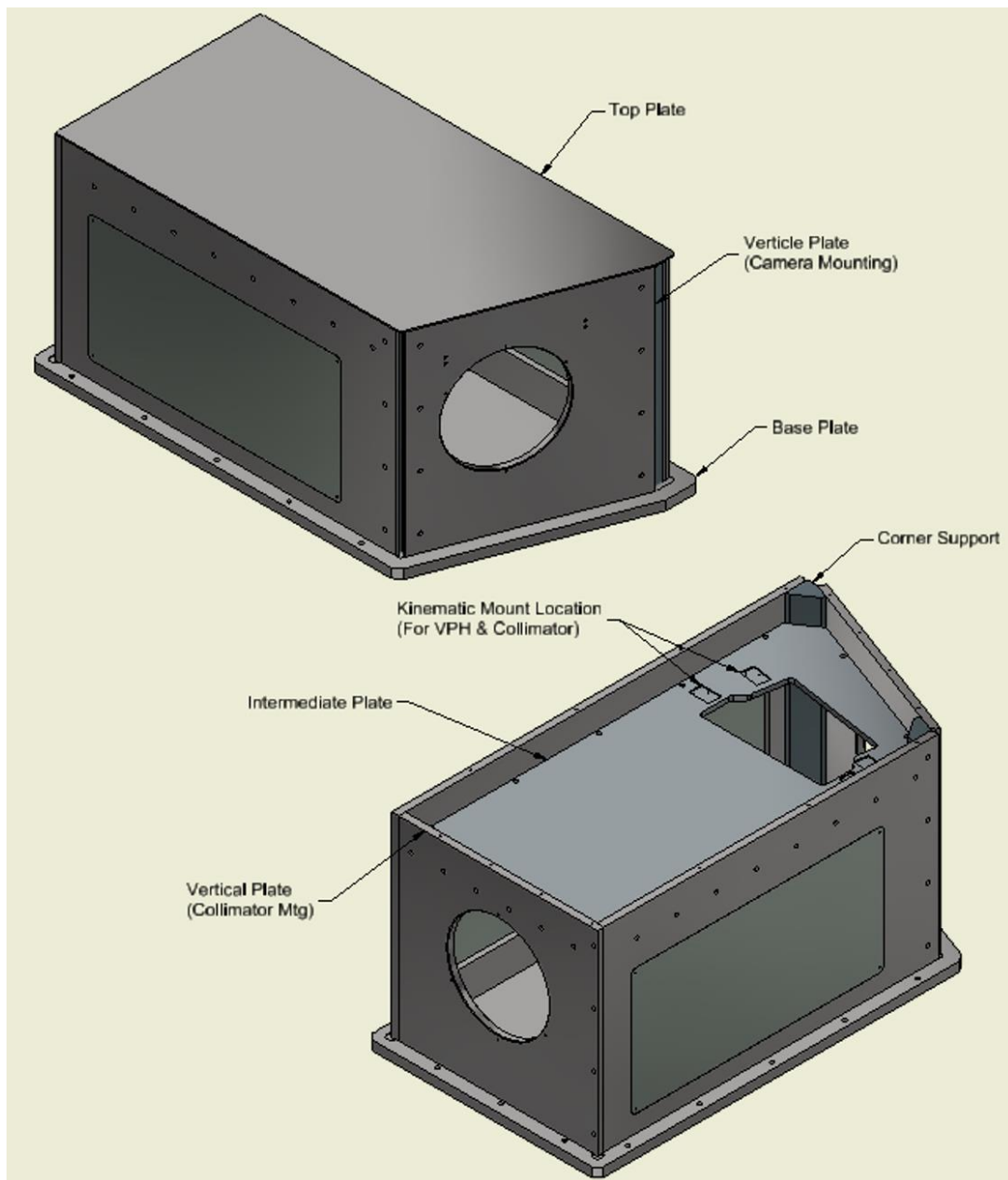


Figure 31. Features of spectrograph structural assembly.

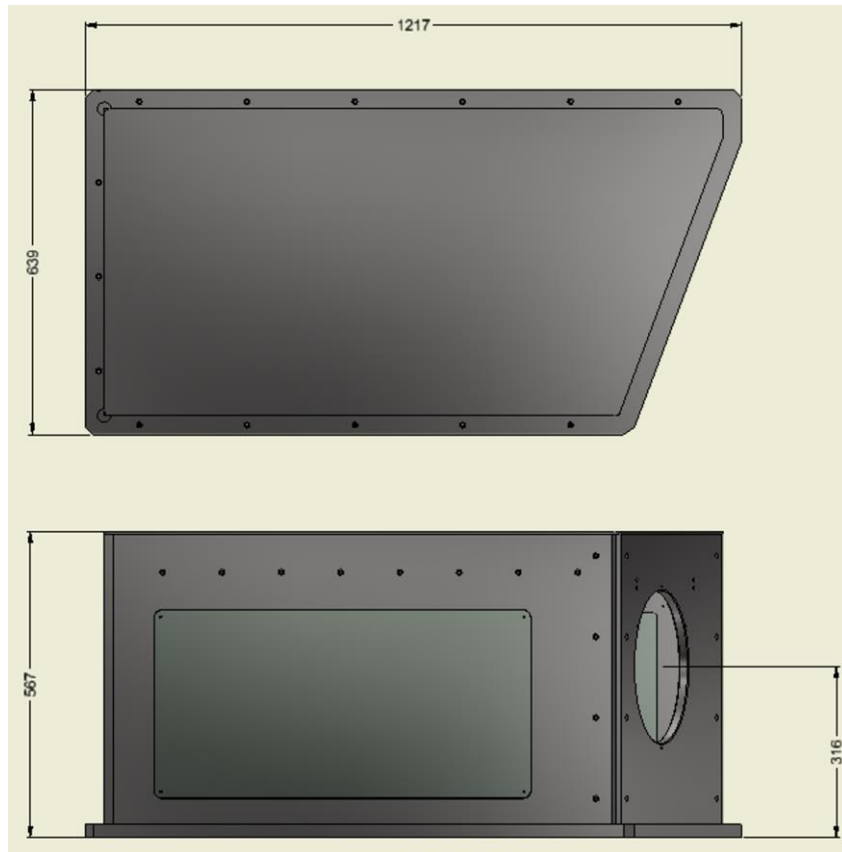


Figure 32. Dimensions of spectrograph structural assembly.

5.4 Collimator

The collimator #1 assembly is shown in Figure 33. This assembly mounted directly to the vertical plate of the structural assembly. This collimator #1 assembly is fabricated from an aluminium turning. The collimator lens is mounted to a lens cell using a retainer. The lens cell is mounted to the structure precisely with its optical surface rested to the tangential surface of the cell. The axial retainer ring is threaded which keeps the lens in place. A gap is provided to bond the optics to the mount with elastomer. The lens is accurately mounted in its lens cell using a precision lens alignment station capable of centering to within 10 μm and registering tilt within 10 arcsec to the mechanical reference surface and optical axis.

The collimator lenses #2 and #3 are fixed in the collimator #2/#3 assembly, which is shown in Figure 34. This assembly has a casing to locate and hold lens #1, a casing to locate and hold lens #2, and a third casing to hold the kinematic mounts. Materials used are aluminium and stainless steel. The casings are mounted using screws which are pinned to the correct reference. The complete assembly is connected to kinematic mounts. Gaps are provided to bond the optics to the mounts with elastomer. Again, using a precision lens alignment station.

The collimator #2/#3 assembly is contracted as a complete unit that is then inserted into the optical path from above and attached to the intermediate plate. Provision for adjustment of the complete assembly is provided for in tip, tilt, and rotation through shimming on installation. Further adjustments may be provided during the detailed design phase if necessary. A v-groove is used to locate and align the overall assembly

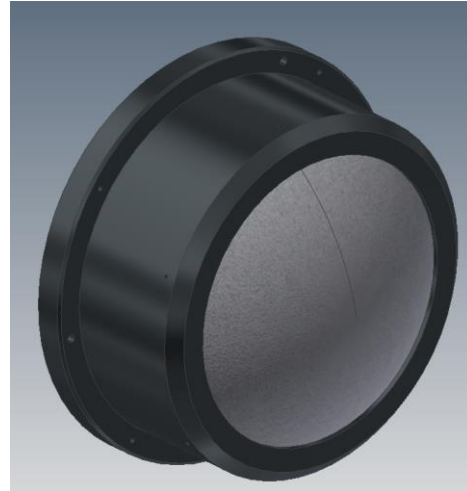
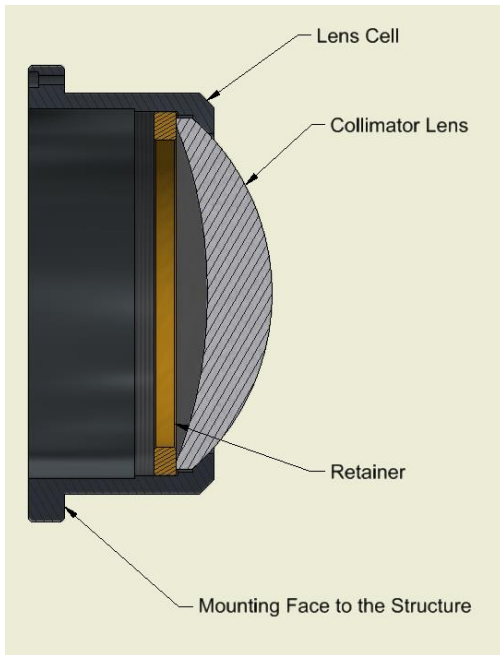


Figure 33. Cross section and model of the collimator #1 assembly.

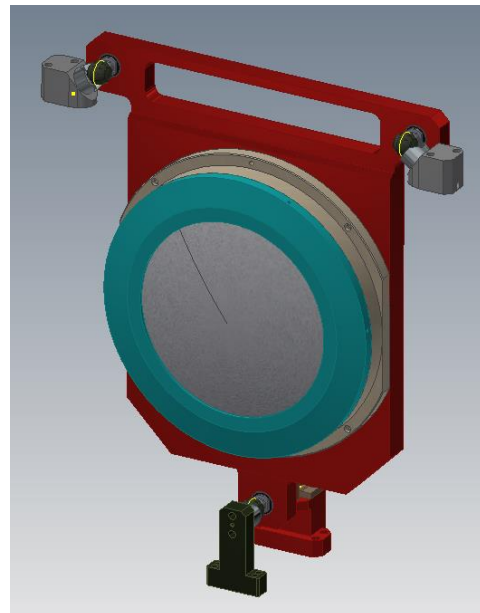
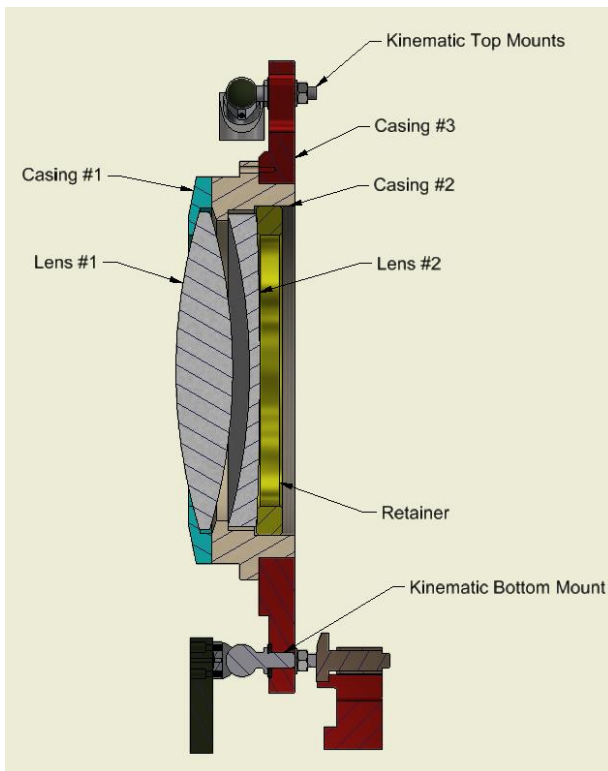


Figure 34. Cross-section and model of the collimator #2/#3 assembly.

5.5 Grating

The grating assembly is shown in Figure 35. It follows many features of the collimator #2/#3 assembly. A casing is used to locate and hold the VPH grating. A cover provides protection for one

side and also can be used as a stop for the optical system. Construction of the assembly is aluminium and stainless steel. Screws are used to mount the cover. The complete assembly is connected to kinematic mounts with gaps provided to bond the optics to the mount with elastomer.

The VPH assembly is constructed as a complete unit that is then inserted into the optical path from above and attached to the intermediate plate. As for the collimator assembly, adjustment is provided for via shimming in tip, tilt, and rotation with further adjustments possible if required. V-grooves are also used to locate and position the overall assembly.

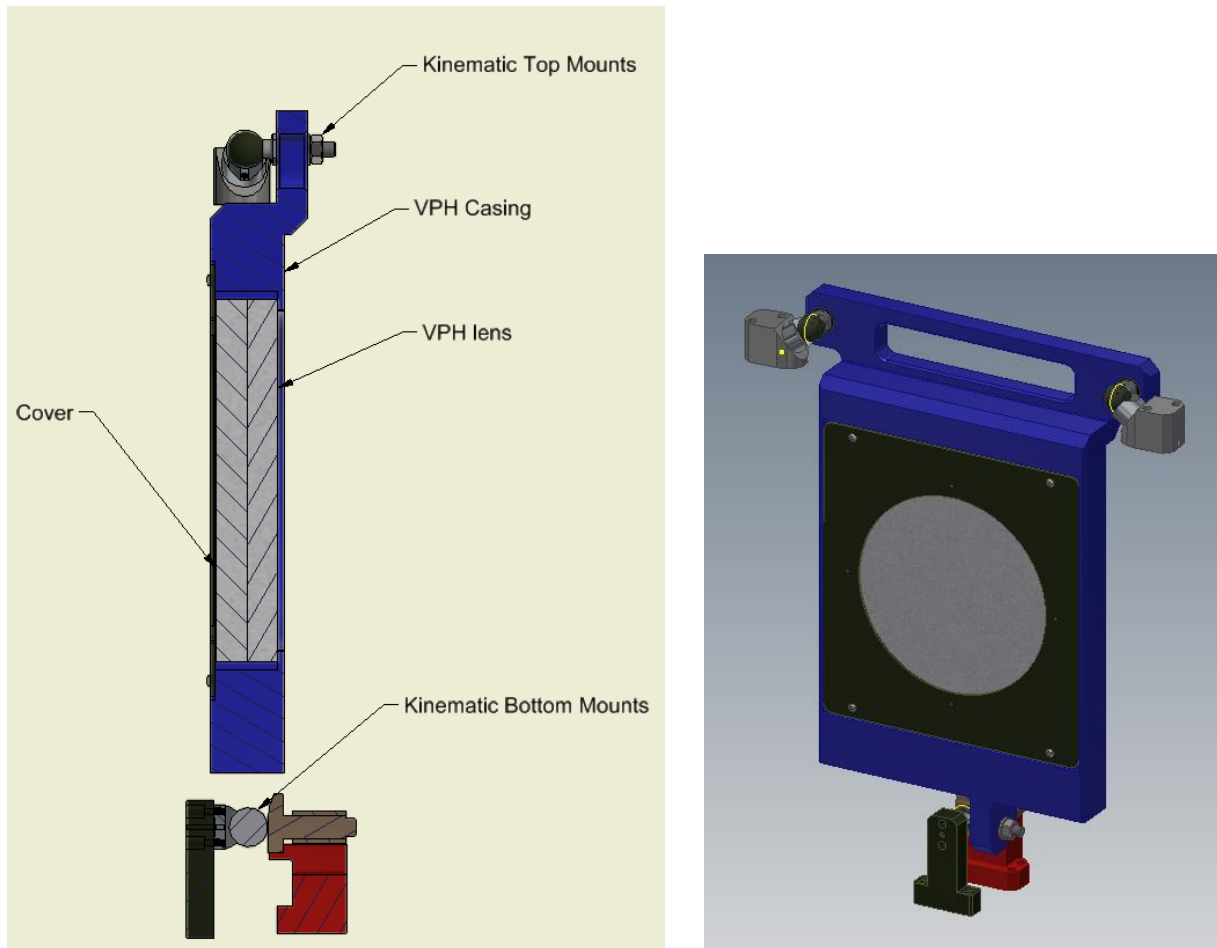


Figure 35. Cross-section and model of the volume phase holographic grating.

5.6 Camera

The camera assembly is shown in Figure 36. Each lens is mounted in an individual lens cell as a subassembly during alignment, with the full assembly built sequentially. The optical surface of the lenses are rested to the tangential surface of the cells. Axial retainers are threaded for each lens to keep the lenses fixed. Gaps are provided to bond the optics to the mount with elastomer. The reference plane is machined into the cell of lens 3 which serves as the structural mounting face for the full assembly. All materials are aluminium.

The complete assembly is built on a precision lens alignment station capable of centering all optics to the accuracy described above.

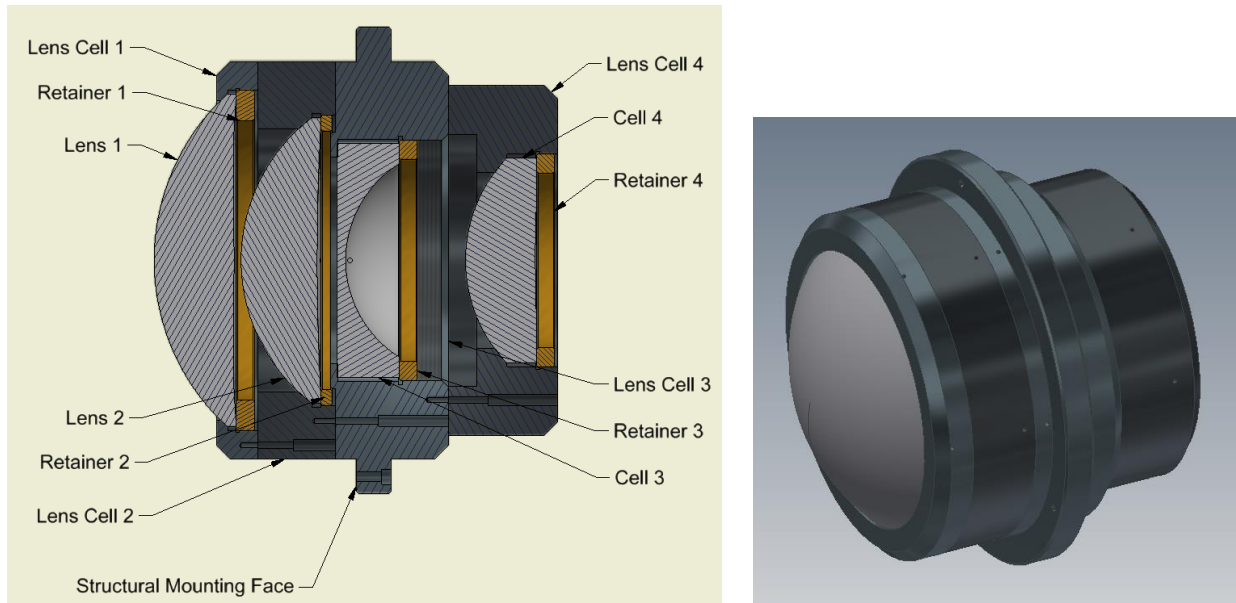


Figure 36. The camera assembly and rendering.

5.7 Detector Cryostat

For both TAIPAN and Hector spectrographs, the detector cryostats are mounted on 5-axis adjustable cradles (Figure 37). These cradles can be manually or automatically adjusted in position to allow focus change when required. The decision on whether to automate the focus mechanism should depend on a detailed thermal analysis based on the properties of the spectrograph room, combined with an understanding of the scientific requirements (i.e., for calibration).

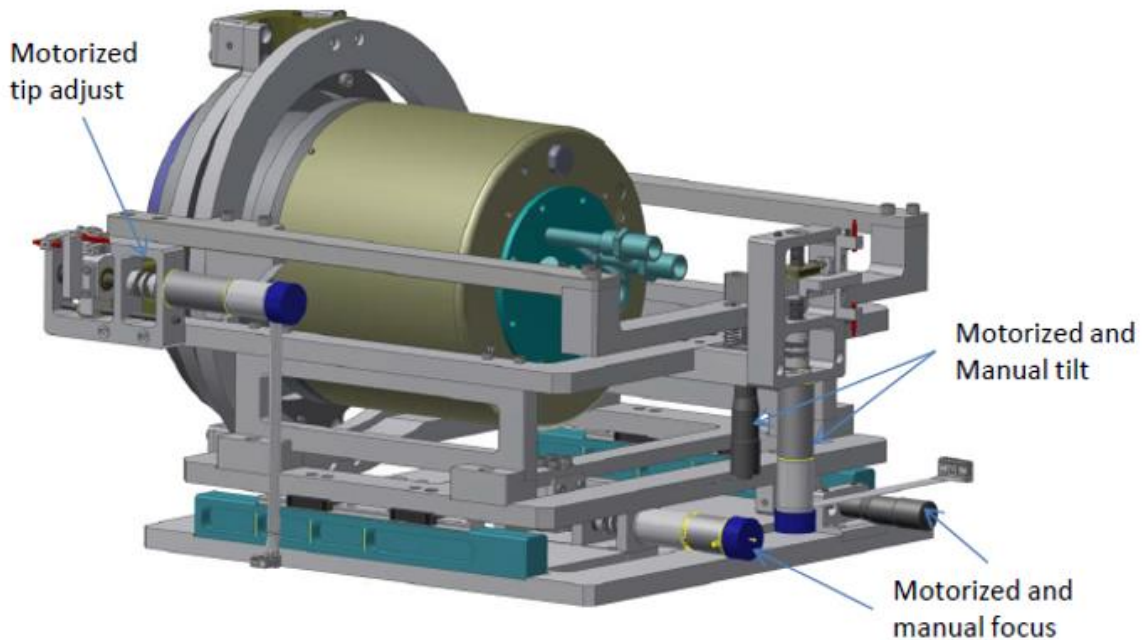


Figure 37. Detector mount cradle design for the Hector spectrograph with 5-axis adjustment.

The last optical element of the spectrograph is a powered lens that is mounted as the front window of the detector cryostat. The tight spacing between the detector surface and the last window is beneficial for control of spectrograph aberrations. Once the optical design is finalized, a new ICD should be developed that details the orientation, spacing, and alignment tolerances between the window and the chip. This should be provided to the vendor/supplier of the cryostat system. The ICD for Hector is shown as an example in Figure 38.

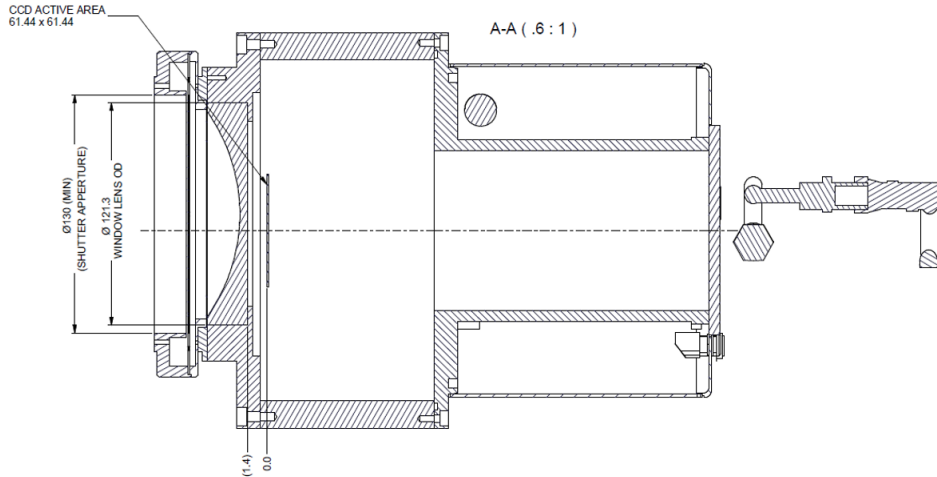


Figure 38. Example of Interface Control Drawing for the Hector spectrograph cryostat.

5.8 Fore-Optics Mechanical Design

We have not provided a design or costing for the mechanical concept for the fore-optics unit. However, it should be noted that the AAO has previous experience with many similar instruments that may be relevant and can be considered. The fore-optics unit for KOALA is shown in Figure 39. This is a 1000 fibre IFU that interface to the Cassegrain focus of the AAT – it also includes an automated mechanism that includes two separate plate scales. Similar fore-optics units have been built for CYLCOPS2, GNOSIS, PRAXIS, and Veloce.

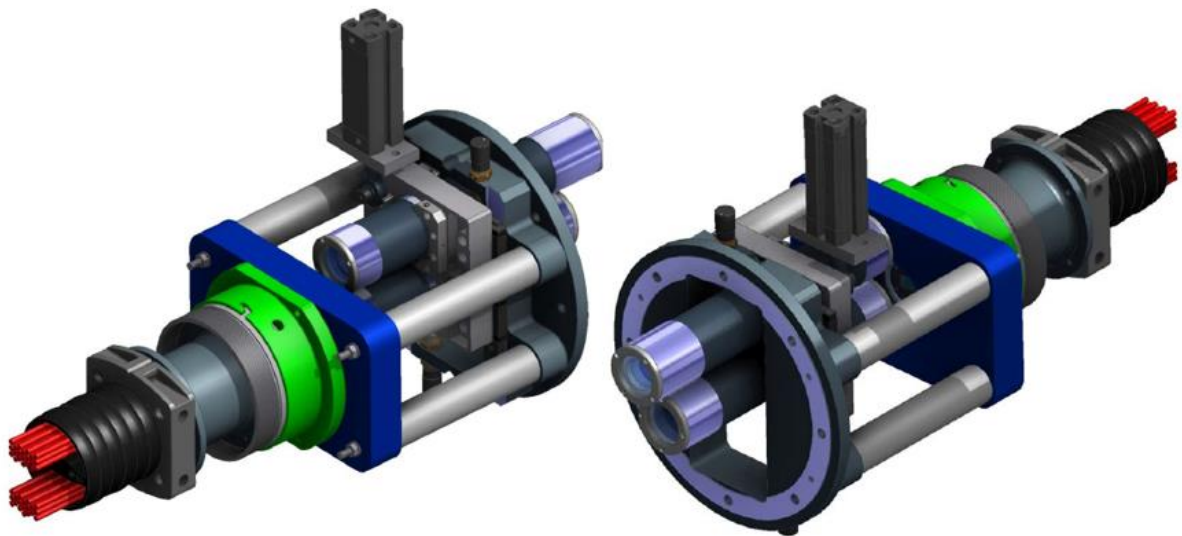


Figure 39. Fore-optics design for the KOALA unit at the AAT.

6 COST AND SCHEDULE TO FINAL DESIGN

6.1 Scope of Work

We present here an estimate for the costing and schedule for AAO-MQ to complete the final design for instrument optics and the spectrograph. This will allow appropriate confidence on costing and schedule for the following build phase. The following tasks are considered part of the final design phase:

- Development of trade-off document on use of MLA or straight fibre injection at input and output of fibre cable, and on chose of key system parameters;
- Finalise the complete instrument system specification that provides for a single spectrograph design option (to include sign-off from the project PI);
- Verification from lens vendors on glass availabilities and search for alternative lens vendors (to include AAO-MQ preferred vendors and also European vendors such as Winlight Optics);
- Finalise the optical design for the fore-optics/MLA at the injection end of the cable;
- Finalise the optical design for the spectrograph;
- Conduct tolerance analysis for the spectrograph based on the final design;
- Document the assembly and alignment procedures for the spectrograph;
- Produce final designs for the mechanical parts of the spectrograph;
- Development of final system testing procedure for the spectrograph;
- Development of full system throughput model (including the telescope injection optics, fibre cable and focal ratio degradation, spectrograph injection, and spectrograph optics);
- Liaise with other partners to finalise ICDs where relevant (for example, on the fore-optics/telescope interface, the spectrograph enclosure interface, the slit interface, and the cryostat interface);
- Develop the cost and schedule for the remainder of the work to complete the full spectrograph assembly and commissioning;
- Produce final design report outlining above items.

6.2 Costing

The cost for AAO-MQ to complete the above workpackages is €137,000 EURO. Increase or reduction in scope to be negotiated prior to commencement of work.

6.3 Schedule

Final review document to be complete 6 months after contract signatures. Deadline assumed trade-offs complete and system specification is agreed with PI at 2 months after contract signatures.

7 COST AND SCHEDULE TO SPECTROGRAPH DELIVERY

7.1 Scope of Work

The following tasks are considered to be in-scope for each spectrograph unit:

- Procurement of all spectrograph lenses;
- Procurement of volume phase holographic gratings;
- Production of parts drawings for the spectrograph;
- Procurement of all mechanics parts (including mounts for all lenses and VPHG, the 5-axis manual adjustment cradle for the cryostat, and the optical table);
- Assembly and integration of all parts of the spectrograph;
- Testing of the complete spectrograph system and documentation of test results.

Out of scope, un-costed items include:

- Fibre slits and test slits (this is assumed the responsibility of the fibre system fabricator);
- Injection optics (belongs to the telescope system);
- Shutter mechanisms or shutter control mechanisms (to be determined where the shutter is located and if it belongs with the cryostat system as for Hector);
- Shipping, on-telescope installation, integration with the fibre and cryostat subsystems, and assistance with instrument commissioning (these costs can be calculated once the schedule and plan is developed in more detail);
- Cryostat and detector sub-systems (noting however, that the last powered spectrograph lens is to be provided as this should be the cryostat window);
- Software or control electronics (noting that the spectrograph is fixed format and thus no motion control system is required).

7.2 Cost Estimate

We present here an estimate of the costing and schedule for AAO-MQ to complete the first unit spectrograph to the point that it is ready for shipping. It is assumed that the final design phase has been completed. Also presented is an estimate of the unit costs for the following units, assuming that there is a 1+7 delivery plan (1+12 for the compact version). Other delivery options can be considered, such as ordering all units together and/or shipping 4+4 (or 6+7) for example. In such cases the unit cost for the first spectrograph is likely to drop.

The cost estimate is given in Table 3 based on the above scope of work for the baseline LUCA spectrograph, using bare fibre injection; the LUCA spectrograph with MLA injection; and the compact design. Costs are given in EURO after conversion from USD and AUD using current exchange rates. Note that the estimate should be revised as part of the final design process once all system elements and designs are finalised. It is likely that further cost reductions can be realised in the final design phase, particularly in regards to the unit cost for the second larger shipment.

Table 3. Cost estimates for final delivery

Option	Unit cost for the first spectrograph (EURO)	Unit cost for the remaining spectrographs (EURO)
LUCA spectrograph – baseline bare fibre design	€891,000	€702,000
LUCA spectrograph – MLA design	€911,000	€717,000
LUCA spectrograph – compact design (upper limit)	€587,000	€473,000

7.3 Schedule

A high level estimate for the delivery milestones is provided in Table 4, relative to the milestone start point, T_0 , commence build phase. This assumes that a final design phase has been completed, all designs are accepted, and that a contractual agreement is in place prior to this date. A detailed project plan is to be produced during the final design phase that will take into account glass availabilities and vendor specific timeframes.

The timeframe to achieve the end date could be reduced by commencing procurement of the long lead time items, such as the VPH grating and the glass blanks, during the final design phase.

Table 4. Schedule estimate

Milestone	Due date
Commence build phase	T_0
Order all optics (lenses/ gratings/ dichroic)	$T_0 + 1$ month
Complete mechanical design and release all drawings for manufacture	$T_0 + 4$ months
Procurement complete (all optics received and tested, all mechanical parts fabricated)	$T_0 + 13$ months
Assembly and test complete (ready for shipping)	$T_0 + 17$ months

7.4 Co-Contributions

At this time the AAO-MQ cannot commit any level of in-kind or cash co-contribution to the project. It is possible that some level of co-contribution to the LUCA project could be obtained from Australian funding sources in the future. There are opportunities to apply for funding to the Australian Research Council through a number of grant schemes. The AAO-MQ are willing to explore such opportunities in the next phase if this is of interest. Note that this co-contribution would be based upon some expectation of data availability to Australian astronomers.

8 RISK ANALYSIS

Risk management is an on-going activity throughout a project life-cycle. The preliminary risk register is shown in Table 5. There are no high risk items identified because this project will follow closely other very similar projects using the same vendors for which there is a good track record.

For the remaining project phases, the risk matrix will be further developed and updated with the participation of all team members and in consultation with the key stakeholders. The risk assessment procedure is based on the AS/ISO31000:2009 standard. The risk matrix is applied to both technical risk and commercial risk for: comparing the risks of different design options; identifying components that are critical; identifying potential system hazards; and identifying risks associated with production processes.

Table 5. Preliminary risk register

Risk	Consequence	Likelihood	Mitigation	Risk Rating
Lack of adequate interface information on telescope	Schedule delay	Unlikely	Regular meetings with IAA, documented interfaces with telescope	Low
Staff availability	Schedule delay	Unlikely	Regular monitoring of staff load and prioritization of project at AAO-MQ	Low
Errors in detector interface	Schedule delay	Unlikely	Develop detailed ICD for detector/spectrograph interface	Low
Errors in fibre interface	Schedule delay	Unlikely	Develop detailed ICD for fibre slit/spectrograph interface	Low
Procurement delays	Schedule delay	Possible	Regularly monitor all vendor orders, use vendors with good history	Moderate
Suppliers do not deliver to specification	Reduced performance and/or schedule delay	Possible	Regular and detailed communication with vendors, clear specifications for all items, thorough testing phase after delivery	Moderate
Optical sub-systems do not perform to specification	Reduced instrument performance	Unlikely	Detailed optical engineering, tolerancing, assembly and alignment plan	Low

9 AAO-MQ CAPABILITIES AND HERITAGE

9.1 The AAO-MQ Technology Group

AAO-MQ sits with the Faculty of Science and Engineering at Macquarie University. The group consists of over 50 staff with expertise in a range of disciplines relevant to astronomy instrumentation: project management and systems engineering, optical engineering, mechanical engineering, electronics engineering, software engineering, data science, database management, astronomy and instrument science.

AAO-MQ is internationally recognized as a pioneer of spectrographs, fibre-positioners, fibre systems, imagers, and techniques for astronomy having had extensive experience and highly successful outcomes with the design, development and operation of over 90 instruments for telescopes around the world.

Previous AAO spectrographs have included:

- IRIS2, commissioned in 2002, a Cassegrain-mounted near-infrared imaging spectrograph capable of imaging over a 7x7 arcmin field-of-view in the z, J, H, and K bands, as well as long-slit and multi-object spectroscopy via a changeable slit-mask.
- AAOmega, commissioned in 2006, a general-purpose facility providing multi-object and integral field spectroscopy (Figure 40). This dual beam bench mounted multiple-object spectrograph is fed by ~400 fibres from 2dF providing spectral resolutions ranging from 1,200 to 10,000 with a variety of VPH gratings.
- HERMES, a multi-object spectrograph commissioned at the AAT in 2014 that covers four optical bands simultaneously at a spectral resolution of ~28,000. The HERMES instrument is driven primarily by the ‘Galactic Archaeology’ science project, which aims to reconstruct the history of our Galaxy’s formation from precise element abundances of 1 million stars.

Previous AAO fibre positioning projects have included:

- 2dF, a pick-and-place style fibre positioning system mounted at the AAT prime focus (see Figure 41). This system, commissioned in 1997 has proven extremely reliable (total downtime less than 4% without any major refurbishments). Over the last 5 years the 2dF/AAOmega system has occupied the majority of available telescope time at the AAT and has been used to conduct a series of high profile science projects.
- OzPoz, a fibre positioner that forms part of the FLAMES facility (Fiber Large Area Multi-Element Spectrograph) mounted on the second Unit Telescope of the VLT. The AAO designed and built the OzPoz positioner in 2003, which fed the moderate resolution GIRAFFE optical spectrograph and/or the red arm of the high resolution UVES spectrograph. The spectrographs were built by a consortium of European institutes. Since commissioning there were no major instrument refurbishments or major technical issues.
- FMOS Echidna, a fibre positioning system commissioned at the Subaru telescope in 2010, which feeds dual near-infrared spectrographs. Echidna uses piezo-electric actuators to position a total of 400 fibre-spines at the telescope focal plane. Positioning occurs in parallel with a field configuration time of ~12 minutes.

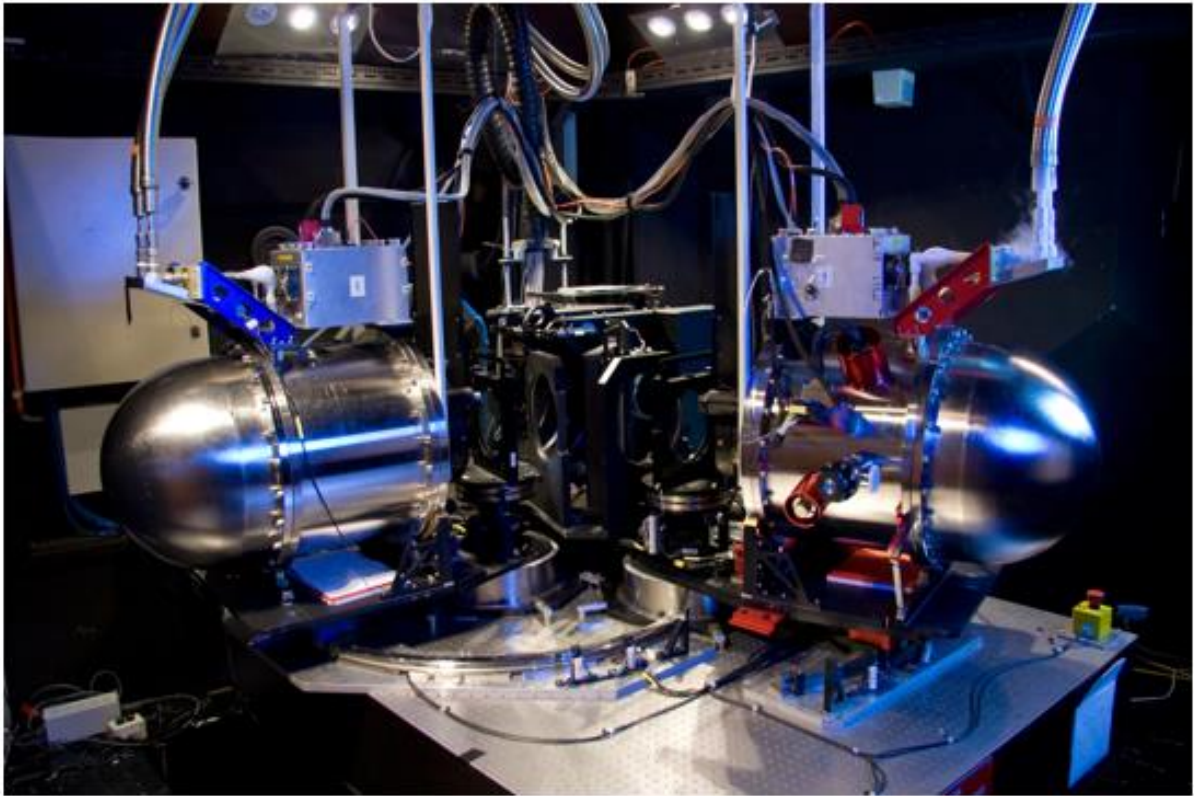


Figure 40. The AAOmega spectrograph at the Anglo-Australian Telescope.



Figure 41. The 2df fibre positioning system at the Anglo-Australian Telescope.

AAO fibre systems have included:

- CYCLOPS2, a fibre image slicer for the high resolution UCLES optical echelle spectrograph at the AAT, commissioned in 2012.
- GNOSIS, a photonic H-band OH suppression upgrade to the IRIS2 spectrograph based on fibre Bragg grating technology developed and tested in 2012.
- SAMI hexabundles and fibre feed commissioned in 2013. AAO-MQ developed this breakthrough technology along with collaborators at the University of Sydney, which allows multiple IFUs to be deployed over a large field-of-view as easily as optical fibres. These hexabundles were used on the SAMI instrument which feeds AAOmega on the AAT, leading to the SAMI galaxy survey, which completed in May 2018 producing spatially resolved spectroscopy for >3000 galaxies.
- KOALA, a 1000 element fibre-IFU for the AAT commissioned in 2014. The KOALA IFU uses dual microlens arrays at the fibre input and interfaced to the AAOmega spectrograph slit at the output.

Current projects of note at AAO-MQ include:

- TAIPAN, a parallel positioning robotic fibre system and spectrograph for the UK Schmidt Telescope (UKST). The fibre positioner uses ‘Starbug’ robots for a target field configuration time of 2 minutes. The spectrograph is a wide wavelength range fixed-format low-resolution (R~2200) all refractive design. The TAIPAN instrument is currently being commissioned and is expected to be ready for science in 2019.
- MANIFEST, a fibre positioner for GMT that will feed all of the GMT seeing limited instruments, G-CLEF and GMACS. MANIFEST is based on the Starbugs parallel positioning technology developed at the AAO.
- AESOP, a fibre positioner for the 4MOST instrument on the European Southern Observatory’s VISTA telescope. AESOP consists of 2500 individual fibre spines using a similar technology for FMOS Echidna.
- GHOST, a high resolution fibre image slicing spectrograph for the Gemini telescope in Chile. AAO are leading this project with responsibility for the positioner and the fibre cable, and software; the Herzberg Institute of Astrophysics in Canada are subcontracted for the spectrograph, with the Australian National University contributing to the instrument software.
- Hector, a new integral-field spectrograph for the AAT, which will allow highly multiplexed (>2000 fibres) observations of more than 20 galaxies simultaneously. AAO-MQ are leading the development of the Hector spectrograph with the overall project run from University of Sydney.

9.2 Key Staff Expertise

Brief biographies are given below for key members of the leadership and project teams that would be expected to contribute towards the LUCA spectrograph development if this project moves to the next phase.

Prof. Jon Lawrence

Jon Lawrence is the Head of Instrumentation at Australian Astronomical Optics, Macquarie University. He has nearly two decades of experience in the development and implementation of instrumentation for astronomy (in Antarctic site testing, astrophotonics research, and telescope facility instrumentation). At AAO-MQ he leads a large team of engineers, managers and scientists, working on an array of instrument projects including: TAIPAN for UKST, GHOST for Gemini, MANIFEST for GMT, 4MOST for VISTA, and AST3-NIR for Antarctic Dome A. He has published over 300 papers.

Dr. Robert Content

Dr Robert Content received his PhD in Physics in 1992, the first PhD on liquid mirror technology. Dr Content spent 1992-1994 at Steward Observatory where he developed the design of a camera suppressing the near infrared OH background. He was a Senior Research Associate at the Centre for Advanced Instrumentation of Durham University for 18 years where he extensively developed the technology of Integral Field Spectroscopy. This includes developments of the theory of fibre-lenslets IFUs and adaptive sampling IFUs, and the inventions of the advanced image slicer (now extensively used on telescopes including the VLT KMOS and MUSE) and the microslice system. He spent 6 years to the AAO designing 3 spectrographs and an Antarctic camera. He has contributed to space projects such as the NASA ATLAS Probe proposal, the original JWST NIRSpec, EUCLID and the ORIGIN proposal where he designed the telescope BIRT and its instrumentation. Dr Content currently runs his own optical design consultancy company.

Dr. Angel Lopez-Sanchez

Angel Lopez-Sanchez is a Senior Lecturer at Macquarie University. He conducts research in the observational astronomy fields of optical spectroscopy, optical and near-infrared imaging, and radio imaging of local star-forming galaxies. His main research topic is galaxy evolution and star formation phenomena in galaxies from a multi-wavelength approach. He has been providing instrument and observing support at the Anglo-Australian Telescope since 2011, and has been instrument scientist for 2dF, AAOmega, KOALA, and IRIS2. Angel has extensive experience with integral-field spectroscopy, being a very active member of the SAMI collaboration and leading the international astronomy survey "HI KOALA IFS Dwarf and irregular galaxy Survey" (Hi-KIDS), that is taking unique, high-quality IFS data of a sample of 100 nearby dwarf and irregular galaxies for which 21 cm H I interferometric data are available.

Dr. Ross Zhelem

Ross Zhelem is an optical engineer at Australian Astronomical Optics, Macquarie University specializing in optical design and analysis, specification, procurement and testing of precision optical components, alignment, integration and verification of instrument subsystems. He started his career in astronomical optics in 2002 joining the Australian National University, worked 6 years at the Ohio State University and has been with the AAO since 2012. Ross was involved in multiple international and local instrumentation projects such as NIFS, GSAOI, WiFeS (at ANU), MODS1 for LBT, OSMOS and Korean Microlensing Telescope (at the OSU), CYCLOPS2, KOALA, PRAXIS, HERMES, TAIPAN, MANIFEST, Veloce, GHOST, and Hector at AAO.

Dr. Jessica Zheng

Jessica Zheng has been with the AAO since 2008. She is currently the optics group manager, where she leads the optics and fiber design, test and integration for all astronomical instruments developing at AAO-MQ. Her research includes innovative liquid prism, fibre miniature wavefront sensors for

adaptive optics and thermal and stray light analysis for infrared camera design. She has been involved in several on-sky telescope demonstrations of liquid prism and multiple-object ground layer adaptive optics system with fiber miniature wavefront sensors. She also specializes in optical system characterisation and testing. She is the project scientist for AST3-NIR camera for Antarctic Dome A.

Ms. Helen McGregor

Helen McGregor is the Mechanical Group Manager at the Australian Astronomical Optics, Macquarie University. Helen has a background in mechanical engineering for astronomy, having held positions at the UK Astronomy Technology Centre and the Institute for Astronomy at the University of Hawaii, working on projects covered multiple applications from large vacuum systems for sub-millimetre, spectrographs for infrared and solar telescopes to high precision positioners. At the AAO, Helen leads the AAOs mechanical complement of over a dozen engineers and technicians in developing opto-mechanical and mechatronic designs for a wide range of instruments.

Mr. Scott Case

Scott Case is a Project Manager within the project group at the Australian Astronomical Optics, Macquarie University. Scott has a technical background in optical fibres and photonics and has worked as a fibre engineer on many of AAO's projects, including HERMES, CYCLOPS2, GHOST, and 4MOST. He is currently managing a number of national and international projects, including DIRAC for the Turkish astronomy community. Scott also manages the AAO's technical support program to the Anglo-Australian Telescope.

9.3 AAO Consortium

The AAO-MQ is part of the AAO consortium, a wider collaboration of institutes in Australia with capabilities in the area of instrumentation for astronomy. Our partners include:

- AAO-Stromlo: a world-class group with extensive experience in developing and testing astronomical instrumentation, small satellites and space payloads, high-speed laser communications, and advanced materials. AAO-Stromlo lies with the Research School of Astronomy and Astrophysics at the Australian National University. It hosts many industry partnerships and research collaborations, and contains one of the world's leading adaptive optics groups.
- AAO-USyd: a research group based at the University of Sydney with specific experience in the development of novel photonic designs and solutions for use in astronomy. Past instrument successes of note include the SAMI multi-IFU spectrograph at the AAT.

9.4 Astronomy Linkages

A key ingredient of the success of AAO-MQ has been the close synergy between instrumentation development and scientific research within the same organization – a principle that continues strongly today. In addition to the AAO-MQ Astronomy group itself, AAO-MQ has strong connections to the astronomy research staff of the Macquarie University Astronomy, Astrophysics and Astrophotonics Research Centre (MQAAAstro), having shared joint staff positions for many years prior to the recent transition. Combined, AAO-MQ and MQAAAstro are one of the largest and fastest-growing astronomical centres of research excellence in Australia, with 20 research-active academic and instrument scientist faculty.

10 ADDITIONAL SCIENCE PROGRAMS

Besides being used for unravelling the fine structure of galaxies in the Local Volume, LUCA can be used for some additional scientific programs that we outline here. LUCA will be a perfect instrument to explore relatively large areas of the sky comprising HII regions and planetary nebulae, as well as could be used for exploring the properties of galaxies, galaxy groups and galaxy clusters that are not located in the Local Universe.

10.1 Galactic HII Regions

During the last decades we have achieved a better understanding of the properties of some Galactic HII regions using very deep optical/NIR echelle and long-slit spectroscopy. The majority of these studies have provided integrated values over small areas of the nebulae. However, observations of Galactic HII regions using IFS (e.g., Sánchez et al. 2007, Mesa-Delgado et al. 2011, 2014) have shown that we are still lacking a complete full picture of the distribution of the physical and chemical properties across HII regions, particularly for large objects. With its wavelength coverage and a 7.62 arcmin² FOV, LUCA will be an excellent instrument to improve our knowledge of Galactic HII regions. Observations with LUCA will be able to derive reliable maps of the distribution of physical (dust extinction, ionization, excitation, electron temperature, electron density, kinematics) and chemical (abundances of helium, oxygen, nitrogen, sulfur, neon, argon, iron..., as well as their ratios) properties, as well as investigate the feedback by massive stars (e.g. Simon-Díaz et al. 2010, García-Rojas et al. 2014), across large Galactic HII regions.

Some exploratory studies of large nebulae (e.g. Sánchez et al. 2007 using PPAK at the 3.5m CAHA to explore the Orion Nebula) suggest that the gas could be not fully ionized when considering the full integrated HII region. This could lead to a systematic underestimation of the chemical abundances, that could have effects even in the calibrations that are later used for estimating the metallicity in external galaxies. LUCA will be able to explore this issue in a large number of Galactic HII regions. Furthermore, there is increasing suspicion that there are dust grains mixed with the emitting gas which could be absorbing the ionizing Lyman-continuum photons, and therefore the simple dust screen model (which is also typically used for HII regions in external galaxies) could be biased. On top of that, there is the well-known problem of the abundance discrepancies in HII regions (i.e., abundances derived using collisional excited lines are up to 0.5 dex higher than those derived using the faint recombination lines). Mapping large regions of extended nebulae will provide key data to trace where these discrepancies are arising (e.g. Mesa-Delgado et al. 2010, 2012, Toribio San Cipriano et al. 2017), and their dependence on other physical properties (e.g., electron density, ionization). The data of Galactic HII regions obtained with LUCA will also be able to trace very local pollution of helium and nitrogen by massive stars of the Wolf-Rayet type (e.g., López-Sánchez et al. 2011, Mesa-Delgado 2014, Esteban et al. 2016) or of any other kind, as well as explore the dynamical effects of stellar winds and supernova explosions in the gas.

10.2 Evolved Low-Mass Stars and Planetary Nebulae

Next to supernova explosions, stellar winds on the asymptotic giant branch (AGB) make significant contributions to the recycling of chemically enriched material to the interstellar medium. Indeed, the physics of AGB mass loss is a key ingredient for our understanding of the evolution of galaxies, as far as the recycling of matter, processed by different stellar populations. In the last decade our theoretical understanding of stellar evolution and mass loss during the AGB phase has considerably

improved, however deep, high quality data of a large area around planetary nebulae (PNe) are not available yet. Planetary nebula (and their haloes) are fossil records of the mass-loss history at the tip of the AGB. These observations must be conducted using IFS (e.g., Tsamis et al. 2008, Monreal-Ibero et al. 2015, Ali & Dopita 2017, Walsh et al. 2018). LUCA will be able to address these problems and, using the very same tools needed for analysing large HII regions, can provide key observational data of a sample of planetary nebulae and their surroundings.

Furthermore, PNe are self-contained laboratories of a wide range of low density ionization conditions, therefore providing important information about the interstellar medium. The gradient in ionization from close to the central star to lower values in the outer regions can be traced using IFS data and will largely help to understand the nebular structure and the role of the local physical conditions of the gas. The large amount of emission lines that are typically found in the central regions of PNe (a consequence of the hardness of the radiation emitted by the white dwarf) also provide an excellent laboratory to explore the distribution of the physical and chemical properties across the nebulae, something that is not typically explored because of the relatively large size of these objects in the sky. However, LUCA, with its large FOV, will be able to map completely many PNe and their haloes.

Furthermore, these data will allow to investigate the s-process enrichment induced during the AGB phase (e.g. García-Rojas et al. 2015) and to further study the metallicity discrepancy problem in ionized nebulae, as the discrepancy in PNe is much larger than that measured in HII regions (Tsamis et al. 2004, Liu et al. 2006, García-Rojas et al. 2013), something recent research suggests could be related to central star binarity (Corradi et al. 2015, Jones & Boffin 2017, Wesson et al. 2018).

10.3 Non-Local Galaxies, Galaxy Groups and Galaxy Clusters

Although LUCA has been designed to survey nearby galaxies of the Local Volume and the Virgo cluster this instrument can also be used for observing more distant galaxies, galaxy groups in the low- and intermediate- z Universe, galaxy clusters, and active galactic nuclei.

Many galaxy groups, as well as hundreds of galaxy clusters, can be observed with LUCA simultaneously targeting multiple galaxies in blank and cluster fields over the full optical spectrum. These data will provide key information not only about the galaxies located in those clusters or groups, but also about their environment and the physical processes that are ruling the evolution of the galaxies. These observations will allow to discover new galaxy members in the clusters and groups, lensed galaxies, clouds of ionized gas (star-formation in tidal streams, ram pressure stripping, galactic winds) and even hints of accretion of cold gas in galaxies via a spatially resolved kinematic and chemical analysis. Kinematics maps of early type galaxies will allow to classify them in slow rotators and fast rotators. In galaxy clusters all these data can be used to obtain their accurate mass reconstruction, at least of their central regions.

Observations of active galactic nuclei (AGNs) with LUCA can also provide key information about the physical phenomena that are triggering their activity, as well as investigate their kinematics (that could reveal features of interactions, merger or gas accretion) and other spatially resolved properties of the gas and the stars in these objects. All this information will also give a better understanding of the physics behind AGN feeding and feedback processes.

APPENDIX C






IFU-6000 spectrograph technical and proposal reports



TECHNICAL REPORT

« FEASABILITY STUDY FOR IFU6000 »

		A
Prepared by :	Date : Name : Function : Visa :	28/03/2019 V.LAPERRE Optical Engineer 
Verified by :	Date : Name : Function : Visa :	28/03/2019 D.SOLER CTO 
Verified by :	Date : Name : Function : Visa :	28/03/2019 T.SANNEJAN Quality Insurance 

<i>Review</i>	<i>Modifications - Reasons</i>
A	First release

Spreading : FILE, CAHA

TABLE OF CONTENT

1 OBJECT 4

2 APPLICABLE DOCUMENTS 4

3 REFERENCE DOCUMENTS 4

4 ASSOCIATED DOCUMENTS 4

5 GENERALITIES 5

5.1 GOAL OF THIS PRELIMINARY STUDY 5

5.2 PRELIMINARY REQUIREMENTS..... 5

6 THE MUSE LIKE DESIGN..... 6

6.1 OVERVIEW 6

6.2 PERFORMANCES 6

6.3 CONCLUSION 7

7 THE DESI LIKE DESIGN 8

7.1 OVERVIEW 8

7.2 PERFORMANCES 8

7.3 OPTIMIZATION – MINOR CHANGES 9

7.4 CONCLUSION 10

8 OTHER POSSIBILTIES 10

8.1 PFS DESIGN 10

8.2 4MOST LIKE DESIGN 11

8.3 CURVED CCD WITH MUSE LIKE DESIGN..... 11

9 THE PROPOSED DESIGN 11

9.1 OVERVIEW 11

9.2 PERFORMANCES 12

9.3 ASPHERE DEFORMATION 14

9.4 MAIN PARAMETERS 15

9.5 CONCLUSION 15

10 CONCLUSION OF DIFFERENT EXPLORED DESIGNS 16

11 DEVELOPMENT PLAN FOR THE PROPOSED DESIGN..... 17

11.1 THE OPTICAL TABLE 17

11.2 THE SLIT 17

11.3 THE COLLIMATOR..... 18

11.4 THE SLIT TO COLLIMATOR LINK 19

11.5 THE SHUTTER 19

11.6 THE GRATING 19

11.7 THE CAMERA 20

11.8 THE COVER 21

12 PRELIMINARY COLABORATION AND INTEGRATION PLAN 22

12.1 THE PRELIMINARY INTEGRATION PLAN 22

12.2 THE POSSIBLE COLLABORATION SCHEME..... 22

13 CONCLUSION 23

14 APPENDICES 24

14.1 PROPOSED DESIGN PRELIMINARY DEFINITION 24

CE DOCUMENT ET LES INFORMATIONS QU'IL CONTIENT SONT CONFIDENTIELS ET SONT LA PROPRIETE EXCLUSIVE DE WINLIGHT SYSTEM. ILS NE DOIVENT ETRE COMMUNIQUEES QU'AUX PERSONNES AYANT A EN CONNAITRE LE CONTENU ET NE PEUVENT ETRE REPRODUITS NI DIVULGUES A TOUT AUTRE PERSONNE SANS L'ACCORD ECRIT DE WINLIGHT SYSTEM.

THIS DOCUMENT AND THE INFORMATION IT CONTAINS ARE PROPERTY OF WINLIGHT SYSTEM AND CONFIDENTIAL. THEY SHALL NOT BE DISCLOSED TO ANY PERSON EXCEPT TO THOSE HAVING A NEED TO KNOW THEM WITHOUT PRIOR WRITTEN CONSENT OF WINLIGHT SYSTEM.

1 OBJECT

This document presents the feasibility study for IFU6000 and explores different spectrograph designs.

2 APPLICABLE DOCUMENTS

- [DA1] : Purchase order email dated December 13th 2018 and Commercial Invoice reference PF/026inD/18 dated November 23th 2018.
- [DA2] : OFWS1780-C – technical and financial offer

3 REFERENCE DOCUMENTS

- None

4 ASSOCIATED DOCUMENTS

- None

<p>CE DOCUMENT ET LES INFORMATIONS QU'IL CONTIENT SONT CONFIDENTIELS ET SONT LA PROPRIETE EXCLUSIVE DE WINLIGHT SYSTEM. ILS NE DOIVENT ETRE COMMUNIQUEES QU'AUX PERSONNES AYANT A EN CONNAITRE LE CONTENU ET NE PEUVENT ETRE REPRODUITS NI DIVULGUES A TOUT AUTRE PERSONNE SANS L'ACCORD ECRIT DE WINLIGHT SYSTEM.</p>										<p>THIS DOCUMENT AND THE INFORMATION IT CONTAINS ARE PROPERTY OF WINLIGHT SYSTEM AND CONFIDENTIAL. THEY SHALL NOT BE DISCLOSED TO ANY PERSON EXCEPT TO THOSE HAVING A NEED TO KNOW THEM WITHOUT PRIOR WRITTEN CONSENT OF WINLIGHT SYSTEM.</p>										
REF. DOC	W	S	3	0	3	3	-	0	0	1	-	R	A	P	0	0	1	-	A	PAGE 4/27

5 GENERALITIES

5.1 Goal of this preliminary study

[DA2] defines the tasks to be carried out in this phase of the project. The revision A of [DA2] explains the necessity and criticality of the time scale for manufacturing the spectrograph:

“This feasibility study should take place from January to June 2018. As per discussion with Francisco Prada, we propose to split the study in two phases :

1st phase : comparison and trade-off between three different designs

One big constrain is that the project would like to have one spectrograph ready looking at the sky for end of 2020. Considering that the studies will last during 2018 and that tenders will be issued beginning of 2019, the beginning of the construction of the first spectrograph would be around mid-2019 at the earlier. The remaining time for design, production and testing of this spectrograph is tight and looks not compatible with the design of a new spectrograph from scratch. Therefore, the initial idea, discussed during our meeting at WINLIGHT on October 27, is to use an existing design that has been already studied and for which production tooling already exists.”

The goal is then to find the best compromise between performances and planning.

5.2 Preliminary requirements

This chapter aims to present the preliminary requirements of an IFU6000 spectrograph. These requirements are taken from different discussions with IAA.

<i>Requirement</i>	<i>Value</i>	<i>Comment</i>
Spectrum	[365 ;736]nm	-
Image plane dimension	CCD 4kx4k, 15 μ m pitch	61.44x61.44mm
Number of fiber per spectrograph	600	Depends on image quality and cross talk specification
Image quality	Spot radius <9 μ m RMS	Preliminary value.
Fiber core diameter	\varnothing 150 μ m	At slit plane
Object numerical aperture	0.14 baseline	DESI baseline. Wider for 4MOST/PFS like designs

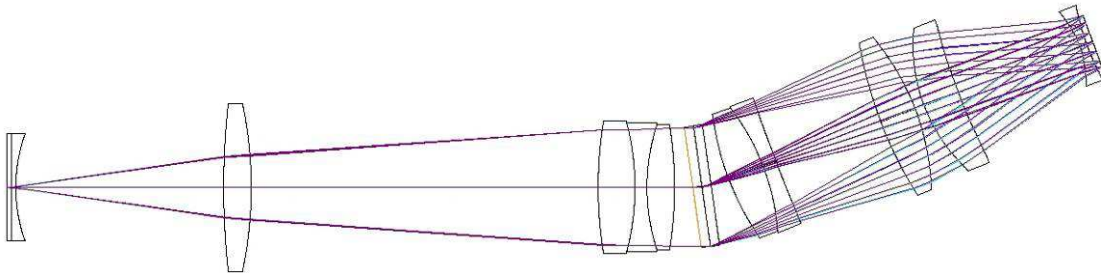
6 THE MUSE LIKE DESIGN

6.1 Overview

Winlight has already realized MUSE like spectrographs :

- MUSE : working at ESO VLT with a coverage in wavelength starting at 465nm.
- Multiplex : a fiber fed spectrograph for bluer wavelengths, but for medical applications.

Both of them are using some glasses that are very absorbent at $\lambda=365\text{nm}$. Therefore the optical design must be reoptimized to cover the [365;736]nm bandwidth.



The numerical aperture is set to 0.14 (as for DESI and Multiplex fibers). The fibers are arranged in a flat plane, in front of the object field lens (interface used for Multiplex).

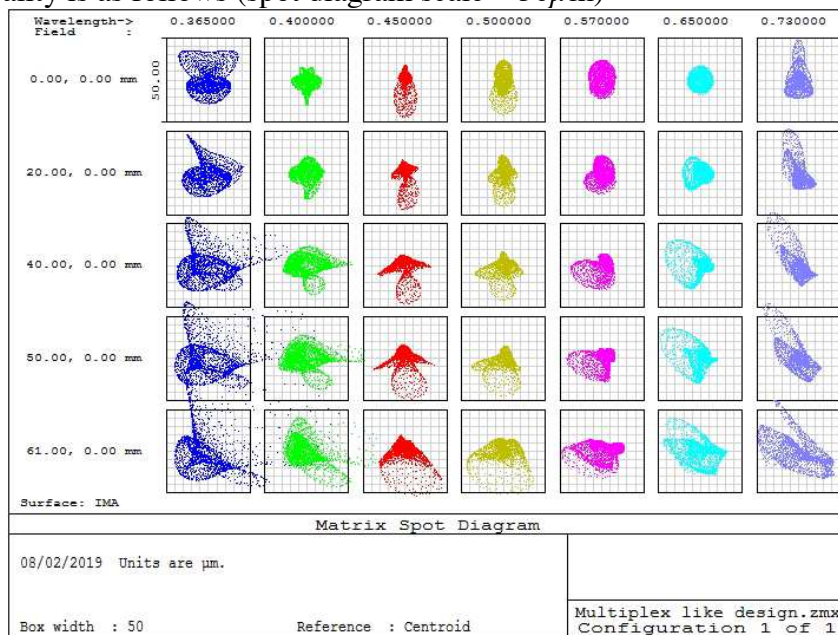
There are 10 lenses in the design (with a triplet and a doublet). There are 2 aspheres (front lens of the camera and the first face of the field lens).

The glasses are fused silica, CaF2, PBL25Y, PBL6Y and N-BAK2 to optimize the throughput at 365nm and are available is sufficient size ($\varnothing > 160\text{mm}$).

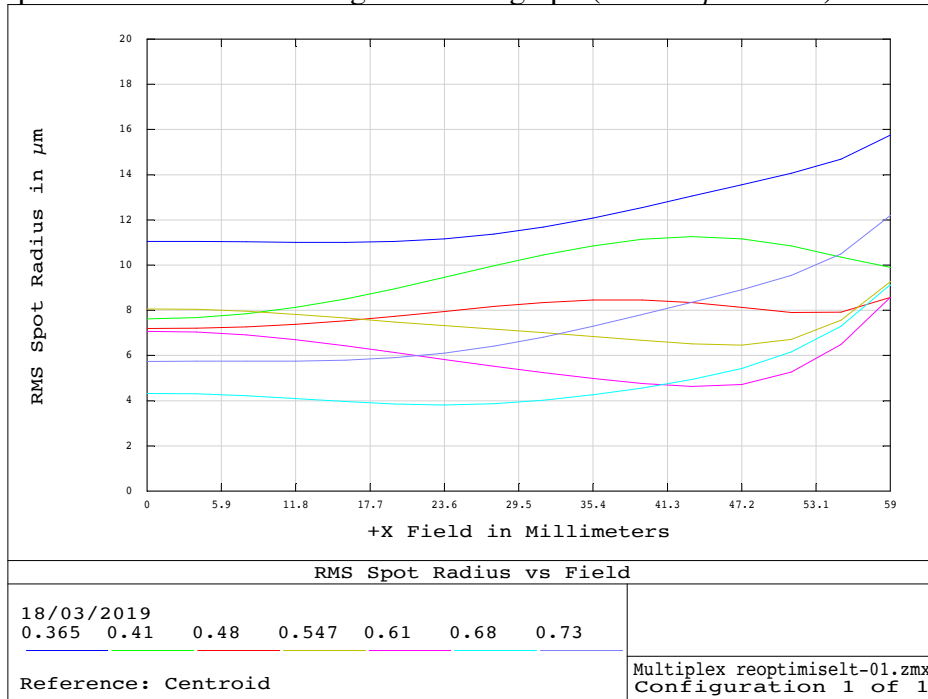
The image plane has been kept voluntary flat for a 4kx4k CCD as specified. The field lens + CCD assembly are tilted and decentered to correct a part of the chromatism.

6.2 Performances

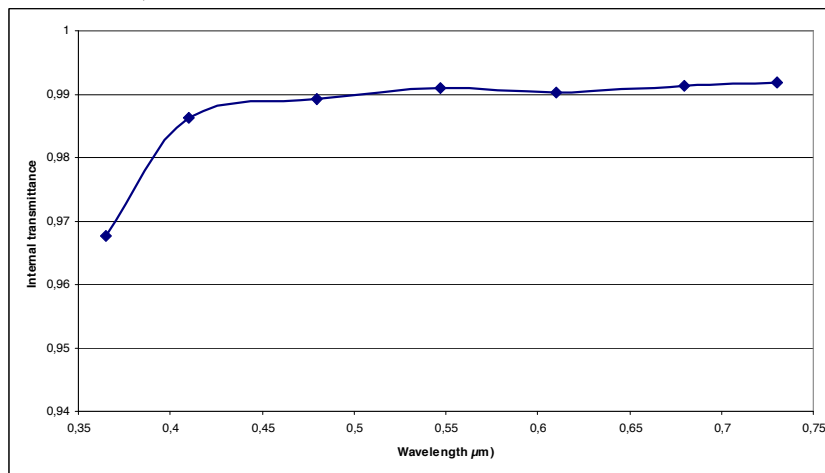
The image quality is as follows (spot diagram scale = $50\mu\text{m}$)



The RMS spot values in the field are given in the graph (scale $20\mu\text{m}$ RMS).



The transmittance of glasses performs well with a value greater than 96.5% at 365nm (VPHG efficiency not considered).



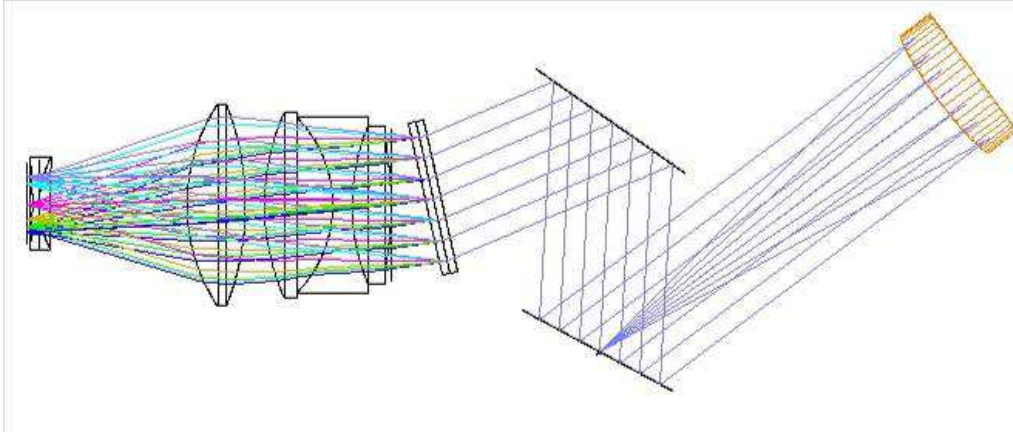
6.3 Conclusion

The MUSE like design must be reoptimized to adapt for the spectrum and interfaces. The image quality is not good enough (nominally $16\mu\text{m}$ RMS max), and the number of elements is important (10 lenses, so 20 faces to polish). The number of different glasses may be a risk in the planning, at least for the first spectrograph.

7 THE DESI LIKE DESIGN

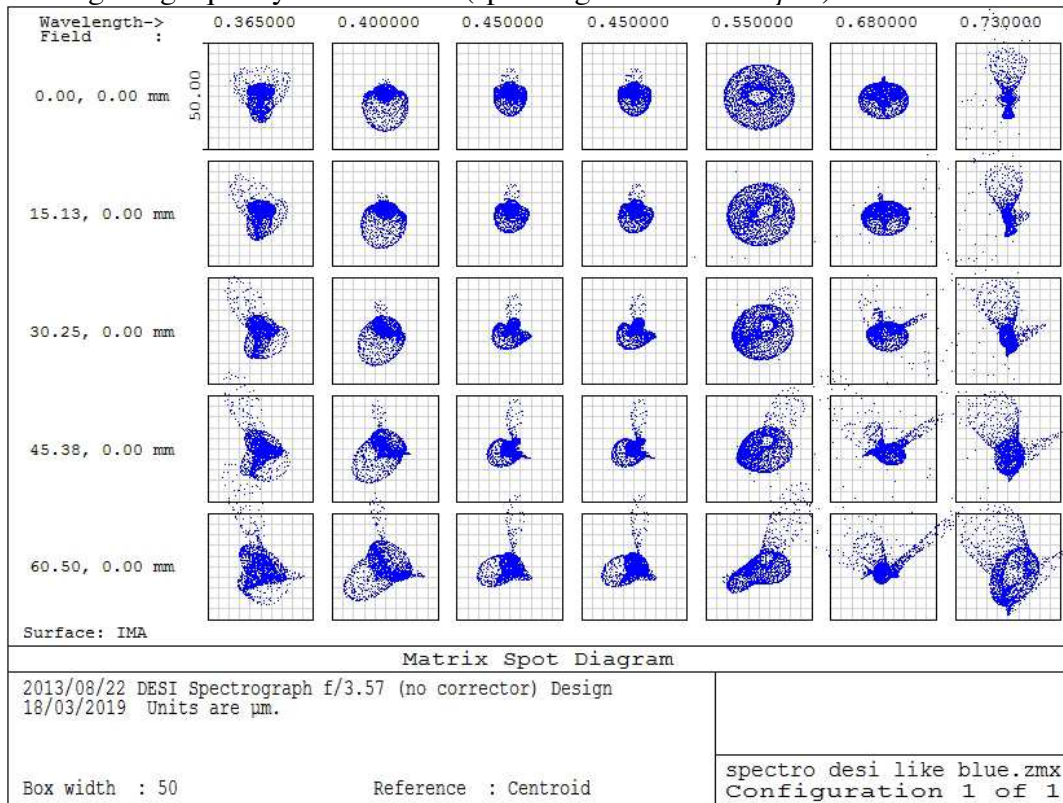
7.1 Overview

The original idea was to update the DESI design (Blue channel) to cover the IFU6000 bandwidth. This can be done by removing the dichroics (not done on the simulation), and changing the VPHG parameters (incidence, line frequency) and adapt camera position:

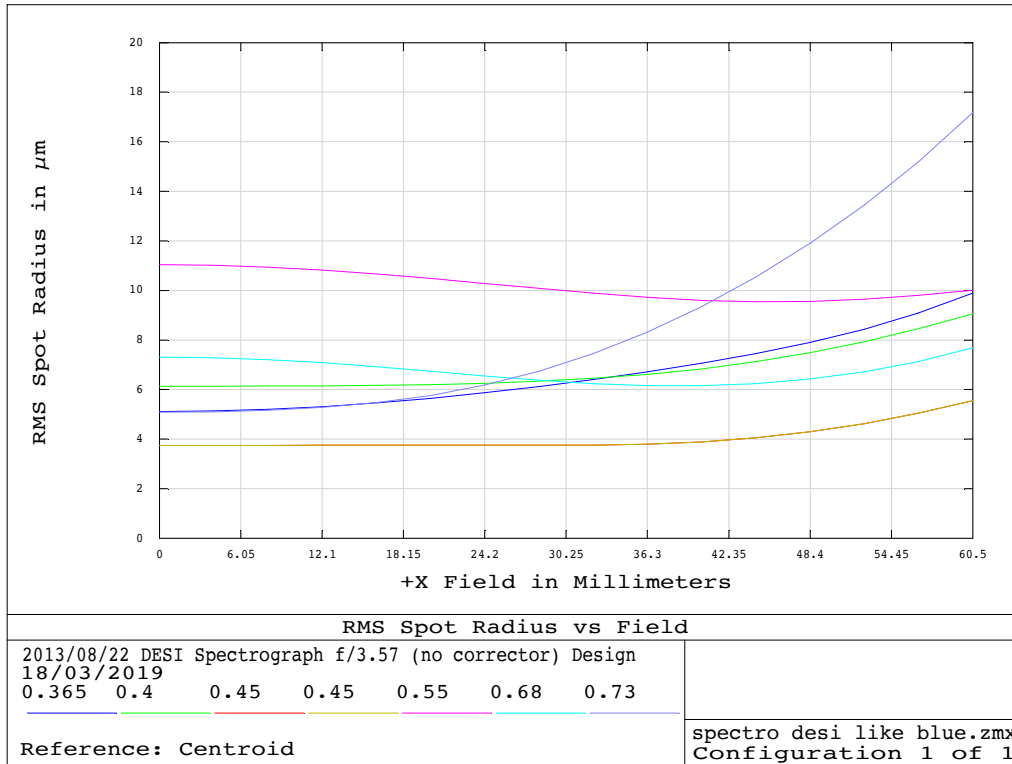


7.2 Performances

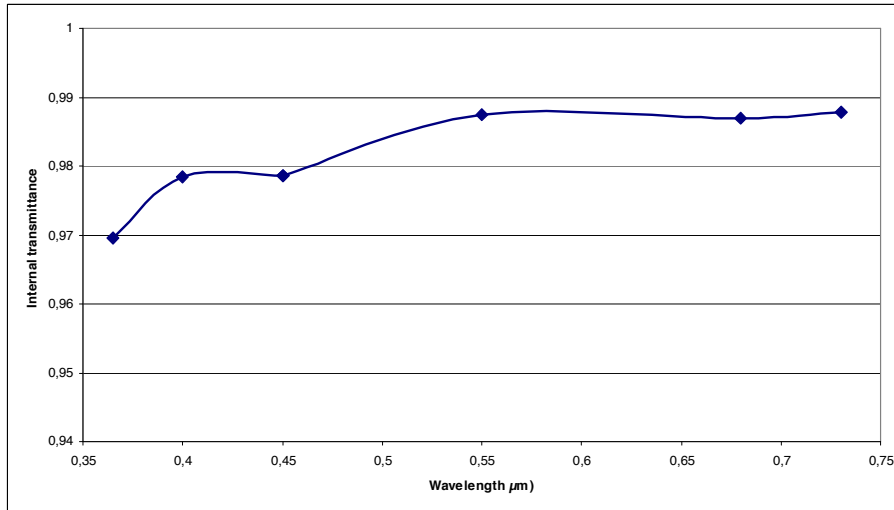
The resulting image quality is as follows (spot diagram scale = 50μm)



Below are given the RMS spot radius for a half slit and the different wavelengths (scale 20μm RMS).

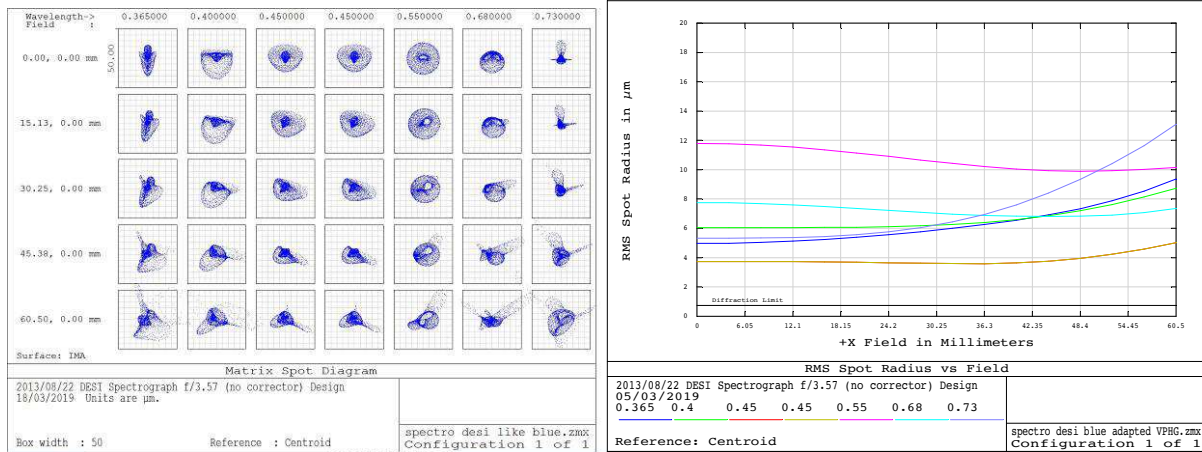


The transmittance of glasses performs well with a value greater than 96.5% at 365nm (mirror coating and VPHG efficiency not considered).



7.3 Optimization – minor changes

A reoptimization of the camera has been done to find a better image quality over the spectrum. The result is given below: the chromatism remains important and the image quality not good enough.



7.4 Conclusion

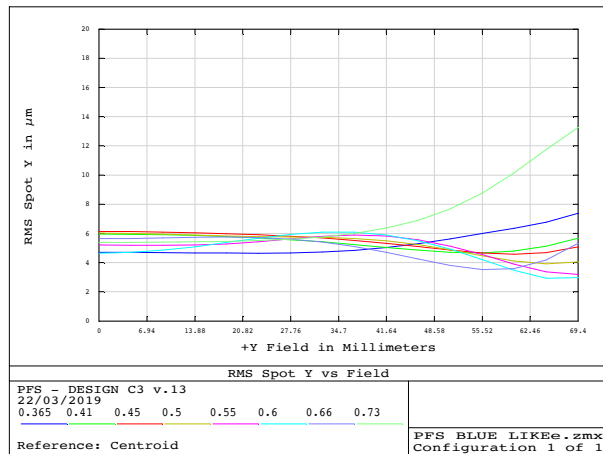
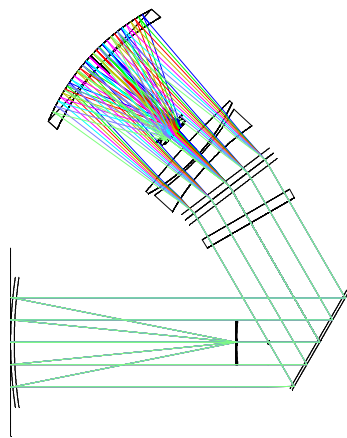
Keeping the DESI design as it is, by only changing the VPHG parameters and camera position gives a spectrograph which is not optimized for the entire spectrum(spot RMS >9μm). Even an optimization of the camera radii does not really improve the image quality. This design has the advantage of keeping DESI interfaces and tooling, but is not optimized for IFU6000 spectrum.

8 OTHER POSSIBILITIES

Some other design possibilities have been studied :

- PFS design
- 4MOST like design
- MUSE like design with curved CCD

8.1 PFS design



Without reoptimization, the image quality is good (except at the edge of the field at 730nm). The problems of such design are :

- the dimensions of the components (>300mm diameters with 5 aspherical faces, very long to produce)
- the very complex interfaces within the cryostat

This design is not compatible with the schedule of IFU6000. This solution has not been considered.

8.2 4MOST like design

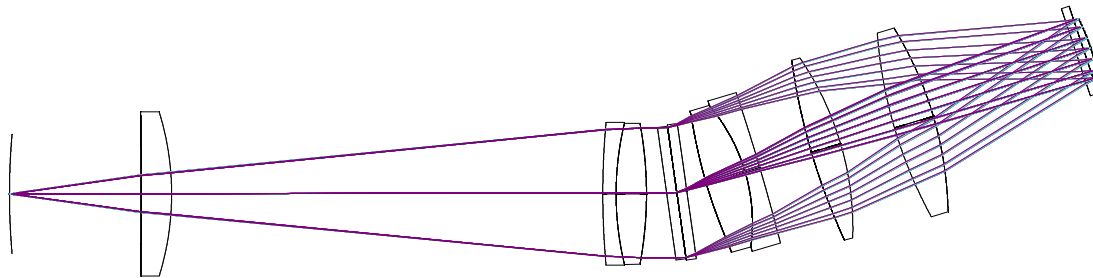
The 4MOST design does not fit with requirements of IFU6000 :

- The design is based on 6kx6k flat CCD.
- The complexity of the collimator and camera are not compatible with IFU 6000 schedule (long glass blank procurement for diameter above 270mm)

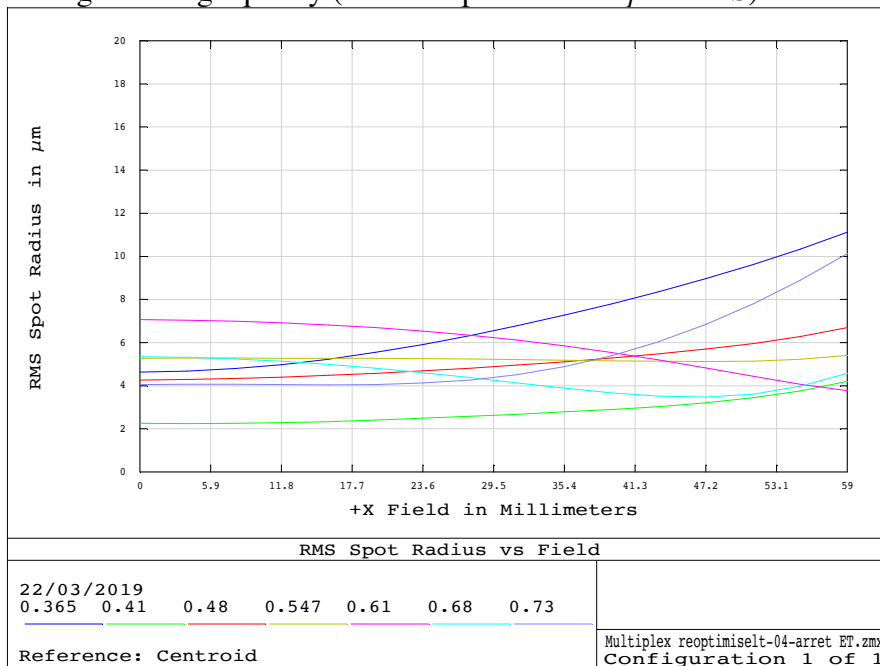
This solution has not been considered, nor simulated.

8.3 Curved CCD with MUSE like design

The optimization of a MUSE like design, using a curved CCD (and a window as dewar window) shows good results with few elements:



Only 7 lenses (mixed CaF2 and i-line glasses), 1 aspherical face, a silica window and a curved CCD show rather good image quality (scale of spot radius 20µm RMS) :

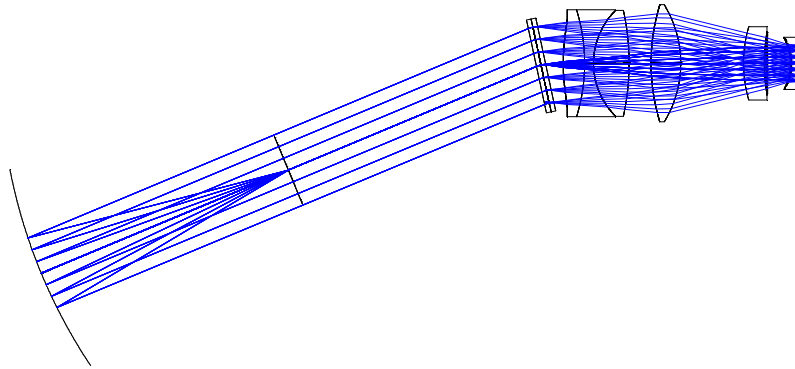


The maturity of curved CCD is not known at the moment to propose such a solution.

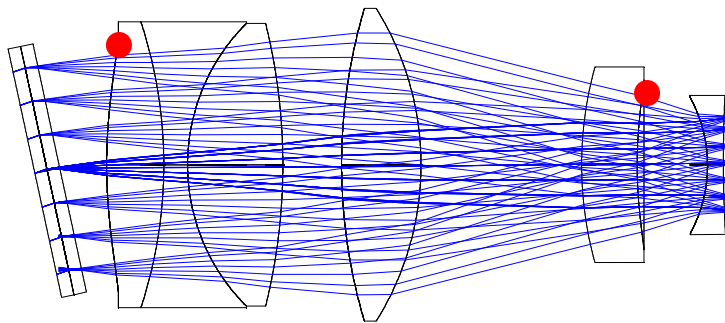
9 THE PROPOSED DESIGN

9.1 Overview

The proposed design is an update of the DESI blue optical configuration (fiber na=0.14, curved slit and spherical collimator mirror), the main difference being the addition of a lens. The asphere is also moved from the field lens to this new lens. The collimator is also slightly updated.

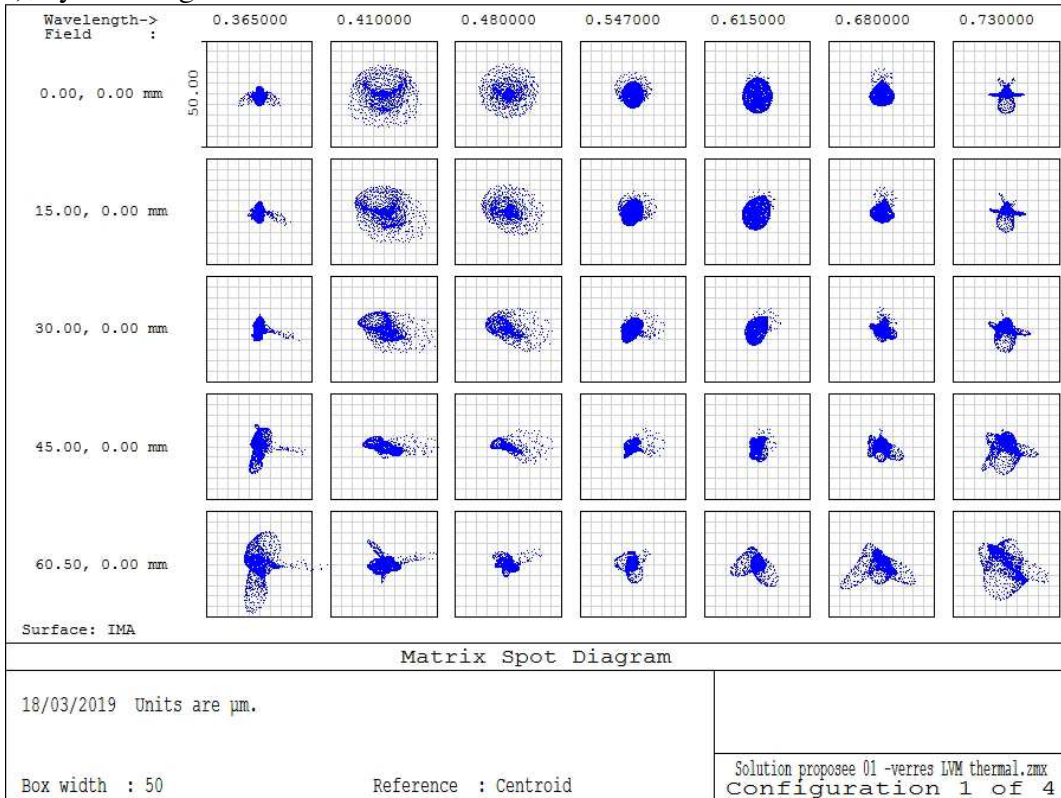


The next picture shows the camera design. The first CaF2 lens is aspheric, same as the PBL25Y L5 lens (red dots). The field lens and the other faces are purely spherical.

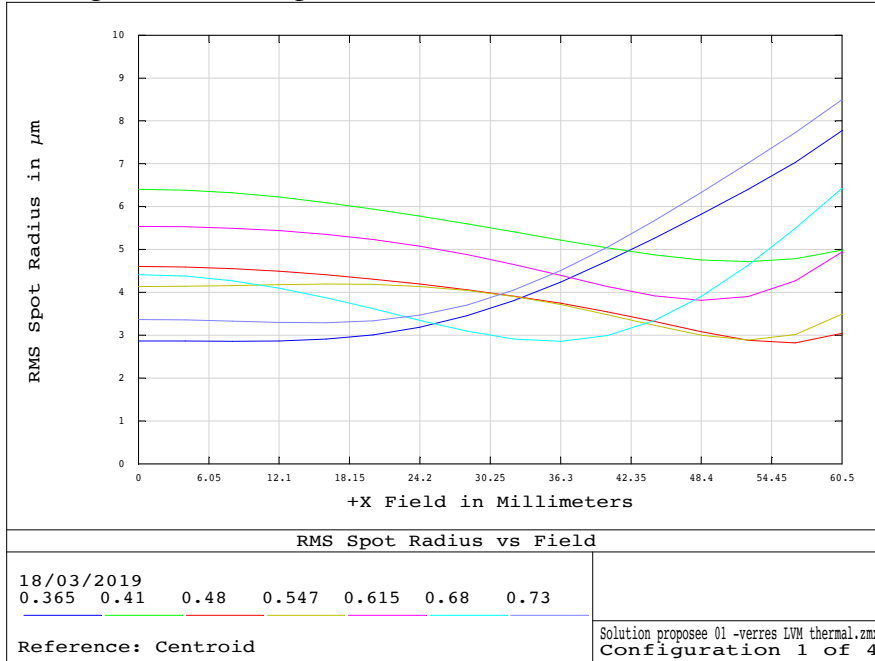


9.2 Performances

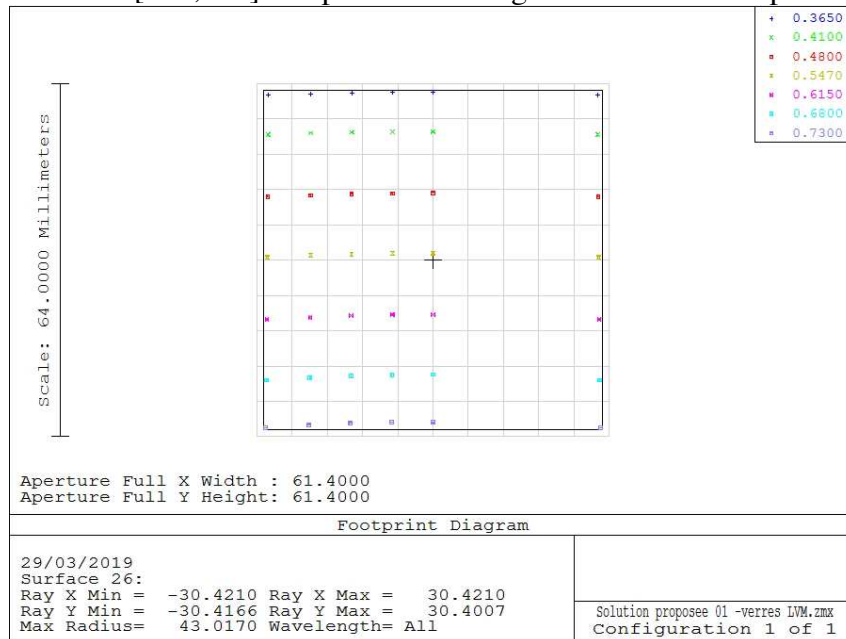
The next spot diagram shows the RMS spot radius (scale 50μm) for a half slit for the different wavelengths over IFU6000 spectrum. The image quality is improved (regarding DESI design), by reducing the residual chromatism.



The RMS spot size curves are as follows (scale $10\mu\text{m}$ RMS radius). The max RMS spot radius is $8.5\mu\text{m}$ (edge of field and spectrum):

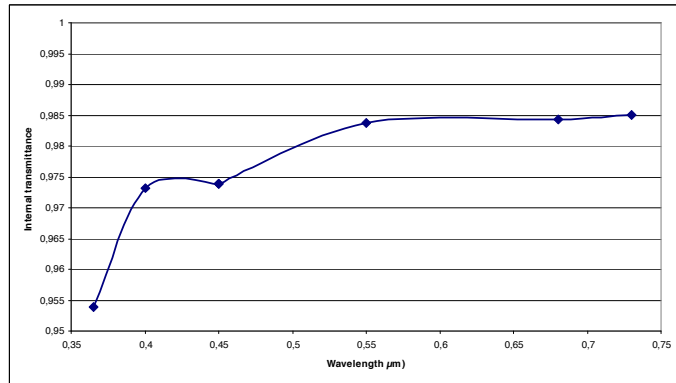


The slit length over the [365;736]nm spectrum is image on the CCD as represented below :



The internal transmittance of the camera is good: more than 95% at 365nm.

<i>Lambda (μm)</i>	<i>Internal transmittance (-)</i>
0,365	0,9538
0,4	0,9731
0,45	0,9739
0,45	0,9739
0,55	0,9837
0,68	0,9844
0,73	0,9850

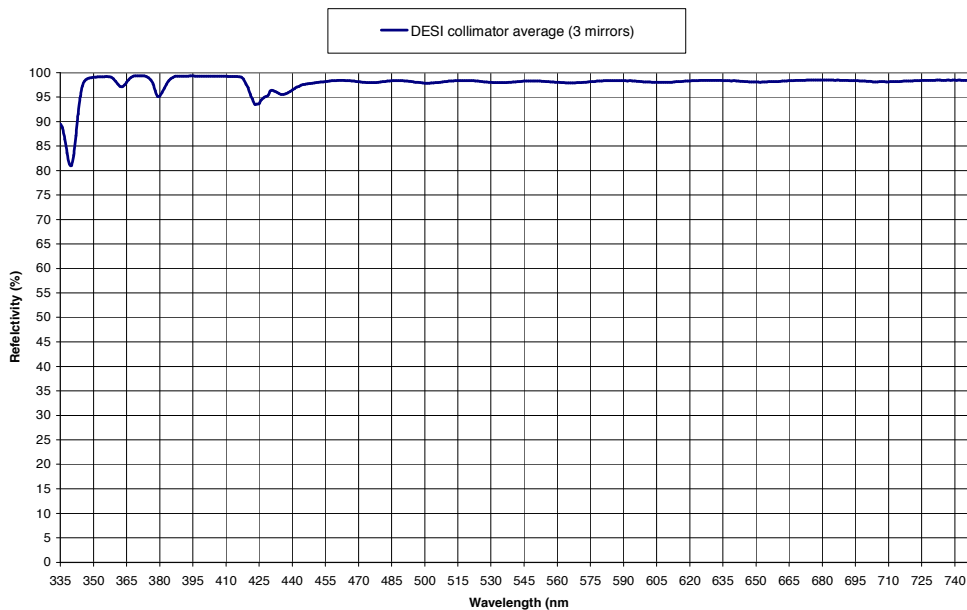


Note that it does not take into account the index of oil or glue absorbance, and the coating are considered perfect.

The AR coatings could be efficient at $R \approx 0.5\% / 0.6\%$ in average over the bandwidth.

The other contributors will be :

- the collimator mirror, which will be coated with a blue enhanced silver coating as for DESI ones (see curve below)
- the VPHG efficiency, which is not known at that time, but it will be the main contributor for sure.



9.3 Asphere deformation

The aspherical of the proposed design present the following departures from best sphere over the mentioned diameter:

<i>Asphere</i>	<i>Departure from best sphere</i>	<i>Diameter</i>
Asphere on L1	677 μm	160 mm
Asphere on L5	278 μm	110 mm

The aspherical surfaces are manufacturable.

9.4 Main parameters

The next table summarizes the main parameters of the proposed spectrograph :

<i>Parameter</i>	<i>Value</i>	<i>Comment</i>
Fiber numerical aperture	0.14	-
Slit length	121 mm	-
Useful diameter of VPHG	130mm	-
Line spacing of grating	0.70746 lines/ μm	Silica substrate
Camera focal length	221mm	-
Camera F/#	1.7	-
Vignetting	0%	Over the full field of view
Lateral magnification	0.496	At 547nm calculated for 60.5mm object height (30.026 on CCD)

The full optical combination is given in appendix 1

9.5 Conclusion

This design presents a good image quality, nominally better than $8.4\mu\text{m}$ RMS ($5\mu\text{m}$ in average), and uses a limited number of elements (1 spherical mirror and 6 lenses).

The glass blanks for CaF₂ and N-BAK2 are DESI compatible (same size), and the PBL25Y can be cut in a standard blank from Ohara (the homogeneity is guaranteed to 2.10^{-6} for these size of i-line glasses and PBL25Y is melted with the highest frequency).

The mechanical design can be very close to the DESI one, but is different due to this new lens. The interface principles can be kept and adapted.

The grating aperture has been limited to $\varnothing 130\text{mm}$ useful diameter (same as DESI size).

10 CONCLUSION OF DIFFERENT EXPLORED DESIGNS

This document has presented the different possibilities in the design of IFU6000. Most of them are not compatible with the schedule of the project.

We propose an alternative design, that will fulfil the requested performances, and that could be manufactured in the given time scale.

Note : in this document, we have not defined how many spectrographs are needed to integrate the 6000 fibers. The number of spectrographs will depend on different parameters that are not known :

- The final image quality specification
- The possible level of crosstalk between adjacent fibers
- The final dimension of fiber core at slit plane.

CE DOCUMENT ET LES INFORMATIONS QU'IL CONTIENT SONT CONFIDENTIELS ET SONT LA PROPRIETE EXCLUSIVE DE WINLIGHT SYSTEM. ILS NE DOIVENT ETRE COMMUNIQUEES QU'AUX PERSONNES AYANT A EN CONNAITRE LE CONTENU ET NE PEUVENT ETRE REPRODUITS NI DIVULGUES A TOUT AUTRE PERSONNE SANS L'ACCORD ECRIT DE WINLIGHT SYSTEM.

THIS DOCUMENT AND THE INFORMATION IT CONTAINS ARE PROPERTY OF WINLIGHT SYSTEM AND CONFIDENTIAL. THEY SHALL NOT BE DISCLOSED TO ANY PERSON EXCEPT TO THOSE HAVING A NEED TO KNOW THEM WITHOUT PRIOR WRITTEN CONSENT OF WINLIGHT SYSTEM.

11 DEVELOPMENT PLAN FOR THE PROPOSED DESIGN

The most important step is the optical final specifications that must be agreed with CAHA and consortium if any. The non exhaustive list is :

- the magnification ratio (margin of imaged fibers with respect to CCD size)
- the final image quality level (for tolerancing)
- the final throughput specification (for coatings)
- the ghost image analysis verification
- the final grating definition

This will allow to create the definition file of IFU6000 for manufacturing.

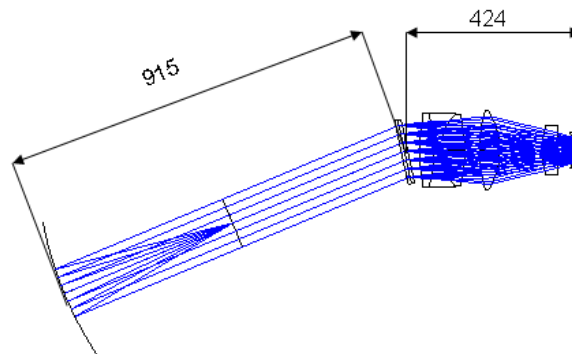
The proposed spectrograph is very similar to DESI one to reduce study work, but adaptation must be done anyway:

- The global foot print on the optical table
- The slit is different (curvature)
- The collimator has its radius of curvature different
- There is no dichroic
- The shutter may be different (smaller)
- The grating is different (incidence, line spacing, dimensions ?)
- The camera is different (radii, thicknesses, on more lens)
- The cryostat may be different
- The external cover will be different

The next paragraphs shows briefly the work to be done.

11.1 The optical table

The optical table must be chosen to fit at best the foot print of the spectrograph. The layout below gives the optical lengths, for which margin must be added for the collimator mount and thickness.



11.2 The slit

The slit curvature is different, but the concept is similar. Since its length is identical, and that the collimator size is very similar, the DESI interface can be kept.

The process for slit alignment can be kept also.

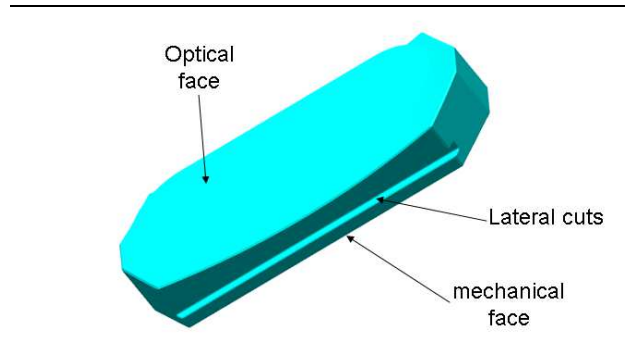
The tool used at Winlight to test and verify the spectrograph must be updated in accordance, based on the same conceptual design.

The slits for the DESI spectrographs have been supplied by Durham.

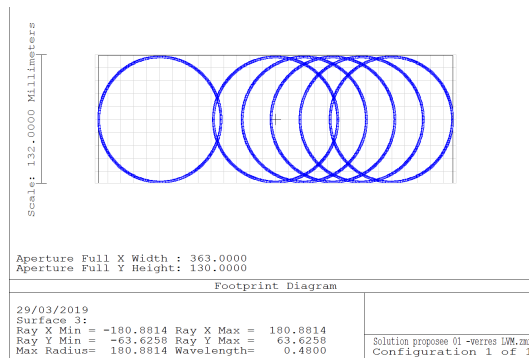
11.3 The collimator

The only difference with DESI collimator mirror is the radius of curvature (small change). It means that the mechanical design can be kept. Indeed the mechanical maintain is done at the back of the mirror by clamping the back surface through the lateral cuts.

It means also that the protective packages used for shipping the mirror already exists.



Below is shown the footprint of IFU6000 on the collimator having the nominal aperture of DESI mirror: it fits.



The collimator structure, as well as the Hartman doors shown beside can be reused without modification.

It is to be note that the collimator structure and the Hartman doors (mechanic and electronics) have been supplied for DESI by Ohio State Univeristy.

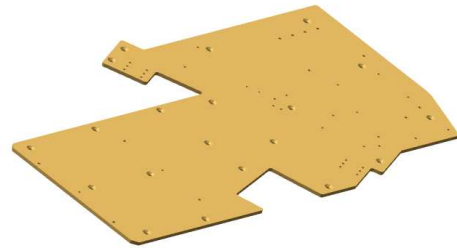
3 different possibilities must be considered :

- A - OSU accepts to deliver such assembly for IFU6000
- B - OSU accepts to share the definition files of it and Winlight manufacture and test it accordingly.
- C - OSU refuses the 2 first possibilities, and the mechanical / electronical designs must be done from the beginning.



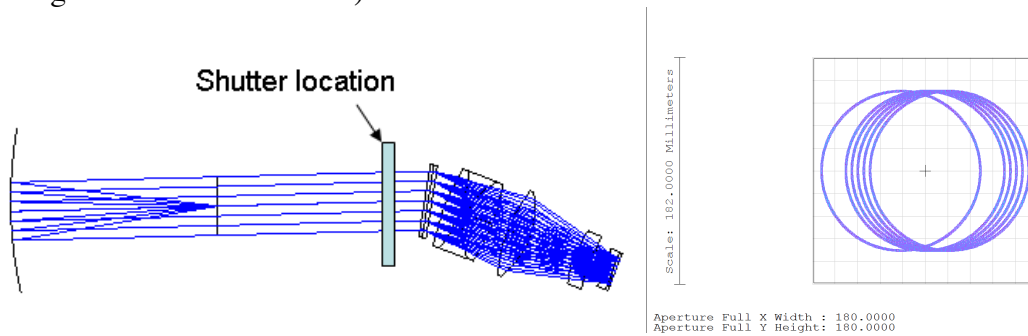
11.4 The slit to collimator link

The link between the collimator and the slit is done with an additional plate fixed on the bench that must be adapted to the IFU6000 final design.

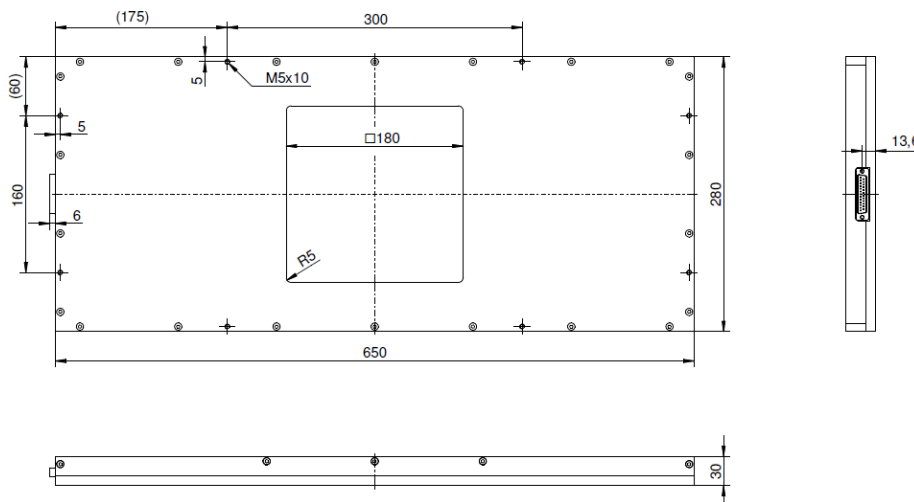


11.5 The shutter

On DESI the shutters are close to the dichroics (both components are supplied by DESI consortium). For IFU6000 it can be placed closer to the pupil (e.g. the VPHG). That allows to reduce the size of the shutter and to use on the shelf Bonn shutter. For example the 180x180 aperture shutter can be used if it is placed not far away than 150mm from the VPHG (see foot print diagram in that case below).

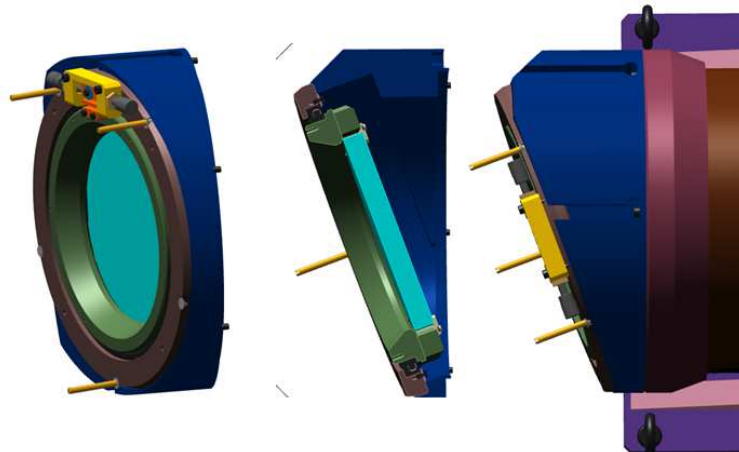


It implies to create a mount for this shutter, which is rather simple because no thermal effect or critical positioning is requested, and the interface is also simple (see drawing below, 4xM5 L10). This structure can be a part of the external cover.



11.6 The grating

The VPH grating is different. The same DESI geometry can be kept so that the individual cell can be kept (all parts except the blue one in the picture below).



In terms of general implantation there are 2 possibilities:

- To keep the VPHG on the camera barrel.
- To place the VPHG on the bench with a new structure.

If the VPHG is fixed on the camera, its orientation with respect to the collimator is modified when the camera is tilted to center the spectrum on the CCD: the settings camera and VPHG are coupled!

If the VPHG is placed on the bench, the AIT is highly simplified, because the VPHG is set according to the {slit+collimator} position, then it is fixed and does not move anymore.

The protocol to set the VPHG in that case is easy and accurate :

- to fix the orientation of the VPHG, a theodolite points the central fiber through the collimator and order 0 of the VPHG, and then points the face of the VPHG to set the incidence angle in vertical and horizontal directions.
- The different fibers, through the 0 order, give the geometrical axis of the slit in the VPHG space.
- Then the theodolite points the order 1 with few wavelengths (or white light) to set the dispersion axis perpendicular to the geometrical axis.

Once these settings are done, the VPHG will never be modified.

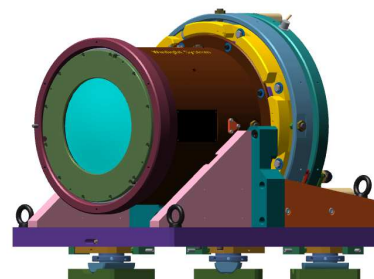
If it is placed on the camera, when the camera is tilted (to center the spectrum) or clocked (to align columns of CCD with fibers and spectra) the settings are strongly linked.

Making them independent is a strong upgrade of the DESI like design.

11.7 The camera

The camera general mechanical design and concept can be kept, there is no strong difference to implement except 2 points :

- the addition of the lens
- the cryostat interface



There shall be enough place and the adaptation seems not too difficult to add the new lens.

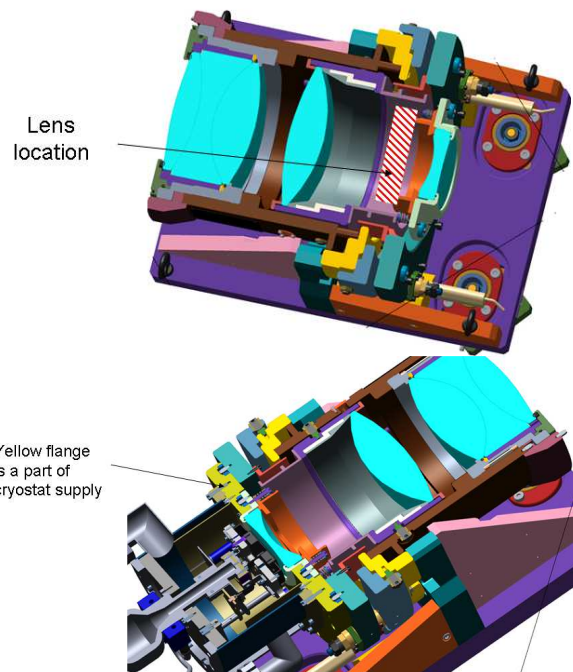
Indeed the mechanical cut beside shows that there is enough place for this modification.

The field lens is mounted in an individual barrel, which is then mounted onto the cryostat main flange.

The design of this barrel is made in collaboration with the cryostat supplier (CEA in the case of DESI).

The final camera+field lens interface is strongly linked to the cryostat supplier.

This is one of the critical point, if CEA can not supply a cryostat.



11.8 The cover

The cover must be redesigned any way because the spectrographs are really different. The proposed design is fully compatible with the technology used for DESI spectrograph (Dibond plates fixed in aluminium frames, and Viton flexible baffles between VPHG and camera).

12 PRELIMINARY COLABORATION AND INTEGRATION PLAN

12.1 The preliminary integration plan

This chapter aims to develop a very preliminary integration plan.

<i>Integration step</i>	<i>Protocol and required tooling</i>
Slit interface mounting.	The slit tool is required. It is based on the existing one, but updated to fit with IFU6000 slit definition.
Mounting and alignment of the collimator mirror with respect to the slit.	Same procedure and tooling as for DESI. Tooling already exists
Mounting and alignment of the grating with respect to collimator and slit	Only a theodolite
Camera mounting and setting	A dummy flange is required to hold a field lens during the test. For image quality verification, the tooling already exists. Light sources already exist
Integration of the cover and shutter	None
Mounting of the cryostat	None
Final verification with a specific slit (if needed)	The specific slit is from CAHA or consortium and aims to simulate the final slit.

The only tooling which must be manufactured is a slit like tool for alignment and image quality verification.

12.2 The possible collaboration scheme

This chapter aims to initiate a possible collaboration scheme taking into account the different subassembly and qualification steps. The next table gives the possible collaboration/participations.

<i>Subassembly / Qualification steps</i>	<i>Possible collaboration with</i>	<i>Comment</i>
Collimator and Hartman doors	Ohio State University	IFU6000 100% compatible with existing DESI supply
Fiber slit assembly (final and tooling)	Durham	IFU6000 very similar to existing DESI supply
Shutter	Not critical	Must be completely redesign and can be on the shelf Bonn shutter
VPHG	Who wants.	Subcontractors could be KOSI or Wasatch Photonics Specific inspection at delivery requests knowledge and specific optical means
Cryostat	CEA	IFU6000 100% compatible with existing DESI supply
Final qualification of the assembled spectrograph	OHP / LAM	Tooling and procedure exists at OHP/LAM (DESI)

13 CONCLUSION

The proposed optical design will met good optical performances.

It is designed such that most of the tools used by Winlight to integrate and test DESI spectrographs can be adapted.

It is shown that most of the elements can be handled by Winlight except the slit, the grating and the cryostat with detector, which are very critical.

CE DOCUMENT ET LES INFORMATIONS QU'IL CONTIENT SONT CONFIDENTIELS ET SONT LA PROPRIETE EXCLUSIVE DE WINLIGHT SYSTEM. ILS NE DOIVENT ETRE COMMUNIQUEES QU'AUX PERSONNES AYANT A EN CONNAITRE LE CONTENU ET NE PEUVENT ETRE REPRODUITS NI DIVULGUES A TOUT AUTRE PERSONNE SANS L'ACCORD ECRIT DE WINLIGHT SYSTEM.										THIS DOCUMENT AND THE INFORMATION IT CONTAINS ARE PROPERTY OF WINLIGHT SYSTEM AND CONFIDENTIAL. THEY SHALL NOT BE DISCLOSED TO ANY PERSON EXCEPT TO THOSE HAVING A NEED TO KNOW THEM WITHOUT PRIOR WRITTEN CONSENT OF WINLIGHT SYSTEM.										
REF. DOC	W	S	3	0	3	3	-	0	0	1	-	R	A	P	0	0	1	-	A	PAGE 23/27

14 APPENDICES

14.1 Proposed design preliminary definition

System/Prescription Data					
File : D:\VL\DATA WS\Affaires\AF3033 - IAA - IFU6000\6 - Etude optique\Solution proposee 01 - verres LVM.zmx					
Title:					
Date : 22/03/2019					
GENERAL LENS DATA:					
Surfaces	: 24				
Stop	: 1				
System Aperture	: Object Space NA = 0.14				
Glass Catalogs	: SCHOTT DVMISC DIVERS-ESPRESSO KCRM_REDRX				
Ray Aiming	: Off				
Apodization	: Uniform, factor = 0.00000E+000				
Temperature (C)	: 2.00000E+001				
Pressure (ATM)	: 1.00000E+000				
Adjust Index Data To Environment	: Off				
Effective Focal Length	: 712.8111 (in air at system temperature and pressure)				
Effective Focal Length	: 712.8111 (in image space)				
Back Focal Length	: 339.7032				
Total Track	: 1341.15				
Image Space F/#	: 5.461466				
Paraxial Working F/#	: 1.715957				
Working F/#	: 1.727539				
Image Space NA	: 0.2797487				
Object Space NA	: 0.14				
Stop Radius	: 65.25822				
Paraxial Image Height	: 29.35743				
Paraxial Magnification	: -0.4852468				
Entrance Pupil Diameter	: 130.5164				
Entrance Pupil Position	: 0				
Exit Pupil Diameter	: 95.08156				
Exit Pupil Position	: -154.7966				
Field Type	: Object height in Millimeters				
Maximum Radial Field	: 60.5				
Primary Wavelength	: 0.365 μ m				
Lens Units	: Millimeters				
Angular Magnification	: 1.413315				
Fields	: 6				
Field Type	: Object height in Millimeters				
#	X-Value	Y-Value	Weight		
1	0.000000	0.000000	1.000000		
2	15.000000	0.000000	1.000000		
3	30.000000	0.000000	1.000000		
4	45.000000	0.000000	1.000000		
5	60.500000	0.000000	2.000000		
6	-60.500000	0.000000	0.000000		
Vignetting Factors					
#	VDX	VDY	VCX	VCY	VAN
1	0.000000	0.000000	0.000000	0.000000	0.000000
2	0.000000	0.000000	0.000000	0.000000	0.000000
3	0.000000	0.000000	0.000000	0.000000	0.000000
4	0.000000	0.000000	0.000000	0.000000	0.000000
5	0.000000	0.000000	0.000000	0.000000	0.000000
6	0.000000	0.000000	0.000000	0.000000	0.000000
Wavelengths	: 7				
Units:	μ m				
#	Value	Weight			
1	0.365000	2.000000			
2	0.410000	1.000000			
3	0.480000	1.000000			
4	0.547000	1.000000			

5	0.615000	1.000000				
6	0.680000	1.000000				
7	0.730000	1.500000				
SURFACE DATA SUMMARY:						
Surf	Type	Radius	Thickness	Glass	Diameter	Conic
Comment						
OBJ	STANDARD	438.9358	461.5394		121	0
fibers						
STO	STANDARD	Infinity	-461.5394		130.5164	0
pup						
2	STANDARD	Infinity	-451.7717		123.304	0
3	STANDARD	909.6449	451.7717	MIRROR	361.7628	0
4	STANDARD	Infinity	448.7945		246.5986	0
5	COORDBRK	-	0		-	-
tilt	grating					
6	STANDARD	Infinity	8	SILICA	160	0
7	DGRATING	Infinity	0	SILICA	134.1684	0
8	STANDARD	Infinity	8	SILICA	134.1684	0
9	STANDARD	Infinity	0		160	0
10	COORDBRK	-	0		-	-
11	STANDARD	Infinity	30		134.4868	0
12	EVENASPH	327.0892	36	LITHOTEC-CAF2	160	0
L1						
13	STANDARD	-288.0132	15	N-BAK2	180	0
14	STANDARD	125.4764	60	LITHOTEC-CAF2	178	0
15	STANDARD	-370.3372	37.03788		178	0
16	STANDARD	345.3132	50	LITHOTEC-CAF2	197	0
L4						
17	STANDARD	-185.9449	101.2168		197	0
18	STANDARD	230.6097	35	PBL25Y	123.0761	0
L5						
19	EVENASPH	287.8174	4.304116		106.8075	0
20	STANDARD	Infinity	40		106.8075	0
21	COORDBRK	-	0		-	-
22	STANDARD	-89.44228	10	SILICA	86.23526	0
23	STANDARD	848.5682	6.025		87.66635	0
IMA	STANDARD	Infinity			85.98856	0
SURFACE DATA DETAIL:						
Surface OBJ STANDARD fibers						
Surface STO STANDARD pup						
Surface 2 STANDARD						
Surface 3 STANDARD						
Mirror Substrate : None						
Surface 4 STANDARD						
Surface 5 COORDBRK tilt grating						
Decenter X : 0						
Decenter Y : 0						
Tilt About X : 10.46						
Tilt About Y : 0						
Tilt About Z : 0						
Order : Decenter then tilt						
Surface 6 STANDARD						
Aperture : Floating Aperture						
Maximum Radius : 80						
Surface 7 DGRATING						
Lines / μm : 0.70745995						
Diffraction Order : 1						
Surface 8 STANDARD						
Surface 9 STANDARD						
Aperture : Floating Aperture						
Maximum Radius : 80						

```

Surface 10 COORDBRK
Decenter X      :          0
Decenter Y      :          2
Tilt About X    :      12.161372
Tilt About Y    :          0
Tilt About Z    :          0
Order           : Decenter then tilt

Surface 11 STANDARD

Surface 12 EVENASPH L1
Coefficient on r^ 2      :          0
Coefficient on r^ 4      : -4.9952428e-008
Coefficient on r^ 6      : -2.6501307e-012
Coefficient on r^ 8      :  4.3822839e-016
Coefficient on r^10     : -9.2740884e-020
Coefficient on r^12     :  6.5753739e-024
Coefficient on r^14     :          0
Coefficient on r^16     :          0
Aperture           : Floating Aperture
Maximum Radius      :          80

Surface 13 STANDARD
Aperture           : Floating Aperture
Maximum Radius      :          90

Surface 14 STANDARD
Aperture           : Floating Aperture
Maximum Radius      :          89

Surface 15 STANDARD
Aperture           : Floating Aperture
Maximum Radius      :          89

Surface 16 STANDARD L4
Aperture           : Floating Aperture
Maximum Radius      :          98.5

Surface 17 STANDARD
Aperture           : Floating Aperture
Maximum Radius      :          98.5

Surface 18 STANDARD L5

Surface 19 EVENASPH
Coefficient on r^ 2      :          0
Coefficient on r^ 4      : -3.3563967e-008
Coefficient on r^ 6      : -1.8277789e-011
Coefficient on r^ 8      :  2.3568062e-015
Coefficient on r^10     : -8.0910827e-019
Coefficient on r^12     :          0
Coefficient on r^14     :          0
Coefficient on r^16     :          0

Surface 20 STANDARD

Surface 21 COORDBRK
Decenter X      :          0
Decenter Y      :     -0.099866309
Tilt About X    :     -0.24397842
Tilt About Y    :          0
Tilt About Z    :          0
Order           : Decenter then tilt

Surface 22 STANDARD

Surface 23 STANDARD
Aperture           : Floating Aperture
Maximum Radius      :      43.833174

Surface IMA STANDARD
Aperture           : Rectangular Aperture
X Half Width      :          30.7

```

Y Half Width	:	30.7
--------------	---	------

CE DOCUMENT ET LES INFORMATIONS QU'IL CONTIENT SONT CONFIDENTIELS ET SONT LA PROPRIETE EXCLUSIVE DE WINLIGHT SYSTEM. ILS NE DOIVENT ETRE COMMUNIQUEES QU'AUX PERSONNES AYANT A EN CONNAITRE LE CONTENU ET NE PEUVENT ETRE REPRODUITS NI DIVULGUES A TOUT AUTRE PERSONNE SANS L'ACCORD ECRIT DE WINLIGHT SYSTEM.

THIS DOCUMENT AND THE INFORMATION IT CONTAINS ARE PROPERTY OF WINLIGHT SYSTEM AND CONFIDENTIAL. THEY SHALL NOT BE DISCLOSED TO ANY PERSON EXCEPT TO THOSE HAVING A NEED TO KNOW THEM WITHOUT PRIOR WRITTEN CONSENT OF WINLIGHT SYSTEM.



IFU6000 spectrographs Study and first spectrograph CAHA

TECHNICAL AND FINANCIAL PROPOSAL Ref. OFWS1780-1-A



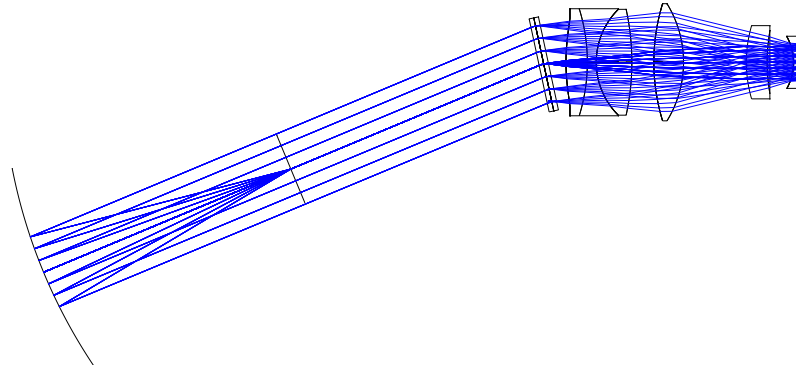
Date : 30 April 2019

	Technical Contact	Commercial Contact
Name :	Vincent Lapère	Philippe Godefroy
Tel. :	+33 (0)4 90 07 78 60	+33 (0)4 90 07 78 60
Fax :	+33 (0)4 90 77 76 31	+33 (0)4 90 77 76 31
Email :	vincent.lapere@winlight-system.com	philippe.godefroy@winlight-system.com

A – TECHNICAL PROPOSAL

1. SUBJECT

This proposal deals with the study and manufacturing of the spectrograph for IFU6000 project. The optical design of the spectrograph unit is as shown below. More details are given in the document Ref WS3033-001-RAP001-A.



IFU6000 is working with 6000 optical fibers. Therefore few spectrograph units are requested to cover this number of fibers. This offer deals with the design and manufacturing of one spectrograph unit.

2. DESCRIPTION OF THE TASKS and DELIVERABLES

a. Optical and mechanical design

The spectrograph design is not a copy of an existing spectrograph. The definition file must be created to allow its manufacturing. During this study some optical and mechanical work is done:

- Optical sensitivity analysis and tolerancing
- Ghost image analysis
- Thermal optical and mechanical analysis
- Mechanical design of the camera assembly, of the grating assembly, of the shutter and cover assembly, and possibly of the collimator assembly (the slit and cryostat assembly are not part of the supply)

Our offer includes:

<i>TASKS TO BE DONE</i>	<i>DELIVERABLES</i>
Optical and mechanical study	Justificative Design Report.
Final manufacturing drawings	Final mechanical design with interfaces CAD model

Our offer does not include:

- Finite Elements Analysis (FEA)
- Thermal impact of the shutter if any
- Everything not specified on “the offer includes”

b. Manufacturing integration and testing

The manufacturing, integration and test of the spectrograph unit will be organized as follows regarding Winlight activities and deliverables:

- Optical manufacturing of the collimator mirror and camera lenses
 - Glass blanks procurement
 - Grinding, polishing of optical elements
 - Coating of elements
- Mechanical pieces procurements
 - Procurement of mechanical pieces
 - Procurement of the shutter (180x180 Bonn)
- Mounting of assemblies :
 - Bench assembly
 - Grating assembly (to be supplied by CAHA)
 - Field lens assembly (with vacuum sealing verification)
 - Camera assembly
 - Shutter and cover assembly
 - Collimator mechanical assembly (without Hartman doors)
- Alignment and tests
 - Alignment of assemblies :
 - Slit interface verification
 - Collimator mirror alignment
 - Grating assembly
 - Camera and field lens assembly

Our offer includes:

<i>TASKS TO BE DONE</i>	<i>DELIVERABLES</i>
Procurement of glass blanks	Certificate of Compliancy
Manufacturing and coating of the lenses	Inspection reports
Manufacturing of mechanical pieces	-
Integration, alignment and testing of the spectrograph assemblies	Inspection report
Delivery of spectrograph packed safely and shipped	Full integrated assemblies on optical bench

Our offer does not include:

- the slit
- the cryostat assembly
- the VPHG
- the Hartmann doors
- final slit mounting and verification are not considered.
- work on or with cryostat is not considered.
- everything not specified on “the offer includes”

Note : if parts to be delivered by the project are not delivered in due time (for instance VPHG), Winlight will not be held responsible for delay. In case, this leads to delay the schedule by more than 6 months, Winlight will be allowed to complete its work up to what is possible without this missing part and to invoice the total amount of the contract.

B – FINANCIAL PROPOSAL

1 - DELIVERY DATE

T0 : date of receipt of the order and/or kick off meeting.

The delivery dates are the followings (August should be neutralized) :

<i>Phase</i>	<i>Delivery time</i>
Study	T0 + 8 months
Glass blank procurement (will start at T0+ 3months)	T1 + 6 months = T0 +9 months
Optical manufacturing (including coating)	T1 + 12 months = T0 + 15 months
Integration, alignment and testing of the spectrograph	T1 + 16 months= T0 + 19 months
Delivery	15 days after acceptance

August has to be neutralized for summer holidays.

2 - PRICES

The tasks as proposed in our technical proposal can be realized for the following amounts:

Item 1 : Optical and mechanical study and non recurrent costs (tooling)

88 000 €

Item 2 : Manufacturing, integration and test of the first spectrograph

273 000 €

Item 3 : Manufacturing, integration and test of spectrographs

To be discussed later

Our prices are without VAT and DAP your laboratories in Spain.

Item 2 cannot be ordered without Item 1.

Item 2 should be ordered not later than 5 months after Item 1.

3 – SALES CONDITIONS

3.1 - Validity of our offer: our offer is valid 3 months from the date of page 1.

3.2 - Payments schedule: our offer is established taking into account the following payment schedule:

Item 1 :

- 30% with the order
- Balance at delivery

Item 2 :

- 30% with the order
- 30% at glass blanks receipt
- Balance at delivery

3.3 - Way of payment: By bank transfer within 30 days at receipt of the invoice. Initial down payment shall be paid within 10 days after placement of the order. The bank transfer costs remains at your charge. It is not included in our prices charges for the supply of bank guarantee or performance bonds which can be supplied upon request.

3.4 - Guarantee: Our products are guaranteed 12 months. This guarantee is intended for repairs done in our workshop, the packing insurance and transport costs being excluded. The date of the beginning of the guarantee is the date of delivery.

3.5 - Ownership reserve: WINLIGHT SYSTEM keeps the entire ownership of the good until the effective payment of the total price amount. The non-payment of any expired date can involve the claim of the goods. These clauses do not obstruct the transfer to the buyer, from delivery, of losses or damage risk on the sold goods as well as damages they could induce.

3.6 - Limit of responsibility : our products are manufactured according state of the art techniques. Therefore, we cannot be held responsible for any consequences caused by either delay or failure of our products.

Philippe Godefroy

C.O.O.






APPENDIX D




IFU-6000 Instrument Control System Feasibility Study

Document Title	LUCA@CAHA35-Instrument Control System Feasibility Study
Document Number	LUCA35-ICS-FS-001
Issue	V 1.0
Date	12/07/2019

Prepared By	José Miguel Ibáñez	Signature	
	Control Engineer / IAA-CSIC	Date	12/07/2019
Approved By	Francisco Prada	Signature	
	Principal Investigator	Date	12/07/2019
Released By	Francisco Prada	Signature	
	Principal Investigator	Date	12/07/2019

Contributors	Francisco Prada, Justo Sánchez del Río
Description	This document describes the design of the ICS sub-system
Distribution	LUCA Team




	<p>LUCA@CAHA35-Instrument Control System Feasibility Study</p>	<p>Reference: LUCA35-ICS-FS-001 Issue: V 1.0 Date: 12/07/2019 Page 2 of 30</p>
---	--	--

Change Record

Issue	Date	Changed by	Sections Affected	Change Description
0d1	15/05/19	JM.Ibáñez	All	First draft
0d2	04/06/19	JM.Ibáñez	All	Second draft
0d3	18/06/19	JM.Ibáñez	6	Add cost estimation
1.0	11/07/19	JM.Ibáñez	All	Consider AAO design as main solution

Table of Contents

Change Record.....	2
List of Figures	5
List of Tables	5
1 Applicable and Reference documents	6
1.1 Applicable Documents	6
1.2 Reference Documents	6
1.3 List of Abbreviations	6
1 Introduction.....	8
1.1 Scope and Purpose of Document.....	8
1.2 Structure of the document	8
2 Instrument Control Electronics (ICE).....	9
2.1 Organization	9
2.2 Devices	10
2.2.1 Calibration Unit	10
2.2.2 Focal Plane Assembly (FPA).....	10
2.2.3 Spectrograph	10
2.2.4 ICE cabinet	11
2.2.5 Motors	11
2.2.6 Shutters.....	11
2.2.7 Lamps	11
2.2.8 Pick-off mirror	12
2.2.9 ADC (TBC).....	12
2.2.10 Cryostats control and monitoring	12
2.2.11 Temp, Hum sensor and Press probes	12
2.3 Environmental conditions.....	12
2.4 Device Controllers	13
2.4.1 Motor controllers	13
2.5 Detector readout sub-system	13
2.5.1 Host data Interface	15
2.6 A&G sub-system.....	16
2.7 Hardware Interfaces	16

	<p>LUCA@CAHA35-Instrument Control System Feasibility Study</p>	<p>Reference: LUCA35-ICS-FS-001 Issue: V 1.0 Date: 12/07/2019 Page 4 of 30</p>
---	--	--


2.8	Deployment.....	17
2.9	Cabinets.....	18
2.9.1	Overall layout.....	18
2.9.2	Common features	18
2.10	Power consumption	18
2.11	Power dissipation.....	18
2.12	Interlock and safety.....	19
3	Instrument Control Software (ICSW).....	19
3.1	Organization	19
3.2	General specifications	20
3.3	Software architecture overview	21
3.3.1	Telescope I/F	22
3.3.2	Spectrograph and Calibration Unit control.....	22
3.3.3	Detector Control Software (DCS)	22
3.3.4	A&G	23
3.3.5	Third-party controllers.....	23
3.3.6	Thermal control and monitoring.....	24
3.3.7	Interfaces and protocols	24
3.4	Observation Tool	25
3.5	Software development Environment.....	25
4	Data Handling System (DHS).....	26
4.1	Data rate estimation.....	27
4.2	Storage format	27
4.3	Data processing.....	28
5	Costing	28
5.1	Personnel.....	28
5.1.1	Feasibility study (1-Oct-2018 to 12-Jul-2019).....	28
5.1.2	Development and AIV phases (5 years).....	28
5.2	Hardware costs	28
6	Overall feasibility and compliance assessment with the CAHA software framework and hardware recommendations	30

List of Figures

Figure 1-1 LUCA@CAHA3.5m ICS PBS.....	8
Figure 2-1 ICSW PBS.....	9
Figure 2-2 Embedded Beckhoff PC-PLC	13
Figure 2-3 Example of Beckhoff stepper motor controller and resolver modules	13
Figure 2-4 Archon CCD controller	14
Figure 2-5 Hardware Architecture for the LUCA data acquisition sub-system.....	15
Figure 2-6 A&G cameras distribution	16
Figure 2-7 Hardware architecture.....	18
Figure 3-1 ICSW PBS.....	20
Figure 3-2 Software Architecture.....	21
Figure 3-3 DCS architecture.....	23
Figure 3-4 IWS-PLC protocol interface.....	25
Figure 4-1 LUCA@CAHA-3.5m Data Handling System.....	26

List of Tables

Table 1: CAL device list.....	10
Table 2: FPS device list.....	10
Table 3: Spectrograph device list	11
Table 4: ICE cabinet device list	11
Table 5 Data rate estimation	27
Table 6 Estimated personnel resources (FTE).....	28

	<p style="text-align: center;">LUCA@CAHA35-Instrument Control System Feasibility Study</p>	<p>Reference: LUCA35-ICS-FS-001 Issue: V 1.0 Date: 12/07/2019 Page 6 of 30</p>
---	--	--

1 Applicable and Reference documents

1.1 Applicable Documents

Ref No	Document Number and Document Title	Issue Number & Date
[AD-01]	CAR_RPT_001_LUCA_Feasibility_Study_V2	Rev 2 , 1–July-2019

1.2 Reference Documents

Ref No	Document Number and Document Title	Issue Number & Date
[RD-01]	Archon: A modern controller for high performance astronomical CCDs.	SPIE, Volume 9147, id. 91475B 11 pp. (2014)
[RD-02]	The Zwicky Transient Facility Camera	SPIE, Volume 9147, id. 914779 13 pp. (2014)
[RD-03]	An electro-optical test system for optimising operating conditions of CCD sensors for LSST	Journal of Instrumentation, Volume 12, Issue 12, pp. C12019 (2017).

1.3 List of Abbreviations

The following abbreviations and acronyms are used in this document:

AAO	Anglo-Australian Observatory
ADC	Atmospheric Dispersion Corrector / Analog Digital Converter
AIV	Assembly, Integration and Verification
API	Application Programmatic Interface
ATP	Acceptance Test Plan
CCD	Charge Coupled Device
DCS	Detector Control System
DFE	Detector Front-End Electronics
DRS	Data Reduction Software
FCS	Function Control System
FDR	Final Design Review
FITS	Flexible Image Transport Format
FWHM	Full Width Half Maximum



LUCA@CAHA35-Instrument Control
System Feasibility Study

Reference: LUCA35-ICS-FS-001

Issue: V 1.0

Date: 12/07/2019

Page 7 of 30

GUI	Graphical User Interface
HW	Hardware
ICE	Instrument Control Electronics
ICS	Instrument Control System
ICSW	Instrument Control Software
INS	Instrumentation Software
ISDD	Instrument Software Design Description
ISFS	Instrument Software Functional Specification
ISURS	Instrument Software User Requirements Specification
ISUMM	Instrument Software User and Maintenance Manual
IWS	Instrument Workstation
LAN	Local Area Network
LCU	Local Control Unit
MS	Maintenance Software
MTBF	Mean Time Between Failures
MTBS	Mean Time Between Service
N/A	Not Applicable
OB	Observation Block
OBD	Observation Block Descriptor
OLAS	On-Line Archive Subsystem
OO	Object Oriented
OCS	Observation Coordination System
OT	Observation Tool
PAF	Parameters File
PDR	Preliminary Design Review
RPC	Remote Procedure Call
SW	Software
TBC	To Be Confirmed
TBD	To Be Defined
TCCD	Technical CCD
TCS	Telescope Control Software

WS	Workstation
----	-------------

1 Introduction

1.1 Scope and Purpose of Document

The purpose of this document is to present the scale and feasibility of the LUCA@CAHA3.5m Instrument Control System (ICS) work package, including: electronics, number of motor/actuators/sensors, cabinet control and distribution, power consumption, data rates, control software, observation software tools, GUIs, data handling, etc., and also assess the compliance of the ICS with the hardware recommendations applicable to the CAHA Observatory. It forms part of the documentation set to be revised by the review panel of the Feasibility Study, and contains the technological baseline and will be the reference for further [LUCA@CAHA3.5m](#) activities during the preliminary and detailed design phases.

The document gives a general description of the LUCA@CAHA3.5m control electronics and software, and suppose the **AAO optical design** described in the specific document [AD-01], consisting in ten 1-arm spectrographs, and employing 600 fibres per slit/spectrograph. From the point of view of the system control, that design is simpler compared with the other conceptual instrument based on **Winlight DESI-like 1-arm**, mainly due to the number of spectrographs required, so the AAO case is considered to study in this document.

Standard features, such as e.g. data processing, cryogenic control, telescope control, are not addressed in detail at this phase of the project. Some specifications from CAHA that are specifically driving the design are extracted from the various applicable documents and highlighted in this document.

1.2 Structure of the document

The structure of the document is mapped to the ICS Product Breakdown structure. Section 2 addresses the electronics, section 3 describe the software and section 4 is about the data handling system.

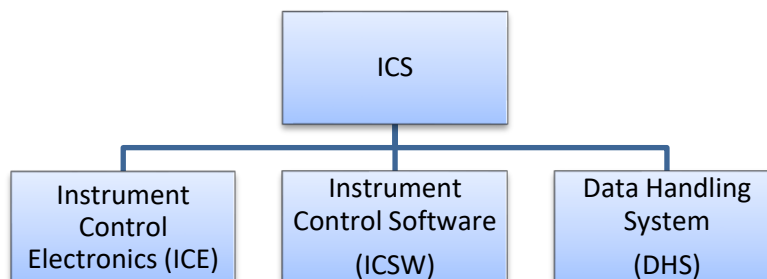


Figure 1-1 LUCA@CAHA3.5m ICS PBS

2 Instrument Control Electronics (ICE)

2.1 Organization

Next figure is the detailed product breakdown structure of the ICE that is part of the ICS work package.

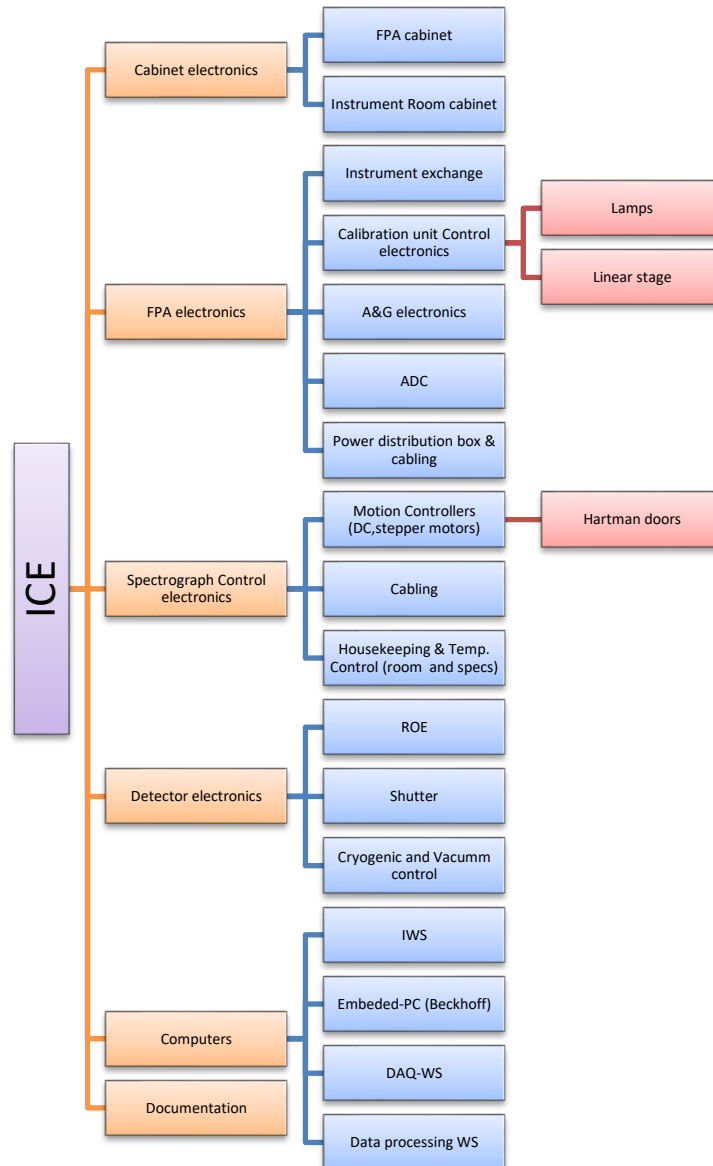


Figure 2-1 ICSW PBS

The LUCA@CAHA-3.5m instrument control electronics (ICE) package consists of several hardware components to control the devices of the instrument. The choice of the hardware components will be driven by well established industrial standards and Commercial Off-the-Shelf (COTS) products and compliance with CAHA requirements.

The control of the cryogenic and vacuum part of the detector sub-system is entirely of the responsibility of Cryostat work package (TBC), and only I/F for supervision and monitoring are considered here.

2.2 Devices

The following tables list all the devices of the instrument, grouped per work sub-package.

2.2.1 Calibration Unit

The calibration unit supposed to be like PMAS instrument at [CAHA@3.5m](#), requiring a positioning mechanism, several light sources and optics elements.

Table 1: CAL device list

WP	Device	#	Device type	Detailed device type
CAL	VIS wavelength calibration source	4	Light source	Lamp (spectral)
CAL	VIS flat field calibration source	2	Light source	Lamp (halogen)
CAL	Calibration shutter	1	Shutter	Shutter (TBC)
CAL	Power supply for spectral lamps	4	Power Supply	Power Supply

2.2.2 Focal Plane Assembly (FPA)

Table 2: FPS device list

WP	Device	#	Device type	Detailed device type
FPA	ADC (TBC)	1	Atm. Disp. Corrector	Circular movement (2 motors)
FPA	Instrument Pick-off mirror (CARMENES-LUCA)	1	linear movement	Medium stepper motor
FPA	HSK temperature sensors	2	Temperature sensor	Temperature sensor (for monitoring)
FPA	Instrument Pick-off mirror, ADC and Calibration positioning switches	3	Switch	Switch
FPA	Calibration unit linear stage	1	Linear movement	Stepper motor

2.2.3 Spectrograph

The spectrograph assembly, made by *Winlight Systems*, and its major mechanical components includes the optical bench, cameras and cryostats, optical elements, the shutters and the Hartmann doors.


	<p style="text-align: center;">LUCA@CAHA35-Instrument Control System Feasibility Study</p>	<p>Reference: LUCA35-ICS-FS-001 Issue: V 1.0 Date: 12/07/2019 Page 11 of 30</p>
---	--	---

Table 3: Spectrograph device list

WP	Device	#	Device type	Detailed device type
SPEC	science detector	8	Science e2v 4kx4k	Science camera (VIS)
SPEC	Shutter	8	Shutter	Uniblitz/Bonn shutter (TBC)
SPEC	HSK Temperature sensors in spectrographs	16	Temperature sensor	Temperature sensor (for monitoring); 2 per SPEC
SPEC	Motorized Detector tip	8	Linear movement	Stepper Motor (1 per detector)
SPEC	Motorized Detector tilt	8	Linear movement	Stepper Motor (1 per detector)
SPEC	Motorized Detector focus	8	Linear movement	Stepper Motor (1 per detector)
SPEC	JUMO Imago 500	8	Temp monitor and controller for SPEC and detector	Temp. monitor and controller

2.2.4 ICE cabinet

Table 4: ICE cabinet device list

WP	Device	#	Device type	Detailed device type
ICE	Varistar LHX3 Cabinet cooled	1	42 U Cabinet	Varistar LHX3
ICE	Workstation	5	Rack Computer	DELL PowerEdge R7415
ICE	STA Archon ROE	2	CCD ROE	CCD Read out controller
ICE	PC-PLC	2	Embedded Sw PLC	Beckhoff PLC CX2030
ICE	Network Switch	2	Network Switch	Network Switch
ICE	Power Distribution Supply	2	Power Supply	General PS

2.2.5 Motors


Motors (for CCD tip/tilt and focus) will be standard DC or stepper motors (no brushless). In general, these motors are compatible with the standard Beckhoff hardware controllers.

2.2.6 Shutters

Shutters purposed will be based on COTS components, as Bonn Univ. or Uniblitz brands. They will have their own controller, which will be triggered by the Archon output TTL signal providing a reference signal synchronous to the all CCD sensors.

2.2.7 Lamps

The calibration lamps purposed for the calibration unit are four HCL lamps (Hg, Ne, ThAr and TBD) with its own power supply (Photron), controlled via USB. This power supply provides a precision current source to correctly drive hollow cathode lamps (HCL) at a specific current.

	<p>LUCA@CAHA35-Instrument Control System Feasibility Study</p>	<p>Reference: LUCA35-ICS-FS-001 Issue: V 1.0 Date: 12/07/2019 Page 12 of 30</p>
---	--	---

Additionally, two halogen (HL) continuum lamp will be included for flat field calibrations. These lamps will not require any special power supply.

2.2.8 Pick-off mirror

Due to the Cassegrain focus will be shared between CARMENES and LUCA, the FPA will include a pick-off mirror to select the instrument light path. This mirror will be mounted on its linear stage, and two positions will be defined: mirror in beam for CARMENES observations and mirror out of beam to clear the LUCA FoV.

2.2.9 ADC (TBC)

The FPA fore-optics section contains an ADC which requires 2 continuous rotary mechanisms. These will utilize a stepper motor and worm gear to produce the required slow speed continuously variable motion according to telescope coordinates.

2.2.10 Cryostats control and monitoring

The control of the cryogenic and vacuum part of the detector sub-system is entirely of the responsibility of Cryostat work package (TBC), and only I/F for supervision and monitoring are considered here.

The thermal supervision and monitoring of the 8 detector cryostats heads will be handled and monitored by a unit based on an industrial Program Controller (JUMO Imago 500). The Imago 500 can control and monitor:

- Detector temperature
- Cold plate temperature
- N2 exhaust gas temperature
- Vacuum pressure

There will be numerous interlocks for temperature and pressure to guarantee the detector safety. We will use a JUMO Imago 500 per detector, connected via Profibus-DP to the master controller.

2.2.11 Temp, Hum sensor and Press probes

Temperature, humidity and pressure sensors will be compliance with an Ethercat field bus control, and read with the embedded PC-PLC. Industrial solutions based on JUMO Imago 500 will be used to read out the sensor and probes.

2.3 Environmental conditions

All motors should comply with the CAHA@3.5m environmental conditions, i.e. operational conditions of [0;15] °C and functional conditions of [-5, 20]°C. All movements shall be tested at -5°C.

For information, the spectrograph internal temperature range will be [0-15] °C (not regulated).

2.4 Device Controllers

The core technology proposed for LUCA devices control (i.e. motorized functions, shutters, lamps, environment sensors) is PLC-based. PLCs are wide spread devices used by industry since decades in automation technology. They are essentially hard real-time systems where outputs are produced based in response of input conditions. The way outputs are done is fully programmable and this offers a huge flexibility allowing with the same PLC to control almost any functionality the system will require.

The choice of PLC controllers will be driven by CAHA-IAA recommendations, in particular this one: well-established industrial standards and Commercial Off-The-Shelf (COTS) products are promoted and custom-built solutions are strongly discouraged. We also wish to integrate controllers that are widely used in ESO new instruments.

As a rule, all low level control will be done with Beckhoff Ethercat modules, including the cryogenic control and all safety-relevant devices.



Figure 2-2 Embedded Beckhoff PC-PLC

2.4.1 Motor controllers

In this phase A study, we consider that every motor has its own dedicated controller (Beckhoff modules).

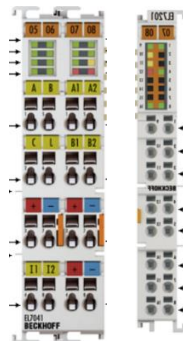


Figure 2-3 Example of Beckhoff stepper motor controller and resolver modules

2.5 Detector readout sub-system

The instrument is equipped with 8 science CCD detector cameras of type CCD231-84, with 15µm and 4096 x 4096 pixels, four outputs and readout rates up to 3 MHz

For the detector readout sub-system, two options has been considered: one based on ARC controller (from Astronomical Research Cameras, Inc.), and a second one based on the Archon CCD controller. We consider the Archon controller a more compact, modular and updated solution, so in this study we will detail that option.

The Archon [RD-01] controller consists of a FPGA with an instantiated 32-bit CPU, supporting memory and Ethernet controller. The system receives configuration information from and send status and image data to the host PC (IWS) via gigabit Ethernet connection (either copper or fibre).

This highly modular system can incorporate up to 4 ADC 16-bit ADC modules for 16 total CCD output channels. Considering that the CCD detector (e2v 231-84 BI) has 4 output channels, one such ADC modules (4-output channel) will be utilized per CCD detector, allowing to operate four-CCDs with one single Archon controller. As result, only three Archon controllers (each of them controlling four different detectors) will be required for the readout of the 8 CCD detectors.

To minimize noise insertion, the Archon system will be located immediately on top of the CCD's giving the minimal possible cabling from the raw analog CCD raw output to the input preamps on the ADC modules.

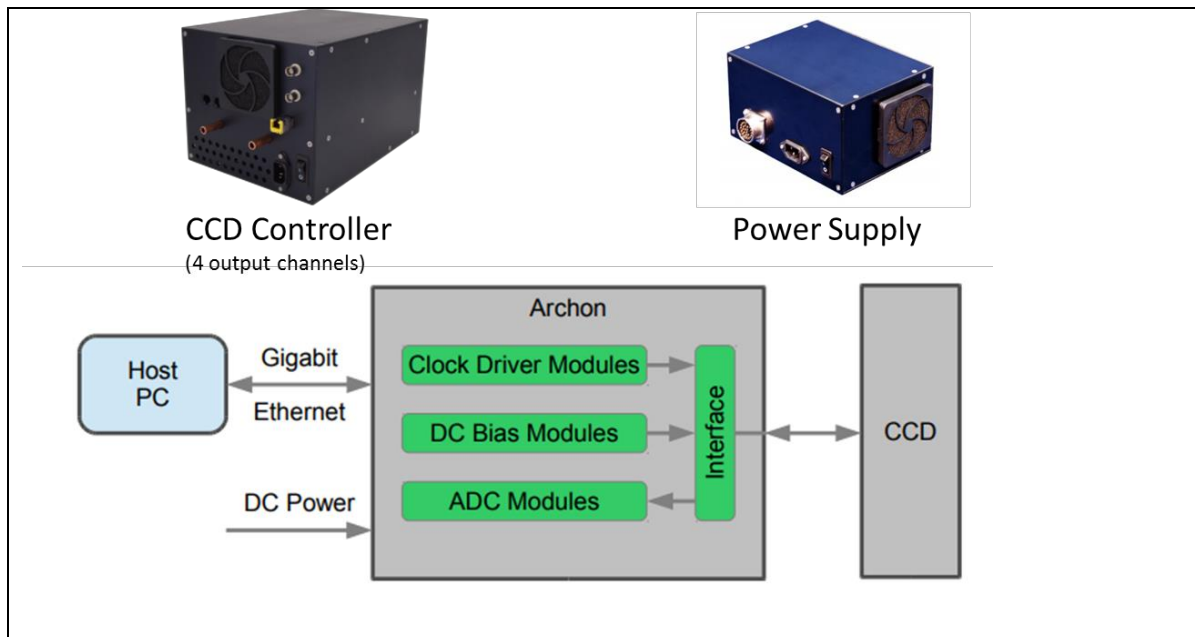


Figure 2-4 Archon CCD controller

The CCD detector to be operated is connected to the Archon through a custom interface board, build to route signals from the CCD cabling to the internal Archon module connectors.

Power is supplied to Archon through a circular connector carrying the DC voltages necessary for a particular system, or through a standard AC power cable for the Archon AC variant.

Next figure shows the architecture of the data acquisition system required for the readout and saving of the frames from all CCDs.

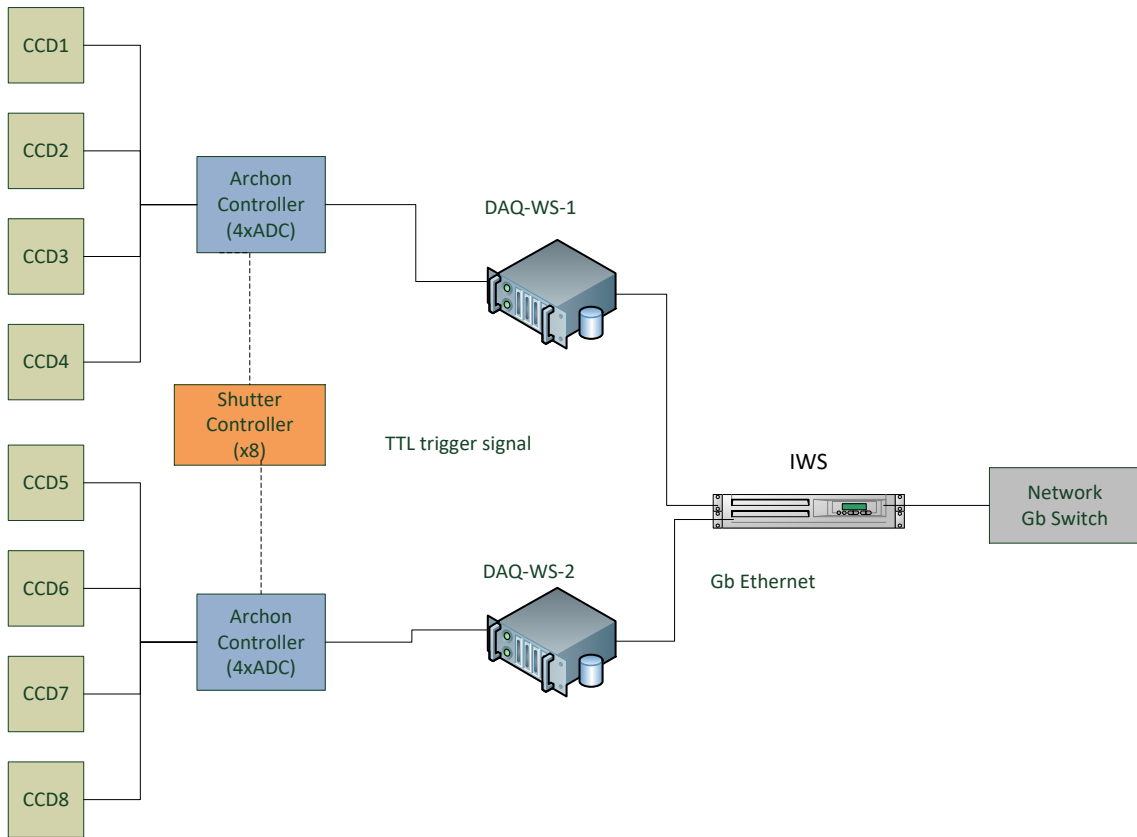


Figure 2-5 Hardware Architecture for the LUCA data acquisition sub-system

A synchronization mechanism has to be implemented to ensure that the shutters are opened when all the detectors are ready to collect the radiation and that all the cameras start the readout when the shutters have been completely closed. Synchronizing the three Archon controllers is still TBD, but suffice it to say that one controller is going to produce a single image multi-extension FITS file from the CCDs (four or two) which it controls. Then, in the IWS, the *Data Product Manager* process will merge and build a full multi-extension FITS file with 8-extension (one per detector). Then, this synchronization will be performed via software through status messages among the cameras and the supervisor.

The choice of the Archon controller is based on its use on other instruments as ZTF [RD-02] and LSST [RD-03].

2.5.1 Host data Interface

Host to controller communication takes place over a standard gigabit Ethernet interface, on a single TCP/IP port. This avoids the driver and compatibility issues sometimes associated with CameraLink, USB, or proprietary interfaces. The TCP/IP interface is implemented in hardware in the FPGA and can sustain full gigabit data rates. For example, fetching a 12000 x 10600 pixel frame (250 Mbytes of data) takes 3.8 seconds.

2.6 A&G sub-system

The A&G sub-system will consist of four technical guide cameras fed by four fiber bundles (3'x3' arc) attached to the FPA around the IFU. The four guide cameras will be Peltier cooled monochrome CCDs, and will be controlled and read using a USB3 or GigE interface (TBD). The purposed models at the moment of this study are the CCD Atik 414EX (1392 x 1040 pixels, 6.45 μm) and the Allied Vision CCD Bigeye G-132 (TBC).

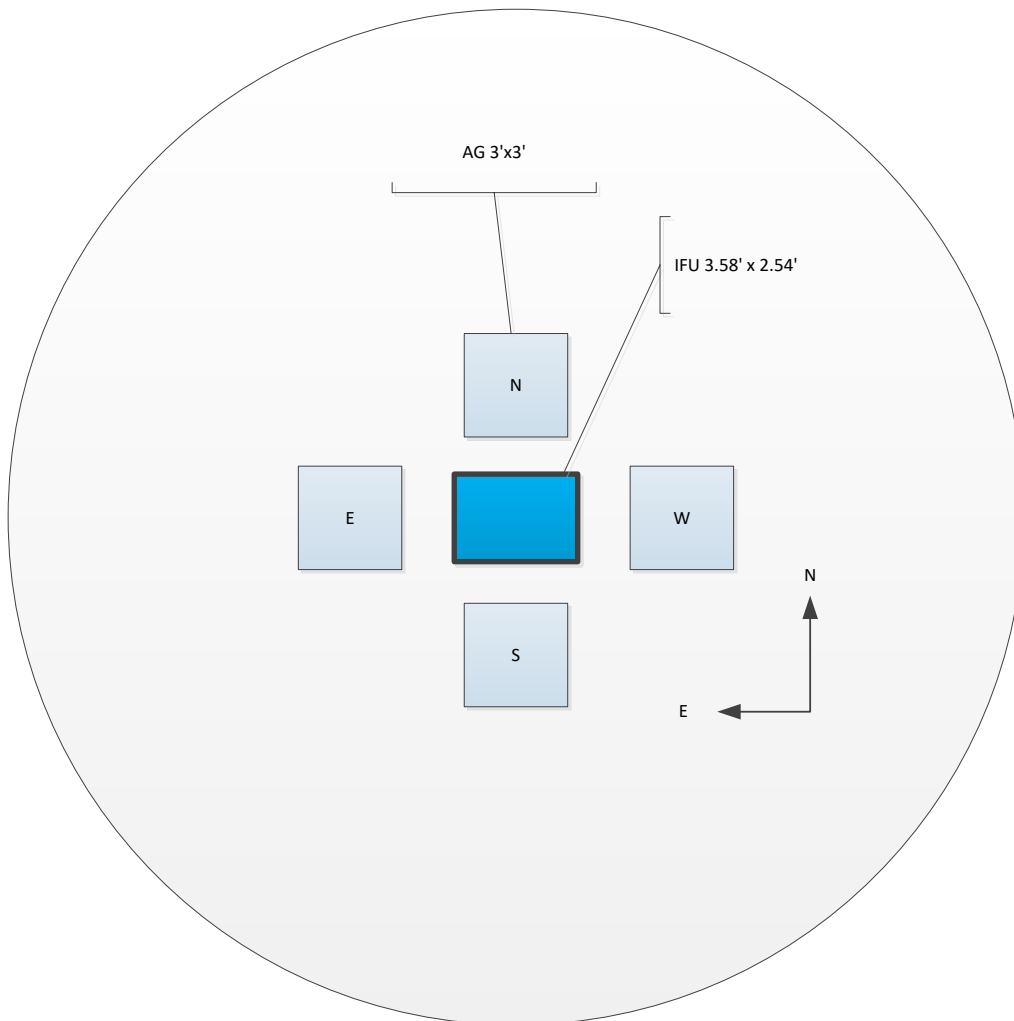
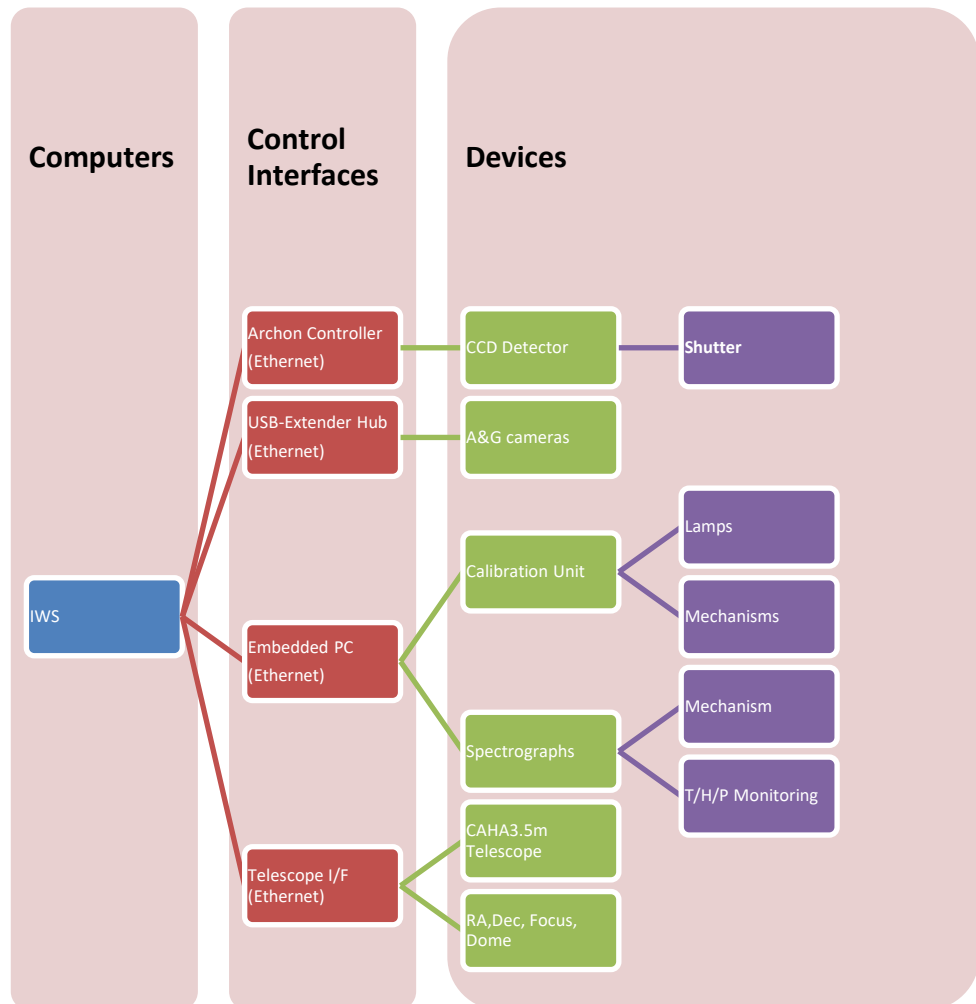


Figure 2-6 A&G cameras distribution

In principle, a field of 3 x 3 arcminutes should be sufficient to find a guide star brighter than $m_v = 18$ mag.

2.7 Hardware Interfaces

Next figure shows the hardware interfaces involved in the control of the hardware devices purposed for the ICE.



2.8 Deployment

The device control will be split over 3 embedded PC-PLCs:

- one PLC will be dedicated to the safety cryogenic and vacuum control devices
- one PLC will control the devices belonging to the Spectrographs control system
- one PLC will control the rest of the devices (calibration unit, FPA mechanism, ADC, A&G)

The final instrument will have only one IWS, where the observation will be orchestrated and managed with the Observation Tool and its software components.

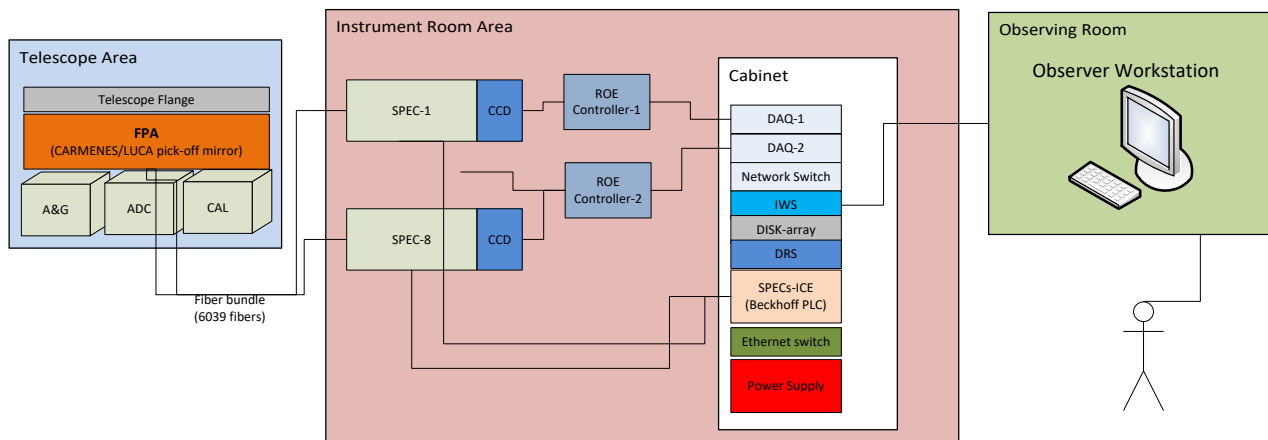


Figure 2-7 Hardware architecture

2.9 Cabinets

2.9.1 Overall layout

- Telescope FPA: small rack with A&G, ADC and CAL front-end electronics.
- Instrument Room at telescope building, with 42U thermal controlled cabinet
- Observer Control Room

2.9.2 Common features

All cabinets will be equipped with:

- a glycol cooling system (only in instrument room area)
- temperature monitoring, thermal switch and smoke sensor acting as an hardware interlock to the electrical supply upon the event of an over-temperature or detection of smoke

2.10 Power consumption


The power budget is not described in this document (average, peak, safety, computer room average, computer room safety), but in principle it is not foreseen a main concern about it.

2.11 Power dissipation

Instrument outer surfaces that are bound to radiate heat are:

- Cabinet skins
- Motors
- Sensors
- Any kind of proximity electronic boxes (encoder interpolation boxes, etc...)
- Any equipment in the Cassegrain FPA itself (lamps, power supply, AG cameras, etc.)

This specification can be checked:

	<p>LUCA@CAHA35-Instrument Control System Feasibility Study</p>	<p>Reference: LUCA35-ICS-FS-001 Issue: V 1.0 Date: 12/07/2019 Page 19 of 30</p>
---	--	---

- By design, for example, we can calculate the heat radiated inside a cabinet and assess the cooling efficiency

And

- By test, for example with IR imaging on a mock-up or a cabinet.

At this stage of the study, no deeper specifications or assumptions are done.

2.12 Interlock and safety

Interlocks have to be implemented for all conditions that could endanger personnel, environment or equipment. Their implementation shall be in accordance with the requirements resulting from the hazard analysis and risk assessment either in software, in hardware or on a dedicated safety related control system. The ICS high-level software shall not be involved in safety critical systems except to display the status of alarm signals.

A separate communication channel should be dedicated to interlock and safety information, as part of the ILS (Interlock and Safety System).

3 Instrument Control Software (ICSW)

The Instrument Control Software (ICSW) will allow the user to command, control and monitor the various components of [LUCA@CAHA3.5m](#). It will also communicate with the TCS to get and return any relevant information related to the operation of the telescope and instrument (guiding offset, focussing and current pointing for ADC).

The ICSW will also acquire and route science data from the instrument to the data processing software (pipeline) at the DHS.

3.1 Organization

Figure 3-1 is the detailed product breakdown structure of the ICSW that is part of the ICS work package.

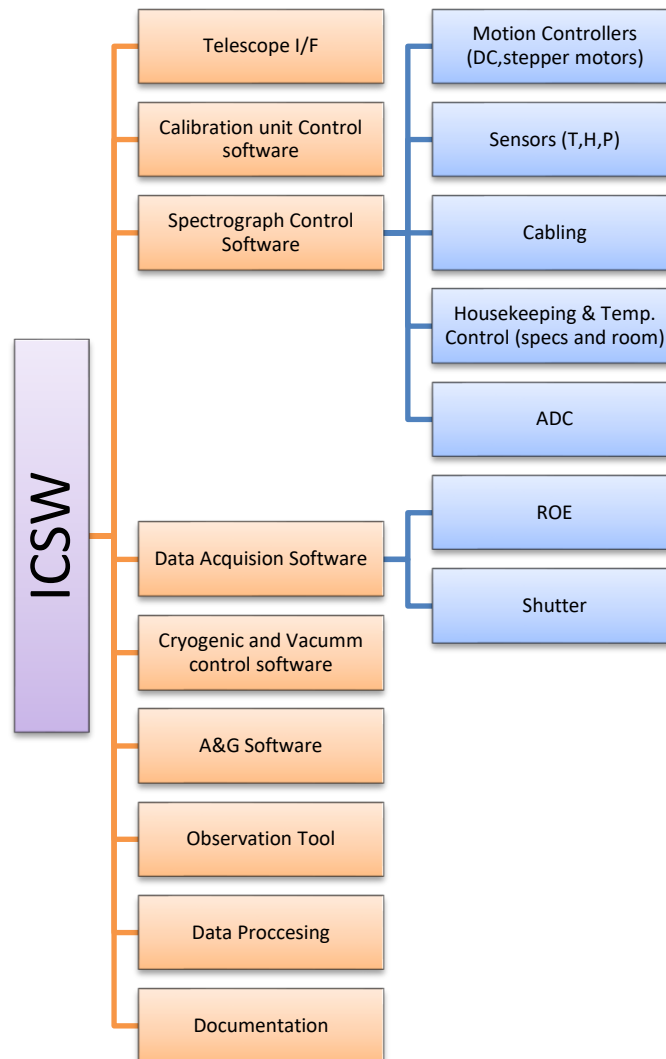


Figure 3-1 ICSW PBS

3.2 General specifications

Requirements on the ICS flow directly from the LUCA science goals and survey design. The following list represent the main software requirements that were identified during the feasibility study effort. This list will serve as a high-level baseline from which a detailed set of instrument software requirements will be derived during the development.

- The ICSW shall provide a command interface to the LUCA motors, actuators, mechanisms and cryogenic subsystem.
- The ICSW shall provide a command interface to configure and control the detector controllers.
- The ICSW shall be capable of acquiring data from the detector controllers at a rate of 100 Mbps.
- The ICSW shall be capable of timestamping acquired data at a minimum accuracy of a few milliseconds (TBD).

- The ICSW shall be route the instrument science data and associated engineering data to the Data Processing Software.
- The ICSW shall continuously monitor the operational parameters of the LUCA instrument and must archive these parameters and other telemetry information for offline analysis. Observer support has to include consoles with graphical user interfaces, alarm and error notification systems and support for secure remote access. An additional important requirement on the ICSW architecture is the need to support small-scale test systems and sub-component integration tasks.

3.3 Software architecture overview

The following block diagram in Figure 3-2 illustrates the design of the ICSW, as well as the interface to the Data Processing Software. The top half of the diagram illustrates the design of the Observation Control software and its related components; the bottom half of the diagram illustrates the design of the Detector control software (DCS) and Spectrographs control software (SCS). The right side of the diagram shows the Data Processing Software, which also executes the Quick Look tool for quick data inspection during the observation.

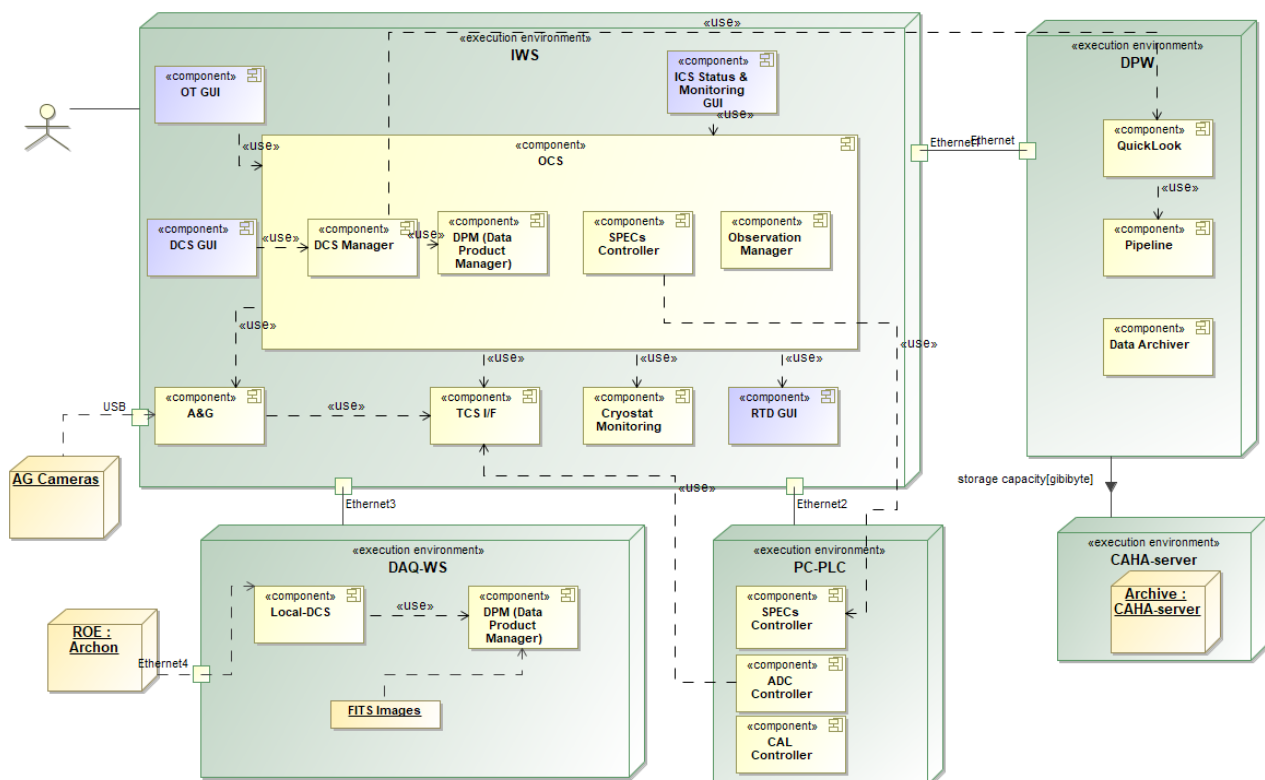



Figure 3-2 Software Architecture

	<p>LUCA@CAHA35-Instrument Control System Feasibility Study</p>	<p>Reference: LUCA35-ICS-FS-001 Issue: V 1.0 Date: 12/07/2019 Page 22 of 30</p>
---	--	---

3.3.1 Telescope I/F

The ICSW will implement the interface required to command the CAHA 3.5m telescope in order to:

- Pointing the telescope
- Offsetting the telescope
- Auto-guiding
- Focussing the telescope
- Acquire telescope coordinates and status information to be included into the FITS headers

3.3.2 Spectrograph and Calibration Unit control

The low-level control software of the Spectrographs (SCS) and Calibration Unit (CAL) will run on the instrument control embedded PC-PLCs. This software will fulfil the PLC software IEC-61131 development standard and it will be based on the TwinCAT software libraries and modules. When there is no a directly usable library component to control some specific hardware, that library component will be developed by the LUCA team.

3.3.3 Detector Control Software (DCS)

The DCS will be in charge of all sub-systems functions involved in detector control and data transfer. The Archon detector controller manufacturer (STA) provides the science detector control low-level software, and the high-level detector control software (DCS) will be based on it, following a distributed architecture. There will be three data acquisition subsystems (DAQ[1-3] computers) running a local DCS component which will readout the CCDs through the Archon controller interface. Then, at the IWS the DCS-Manager will read the local DCS and finally the Data Production Manager will build the final multi-extension FITS file with the data from all the CCDs. The DCS will also include an advanced user-friendly GUI to display the raw data of the 8 science detectors, what is called the Real Time Display (RTD).

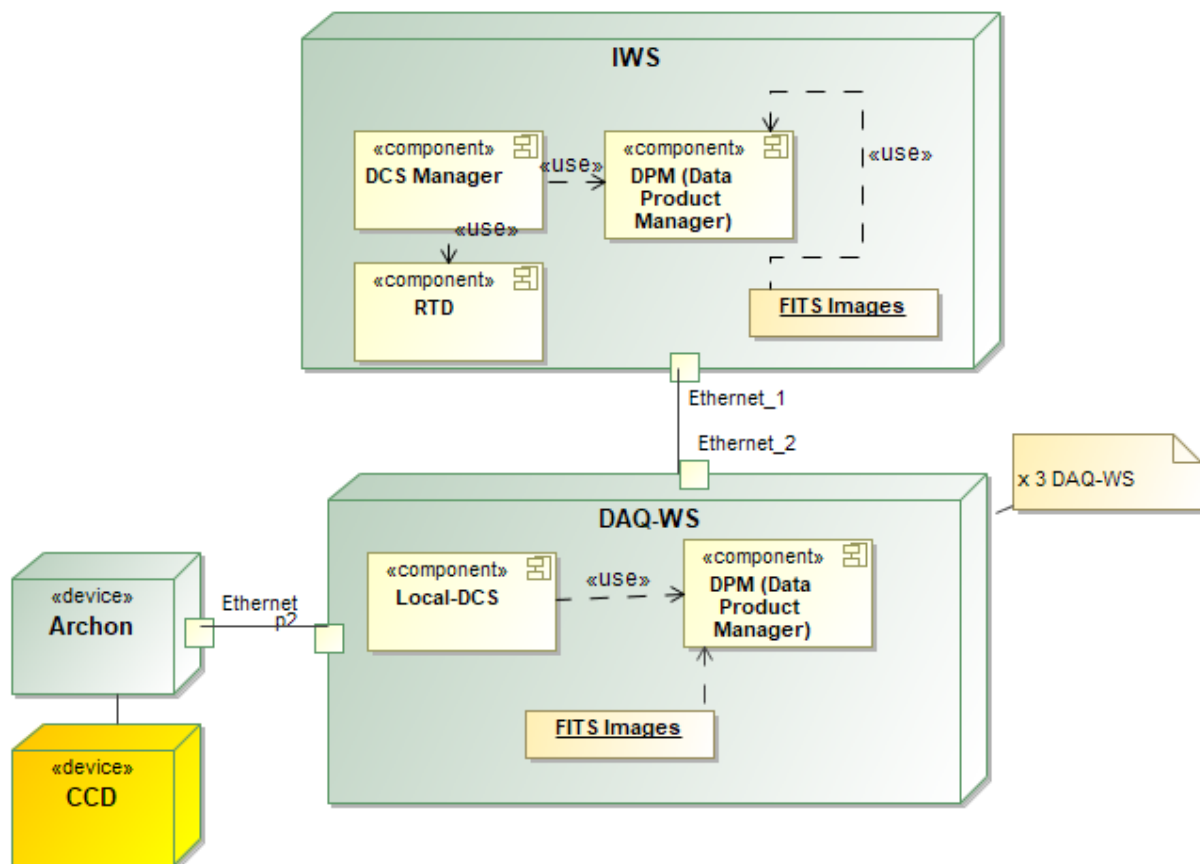



Figure 3-3 DCS architecture

3.3.4 A&G

The ICS will implement a slow guiding system to remove the effects of the differential drifts between the telescope guide probe and the instrument, by tracking a set of auto-selected guide stars in order to reach a high image stability ($< \text{TBD arcsec RMS}$).

3.3.5 Third-party controllers

LUCA ICS foresees a number of third-party controllers (e.g., manufactured by Physical Instruments, Bonn/Uniblitz shutters, power supplies, JUMO Imago) for the control of a linear/rotation stages, linear actuator, and several high-accuracy translation stages in its calibration or spectrograph unit. Unfortunately, there is no straight-forward way to integrate these devices into the software running on the PLCs. All these controllers support a common command interface, however, and can communicate with the outer world via an Ethernet connection. It is therefore relatively easy to implement a function block on the PLC which acts as a “translator” between higher levels in the LUCA software and the controllers: Commands received via the OPC UA interface of the PLC are simply translated into commands which are understood by the

	<p>LUCA@CAHA35-Instrument Control System Feasibility Study</p>	<p>Reference: LUCA35-ICS-FS-001 Issue: V 1.0 Date: 12/07/2019 Page 24 of 30</p>
---	--	---

controllers and are sent on via Ethernet. (Of course, additional topics as error handling, connection setup/shutdown, timeouts, and so on have to be handled by the regarding function block, too).

3.3.6 Thermal control and monitoring

3.3.6.1 Spectrographs and instrument room

LUCA spectrographs will be located in a dedicated room next to the telescope in the same dome building. That room shall be thermal controlled to manage the heat dissipation and at the same time, the spectrographs units shall have a local thermal control.

The, the ICS will run three independent thermal control systems in parallel:

- The coarse thermal control of the instrument room regulated to ± 1 C; it is located in the control PLC
- The local thermal control of the spectrograph units, regulated to ± 1 C (TBC);
- The thermal control of the electronics cabinets in the instrument room to control the heat dissipation from the electronics sources.

These thermal loops will be handled by industrial JUMO Imago 500 Multichannel Process Controllers; they will operate independent and only publish their control data via Profibus-DP towards the thermal control PLC. These values will be monitored by the *ThermalMonitorController* software component.

3.3.6.2 Cryostats control and monitoring

The thermal control of the 8 detector cryostats heads will be handled and monitored by a unit based on a industrial Program Controller (JUMO Imago 500). These controllers will be connected via Profibus-DP to the master cryostat controller and monitoring software component. These values will be monitored by the *ThermalMonitorController* software component.

3.3.7 Interfaces and protocols

3.3.7.1 ICS-TCS

The communication between the ICS and the [CAHA@3.5](#) telescope control system will use the CAHA protocol (t_command/t_request) already defined and based on TCP/IP.

3.3.7.2 IWS-PLC

The communication between PLCs and higher software layers will use the OPC UA protocol (an OPC UA server is running on all PLC).

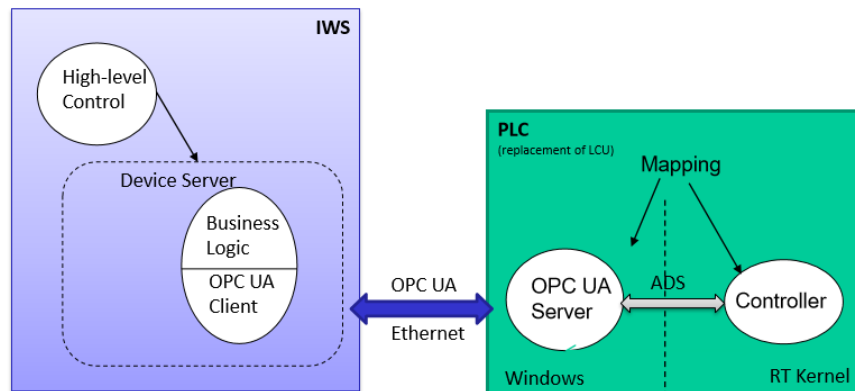


Figure 3-4 IWS-PLC protocol interface

3.4 Observation Tool

This is the highest layer in the LUCA@CAHA3.5m instrument software, which has a number of responsibilities, e.g.:

- Observation preparation and planning
- The coordination of the various subsystems in LUCA (as detector control system or function control system)
- The handling of the exposure life-cycle (setup of detectors, exposure, creation of FITS headers, trigger of archiving, and so on)
- security checks
- telescope pointing and guiding (to correct for slow drifts in plate scale, rotation, or centering)

3.5 Software development Environment

The ICS will be designed within the constraints of the CAHA control requirements and communication standards to be developed. Standard software engineering methods (use cases, UML, etc) will be used during the design and development process of the ICS.

The software will be developed in the C/C++ and Python programming languages, using standard open source tools and compilers. Qt libraries for GUI and TwinCAT3 environment for embedded PC, will also be used. The specific compilers versions will be determined as one of the initial planning tasks in the development phase.

The instrument control workstation (IWS) and data acquisition workstations (DAQ-WS) will be based on Linux *CentOS* operating system, and the Beckhoff embedded PC will run *WindowsCE* OS.

The GIT revision control software will be used for software configuration management. The *Redmine* web application will be used capture and track software problems reports and change request.

4 Data Handling System (DHS)

DHS will provide the infrastructure and procedures needed to store the raw data (FITS files) generated by the instrument and the data produced by the data reduction pipeline. In principle, night data will be stored in the IWS with a storage capacity for at least one month. Then, data will be copied daily to the LUCA Data Processing Workstation (DPW) for its processing and to the CAHA Archive.

The instrument data handling system (DHS) will be composed by three computer systems: The Instrument Control Workstation (IWS), the Data Acquisition workstation (DAQ-WS) and the Data Processing Workstation (DPW). Additionally, the data obtained will be copied daily to the CAHA Archive system.

- **Instrument Control Workstation (IWS)**
 - Run Observation Tool and Display Tool
 - Enough room to store 1-month raw science and calibration data, with fast storage disks (SSD RAID1)
- **Data Acquisition Workstations (DAQ-WS)**
 - Acquisition Interface with the detector readout (Archon Controller)
 - Three DAQ-WS will be required to acquire frames from the 8 CCD science detectors; each DAQ-WS can handle data from up to 4 CCD detector.
- **Data processing Workstation (DPW)**
 - Run Pipeline and QL
 - Massive Storage Disks for LUCA Survey (RAID5)
 - Run Web server for web front-end
- **CAHA Archive**
 - LUCA data will be transferred in a regular basis to CAHA Archive for final storage of raw and processed data.

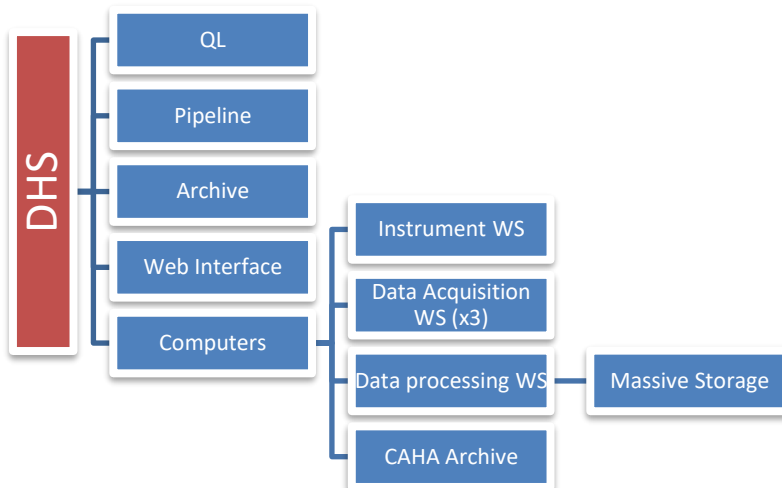


Figure 4-1 LUCA@CAHA-3.5m Data Handling System

4.1 Data rate estimation

Due to long exposition times (typical 1800s), the instrument will not generate a large volume of data. Considering 16-bit integers:

One image detector: 4k x 4k x 16 bits → **32 MB** (plus header and FITS tables)

If we suppose 2 images per hour, and 10 observing hours per night, we have $32 \times 2 \times 10 = 640$ MB per detector/night. Then, the 8 spectrographs will generate about **5120 MB** of raw science data per night. We should also add the calibration data, and assuming around 100 calibration files per detector, we have to add **25600 MB**. It means, that in one night, around $25600 + 5120 = 30720$ MB per night. Therefore, we could estimate about **30 GB** of raw data per night.

The following table summarize these numbers:


One image detector: 4k x 4k x 16 bits	32 MB
# images per detector/night	120 files
Raw science data per night	5120 MB
Calibration data per night	25600 MB
Total raw data (sci + cal) per night	30720 MB

Table 5 Data rate estimation

Storage disks will be installed in the ICS computer room with enough room to store 1 month of raw science and calibration data (TBC). The data size per night will be assessed in phase B. This storage will be done on 19" disks mounted in an electronic cabinet as presented in Figure 2-7.

4.2 Storage format

Data (calibration and science) acquired from the science detectors will be stored in FITS files, following the FITS standard (v 4.0, July 2016). Every exposure will be saved as a multi-extension FITS file, containing an extension per each science detector. The FITS header information will consist of a detector, TCS, and instrument part. Additionally, all monitored values provided by the different sensors (temperatures, pressure, etc.) shall be included.

	<p>LUCA@CAHA35-Instrument Control System Feasibility Study</p>	<p>Reference: LUCA35-ICS-FS-001 Issue: V 1.0 Date: 12/07/2019 Page 28 of 30</p>
---	--	---

4.3 Data processing

The DRS will automatically be triggered once raw FITS files are produced via the LUCA Control Software, and in visitor mode it could also be used offline step by step. The DRS will also offered to any user for offline data processing. The details of the steps for data processing will not be addressed in this document.

5 Costing

Next figures are based on experience with previous projects and does not include a 20% contingency.

5.1 Personnel

5.1.1 Feasibility study (1-Oct-2018 to 12-Jul-2019)

To accomplish this feasibility study of the ICS, from 1-Oct-2018 to 12-July-2019, it was required the human resources described below:

0.25 FTE Hardware/Software Control Engineer during **9 months** approx.

5.1.2 Development and AIV phases (5 years)

A preliminary and raw estimation of human resources required in develop, implement, and verify the ICS with a planned ramp-up in operation over a 5 year period is as follow:

	Year 1	Year 2	Year 3	Year 4	Year 5	Total (FTE)
Control Software Engineer	0,5	1	1	1	1	4,5
Data Science Engineer	0,5	1	1	1	1	4,5
Electronic Engineer	0,5	1	1	1	1	4,5
Detector Engineer	0,5	0,5	0,5	0,5	0,5	*
Total FTE	1,5	3	3	3	3	13,5


Table 6 Estimated personnel resources (FTE)

(*) Consultancy services

For the **Winlight DESI-like 1-arm**, that includes other kind of mechanisms (Hartman doors), the personnel cost estimation would be similar.

5.2 Hardware costs

Next figures are a preliminary estimation of the hardware cost for the **AAO design**, and actual quotations shall be requested during the Final Design phase, therefore a 20% contingency should be factored into these baseline estimates. For the **Winlight DESI-like 1-arm**, that includes other kind of mechanisms

	<p style="text-align: center;">LUCA@CAHA35-Instrument Control System Feasibility Study</p>	<p>Reference: LUCA35-ICS-FS-001 Issue: V 1.0 Date: 12/07/2019 Page 29 of 30</p>
---	--	---

(Hartman doors), the hardware cost estimation per spectrograph would be quite similar than current AAO design.

Item	Description	Cost	Quantity	Sub-total
Shutter	Uniblitz CCD Shutters	500	9	4500
Shutter driver D880C	Shutter Controller	500	9	4500
Lamp PS	Power Supply for spectral lamps	2000	4	8000
HCL Calibration lamp	Spectral Calibration lamp	500	4	2000
Halogen Lamp	VIS FF calibration lamp	100	2	200
Motors	Stepper/DC motors	300	24	7200
JUMO Imago 500	Temp. Controller	1500	8	12000
Varistar LHX3 Cabinet	42 U Cabinet watercolled & accesories	6000	1	6000
Beckhoff CX2030	PLC CPU	4500	3	13500
Beckhoff Modules	PLC Modules	10000	1	10000
Power Supply	Serveral power supplies	5000	1	5000
Subtotal Specs Control				67900
STA Archon ROE	CCD Read-out	45000	2	90000
Subtotal ROE				90000
DAQ-WS	Acquisition Computer	4000	2	8000
ICS-WS	Control SW Computer	6000	2	12000
DRS-WS	Data Reduction Computer	25000	1	25000
Network Switch	Network Switch	1500	2	3000
Subtotal Computers				48000
Sensors, cabling, connectors	Misc electronics stuff	6000	1	6000
Laboratory Misc	Laboratory miscelaneus AIT tools and infraestructure	6000	1	6000
Shipping	Misc shipping	3000	1	3000
Sub-contrating	Cabling & Misc subcontrating	6000	1	6000
Subtotal Lab & AIV				21000
A&G TCCD	CCD Atik 414EX	1.500,00 €	4	6.000,00 €
Science CCD	E2V CCD 231-84	100.000,00 €	8	800.000,00 €
Subtotal detectors				806.000,00 €
Total				1.032.900,00 €


	<p>LUCA@CAHA35-Instrument Control System Feasibility Study</p>	<p>Reference: LUCA35-ICS-FS-001 Issue: V 1.0 Date: 12/07/2019 Page 30 of 30</p>
---	--	---

Table 1 Hardware cost estimation

6 Overall feasibility and compliance assessment with the CAHA software framework and hardware recommendations

The scale of the LUCA@CAHA3.5m control command is unprecedented in CAHA Observatory, as is the scale of the LUCA instrument itself. The most challenging parts identified is the simultaneous readout of the 10 CCD detectors, because of their complexity and the number of devices involved.

However, we can conclude at the moment of this study that no electronics or software feasibility issue was raised.